
Structural Studies of Ionic Liquids and their Use in Synthesis.

Jennifer M. Pringle

A thesis presented for the degree of
Doctor of Philosophy
The University of Edinburgh
2001.



Abstract.

Ionic liquids represent a new type of solvent with a range of advantageous properties such as a large liquid range and negligible vapour pressure. This investigation is concerned with ionic liquids containing the imidazolium cation and reports both utilisation of these ionic liquids in new synthetic reactions and also investigations into the relationship between the structure and physical properties of these compounds by synthesis of a range of new imidazolium-based ionic liquids.

The fluorination of organic and inorganic compounds in the 1-butyl-3-methyl imidazolium hexafluorophosphate ionic liquid was investigated, utilising calcium fluoride as the fluorinating agent.

The asymmetric hydrogenation of prochiral ketones by both homogeneous and heterogeneous hydrogenation was investigated using the chiral ionic liquid 1-butyl-3-methyl imidazolium lactate.

Investigations into the relationship between the structure and physical properties of imidazolium ionic liquids were performed by changing the cation or anion of the compound to synthesise a range of new ionic liquids.

Changes to the cation of the ionic liquid were effected by substitution of the acidic proton at the 2-position of the imidazole ring by methyl and phenyl groups. Methylation at this position results in an unexpected increase in melting point. The crystal structures of 1-butyl-3-methyl imidazolium chloride and 1-butyl-2,3-dimethyl imidazolium chloride are reported and analysis of the extent of hydrogen bonding within these structures used to explain this phenomenon.

The effect of changing the anion of the ionic liquid was investigated and the crystal structures of 1-butyl-3-methyl imidazolium bromide, 1-butyl-2,3-dimethyl imidazolium hexafluorophosphate, 1-butyl-2,3-dimethyl imidazolium tetrafluoroborate and 1-butyl-2-phenyl-3-methyl imidazolium hexafluorophosphate are reported.

The changes to the structure of the compounds in the liquid phase on alteration of the cation and anion were investigated electrochemically using AC Impedance Spectroscopy.

Acknowledgements.

I am very grateful for all the help and support I have been given during the course of my PhD. My particular thanks to;

My supervisors, Dr Colin Pulham and Dr Andy Mount. Without their help, support and infectious enthusiasm completion of this work would not have been possible or as enjoyable.

My supervisors at Avecia, Dr Dave Moody and Dr Paul McCormac, for the suggestions and funding.

The x-ray crystallographers, Dr Simon Parsons, Andy Parkin, Alice Dawson and Pam M^cGregor. Additional thanks to Andy for his work with particularly difficult samples, and all the other help and support.

Brian Manzor at Avecia for his help with the viscosity measurements.

The Departmental services; NMR, elemental analysis and mass spectrometry for all their hard work.

Prof. Seddon for the samples of C₆mimPF₆, C₈mimPF₆ and C₁₀mimPF₆.

The EPSRC, for funding both the PhD and attendance at a number of conferences.

Finally, I would like to thank my friends and family for their unfailing support.

Contents.

Declaration.....	I
Abstract.....	II
Acknowledgements.....	III
Contents.....	IV
Abbreviations.....	VIII

1. Imidazolium-Based Ionic Liquids.

1.1. Introduction.....	1
1.2. Historical Review.....	2
1.3. Air and water stable imidazolium-based ionic liquids.....	5
1.4. Diels Alder Reactions.	6
1.5. Friedel Crafts Reactions.	8
1.6. Oxidations.	9
1.7. Hydroformylations.....	10
1.8. The Heck Reaction.	12
1.9. Dimerisations.	14
1.10. Oligomerisations.....	15
1.11. Stille Coupling.	16
1.12. The Baylis-Hillman Reaction.	17
1.13. Allylation.	18
1.14. Reformatsky Reactions.	19
1.15. Cycloaddition of Carbon Dioxide.....	20
1.16. Radical Reactions.....	21
1.17. The Tetrahydropyranylation of Alcohols.	22
1.18. Carbonylation of Aryl Halides.....	23
1.19. Fluorodediazotiation.	24
1.20. Electrochemical Deposition.....	25
1.21. Enzymatic Catalysis.....	26
1.22. Liquid – Liquid Extraction.	27
1.23. Stationary Phases in Gas Chromatography.	28
1.24. Use with Supercritical Carbon Dioxide.	29
1.25. Conclusions.	31

2. Experimental Techniques.

2.1. Manipulation of Air or Moisture Sensitive Compounds.....	32
2.2. Analytical Techniques - Liquid Samples.....	34
2.2.1. NMR Spectroscopy.....	34
2.2.2. Infrared Spectroscopy.....	34
2.2.3. Mass Spectrometry.....	35
2.2.4. Elemental Analysis.....	35

2.2.5. Viscosity Measurements.....	36
2.2.6. Cyclic Voltammetry.....	37
2.2.7. AC Impedance Spectroscopy.....	38
2.2.8. Optical Activity.....	38
2.3. Analytical Techniques - Solid Samples.....	39
2.3.1. Differential Thermal Analysis.....	39
2.3.2. X-ray Crystallography.....	41
2.3.3. Powder Diffraction.....	42
3. Room Temperature Ionic Liquids.	
3.1. Introduction.....	43
3.2. 1-butyl-3-methyl imidazolium chloride.....	44
3.3. 1-butyl-3-methyl imidazolium hexafluorophosphate.....	45
3.4. 1-butyl-3-methyl imidazolium tetrafluoroborate.....	50
3.5. 1-butyl-3-methyl imidazolium thiocyanate.....	53
3.6. Conclusions.....	54
3.7. Experimental.....	55
4. Uses of bmimPF ₆ in Synthesis.	
4.1. Fluorination reactions in ionic liquids.....	58
4.1.1. Introduction - halogen exchange reactions.....	58
4.1.2. Fluorination reactions in ionic liquids.....	60
4.1.3. Organic fluorinations using calcium fluoride.....	61
4.1.3.1. Fluorination of <i>p</i> -chloronitrobenzene.....	61
4.1.3.2. Fluorination of 1-chloro-2,4-dinitrobenzene.....	62
4.1.4. Fluorinations of other organic compounds.....	68
4.1.4.1.1-chloroheptane.....	68
4.1.4.2. Benzyl chloride.....	69
4.1.5. Fluorination of inorganic compounds – chlorotrimethylsilane.....	69
4.2. Reduction Reactions in 1-butyl-3-methyl imidazolium hexafluorophosphate.....	71
4.2.1. Reduction of cyclohexanone.....	72
4.2.2. Reduction of nitrobenzene.....	73
4.2.3. Reduction of other organic compounds.....	73
4.2.4. Reaction of imidazoles with sodium tetrahydroborate.....	74
4.3. Synthesis of tin compounds in ionic liquids.....	75
4.3.1. Stannane.....	75
4.3.2. Tin (IV) fluoride.....	76
4.3.3. Hexachlorostannate (IV) derivative.....	77
4.4. Future Work.....	78

5. Hydrogenation Reactions in Chiral Ionic Liquids.

5.1. Heterogeneous Hydrogenation.....	79
5.1.1. Introduction.....	79
5.1.2. Raney Nickel.....	80
5.1.3. Synthesis of a chiral ionic liquid.....	83
5.1.3.1.Synthesis of <i>bis</i> -(1-butyl-3-methyl imidazolium) tartrate.....	83
5.1.3.2.Synthesis of 1-butyl-3-methyl imidazolium lactate.....	85
5.1.4. Suitability of 1-butyl-3-methyl imidazolium lactate as a hydrogenation solvent.....	86
5.1.4.1.Hydrogenation using hydrogen gas.....	86
5.1.4.2.Hydrogenation using a hydride donor.....	87
5.1.5. Use of a chiral ionic liquid as an asymmetric hydrogenation solvent.....	88
5.1.6. Decomposition of bmim lactate with Raney nickel.....	88
5.1.7. Conclusions.....	90
5.2. Homogeneous hydrogenation.....	91
5.2.1. Introduction.....	91
5.2.2. Homogeneous hydrogenations in ionic liquids.....	92
5.2.3. Asymmetric homogeneous hydrogenation in ionic liquids.....	96
5.2.4. Wilkinson's catalyst.....	97
5.2.5. 1-butyl-3-methylimidazolium lactate as solvent for hydrogenation..	98
5.2.5.1.Using hydrogen gas.....	98
5.2.5.2.Using a hydride donor.....	100
5.2.6. Decomposition of the ionic liquid.....	101
5.2.7. Interaction of the lactate ionic liquid with Wilkinson's catalyst.....	102
5.2.8. Conclusions.....	102
5.2.9. Future work.....	103
5.2.10. Experimental.....	104

6. Substituted Imidazolium Ionic Liquids.

6.1. Introduction.....	109
6.2. Methyl-Substituted Imidazolium Ionic Liquids.....	110
6.2.1. 1-butyl-2,3-dimethyl imidazolium chloride.....	111
6.2.2. 1-butyl-2,3-dimethyl imidazolium hexafluorophosphate.....	112
6.2.3. 1-butyl-2,3-dimethyl imidazolium tetrafluoroborate.....	114
6.2.4. 1-butyl-2,3-dimethyl imidazolium thiocyanate.....	115
6.2.5. The effect of methylation on melting point.....	116
6.2.6. The effect of methylation on viscosity.....	117
6.2.7. 1-butyl-2,3,4,5-tetramethyl imidazolium chloride.....	118
6.2.8. Conclusions.....	119

6.3. Phenyl-Substituted Imidazolium Ionic Liquids.....	120
6.3.1. 1-butyl-2-phenyl-3-methyl imidazolium chloride.....	120
6.3.2. 1-butyl-2-phenyl-3-methyl imidazolium tetrafluoroborate.....	120
6.3.3. 1-butyl-2-phenyl-3-methyl imidazolium hexafluorophosphate.....	121
6.4. Reaction of Phenyl-Substituted Imidazolium Ionic Liquids.....	122
6.4.1. Sulfonation.....	122
6.4.2. Nitration.....	126
6.5. Future Work – Benzyl Substituted Ionic Liquids.....	131
6.6. Experimental.....	133
7. The Structure of Ionic Liquids in the Liquid State.	
7.1. Introduction.....	141
7.2. AC Impedance Spectroscopy.....	143
7.2.1. Introduction.....	143
7.2.2. AC impedance spectroscopy of ionic aqueous solutions.....	145
7.2.3. AC impedance spectroscopy of ionic liquids.....	149
7.2.4. Modelling ionic liquids.....	155
7.2.5. The effect of temperature on ion motion.....	159
7.2.6. The effect of methylation.....	165
7.2.7. The effect of changing the cation.....	171
7.3. Analysis of calcium fluoride in bmimPF ₆	179
7.3.1. AC Impedance spectroscopy.....	180
7.3.2. X-ray powder diffraction.....	183
7.4. Conclusions.....	188
8. The Structure of Ionic Liquids in the Solid State.	
8.1. Introduction.....	190
8.2. The effect of changing the cation.....	192
8.2.1. 1-butyl-3-methyl imidazolium chloride.....	193
8.2.2. 1-butyl-2,3-dimethyl imidazolium chloride.....	195
8.3. The effect of changing the anion.....	197
8.3.1. 1-butyl-3-methyl imidazolium bromide.....	198
8.3.2. 1-butyl-2,3-dimethyl imidazolium hexafluorophosphate.....	200
8.3.3. 1-butyl-2,3-dimethyl imidazolium tetrafluoroborate.....	202

8.4. The effect of substitution of a phenyl group.....	206
8.5. Structural trends within published ionic liquid crystal structures.....	209
8.6. Conclusions.....	216

Appendix.

1. X-ray Crystallography.....	I
A1. 1-butyl-3-methyl imidazolium chloride.....	I
A2. 1-butyl-3-methyl imidazolium bromide.....	III
A3. 1-butyl-2,3-dimethyl imidazolium chloride.....	V
A4. 1-butyl-2,3-dimethyl imidazolium tetrafluoroborate	VII
A5. 1-butyl-2,3-dimethyl imidazolium hexafluorophosphate	X
A6. 1-butyl-2-phenyl-3-methyl imidazolium hexafluorophosphate.....	XII
2. Courses and Lectures Attended.....	XV

Abbreviations.

bmimCl	1-butyl-3-methyl imidazolium chloride
bmimPF ₆	1-butyl-3-methyl imidazolium hexafluorophosphate
bmimBF ₄	1-butyl-3-methyl imidazolium tetrafluoroborate
bmimSCN	1-butyl-3-methyl imidazolium thiocyanate
bmmimCl	1-butyl-2,3-dimethyl imidazolium chloride
bmmimPF ₆	1-butyl-2,3-dimethyl imidazolium hexafluorophosphate
bmmimBF ₄	1-butyl-2,3-dimethyl imidazolium tetrafluoroborate
bmmimSCN	1-butyl-2,3-dimethyl imidazolium thiocyanate
bpmimCl	1-butyl-2-phenyl-3-methyl imidazolium chloride
bpmimPF ₆	1-butyl-2-phenyl-3-methyl imidazolium hexafluorophosphate
CDCl ₃	deuterated chloroform
CD ₃ OD	deuterated methanol
DMF	dimethyl formamide
dmsO	dimethyl sulfoxide
d ₆ -dmsO	deuterated dimethyl sulfoxide
EI-MS	electron impact mass spectrometry
FAB-MS	fast atom bombardment mass spectrometry
IR	infra-red spectroscopy
M	mol dm ⁻³
mol	moles
mmol	milli moles
<i>m/z</i>	mass per unit charge
M.P.	melting point
NMR	nuclear magnetic resonance
SD	standard deviation
THF	tetrahydrofuran
Z	impedance

1 Imidazolium-Based Ionic Liquids.

1.1 Introduction.

Ionic liquids represent an exciting, new type of solvent, which differ from conventional solvents both in their composition - a combination of large organic cations and organic/inorganic anions - and in the physical properties that they display, such as a negligible vapour pressure and a large liquid range. The first commercial process utilising an ionic liquid has been developed and is now ready for licensing.¹ This marks the next stage in the rapid advancement of ionic liquids as alternatives to conventional molecular solvents.

This chapter is intended to give a brief outline of the history of this new technology and to give a comprehensive review of the uses of 1-butyl-3-methyl imidazolium hexafluorophosphate (bmimPF₆) and 1-butyl-3-methyl imidazolium tetrafluoroborate (bmimBF₄) reported to date and their potential advantages over conventional molecular solvent systems.

¹ H. Olivier-Bourbigou, H. Chodorge and P. Travers, *Petrol. Technol. Q.*, 1999, 4, 141-149.

1.2 Historical Review.

The melting point of pure lithium chloride is 610 °C. This can be reduced by combination with a different inorganic salt to produce a solution that has a eutectic point lower than that of either of its components. For example, combination of lithium chloride and caesium chloride in a 60:40 molar ratio lowers the melting point to 355 °C.² To devise a medium suitable for organic synthesis it is clearly necessary to reduce the melting point further. This can be achieved by use of a large organic cation in combination with the small inorganic anion. As explained by the Kapustinskii equation (1) this results in a significant decrease in lattice energy, U , and thus a concordant decrease in the melting point of the material.

$$U = 287.2 \sum_n \frac{\eta_A \eta_B}{r_C + r_A} \left(1 - \frac{0.345}{r_C + r_A} \right) \quad (1)$$

Where r_A and r_C are the ionic radii of the ions (Å), η is their respective ionic charge and n is the number of ions in the molecule. It can clearly be seen from this equation that an increase in the size of the cation or anion decreases the lattice energy.

This effect was first reported for salts containing an organic cation in 1914 when Smith *et al.*³ prepared ethylammonium nitrate and noted an abnormal *parachor* for this species,⁴ and a melting point of 8 °C.

The early work on the development of ionic liquid chemistry largely centred on the use of the tetrachloroaluminate(III) anion. The first of these was developed in 1948 by Hurley *et al.*⁵ for the electroplating of aluminium, but work did not continue on these systems until Osteryoung *et al.*⁶ successfully prepared chloroaluminate melts that were liquid at ambient temperatures. They noted that the system developed by Hurley, which comprised 67 mol % AlCl_3 and 33 mol % ethylpyridinium bromide,

² K. R. Seddon, *J. Chem. Tech. Biotechnol.* 1997, **68**, 351 – 356.

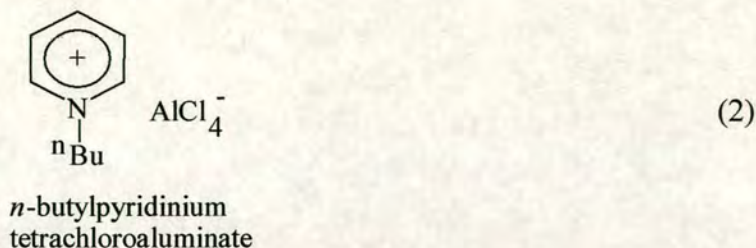
³ S. Sugden and H. Wilkes, *J. Chem. Soc.*, 1929, 1291 – 1298.

⁴ The *parachor* is an empirical measurement of the molecular volume of a material and was used to assess the constitution of organic and inorganic compounds. *The Penguin Dictionary of Chemistry*, D. W. A. Sharp, 2nd Ed.

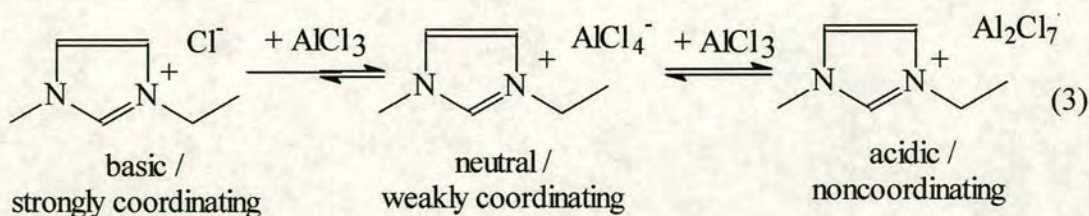
⁵ F. H. Hurley, *Chem. Abs.*, 1949, **43**, P7645b.

⁶ H. L. Chum, V. R. Koch, L. L. Miller and R. A. Osteryoung, *J. Am. Chem. Soc.*, 1975, **97**, 3264 – 3265, J. Robinson and R. A. Osteryoung, *J. Am. Chem. Soc.*, 1979, **101**, 323 – 327.

was only molten at room temperature for this particular composition and an increase in the amount of AlCl_3 resulted in a significant increase in the melting point. Thus, the *n*-butylpyridinium chloride – aluminium chloride system was developed, which is molten at room temperature over a larger composition range.



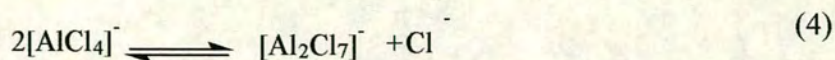
Three years later the same group published the first report of an imidazolium-based ionic liquid, again utilising the tetrachloroaluminate anion.⁷ The development of this alternative cation was prompted by observations that the pyridinium cation was reduced by aluminium in the melt, resulting in a significant decrease in the electrochemical window of the solvent, thus diminishing the extent to which this system could be used in electrochemical applications. The imidazolium-based species also had the added advantage of being liquid at room temperature over the entire composition range. This is important as the composition of the mixture determines its Lewis acidity.² Compositions containing greater than 50 mol % of AlCl_3 are termed acidic and those with less than 50 mol % AlCl_3 are termed basic. This also represents a change in the coordinating ability of the ionic liquid, which is essentially dictated by the nature of the anion.⁸



The equilibrium governing the behaviour of these tetrachloroaluminate ionic liquids is given in equation 4.

⁷ J. S. Wilkes, J. A. Levisky, R. A. Wilson and C. L. Hussey, *Inorg. Chem.*, 1982, **21**, 1263 – 1264.

⁸ P. Wasserscheid and W. Keim, *Angew. Chem. Int. Ed.* 2000, **39**, 3772 – 3789.



Both of the tetrachloroaluminate systems display the advantageous physical properties that have driven the development of these systems as new reaction media. These include a high solubility of a range of organic, organometallic and inorganic compounds, a large liquidus range, and high specific conductivities. Utilisation of the imidazolium cation also results in a large electrochemical window (2.5 V for the 1-ethyl-3-methyl-imidazolium tetrachloroaluminate salt).

Work on the chloroaluminate ionic liquids largely centred on their electrochemical uses until the 1980s when attention also began to focus on their use with transition metal complexes, as new reaction media and as catalysts. However, although these species have been widely investigated and are still being utilised for a range of applications, a specific problem with their use as replacements for conventional solvents in the laboratory is their instability to air and water.

1.3 Air- and Water-Stable Imidazolium-based Ionic Liquids.

The discovery by Wilkes *et al.*⁹ of an air- and water-stable ionic liquid led to a significant increase in the interest in room temperature ionic liquids and was a major step in the development of these systems as widely applicable reaction media. The enhanced air and water stability was the result of a change in the anion of the 1-ethyl-3-methyl imidazolium ionic liquid. Wilkes reported the use of BF_4^- , NO_2^- , NO_3^- , MeCO_2^- , I^- , and SO_4^{2-} as alternative anions, of which the BF_4^- and MeCO_2^- salts were liquid at room temperature. The 1-ethyl-3-methyl imidazolium salts have found applications in a range of reactions, but their use is hindered by their relatively high melting point.⁸

The use of the 1-butyl-3-methyl imidazolium cation was first reported in 1996 and resulted in ionic liquids with significantly decreased melting points.¹⁰ The 1-butyl-3-methyl imidazolium hexafluorophosphate and tetrafluoroborate ionic liquids are now the most widely used of all the air- and water-stable species.

Room temperature ionic liquids have stimulated significant interest as new solvents for industrial processes, particularly with a view to reducing the environmental impact of these processes. The negligible vapour pressures of these compounds when used as solvents offers advantages over conventional organic solvents and allows for easy separation of reaction products. However, for ionic liquids to be seriously considered as alternatives to the well-established molecular solvents, their uses and advantages have to be clearly demonstrated.

The predominant area of interest in ionic liquids is in their use in homogeneous catalysis. Chemical reactions tend to proceed faster and with more control when they take place in liquids because better mixing can occur than in heterogeneous reactions. This normally necessitates the use of organic solvents, which causes both environmental problems and difficulties with product separation. However, ionic liquids are immiscible with a number of organic solvents, particularly linear hydrocarbons and alicyclic compounds such as pentane, and this can be exploited by

⁹ J. S. Wilkes and M. J. Zaworotko, *J. Chem. Soc., Chem. Commun.*, 1992, 965 – 967.

¹⁰ P. A. Z. Suarez, J. E. L. Dullius, S. Einloft, R. F. De Souza and J. Dupont, *Polyhedron*, 1996, **15**, 7, 1217 – 1219.

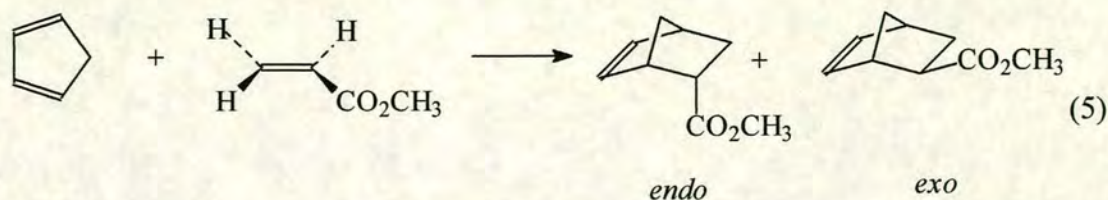
using the ionic liquid in biphasic catalysis. In this procedure the transition metal catalyst is dissolved in the ionic liquid while the organic reactant and product form an immiscible upper layer. The solution is stirred to effect sufficient mixing of the two layers for reaction to occur, and on completion of the reaction the product can be easily removed by decantation. This method has been utilised for a number of different reactions and the transition metal catalyst dissolved in the ionic liquid can normally be recycled with only a small decrease in activity. Clearly, this is an advantageous technique provided the activity of the catalyst in the ionic liquid is comparable to its activity in the conventional solvent system. The recycling of transition metal catalysts is of particular interest as these tend to be very expensive.

1.4 Diels-Alder Reactions.

The Diels-Alder reaction is one of the most useful carbon-carbon bond-forming reactions in organic chemistry and utilisation of a range of ionic liquids as media for this reaction has been investigated.

The Diels-Alder reaction involves combination of a diene and a dienophile to form a cycloadduct. Two isomers are formed when the dienophile is unsymmetrical and the *endo/exo* ratio obtained has been studied extensively in molecular solvents. It is understood to be dependent on the polarity of the solvent system - a more polar solvent leads to the increased stability of the more polar, *endo*, product. The use of an ionic liquid in the Diels-Alder reaction was therefore considered of additional interest as a means of probing the polarity of ionic liquids compared to molecular solvents.

Fischer *et al.* studied the reaction between 0.3 M cyclopentadiene and methyl acrylate in neat bmimBF_4 at 25 °C.¹¹



This ionic liquid was found to exhibit strong *endo* selectivity (6.1:1) compared to diethyl ether (2.9:1) under the same conditions. The selectivity observed is characteristic of hydrogen-bonded, polar organic solvents such as methanol (6.7:1) or ethanol (5.2:1).

The addition of lithium perchlorate to diethyl ether results in increased selectivity to 7.4:1, better than that observed in bmimBF₄. However, bmimBF₄ is clearly a safer solvent system and potentially less harmful to the environment. It is interesting to note, however, that the selectivity in water - the safest and most environmentally benign of all the solvent systems - is 9.2:1 under similar conditions. However, the use of moisture-sensitive reagents is clearly precluded. In ionic liquids, as for molecular solvents, *endo* selectivity is decreased as the temperature and reagent concentration are increased.

Earle *et al.*¹² studied the Diels-Alder reaction of three different dienes and dienophiles in bmimPF₆ and bmimBF₄ over a range of temperatures and reagent concentrations. After one hour, conversion rates intermediate between those of water and 5M lithium perchlorate in diethyl ether were observed for both ionic liquids. The ionic liquids were also reported to be fully recyclable after extraction with diethyl ether or petrol.

In the most recent and promising publication, Song *et al.*¹³ reported the use of ionic liquids in Diels-Alder reactions catalysed by scandium triflate. The reaction between 1,4-naphthaquinone and 3 equivalents of 2,3-dimethylbuta-1,3-diene with 0.2 mol % Sc(Otf)₃ in bmimPF₆ proceeded to completion within 2 hours at room temperature. This is significantly faster than the reaction in CD₂Cl₂, which is only 22 % complete after this time. It was also noted that the use of only one equivalent of the bmimPF₆ as an additive in the CD₂Cl₂ was sufficient to achieve similar rate enhancements. Improved *endo:exo* selectivities compared to the dichloromethane reaction were also observed.

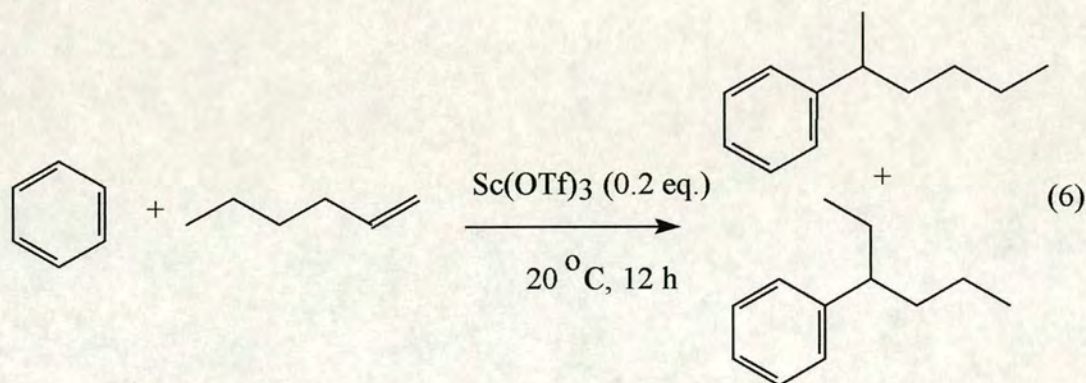
¹¹ T. Fischer, A. Sethi, T. Welton and J. Woolf, *Tetrahedron. Lett.*, 1999, **40**, 793 – 796.

¹² M. J. Earle, P. B. McCormac and K. R. Seddon, *Green Chemistry*, 1999, **1**, 1, 23 – 25.

¹³ C. E. Song, W. H. Shim, E. J. Roh, S. Lee and J. H. Choi, *Chem. Commun.*, 2001, 1121-1123.

1.5 Friedel Crafts Reactions.

The use of ionic liquids in the Friedel-Crafts reaction have focused almost exclusively on the use of the chloroaluminate species. This is unsurprising as the reaction is typically catalysed by the use of aluminium(III) chloride. However, Song *et al.*¹⁴ report the use of a range of ionic liquids with a scandium(III) triflate catalyst for the alkylation of aromatic compounds with alkenes. The use of lanthanides for the catalysis of Friedel-Crafts alkylation is relatively new and had not previously been used for alkylation with alkenes. The alkylation of benzene with hex-1-ene was studied in a variety of ionic liquids including bmimBF₄ and bmimPF₆ and, although the reaction is reported to proceed in >99 % yield in bmimPF₆, no reaction was observed in bmimBF₄.



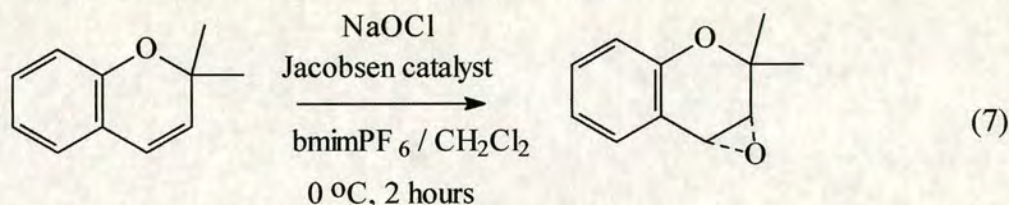
Similar results were obtained for the other ionic liquids studied - the reaction proceeded to completion in the hydrophobic ionic liquids, such as emimSbF₆, bmimPF₆, and bmimSbF₆, but no reaction occurred in the hydrophilic species emimBF₄, bmimBF₄, or bmim triflate.

¹⁴ C. E. Song, W. H. Shim, E. J. Roh and J. H. Choi, *Chem. Commun.*, 2000, 1695 – 1696.

1.6 Oxidations.

There are only two reports of oxidation reactions in bmimPF_6 or bmimBF_4 , but both show promising results. It is known from electrochemical studies that these ionic liquids are relatively stable to oxidation,¹⁵ suggesting that these may be ideal media for such reactions and that this is probably one area of application that will be the subject of considerable interest in the future.

The first report of a transition metal catalysed oxidation reaction in an ionic liquid was published in 2000 by Song *et al.* and reported the use of Jacobsen's chiral $\text{Mn}^{\text{III}}(\text{salen})$ catalyst for epoxidation reactions.¹⁶ BmimPF_6 is reported as the ionic liquid of choice as a result of its immiscibility with water. Using this ionic liquid with dichloromethane in a 1:4 v/v ratio a significant enhancement was reported for the activity of the catalyst, [*N,N'*-bis(3,5-di-*tert*-butylsalicylidene)-1,2-cyclohexanediamine] manganese(III) chloride.



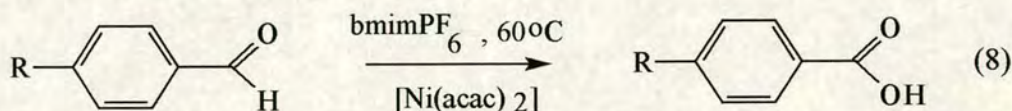
The epoxidation of 2,2-dimethylchromene, shown in equation 2, proceeded with 86 % conversion after two hours using this solvent system. In the absence of the ionic liquid it took six hours to achieve the same conversion. Additionally, the enantiomeric excess of this reaction was 96 % and the catalyst system could be recycled. The organic phase was washed with water and the ionic liquid extracted with hexane leaving the catalyst in the ionic liquid to be reused. After five runs the catalyst activity had dropped from 86 % to 53 % and the % ee had dropped from 96 % to 88 %. It is puzzling, however, that the authors require the use of significant quantities of dichloromethane as a means of maintaining the solvent system as a

¹⁵ P. A. Z. Soares, V. M. Selbach, J. E. L. Dullius, S. Einloft, C. M. S. Piatnicki, D. S. Azambuja, R. F. de Souza and J. Dupont, *Electrochimica Acta*, 1997, **42**, 16, 2533 – 2535.

¹⁶ C. E. Song and E. J. Roh, *Chem. Commun.*, 2000, 837 – 838.

liquid at the reaction temperature of 0 °C. They also report that bmimPF₆ is a solid at this temperature, although it is well established that bmimPF₆ is a liquid at this temperature. It is possible that even greater enhancements of rate could be obtained by using of the neat ionic liquid and this is suggested as an area of further investigation.

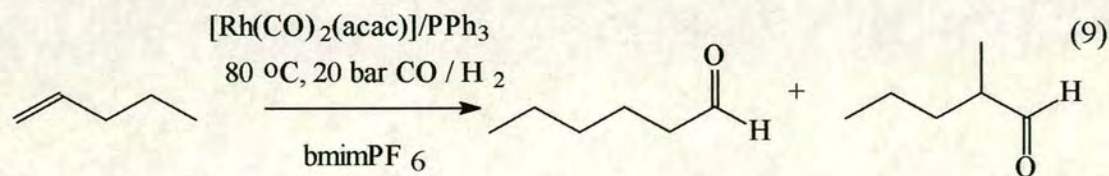
The only report of the oxidation of an aromatic aldehyde in an ionic liquid was published by Howarth and again used the bmimPF₆ ionic liquid.¹⁷ Using a nickel(II) acetylacetonate catalyst a range of aromatic aldehydes were oxidised with yields ranging from 66 % for R = H, to 47 % for R = CO₂H.



The reactions were successfully repeated three times using the same catalyst/ionic liquid system, again indicating the potential for recycling these systems.

1.7 Hydroformylations.

Investigations into the use of room temperature ionic liquids for hydroformylation reactions were first reported by Chauvin *et al.*^{18, 19} Hydroformylation is a form of carbonylation reaction, normally utilising either a cobalt or rhodium catalyst, whereby the reaction of an alkene with carbon monoxide and hydrogen yields either an aldehyde or primary alcohol. Chauvin *et al.* studied the two-phase hydroformylation of pent-1-ene using the [Rh(CO)₂(acac)]/PPh₃ catalyst (acac = acetylacetonate) in bmimPF₆ and high catalytic activity was observed.



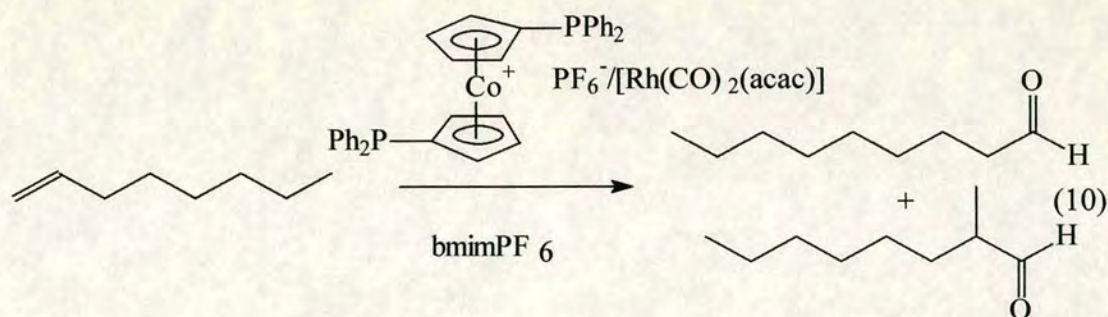
¹⁷ J. Howarth, *Tetrahedron Lett.*, 2000, **41**, 6627 – 6629.

¹⁸ Y. Chauvin, L. Mussmann and H. Olivier, *Angew. Chem. Int. Ed. Engl.* 1995, **34**, 23/24, 2698 – 2700.

¹⁹ H. Olivier and Y. Chauvin, *Electrochemical Society Proceedings*, 1996, **96**, 7, 70 – 73.

The turnover frequency (TOF) of this system was reported to be 333 h^{-1} , a slight improvement compared to toluene ($\text{TOF} = 297 \text{ h}^{-1}$). As this was a biphasic reaction, the organic phase could be removed and re-use of the ionic phase was possible with only a slight loss in activity. However, a small amount of the catalyst leached into the organic phase, prompting attempts to immobilise the catalyst in the ionic liquid. For the bmimPF_6 system, monosulfonated triphenylphosphine was used in place of the PPh_3 , but this resulted in a significant drop in activity ($\text{TOF} 59 \text{ h}^{-1}$).

This observation prompted further investigations by Wassercheid *et al.* to determine whether this was an effect of the ligand or the ionic liquid.⁸ Brasse *et al.*²⁰ prepared a range of ionic phosphine ligands with cobaltocenium backbones and the ligand 1,1'-bis(diphenylphosphino)cobaltocenium hexafluorophosphate, in particular, showed good activities for the biphasic hydroformylation of 1-octene ($\text{TOF} = 810 \text{ h}^{-1}$).



Leaching of catalyst using this ligand was less than 0.5 %, the selectivity for the linear aldehyde was acceptable (linear:branched 16.2:1) and the potential for catalyst recycling was demonstrated. The bmimPF_6 system appears to provide an ideal weakly coordinating medium for the rhodium catalyst whilst at the same time displaying limited, but sufficient, solubility for the 1-octene to allow high reaction rates.

²⁰ C. C. Brasse, U. Englert and A. Salzer, *Organometallics*, 2000, **19**, 3818 – 3823.

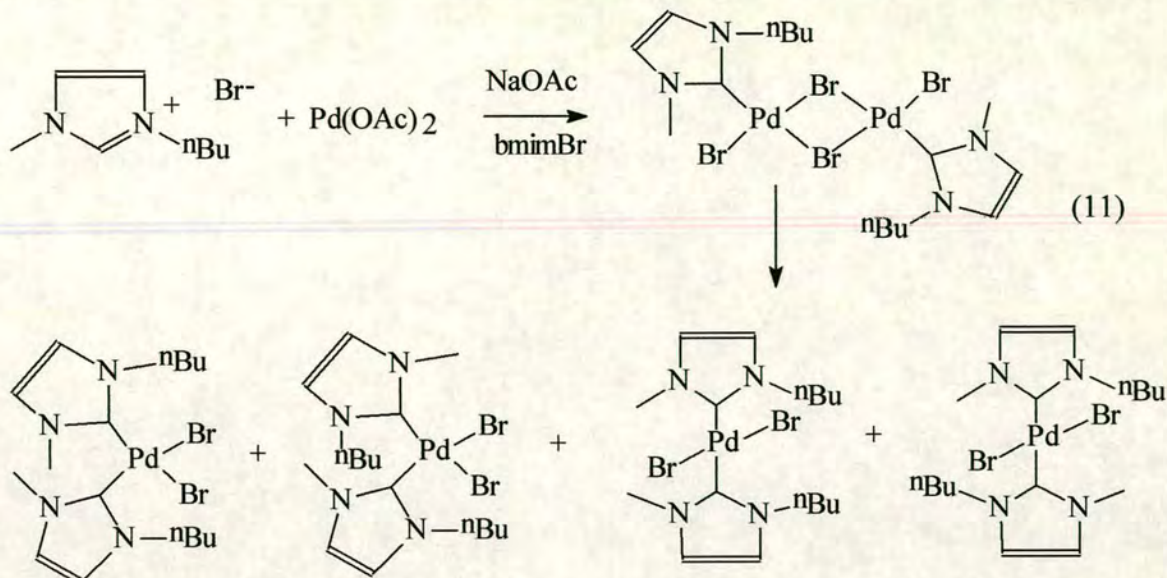
1.8 The Heck Reaction.

The Heck reaction is the palladium-catalysed C-C coupling of an aromatic halide or anhydride with an alkene and is of significant importance in organic chemistry. One major use for this is the synthesis of cinnamic acid and its derivatives, which are widely used as flavourings and UV absorbers. However, a major disadvantage of the reaction is that the catalyst is often lost at the end of the reaction. The possibility of developing a recyclable catalyst system is therefore a significant driving force in the investigation of this reaction in ionic liquids.

Carmichael *et al.* have investigated a wide range of Heck coupling reactions of aryl halides or benzoic anhydride with alkenes and demonstrated the applicability of a range of ionic liquids to these reactions.²¹ The reaction between iodobenzene and ethyl acrylate to give *trans*-ethyl cinnamate in bmimPF₆, with 2 mol % Pd(OAc)₂, proceeded in more than 95 % yield. For this reaction a three-phase catalyst system was used with the catalyst in the ionic liquid forming the lower layer, with water and cyclohexane forming the middle and upper layers respectively. The salt by-products were dissolved in the water layer and the products dissolved in the organic layer. The addition of a phosphine ligand was found to promote the reaction in bmimPF₆. The authors also noted a significantly higher yield in the imidazolium-based ionic liquids compared to the pyridinium species and suggest the deprotonation of the imidazole and subsequent formation of a carbene as an explanation. It is proposed that the carbenes act as ligands forming an imidazolylidine-palladium carbenoid species. This was subsequently confirmed by Xu *et al.* who studied the Heck reaction in bmimBF₄ and bmimBr.²² The palladium catalyst was observed to exhibit greater activity and stability in the bromide species than in the tetrafluoroborate analogue and this was explained by the isolation and characterisation of two 1-butyl-3-methylimidazol-2-ylidene complexes of palladium.

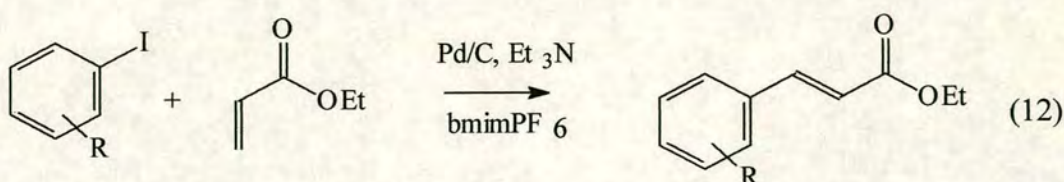
²¹ A. J. Carmichael, M. J. Earle, J. D. Holbrey, P. B. McCormac and K. R. Seddon, *Organic Letters*, 1999, **1**, 7, 997 – 1000.

²² L. Xu, W. Chen and J. Xiao, *Organometallics*, 2000, **19**, 1123 – 1127. L. Xu, W. Chen, J. Ross and J. Xiao, *Organic Letters*, 2001, **3**, 2, 295 – 297.



The palladium-carbene complexes were themselves found to be active catalysts for the Heck reaction when isolated and redissolved in bmimBr.

The applicability of the Heck reaction in ionic liquids was demonstrated further by Hagiwara *et al.* who used bmimPF₆ for heterogeneous Heck reactions.²³ A range of reactions was studied using 3 mol % Pd/C with ethyl acrylate and different aryl iodides at 140 °C and yields were generally good. Ethyl cinnamate (R = H) was produced in 92 % yield after one hour and 95 % yield after twelve hours. Aryl bromides appeared slightly less effective and aryl triflates were completely unreactive under these conditions.



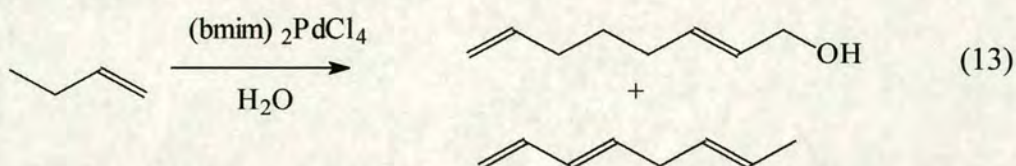
For conventional homogeneous Heck reactions the palladium catalyst deteriorates and palladium black is deposited out of the reaction and recycling is not generally possible. In this system, however, the Pd/C remains suspended in the ionic liquid, the products were decanted off and the catalyst system reused. A decrease in yield was

²³ H. Hagiwara, Y. Shimizu, T. Hoshi, T. Suzuki, M. Ando, K. Ohkubo and C. Yokoyama, *Tetrahedron Lett.*, 2001, **42**, 4349 – 4351.

observed after the second re-use but activity was fully restored by washing the ionic liquid layer with water. The authors preclude the possibility of the formation of an imidazolyldine-palladium carbenoid compound as the active species in this reaction because analysis of the filtered ionic liquid showed negligible concentrations of palladium.

1.9 Dimerisations.

Dullius *et al.* reported the use of a palladium compound to catalyse the reaction of 1,3-butadiene to the dimer (dimerisation) and trimer (telomerisation) in bmimBF_4 .²⁴



The reaction was successfully performed in bmimBF_4 , in the absence of carbon dioxide, with turnover frequencies of 118 h^{-1} , which increased to 204 h^{-1} with high-pressure carbon dioxide. Lower turnover frequencies were observed when bmimPF_6 was used. Carbon dioxide is commonly used to effect the hydrodimerisation of 1,3-butadiene, but the reasons for its effectiveness are not fully understood. It is proposed that carbon dioxide facilitates the formation of an HCO_3^- species from the water, which enhances the nucleophilic attack of the allyl-palladium species. The authors propose a similar effect of the ionic liquid, whereby the bmimBF_4 promotes the ionisation of water. This may explain the lower activity observed using bmimPF_6 as this species is significantly less miscible with water.

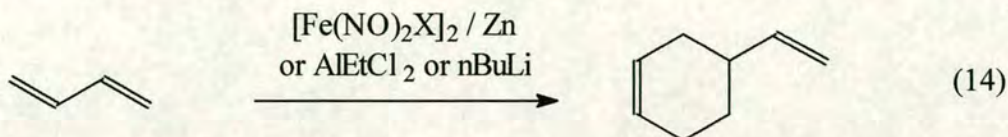
However, the coupling of aryl halides was successfully effected in bmimPF_6 by Howarth *et al.* using a nickel catalyst.²⁵ Zinc powder was used to reduce *bis*(triphenylphosphine)nickel(II) dichloride in the presence of triphenyl phosphine in bmimPF_6 , producing $[(\text{PPh}_3)_n\text{Ni}(0)]$ to which diaryl was added. Heating the solution at $80 \text{ }^\circ\text{C}$ for 48 hours was sufficient to produce a range of biaryls from the

²⁴ J. E. L. Dullius, P. A. Z. Suarez, S. Einloft, R. F. De Souza and J. Dupont, *Organometallics*, 1998, **17**, 815 – 819.

²⁵ J. Howarth, P. James and J. Dai, *Tetrahedron Lett.*, 2000, **41**, 10319 – 10321.

corresponding aryl iodides. Yields were comparable to the conventional dimethylformamide reaction, but the potential for recycling the catalyst system was demonstrated thereby indicating the advantage of the ionic liquid system.

The cyclodimerisation of 1,3-butadiene was effected in bmimPF_6 and bmimBF_4 using an iron-nitrosyl catalyst, prepared *in situ* by reduction of $[\text{Fe}(\text{NO})_2\text{Cl}]_2$.²⁶ Of the three reducing agents tested, metallic zinc gave the best conversion and selectivity.



The reaction proceeded with higher turnover frequencies (TOF) in bmimBF_4 than bmimPF_6 at 10 °C, but the trend was reversed at 50 °C. The conversion and TOF are higher than those obtained in toluene (94 %, 1404 h⁻¹ respectively in bmimPF_6 compared to 90 % and 253 h⁻¹ in toluene). The catalyst/ionic liquid system was recycled three times without any loss in activity.

1.10 Oligomerisations.

The oligomerisation reactions reported in the literature almost exclusively deal with the use of tetrachloroaluminate ionic liquids. In fact it is one of these reactions that now awaits licensing as the first commercial process utilising an ionic liquid. This has been developed by Olivier-Bourbigou *et al.*¹ at the French Petroleum Institute (IFP) and is a variation of the process for synthesising octene. This is a major feedstock for the production of phthalates and the conventional process used by the IFP produces 200 000 tonnes of octene a year.²⁷ Use of the ionic liquid allows recycling of the expensive nickel catalyst that is normally lost at the end of the reaction.

²⁶ R. A. Ligabue, J. Dupont, R. F. de Souza, *J. Molecular Cat. A: Chemical*, 2001, **169**, 11 – 17.

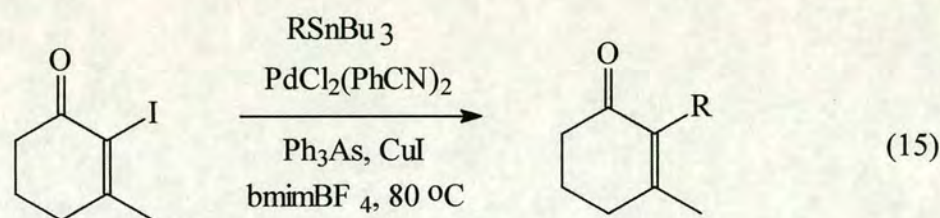
²⁷ D. Adam, *Nature*, 2000, **407**, 938 – 940.

The use of bmimPF_6 for oligomerisations has been investigated by Chen *et al.*²⁸ using the nickel catalyst (η^3 -methallyl)[bis(diphenylphosphanyl)methane-monoxide- κ^2 -P,O]nickel(II) hexafluoroantimonate. Dichloromethane is the best organic solvent for the oligomerisation of ethylene using this catalyst system but the activity was increased seven fold by changing this solvent to bmimPF_6 .

The palladium catalysed dimerisation of butadiene has also been observed to proceed with a substantial increase in activity when bmimPF_6 or bmimBF_4 is used in place of the tetrahydrofuran normally used.²⁹

1.11 Stille Coupling.

The Stille coupling is a popular form of transition-metal catalysed cross coupling reaction and is used in the preparation of aromatic carbonyl compounds, diaryls and polyenes.



Handy *et al.*³⁰ successfully performed the Stille coupling of α -iodoenone with phenyltributyltin ($\text{R} = \text{phenyl}$) in bmimBF_4 with yields improved on those observed using the traditional organic solvent, *N*-methylpyrrolidinone.

Using the same catalyst system the coupling of *p*-iodoanisole with phenyl tributyl tin effectively produced the diaryl compound in 82 % yield. The Stille coupling is often catalysed by palladium compounds, but the authors report that the use of a variety of palladium catalysts produced little or none of the desired product. By contrast, the coupling of bromobenzene with phenyl butyl tin produced biphenyl in poor yield with the tin catalyst, but in excellent yield with a palladium(0) catalyst. Both of these

²⁸ W. Chen, L. Xu, C. Chatterton and J. Xiao, *Chem. Commun.*, 1999, 1247 – 1248.

²⁹ S. M. Silva, P. A. Z. Suarez, R. F. de Souza and J. Dupont, *Polymer Bulletin*, 1998, 40, 401 – 405.

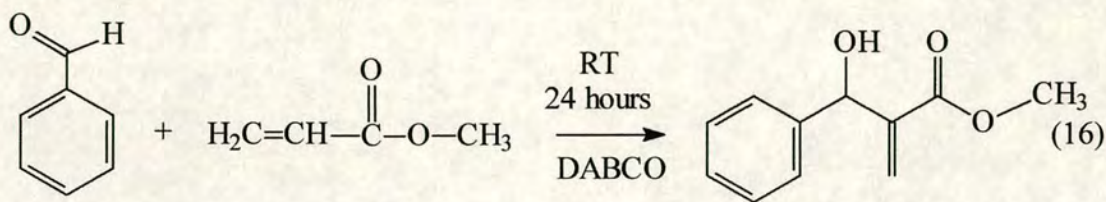
³⁰ S. T. Handy and X. Zhang, *Organic Letters*, 2001, 3, 2, 233 – 236.

catalyst systems were recycled five times, after extraction of the products with diethyl ether, with little loss in activity.

1.12 The Baylis-Hillman Reaction.

The Baylis-Hillman reaction allows the synthesis of highly functionalised compounds in a single step. However, it generally suffers from low yields and the need for high concentrations of catalysts, even when a solvent free system is used.

Rosa *et al.*³¹ reported the use of bmimBF₄ and bmimPF₆ for the condensation of benzaldehyde and methyl acrylate using 1,4-diazabicyclo[2,2,2]octane (DABCO) as the catalyst.

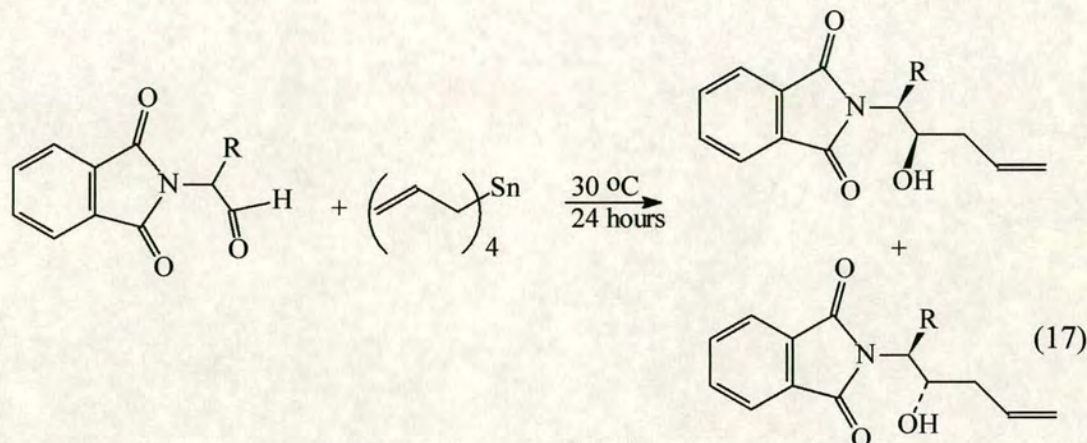


Using 100 mol % catalyst, the reaction proceeded 33.6 times faster in bmimPF₆ than in acetonitrile, the optimum organic solvent. This decreased to 11.1 times faster when the catalyst concentration was dropped to 20 mol %. With 100 mol % catalyst the reaction proceeded 14.1 times faster in bmimBF₄ than in acetonitrile. However, although the rates were excellent, the reported yields are only moderate - 65 % and 57 % for bmimPF₆ and bmimBF₄ respectively. A range of different reactions were studied in bmimPF₆ and in general yields were poor for aliphatic aldehydes (14 – 20 %) and moderate for aromatic aldehydes (39 – 72 %). However, once again the potential for recycling the catalyst/ionic liquid system was demonstrated. The products were extracted with diethyl ether and no drop in yield was observed after four runs.

³¹ J. N. Rosa, C. A. M. Afonso and A. G. Santos, *Tetrahedron*, 2001, **57**, 4189 – 4193.

1.13 Allylation.

Synthesis of *N*-protected homoallylic alcohols and allyl ketones has recently been reported using tetraallylstannane and Weinreb amides in *bmim*BF₄.³² The synthesis of homoallylic alcohols only proceeded with moderate yields after heating for five days at 50 °C. However, synthesis of the alcohols, which starts with the more reactive *N*-protected aminoaldehydes, proceeded with good to excellent yields.



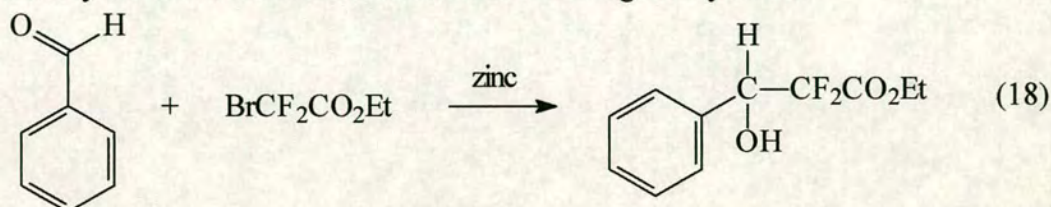
Reaction yields were good, ranging from 82 % ($R = \text{CH}_3$) to 45 % ($R = \text{PhCH}_2$) in *bmim*BF₄, but consistently lower than those in methanol (94 % for $R = \text{CH}_3$, 82 % for PhCH_2). Additionally, there was no advantageous effect of the use of the ionic liquid on the diastereoselectivity of the reaction. Thus, although the novel use of these reagents is an important result, the use of ionic liquids in this reaction presents no immediate advantage.

³² A. McClusky, J. Garner, D. J. Young and S. Caballero, *Tetrahedron Lett.*, 2000, **41**, 8147 – 8151.

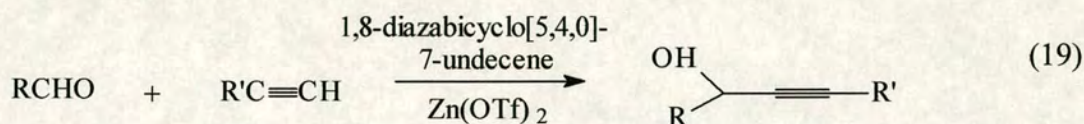
1.14 Reformatsky Reactions.

The use of the ionic liquids bmimPF₆ and bmimBF₄ in combination with zinc reagents was studied recently by Kitazume *et al.*³³ and yields at least as good as those with molecular solvents were achieved.

Addition of benzaldehyde to ethyl bromodifluoroacetate with zinc powder proceeded in bmimBF₄ and bmimPF₆, with yields of 61 % and 69 % respectively. The products were easily extracted from the reaction mixture using diethyl ether.



The applicability of zinc reagents in ionic liquids was further demonstrated by the preparation of propargylic alcohols using zinc trifluoromethanesulfonate.



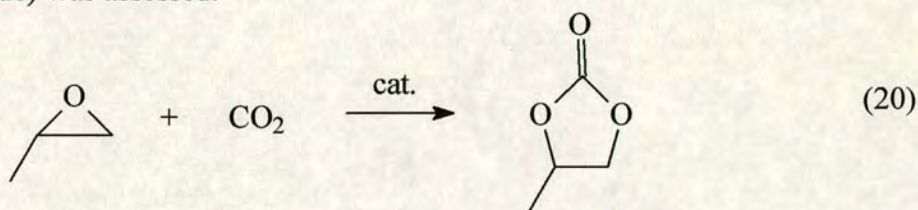
After 48 hours of stirring at room temperature moderate yields were obtained (i.e. for R = Ph, 59 % for bmimBF₄ and 35 % for bmimPF₆).

³³ T. Kitazume and K. Kasai, *Green Chemistry*, 2001, 3, 30 – 32.

1.15 Cycloaddition of Carbon Dioxide.

The addition of carbon dioxide to cyclic epoxides is an important reaction as the products - five-membered cyclic carbonates - are excellent aprotic solvents and are used as intermediates in the production of drugs and pesticides. However, the reaction generally proceeds at a low rate unless high temperatures or high pressures of carbon dioxide are used. A large range of catalysts for this reaction has been studied, including metal halides, MgO, Mg-Al mixed oxides and KI-ZnO.

The addition of carbon dioxide to propylene oxide was studied by Peng *et al.* and the effect of using a catalytic amount of ionic liquid (1.5 mmol ionic liquid in 100 mmol propylene oxide) was assessed.³⁴



BmimPF₆ showed low catalytic activity (11.3 % conversion of propylene carbonate), although this was greatly enhanced (to 45.3 %) by the addition of a small amount (0.2 mmol) of bmimCl. By contrast, bmimBF₄ showed good catalytic activity (80.2 % conversion) but this was only slightly improved (to 90.5 %) by the addition of bmimCl. The bmimBF₄ was recycled five times with only a slight drop in activity. 100 % selectivity for the desired reaction was assumed as no by-products were detected.

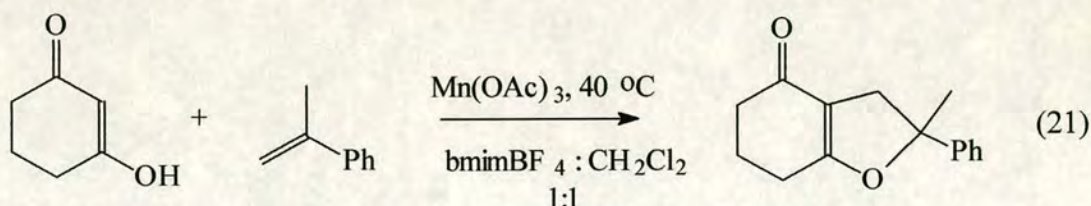
³⁴ J. Peng and Y. Deng, *New J. Chem.*, 2001, **25**, 639 – 641.

1.16 Radical Reactions.

The only report of a polymerisation reaction in bmimPF_6 was published in 2000 and involves a copper(I) radical reaction.³⁵ Transition metal mediated living radical polymerisation is important for the polymerisation of vinyl polymers, but large amounts of catalyst are often required, leading to product contamination.

Polymerisation of methyl methacrylate was effected using a suspension of CuBr in bmimPF_6 with ethyl-2-bromoisobutyrate and proceeded to 87 % conversion within 90 minutes at 70 °C, which is relatively fast compared to the reaction in toluene. The polymer was then collected with negligible copper contamination. This is the only reported living radical polymerisation reaction utilising ionic liquids.

The survival of radicals in ionic liquids was further demonstrated by Bar *et al.*³⁶ who used manganese acetate to mediate the synthesis of tetrahydrofuranone.

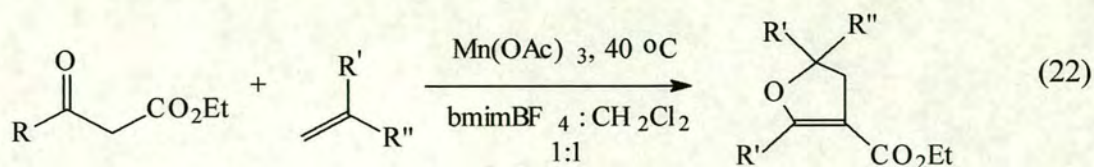


Low yields of the reaction were obtained when neat bmimBF_4 was used but these were increased to 50 % by using a mixture of bmimBF_4 and dichloromethane. In fact, only a catalytic amount of bmimBF_4 appears to be required as use of a 1:19 ratio of bmimBF_4 : dichloromethane gave a 45 % yield. It is also interesting to note that other solvents could be used, such as methanol, acetone or acetonitrile with yields between 27 % and 58 % and that even use of ethyl acetate, which is immiscible with bmimBF_4 , gave a 30 % yield.

Similar yields were obtained for the synthesis of dihydrofurans, further demonstrating the use of manganese acetate in bmimBF_4 .

³⁵ A. J. Carmichael, D. M. Haddleton, S. A. F. Bon and K. R. Seddon, *Chem. Commun.*, 2000, 1237 – 1238.

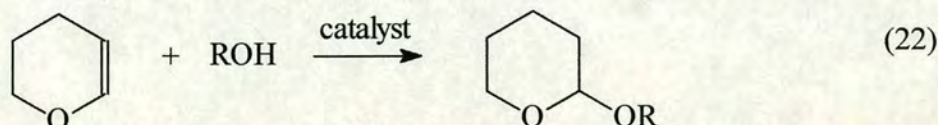
³⁶ G. Bar, A. F. Parsons and C. B. Thomas, *Chem. Commun.*, 2001, 1350 – 1351.



The yields of these reactions were similar or higher to those obtained using acetic acid, without any of the associated problems. When acetic acid is used separation of the products is difficult and often involves generating large quantities of aqueous waste. Using ionic liquids, however, manganese acetate was collected *via* precipitation by addition of more organic solvent and was then reoxidised back to manganese(III) by reaction with potassium permanganate. The bmimBF₄ was then reused with no loss in yield. However, complete removal of the manganese byproducts was more difficult when bmimPF₆ was used.

1.17 The Tetrahydropyranylation of Alcohols.

The tetrahydropyranylation of alcohols is an important reaction for the protection of hydroxyl groups and has been studied in bmimBF₄ and bmimPF₆ by Branco *et al.*³⁷



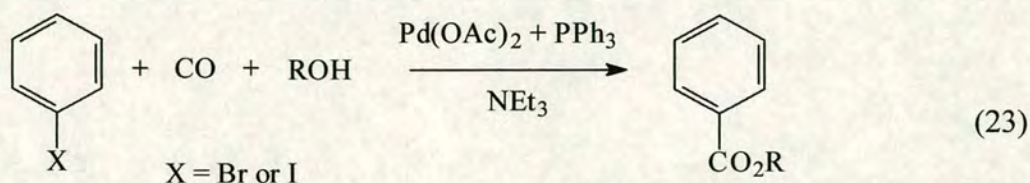
Using pyridinium *p*-toluenesulphonate as the catalyst, the reaction was slightly faster in bmimPF₆ than in dichloromethane, which is the organic solvent of choice, but much faster than in bmimBF₄ (relative rates 5.2 : 3.6 : 1). Similarly satisfactory yields were obtained using triphenylphosphine hydrobromide but results with *p*-toluene sulfonic acid were poor. The product was removed by extraction with diethyl ether and the ionic liquid was recycled at least 22 times without significant loss in activity.

³⁷ L. C. Branco and C. A. Afonso, *Tetrahedron*, 2001, **57**, 4405 – 4410.

1.18 Carbonylation of Aryl Halides.

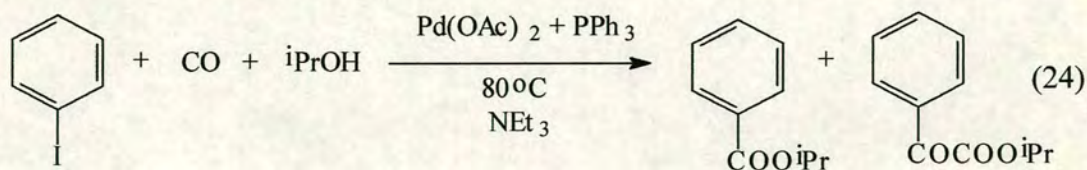
The first example of the palladium-catalysed carbonylation of an aryl halide in an ionic liquid was reported by Mizushima *et al.*³⁸ and the use of both bmimBF_4 and bmimPF_6 were investigated.

The reaction of methanol ($\text{R} = \text{CH}_3$) to form methyl benzoate proceeded with an 82 % yield in bmimBF_4 and with a 68 % yield in bmimPF_6 , compared to the 30 % yield in excess methanol.



The alkoxy carbonylation was studied using a variety of alcohols and all of them displayed higher performances in the ionic liquids. Even the carbonylation of bromobenzene using *tert*-butyl alcohol, which is normally relatively ineffective (7 % yield in excess *tert*-butyl alcohol) proceeds with 28 % yield in bmimBF_4 . The catalyst/ionic liquid system is reported to show good recyclability only when the molar ratio of PPh_3 to Pd(OAc)_2 used in the reaction is increased from four to twenty.

The double carbonylation of iodobenzene using isopropyl alcohol was also found to proceed more efficiently in the ionic liquids than in excess alcohol.



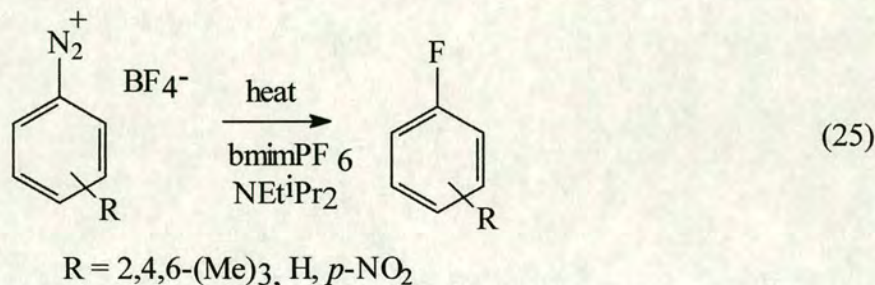
The conversion of iodobenzene was only 8 % in neat isopropanol but was 83 % and 100 % in bmimBF_4 and bmimPF_6 respectively. However, the single carbonylation

³⁸ E. Mizushima, T. Hayashi and M. Tanaka, *Green Chemistry*, 2001, 3, 76 – 79.

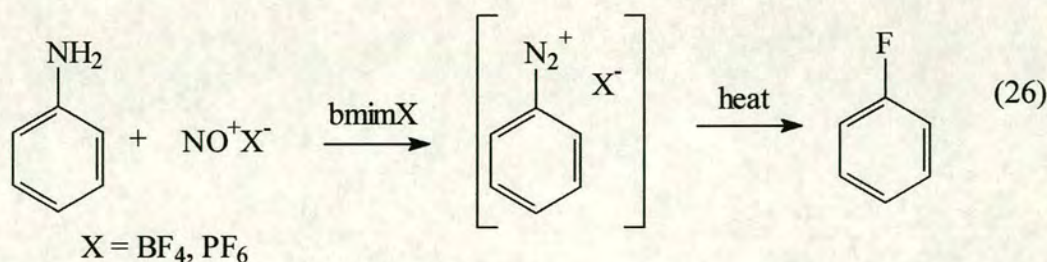
was accelerated to a greater extent than the double carbonylation and hence the selectivity for the doubly-carbonylated product decreased, particularly in bmimPF₆.

1.19 Fluorodediazoniatio.

Fluorodediazoniatio is a classical method for the replacement of a diazonium group with fluorine and is normally referred to as the Baltz-Schiemann reaction. Laali *et al.*³⁹ studied the application of bmimPF₆ and bmimBF₄ for both fluorodediazoniatio (18) and *in situ* diazotisation (19) reactions to synthesise a range of fluorinated aromatics. In most cases the diazonium cation was soluble in the ionic liquid and the products were isolated by ether extraction, hence this is not a biphasic reaction.



This reaction proceeded with 100% yield, at or below 110 °C, in bmimPF₆. The presence of the base was reported to prevent the formation of PF₅ and HF.



The *in situ* reaction also occurred in 100 % yield at 100 °C in both bmimBF₄ and bmimPF₆. This is a significant improvement over the traditional Baltz-Schieman reaction, which often suffers from variable yields depending on the substrate.

³⁹ K. K. Laali, V. J. Gettwert, *J. Fluorine Chem.*, 2001, **107**, 31 – 34.

1.20 Electrochemical Deposition.

The electrochemical uses for the tetrachloroaluminate ionic liquids have been much more thoroughly investigated than the potential electrochemical applications of bmimBF₄ or bmimPF₆. Recently, however, Endres *et al.* have reported the successful electrodeposition of a germanium film from bmimPF₆.⁴⁰ The electrodeposition of elemental semiconductors, such as germanium or silicon, from the tetrachloroaluminate salts is not possible because in acidic melts the aluminium is deposited before the desired semiconductor and in basic melts the chloride ions appear to prevent electrodeposition by complexing the material. However, germanium was successfully deposited onto a gold (111) surface by the electroreduction of germanium tetraiodide in bmimPF₆. This electrodeposition was observed using *in situ* STM and the films produced are reported to be approximately 13 – 16 nm thick.

⁴⁰ F. Endres and C. Schrod, *Physical Chemistry Chemical Physics*, 2000, **2**, 5517 – 5520, F. Endres, *Physical Chemistry Chemical Physics*, 2001, **3**, 3165 – 3174.

1.21 Enzymatic Catalysis.

There are only two examples of the use of ionic liquids for enzymatic catalysis published to date. Erbedinger *et al.*⁴¹ report the use of bmimPF₆ for the catalysed formation of Z-aspartame from carbobenzoxy-L-aspartate and L-phenylalanine methyl ester hydrochloride. Thermolysin was used to catalyse the reaction and the stability of this enzyme was found to be excellent. The rate of reaction in bmimPF₆ was comparable to that of the best organic solvent, ethyl acetate. It is interesting to note, however, that at low concentrations of thermolysin (3 mg mL⁻¹) the enzyme is soluble in the bmimPF₆, but no reaction is observed. It is only at higher enzyme concentrations that a suspension is produced and the reaction proceeds. The system was recycled by washing with water to dissolve the unreacted substrates. The subsequent drying of the ionic liquid under vacuum gave the product as a crystalline precipitate. Future work on this area is proposed, including the use of supercritical carbon dioxide to remove the products. The synthesis of polyesters using lipases in ionic liquids is also under investigation.

The second report on the use of ionic liquids for enzymatic catalysis was published by Cull *et al.*⁴² and involved the use of a bmimPF₆-water biphasic system as an alternative to the organic-water system. In these systems, the substrate is held in the organic phase thereby separating it from the biocatalyst to which it would be inhibitory or toxic at high concentrations. However, organic solvents themselves cause damage to the cell walls of the bacteria, in addition to problems with toxicity, volatility, flammability and potential explosion problems.

The water-bmimPF₆ system was studied as a medium for the conversion of 1,3-dicyanobenzene, first to 3-cyanobenzamide and then to 3-cyanobenzoic acid, using the *Rhodococcus* R312 biocatalyst. The activity of the catalyst in this system was found to be almost an order of magnitude larger than in the alternative toluene/water system. However, the initial rate of the biotransformation was slower in the ionic

⁴¹ M. Erbedinger, A. J. Mesiano and A. J. Russell, *Biotechnol. Prog.*, 2000, **16**, 6, 1129 – 1131.

⁴² S. G. Cull, J. D. Holbrey, V. Vargas-Mora, K. R. Seddon and G. J. Lye, *Biotechnology and Bioengineering*, 2000, **69**, 2, 227 – 233.

liquid system and this is shown to be a result of slower substrate mass transfer in this system.

1.22 Liquid-Liquid Extraction.

The advantageous properties of ionic liquids, such as their negligible volatility, the high solubilities of organic compounds and their miscibilities with a range of organic solvents has been greatly emphasised in the large number of reports into the potential uses of these systems. The ease of extraction of reaction products and subsequent recycling of the ionic liquid has also been highlighted and it is the combination of all of these properties that Huddleston *et al.* suggest make ionic liquids the ideal media for liquid-liquid extraction.⁴³ This separation technique usually employs an organic-aqueous combination, but use of an ionic liquid, in this case bmimPF₆, would reduce the need for organic solvents. The partition coefficient of bmimPF₆ for a variety of charged and uncharged aryl organic compounds such as aniline, toluene, chlorobenzene and benzoic acid is approximately equivalent to those of octan-1-ol. However, the possibility of removing the products by evaporation is an additional advantage of the ionic liquid system. It is also noted that the distribution of a species between the bmimPF₆ and water phase depends on its charge. This is an important observation as it allows for the possibility of using conventional extraction technology, which often utilises changes in pH to extract the desired product.

The potential of bmimPF₆ as a medium for liquid-liquid extraction in multiphase bioprocess operations was investigated by Cull *et al.*⁴² Liquid-liquid extraction is widely used for the recovery and purification of antibiotics, such as penicillin and erythromycin, and actually represents the largest consumption of organic solvents in multiphase processes. Generally the solvent used must display equilibrium partition coefficients, $K > 10$. The extraction of erythromycin using both butyl acetate and bmimPF₆ was studied and extraction coefficients of up to 20 – 25 could be achieved for both systems. It is interesting to note from these studies that equilibrium partition

⁴³ J. G. Huddleston, H. D. Willauer, R. P. Swatloski, A. E. Visser and R. D. Rogers, *Chem. Commun.*, 1998, 1765 – 1766.

coefficient falls dramatically at values of pH >10 in bmimPF₆, although no explanation is given for this phenomenon.

1.23 Stationary Phases in Gas Chromatography.

BmimPF₆ can be coated onto fused silica capillaries and therefore can be used as the stationary phase in gas chromatography. Armstrong *et al.*⁴⁴ studied the behaviour of bmimPF₆ and bmimCl in this application and observed some interesting results that suggest that these media could be useful in the field of separation science. The ionic liquids appear to have dual behaviour in this situation. Analytes that are relatively non-polar, non-acidic or basic, such as butyl acetate, *n*-heptanol, *p*-dichlorobenzene or *n*-dodecane, separated in the same way as observed using conventional nonpolar stationary phases and were spatially resolved. However, polar analytes and molecules that are proton donors, such as weak acids, were strongly retained and in some cases – phenols, diols and carboxylic acids – did not come off at all under the same conditions.

The nature of the anion of the ionic liquid also appears to have an effect of the separation properties. Compounds with no good proton donating or accepting groups, such as aliphatics and aromatics, esters, aldehydes and ketones, were more strongly retained on bmimPF₆, whereas analytes with proton-donating groups such as alcohols, phenols, diols and carboxylic acids were retained more strongly on bmimCl. The behaviour of the ionic liquid as media for gas chromatography is thus suggested as a tool for the analysis of their physical properties. An indication of the proton donor or acceptor capabilities of the ionic liquids can be obtained, in addition to the extent of dipolar interactions within these species.

⁴⁴ D. W. Armstrong, L. He and Y. Liu, *Anal. Chem.*, 1999, **71**, 3873 – 3876.

1.24 Use with Supercritical Carbon Dioxide.

As explained above, the majority of the research undertaken in assessing the potential uses of ionic liquids has centred on their use in biphasic catalysis. Most of the synthetic reactions detailed above utilise this technique in combination with an organic solvent. However, considerable work has recently been focused on the use of ionic liquids in combination with supercritical carbon dioxide (scCO₂).²⁷ Use of this new system for hydrogenation reactions has been investigated and this is reviewed in chapter five. Blanchard *et al.* has assessed the behaviour of a number of ionic liquids in combination with scCO₂ in detail and her results highlight the advantageous properties of this combination.⁴⁵ The miscibility of bmimPF₆ with scCO₂, as for other ionic liquids, is ideal for biphasic reactions because the CO₂ shows high solubility in the ionic liquid but the ionic liquid is effectively insoluble in the scCO₂. This allows the upper scCO₂ layer to be removed with no ionic liquid impurities and thus the product of the reaction can be obtained cleanly. The solubility of CO₂ increases dramatically with pressure up to 0.72 mole fraction CO₂ at 93 bar and 40 °C. As for conventional solvent systems, this solubility decreases with temperature but the temperature dependence is actually unusually small. The preservation of two phases, even at high pressures, is also extremely unusual for a normal liquid-scCO₂ system. However, the authors point out that the water content of the ionic liquid is of extreme importance when dictating the phase behaviour as water saturation results in a decrease in CO₂ solubility from 0.54 mole fraction to 0.13 mole fraction at 57 bar. The formation of carbonic acid by reaction of CO₂ and water can also be a problem with wet ionic liquids and can result in a significant decrease in pH.

The use of bmimPF₆ for the hydroformylation of alkenes using the bmimPF₆/scCO₂ system was reported recently and illustrates the potential of this biphasic system.⁴⁶ The hydroformylation of non-1-ene using [Ph₂PC₆H₄SO₃][bmim] with [Rh₂(OAc)₄] as the catalyst precursor was effected using a constant flow reactor for more than twelve runs with negligible drop in activity, no rhodium leaching and no catalyst oxidation. The alkene, CO₂, H₂ and CO were fed into the apparatus through different

⁴⁵ L. A. Blanchard, Z. Gu and J. F. Brennecke, *J. Phys. Chem. B*, 2001, **105**, 2437 – 2444.

⁴⁶ M. F. Sellin, P. B. Webb and D. J. Cole-Hamilton, *Chem. Commun.*, 2001, 781 – 782.

pipes and combined before being passed through the ionic liquid. These were then removed, still in the supercritical phase, before the pressure was reduced allowing the CO₂ to form a gas and permitting product recovery. This new reaction system allows the use of a rhodium catalyst for hydroformylation reactions. These are high activity catalysts, but are usually overlooked in favour of cobalt catalysts because a combination of the low thermal stability of the catalyst and low volatility of the aldehyde makes product separation difficult.

1.25 Conclusions.

For the ionic liquids bmimBF_4 and bmimPF_6 to be utilised in commercial processes the advantages of this new system have to be demonstrated. The investigations currently underway into the uses of these ionic liquids predominantly focus on their use in biphasic catalysis. Here, their immiscibility with many organic compounds can be fully utilised allowing for the easy separation of reaction products. The potential for recycling the catalyst/ionic liquid system has been well demonstrated, making these environmentally attractive solvents. However, for ionic liquids to replace conventional organic solvents the activity of the catalyst must be at least comparable to the activity achieved in molecular solvents.

Use of supercritical carbon dioxide in combination with ionic liquids is receiving increasing interest and the development of a continuous flow system makes this combination even more attractive. However, the energy efficiency of the process may prove to be a problem as the requirement for high pressures is both expensive and requires specialised equipment. The first commercial applications of ionic liquids will probably be in processes where a change in solvent system does not require significant changes to the current apparatus.

It is evident from the extent and nature of the reports into the uses of bmimPF_6 and bmimBF_4 that interest in these ionic liquids is intense. However, it is also evident that there are still many unanswered questions relating to the behaviour of these species. Many of the reactions studied result in products in unexpected yields or isomeric ratios, or with significantly different results depending on the ionic liquid used. Every unexpected result reported highlights our lack of understanding of these species. The relationship between the structure of the ionic liquids and the physical properties that they display is of particular importance as the ultimate goal is to be able to design ionic liquids with the specific properties required for each application. However, this idea of “designer solvents” is still far from becoming reality and significant investigations into the nature of these species and their physico-chemical properties are required. It is with the relationship between the structure and physical properties of these imidazolium-based ionic liquids that this investigation is based.

2 Experimental Techniques.

2.1 Manipulation of Air- or Moisture-Sensitive Compounds.

The ionic liquids synthesised and used in this investigation are not air-sensitive but do absorb moisture from the atmosphere. The water content of these species, even those that are immiscible with water, can be considerable; 12 wt % for 1-butyl-3-methyl imidazolium hexafluorophosphate and 25 wt % for 1-butyl-3-methyl imidazolium tetrafluoroborate.¹ Even small traces of water can have significant effects on the physical properties, such as viscosity and electrochemical behaviour, so all materials were handled under nitrogen and treated as air-sensitive. This was done using standard Schlenk line techniques and a Vacuum-Atmospheres dry box possessing a vacuum port for entry/withdrawal of equipment and samples. The nitrogen was supplied from cylinders of dry and oxygen-free nitrogen and any traces of oxygen and water were removed from the N₂ gas stream by re-circulating through a reservoir containing copper(I) oxide and 4A molecular sieves. The ionic liquids were dried under vacuum on a high vacuum line where the pressure was reduced to 10⁻² Torr[†] using an oil-filled rotary pump and backed up by a mercury diffusion pump which reduced the pressure to *ca.* 10⁻⁴ Torr. The ionic liquids were stored over 4A molecular sieves that had been dried by heating to 200°C on the high vacuum line.

¹ U. Schröder, J. D. Wadhawan, R. G. Compton, F. Marken, P. A. Z. Suarez, C. S. Consorti, R. F. de Souza and J. Dupont, *New J. Chem.*, 2000, **12**, 1009 – 1015.

[†] 1 Torr = 1 mBar = 133Pa.

The synthetic reactions that were performed using the ionic liquids were also carried out under nitrogen. The ionic liquids were transferred between vessels under nitrogen using a cannula. The high viscosity of these materials meant that gentle heating of the ionic liquids was often necessary to decrease the viscosity. All of the solvents used were dried before use either by distillation from CaH_2 or P_2O_5 followed by storage over molecular sieves.

Unless otherwise stated, chemicals were used as supplied from Aldrich, Fischer-Acros, BDH or Fluorochem.

2.2 Analytical Techniques - Liquid Samples.

2.2.1 NMR Spectroscopy.

Nuclear magnetic resonance spectroscopy was used within this investigation both as a method of determining the purity of the ionic liquids and for the characterisation of reaction products. This analysis technique is primarily useful in this context as a method of identifying any organic impurities within the ionic liquid, which may be present as a result of incomplete reaction during the synthesis of the ionic liquid.

It has been reported that ^1H NMR spectroscopy can be used as a method of assessing the extent of hydrogen bonding within ionic liquids,² particularly with regard to the shift of the H2 on the imidazole ring, but this has since been challenged.³ It is possible to obtain NMR spectra of neat ionic liquids, but signals are generally broad due to the high concentration and viscosity of the samples.

NMR spectra were recorded on Bruker AC250 and AC200 FT spectrometers, either as solutions in CDCl_3 , CD_3OD or d_6 -dmsO or as the neat ionic liquid. Chemical shifts are referenced against $[(\text{CH}_3)_4\text{Si}]$ or the residual solvent protons where present. Spectra were recorded by the departmental service.

2.2.2 Infrared Spectroscopy.

Infrared spectroscopy was primarily used in this investigation for confirming the presence of a particular anion, such as BF_4^- or PF_6^- , within the ionic liquid, thereby indicating the successful metathesis of the chloride ionic liquid. It has been suggested that the positions of the peaks attributed to the aromatic C-H stretching of the imidazolium ring can give an indication of the extent of hydrogen bonding within the ionic liquid,² but these interactions are now considered too weak to be observed unambiguously in the IR spectrum.³ However, infrared spectroscopy can be used as an analytical tool for identifying any water present in the ionic liquids, which produces OH stretching absorbencies in the $3500 - 3800 \text{ cm}^{-1}$ region of the spectrum.

² P. A. Z. Suarez, S. Einloft, J. E. L. Dullius, R. F. de Souza and J. Dupont, *J. Chim. Phys.*, 1998, **95**, 1626 - 1639.

³ J. Holbrey and K. R. Seddon, *J. Chem. Soc., Dalton Trans.*, 1999, 2133 - 2139.

The infra-red spectra of the compounds were obtained using a Perkin-Elmer Paragon 1000 FT-IR Spectrometer, either by preparation of a KBr disk, a Nujol mull or from the neat sample.

2.2.3 Mass Spectrometry.

Mass spectrometry was predominantly used in this investigation for the identification of reaction products and for determining the success of any attempts to substitute the cation of the ionic liquids.

This analytical tool is of limited use in the analysis of ionic liquids, although it has the advantage that it can be used for both solid and liquid samples, and was primarily used to confirm the presence of the desired cation by positive ion mass spectrometry. The anions used in this investigation were too small to be detected by negative ion mass spectrometry. Analysis was predominantly performed using the “soft” ionisation technique, Fast Atom Bombardment (FAB) where xenon atoms bombard the sample. The disadvantage of this technique is that the sample is incorporated into a matrix, which can react with the sample. This was found to be a particular problem for the phenyl-substituted imidazolium ionic liquids. Electron Impact (EI) is a harsher method of obtaining ions from the sample since a high-energy electron beam is used, but this technique does not require the use of a matrix.

Electron impact mass spectrometry was carried out on a Finnigan MAT 4600 quadrupole spectrometer or a Kratos MS50TC. Fast atom bombardment mass spectrometry was carried out using a Kratos MS50TC, in a NOBA or thioglycerol matrix. Analysis was carried out by the departmental service.

2.2.4 Elemental Analysis.

This is a particularly useful technique for determining the purity of the ionic liquids under study and can be used for both liquids and solids. Values for the carbon, hydrogen and nitrogen content are obtained and the presence of any impurities is reflected in these figures. The presence of water in the samples results in an increase in the hydrogen content and a corresponding decrease in the carbon and nitrogen

content. In addition, it is possible to perform the technique under nitrogen, allowing accurate analysis of the hygroscopic ionic liquids. The moisture sensitive samples were analysed by sealing samples into pre-weighed aluminium ampoules under nitrogen using the nitrogen dry box.

Elemental analysis was carried out by the departmental service using a Perkin Elmer 2400 CHN Elemental Analyser.

2.2.5 Viscosity Measurements.

The viscosities of the ionic liquids were measured using a Haake VT 550 cone and plate viscometer at the Avecia laboratories in Grangemouth. Viscosity, η , is a measure of the internal resistance that a liquid offers to the motion of different parts of the liquid. Viscosity can be either Newtonian or non-Newtonian. The viscosity is termed Newtonian if, when a liquid is put between two parallel plates, the shearing force per unit area, σ , is proportional to the velocity gradient between the plates, D , such that $\sigma = \eta D$.

Non-Newtonian behaviour generally occurs in concentrated solutions or dispersions, particularly when the particles are asymmetric or aggregated and there is the formation of a structure throughout the system. The ionic liquids studied were treated as Newtonian and the viscosity results obtained were consistent with this assumption. There are two primary methods for the measurement of viscosity, either using capillary flow methods or rotational methods.⁴ The viscosity of the ionic liquids was measured using a rotational method with a cone and plate viscometer. In this technique the liquid is placed between a cone and a plate and the cone is rotated at increasing speeds, thereby increasing the shear rate. The maximum shear rate used depended on the viscosity of the ionic liquids under study. The maximum shear rate used, for the highest temperatures and least viscous ionic liquids, was 3000 s^{-1} . The shear rate was increased from zero to the maximum value and then back to zero. The viscosity of the ionic liquids remained effectively constant throughout the measurements indicating Newtonian behaviour. If the measurement of the viscosity had caused a change in the internal structure of the ionic liquid, the viscosity would

have been different between the end and the beginning. The temperature of the apparatus was controlled using a water and glycol bath. This mixture was circulated through pipes within the apparatus to maintain the temperature of the ionic liquid.

A plot of shear rate against viscosity was produced for each ionic liquid at each temperature, an example of which is shown in Figure 2.1. The viscosity shows a large deviation at low shear rate just as the cone starts to rotate and the system has to reach equilibrium. The standard deviation of these plots was used as an indication of the error margin within these experiments and was less than 2% for all the ionic liquids studied, which is good accuracy for this type of measurement. The viscosity was taken as the intercept of the line with the y-axis.

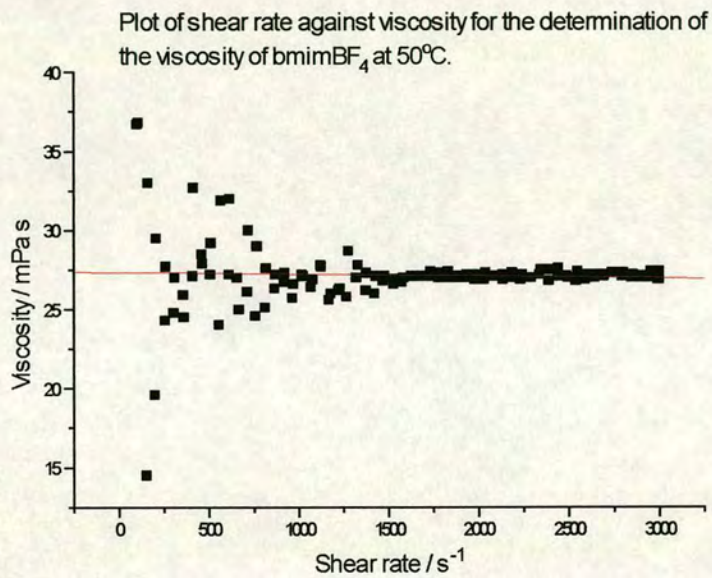


Figure 2.1. Measurement of the viscosity of bmimBF₄ at 50 °C.

2.2.6 Cyclic Voltammetry.

This is a valuable technique for identification of any water or electroactive impurities within the ionic liquids. The cyclic voltammograms were recorded using platinum wire for the reference electrode, platinum foil for the working electrode and platinum gauze for the counter electrode. The measurements were performed under nitrogen, using a water bath to melt the solid ionic liquids where necessary. The

⁴ D. J. Shaw, *Colloid and Surface Chemistry*, 4th Ed. Butterworth and Heinman.

voltammograms were recorded using Visual Designer on the PC *via* a portable potentiostat.

2.2.7 AC Impedance Spectroscopy.

This technique and its application to ionic liquids is discussed in detail in Chapter 7. The ionic liquids under study were contained in a Schlenk tube under a constant flow of nitrogen. The temperature of the system was controlled by insertion into a temperature controlled water bath, with an accuracy of ± 0.05 °C. AC Impedance spectroscopy was then performed using a Sycopel Scientific Ltd. TFA2000A a.c. impedance spectrometer *via* a Voltech TFA2000 frequency response analyser. The data was collected using a 386MHz Toshiba T1900 laptop computer using the TFA2000A control software. The data was saved as an ASCII file that could then be imported into MS Excel and Microcal Origin for further analysis.

2.2.8 Optical Activity.

The presence of a chiral centre within an enantiomerically pure compound was determined by its ability to rotate plane-polarised light, i.e. light with vibrations only in one plane, by analysis using a polarimeter. The amount of rotation depends on the concentration of the sample and the length of sample that the light is passed through so compounds were compared by calculation of their specific rotation, $[\alpha]$, given by:

$$[\alpha] = \frac{\alpha}{l + d} \quad (1)$$

where α is the observed rotation (degrees), l is the length of the sample (dm) and d is the concentration or density of the sample (g dm^{-3}).

Determination of the optical activity of the compounds was performed using a polarimeter from Optical Activity Ltd. using light of wavelength 5893 Å. All samples were dissolved in deionised water and contained within a cell of length 1 dm. The polarimeter was calibrated using deionised water before each measurement.

2.3 Analytical Techniques - Solid Samples.

2.3.1 Differential Thermal Analysis.

Differential Thermal Analysis (DTA) is the most widely used method of thermal analysis and is used to give information on the response of a sample to a specific temperature range, thus allowing determination of melting points, phase changes and decomposition temperatures as well as any enthalpy changes. The procedure simply involves the heating of a sample and a reference material over a chosen temperature range. The reference and sample material are placed in identical metal holders inside a furnace and the temperature of each recorded. The temperatures of the two samples rise identically with the heating of the furnace until an endothermic event, such as melting or a phase change occurs. At this point the sample temperature (T_s) lags behind that of the reference material (T_r) and the temperature difference (ΔT) is noted. This is plotted against the temperature of the reference material, producing a classic DTA curve as shown in Figure 2.2.

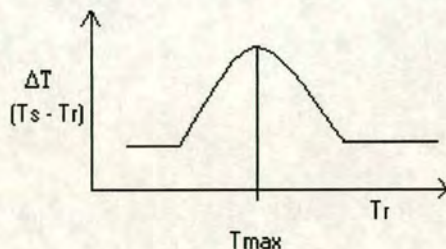


Figure 2.2. A classical Differential Thermal Analysis curve.

ΔT is arbitrarily defined so the direction chosen for an endothermic or exothermic change should be noted.

The reference sample used for the analysis of the ionic liquids was alumina, Al_2O_3 . This is an ideal reference material as it undergoes no phase changes over the temperature range being studied and does not react with the holder or thermocouple. The melting point of the sample can be determined from the DTA curve by extrapolation of the steepest part of the curve to the baseline, shown in Figure 2.3.

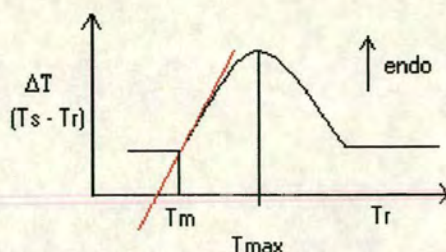


Figure 2.3. Determination of the melting point through analysis of the DTA curve.

For pure substances, this curve is generally very sharp, but for the ionic liquids studied the curves recorded were relatively broad. An example of a DTA curve obtained from the analysis of the ionic liquids is shown in Figure 2.4. The height of the curve obtained was strongly dependent on heating rate, which was kept constant throughout.

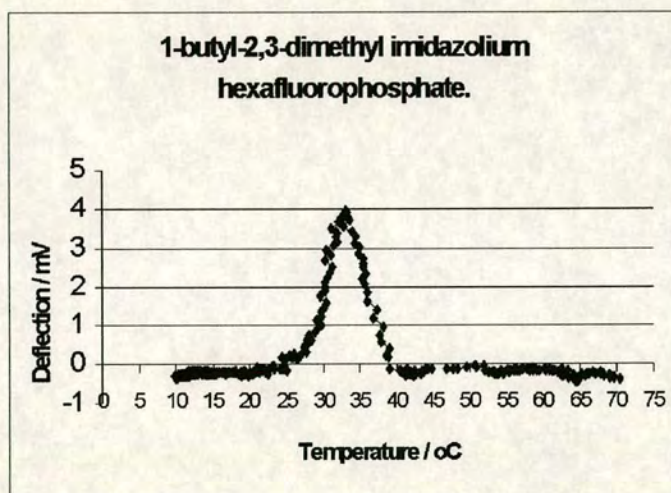


Figure 2.4. The DTA curve obtained for 1-butyl-2,3-dimethyl imidazolium hexafluorophosphate.

The differential thermal analysis equipment was calibrated using ammonium nitrate. This is known to undergo phase transitions at 39.9, 76 and 116.7 °C and is an ideal reference material for calibration of the ionic liquid measurements as the observed phase transitions lie within the temperature range used for study of the ionic liquids. Differential Thermal Analysis was performed using a Stanton Redcroft, model DTA 673-4. The electronic output of the DTA was interpreted by a PC running a

programme written within the university by Dr R. Brown using Q-BASIC. The samples were held in platinum crucibles and analysed under nitrogen.

Melting points not measured by differential thermal analysis were measured using a Gallenkamp melting point apparatus.

2.3.2 X-ray Crystallography.

X-ray crystallography is the most powerful method available for the structural analysis of solids. However, analysis of ionic liquids by this technique has been significantly hampered by the requirement of a single crystal of the material. As explained in Chapter 8, this is a particular problem for the butyl-substituted imidazolium ionic liquids featured in this investigation.

During x-ray crystallography, a single crystal is bombarded by radiation of a fixed wavelength, in this case either Cu-K α or Mo-K α . This interacts with electrons within the crystal and is diffracted. The diffracted radiation is detected and can be transformed using Fourier transformation techniques to give a map of the electron density within the sample. Thus, a map of the atom positions within the sample is produced and accurate geometrical information can be obtained. One common problem encountered using x-ray crystallography is the precise location of hydrogen atoms. This is because they contribute relatively little to the scattering of the x-ray beam, which is dependent on the electron density of the atom. This is normally a particular problem for hydrogen atoms in materials containing heavy atoms, such as metals, that diffract strongly. The hydrogen atoms within the crystal structures of the ionic liquids were placed geometrically. The solution of the structure was performed using computer programs SHELXTL or SIR92. The data collection, solution and refinement conditions for each structure are given in the Appendix.

2.3.3 Powder Diffraction.

X-ray powder diffraction analysis is a useful technique for the analysis of solid materials that do not form single crystals and can be used to gain information on the cell dimensions and symmetry of the compound. The x-rays are scanned across the powder sample from an angle of 10° to 70° and each crystallite within the powder diffracts the beam. The crystallites are randomly orientated within the powder, but each reflection has its own Bragg angle and so the combination of all the reflections results in cones of reflection. Thus, an angle and intensity describe each reflection. The collection of the angle and intensity for each reflection displayed by the crystals within the sample gives the powder diffraction spectra. This can be used as a “fingerprint” of a material and can give structural information, such as particle size, or help identify unknown materials. The powder diffraction patterns were collected using a Philips Diffractometer over a 2θ range of $10 - 70^\circ$ using copper K_α radiation. The data was collected using PC-APD and PC-Identify Philips software and was converted to MS Excel for further analysis. The samples were all thoroughly ground to ensure a random distribution of crystals and were mounted on aluminium slides.

3 Room Temperature Ionic Liquids.

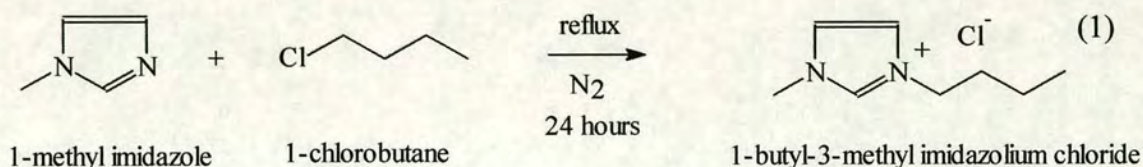
3.1 Introduction

The ionic liquids based on the 1-butyl-3-methyl imidazolium cation have been identified as air- and water-stable species suitable for a number of synthetic reactions, as outlined in Chapter 1. The original impetus behind the work detailed here was to explore the potential of these ionic liquids as media for a range of previously uninvestigated reactions. This chapter outlines the synthetic procedures for each of the room temperature ionic liquids studied, including those described in the literature and those developed in the laboratory, and some physical properties of each species. More details of the investigations into the relationship between the structures and properties of these ionic liquids are given in Chapters 7 and 8.

3.2 1-butyl-3-methyl imidazolium chloride.

1-butyl-3-methyl imidazolium chloride is commonly used as the precursor for the synthesis of other ionic liquids with alternative anions. As an ionic liquid it is not considered a useful medium for synthetic reactions as it is extremely hygroscopic and absorbs moisture from the air sufficiently quickly to turn it from a crystalline solid at room temperature to a colourless liquid within seconds. The water can be subsequently removed by drying under vacuum, producing the solid once more, but this extreme moisture sensitivity makes the compound difficult to manipulate.

The chloride salt was prepared by heating a neat solution of 1-chlorobutane and 1-methyl imidazole under nitrogen for 24 hours. A slight excess of 1-chlorobutane was used to ensure the reaction proceeded to completion and the unreacted 1-chlorobutane was removed under vacuum at the end of the reaction.



This synthetic route is unchanged from that first described by Wilkes *et al.*¹ The crude product was then recrystallised from acetonitrile/ethyl acetate or purified by washing with ethyl acetate.²

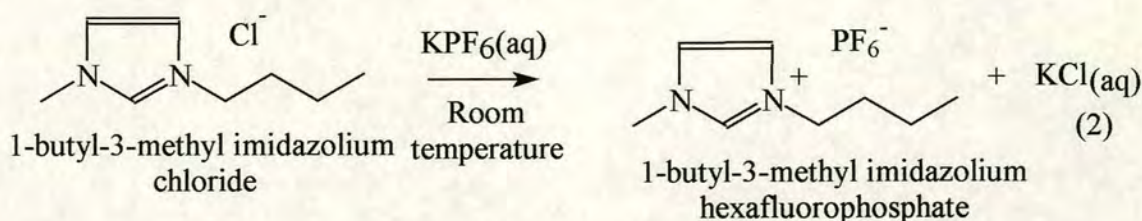
¹ J. S. Wilkes, J. A. Levisky, R. A. Wilson and C. L. Hussey, *Inorg. Chem.*, 1982, **21**, 1263 – 1264.

² J. G. Huddleston, H. D. Willauer, R. P. Swatloski, A. E. Visser and R. D. Rogers, *Chem. Commun.*, 1998, 1765 – 1766.

3.3 1-butyl-3-methyl imidazolium hexafluorophosphate.

1-butyl-3-methyl imidazolium hexafluorophosphate was prepared by metathesis from the chloride salt. There are a number of different synthetic methods for this metathesis reported in the literature. The original report appeared in 1996 and used an acetone solution of bmimCl and sodium hexafluorophosphate.³ Stirring the solution for 24h at room temperature is reported to produce the product in 91% yield. The use of sodium hexafluorophosphate has more recently been replaced by the use of aqueous hexafluorophosphoric acid.^{2,4} Although the use of this reagent is advantageous in the fact that the synthesis is performed in water, hence removing the need for organic solvents, it is worth noting the unpleasant nature of hexafluorophosphoric acid, which is hazardous, corrosive and toxic.⁵ Thermal decomposition of this compound can also result in the evolution of toxic fumes of phosphorous oxide and/or phosphine and as the addition of this acid to bmimCl causes a highly exothermic reaction this is a serious potential hazard.

It was proposed that the advantages of an aqueous synthesis could be maintained without the use of such hazardous materials. The hexafluorophosphate ionic liquid is ideally suited to a water-based synthesis as it is hydrophobic and thus forms a separate layer with water. This allows the product to be easily separated from the reaction mixture by decantation. This unusual property was utilised to develop a water-based synthesis utilising the non-hazardous potassium hexafluorophosphate.



³ P. A. Z. Suarez, J. E. L. Dullius, S. Einloft, R. F. De Souza and J. Dupont, *Polyhedron*, 1996, **15**, 7, 1217 – 1219.

⁴ C. M. Godon, J. D. Holbrey, A. R. Kennedy and K. R. Seddon, *J. Mat. Chem.*, 1998, **8**, 2627 – 2636.

⁵ *The Sigma-Aldrich Library of Chemical Safety Data*, Edition II, Vol 1. Ed. R. E. Lenga.

The 1-butyl-3-methyl imidazolium chloride was added as a melt to an aqueous solution of potassium hexafluorophosphate in a separating funnel. This immediately produced the bmimPF₆ as a lower layer that could be drained off leaving the water containing the potassium chloride by-product. The ionic liquid was then cleaned by washing with water and drying under vacuum.

Reports of the measurement of the physical properties of 1-butyl-3-methyl imidazolium hexafluorophosphate are fairly common in the literature. On the first reported synthesis of this species the melting point is given as -61°C .³ The ionic liquid is a glass below this temperature, which probably accounts for the lack of any crystal structure data for this compound.

The majority of the early investigations into the tetrachloroaluminate ionic liquids centred on their use in electrochemistry so it is probably unsurprising that the first measurements of the physical properties of bmimPF₆ that appeared in the literature were concerned with the measurement of the electrochemical window of this compound.⁶ The electrochemical window of a substance is defined as the difference between the anodic and cathodic decomposition potentials, and for this ionic liquid, as for the tetrachloroaluminate species studied previously, it was found to be relatively large.

The cathodic and anodic limits were found to depend slightly on the electrodes used, as summarised in Table 3.1. Platinum wire was used as the reference electrode in each case.

Electrode	Anodic limit / V	Cathodic limit / V
Tungsten RDE.	>5.00	-2.10
Vitreous carbon RDE	3.85	-2.50
Gold RDE	3.45	-2.50
Platinum RDE	3.40	-2.30
Platinum ume.	3.00	-2.00

Table 3.1 Electrochemical window of bmimPF₆ as measured by Suarez *et al.* RDE = rotating disc electrode. Ume = ultramicroelectrode.

Suarez *et al.* did not analyse the decomposition products of the bmimPF₆ at the solvent limits, but suggested the formation of PF₅ and F₂.⁶

Cyclic voltametry was used to assess the purity of the bmimPF₆ synthesised using the new aqueous route and again a large electrochemical window was observed. Platinum wire was used for the reference electrode, platinum foil for the working electrode and platinum gauze was used as the counter electrode. The cyclic voltammogram obtained is shown in Figure 3.1.

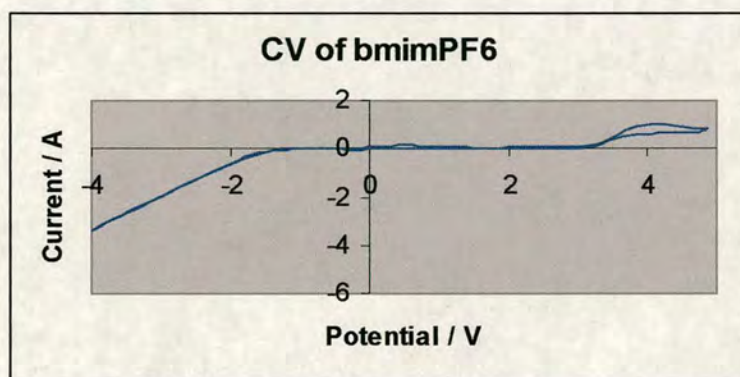


Figure 3.1. Cyclic voltammogram of 1-butyl-3-methyl imidazolium hexafluorophosphate.

The anodic and cathodic potentials were measured as +3.2 V and -1.6 V respectively. The difference in these measurements with those measured by Suarez *et al.* is caused by the difference in working and counter electrode. The absence of any peaks between the cathodic and anodic decomposition potentials indicates that the ionic liquid does not contain any electroactive impurities. The voltammogram also indicates that the species is dry, as absorption of water results in a dramatic decrease in the electrochemical window.⁷

⁶ P. A. Z. Suarez, V. M. Selbach, J. E. L. Dullius, S. Einloft, C. M. S. Piatnick, D. S. Azambuja, R. F. de Souza and J. Dupont, *Electrochimica Acta*, 1997, **42**, 16, 2533 – 2535.

⁷ U. Schroder, J. D. Wadhawan, R. G. Compton, F. Marken, P. A. Z Suarez, C. S. Consorti, R. F. de Souza and J. Dupont, *New J. Chem.*, 2000, **12**, 1009 – 1015.

Following their investigation into the electrochemical behaviour of 1-butyl-3-methylimidazolium hexafluorophosphate, Suarez *et al.* went on to study the IR, NMR, density, viscosity and conductivity of this ionic liquid.⁸

The observation of aromatic C-H stretching frequencies between 3100 and 3200 cm^{-1} in the infrared spectrum is reported to indicate the presence of hydrogen bonding in the liquid. However, this is strongly denied by Holbrey *et al.* who argue such interactions between the cation and anion are too weak to be seen by infrared spectroscopy.⁹

The glass transition temperature, viscosity and density of bmimPF₆ were measured by Suarez *et al.* and are given in Table 3.2.

Tg / K	η_{30} / Poises	ρ_{30} / gcm^{-3}
212	3.12	1.37

Table 3.2. Glass transition temperature, Tg, viscosity, η (30°C) and density, ρ (30°C) for bmimPF₆.

Finally, the specific conductivity of bmimPF₆ is reported as 0.0019 S cm^{-1} (30°C), which is in excellent agreement with that of the bmimPF₆ prepared using the new aqueous route. This was measured using AC impedance spectroscopy (described in Chapter 7) and gave a value of 0.0018 S cm^{-1} at 30 °C.

The polarity of bmimPF₆ has been studied recently by a number of different groups. Carmichael *et al.* used the solvatochromic dye Nile Red to probe the polarity of a range of ionic liquids.¹⁰ A solvatochromic dye is a compound for which the absorption or emission band maxima depend on the polarity of the solvent in which it is dissolved. Nile red is positively solvatochromic so the wavelength of its absorption maximum moves to longer wavelengths as the solvent medium becomes more polar. Using this analysis technique the polarity of bmimPF₆ was found to be the same as 1-butanol and ethanol.¹⁰

⁸ P. A. Z. Suarez, S. Einloft, J. E. L. Dullius, R. F. de Souza and J. Dupont, *J. Chem. Phys.* (1998) **95**, 1626 - 1639.

⁹ J. Holbrey and K. R. Seddon, *J. Chem. Soc., Dalton Trans.*, 1999, 2133 – 2139.

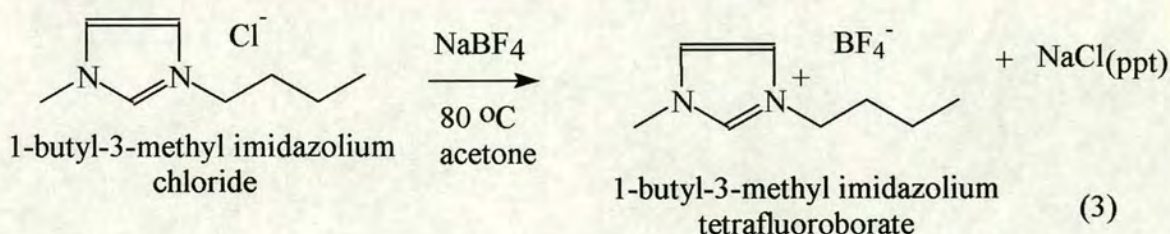
¹⁰ A. J. Carmichael and K. R Seddon, *J. Phys. Org. Chem.*, 2000, **13**, 591 – 595.

Aki *et al.* used a fluorescent probe to measure the polarity of bmimPF₆.¹¹ The fluorescence maximum, fluorescence quantum yield and the fluorescence lifetime of the fluorophore are all dependent on the polarity of the solvent medium hence the polarity of the bmimPF₆ can be measured and compared to conventional solvents using each of these probes. Again, the polarity of the ionic liquid was found to be equivalent to that of the ethanol or butanol. It should be noted, however, that the polarity of the ionic liquids is strongly dependent on the water content. As would be expected given the high polarity of water, the presence of a significant quantity of water increases the polarity of the ionic liquid.

¹¹ S. N. V. K. Aki, J. F. Brennecke and A. Samanta, *Chem. Commun.*, 2001, 413 – 414.

3.4 1-butyl-3-methyl imidazolium tetrafluoroborate.

1-butyl-3-methyl imidazolium tetrafluoroborate was first synthesised from the chloride precursor by metathesis using sodium tetrafluoroborate in acetone.³ The solution was stirred at room temperature for 24 hours and the sodium chloride by-product removed by filtration. As for the hexafluorophosphate analogue, an aqueous route is possible using either expensive silver tetrafluoroborate or the extremely hazardous tetrafluoroboric acid. The cheaper and safer method of synthesising bmimBF₄ used in this investigation utilised sodium tetrafluoroborate, as shown in equation (3).



The by-product was easily removed from the reaction mixture as a white precipitate and washing the bmimBF₄ with acetone followed by drying under high vacuum gave the clean product as a light brown liquid.

The cyclic voltammogram of bmimBF₄ has been recorded and published, and again shows a large electrochemical window, as shown in Table 3.3.⁶

Electrode	Anodic limit / V	Cathodic limit / V
Tungsten RDE	4.50	-1.60
Vitreous carbon RDE	3.65	-1.80
Gold RDE	2.35	-1.85
Platinum RDE	3.00	-1.60
Platinum ume	2.50	-1.50

Table 3.3 Electrochemical window of bmimBF₄ as measured by Suarez *et al.* RDE = rotating disc electrode. Ume = ultramicroelectrode.

The cyclic voltammogram of the sample of bmimBF_4 synthesised in this laboratory was measured and in concordance with the results shown in Table 3.3, a large electrochemical window was observed. As before, platinum wire was used for the reference and working electrode and platinum gauze was used as the counter electrode. The cyclic voltammogram obtained is shown in Figure 3.2 and shows anodic and cathodic limits of 2.4 V and -2.6 V respectively.

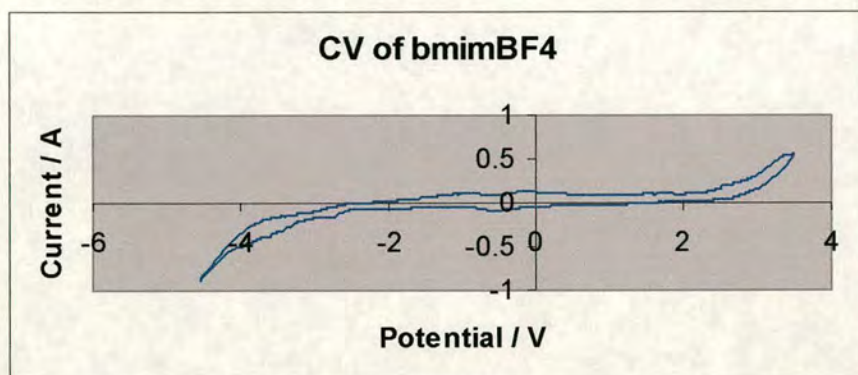


Figure 3.2. Cyclic voltammogram of 1-butyl-3-methyl imidazolium hexafluorophosphate.

The glass transition temperature, viscosity and density were measured for the bmimBF_4 ionic liquid by Suarez *et al.*³ and are presented in Table 3.4. The bmimBF_4 species is less dense and less viscous than the PF_6 analogue. It is postulated that a decrease in hydrogen bonding results in the density and viscosity decrease because the cation and anion are held together less strongly. However, it should be noted that the change in anion size would also be expected to have an effect on these physical properties and a direct comparison of the extent of hydrogen bonding within these systems should not be made solely on this basis.

T _g / K	η_{30} / Poises	ρ_{30} / gcm^{-3}
192	2.33	1.17

Table 3.4. Glass transition temperature, T_g, viscosity, η (30°C) and density, ρ (30°C) for bmimBF_4 .

One striking difference between the bmimBF_4 and PF_6 species is in the affinity of the ionic liquid with water. Whilst bmimPF_6 is observed to be hydrophobic, bmimBF_4 is miscible with water at room temperature. The miscibility of this ionic liquid with water is reported to depend on temperature and composition (the ratio of bmimBF_4 to water).³ A 1:1 (w/w) mixture exists in two phases below 5 °C but is homogeneous above this temperature.

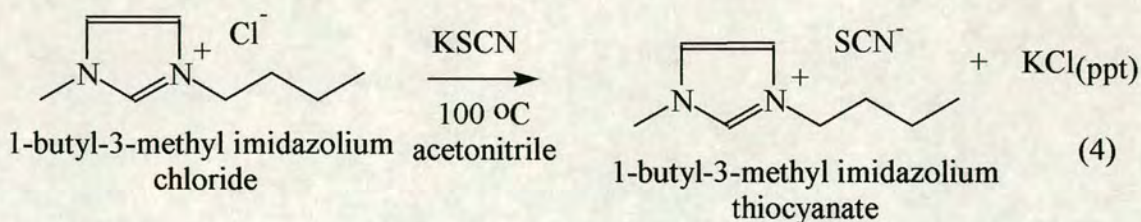
The specific conductivity of bmimBF_4 is reported as 0.0023 S cm^{-1} (30 °C) and again this is in good agreement with that measured using AC impedance spectroscopy (see section 6.1), of 0.0036 S cm^{-1} .

The polarity of the bmimBF_4 was measured using Nile red by Carmichael *et al.* and was found to be slightly higher than the PF_6 analogue.¹⁰ This is to be expected as the BF_4 anion is smaller hence the negative charge is less spread out and the effective anion charge density is larger.

3.5 1-butyl-3-methyl imidazolium thiocyanate.

There are no imidazolium ionic liquids with the thiocyanate anion reported in the literature. However, these can easily be prepared by metathesis from the chloride species *via* a number of routes. A fused mixture of bmimCl and potassium thiocyanate in the absence of solvent rapidly changed consistency on heating and became extremely viscous as bmimSCN was formed. This was then separated from the KCl by-product by extraction with dichloromethane.

Alternatively, for a lower temperature route, acetonitrile can be used as a solvent. Refluxing the solution for 48 hours under nitrogen, followed by removal of the KCl precipitate by filtration, produced bmimSCN as an orange liquid.



The cyclic voltammogram of this new ionic liquid was measured using the apparatus described previously to allow comparison of the electrochemical windows of each species and as a further means for assessing the purity of the compound. The CV obtained is shown in Figure 3.3 and shows anodic and cathodic solvent limits of 0.8 V and -1.8 V respectively. This is a smaller electrochemical window than observed for the bmimPF₆ and bmimBF₄, possibly indicating the lower stability of the thiocyanate ion towards oxidation compared to the tetrafluoroborate or hexafluorophosphate ion. However, the CV shows no peaks due to any electroactive impurities.

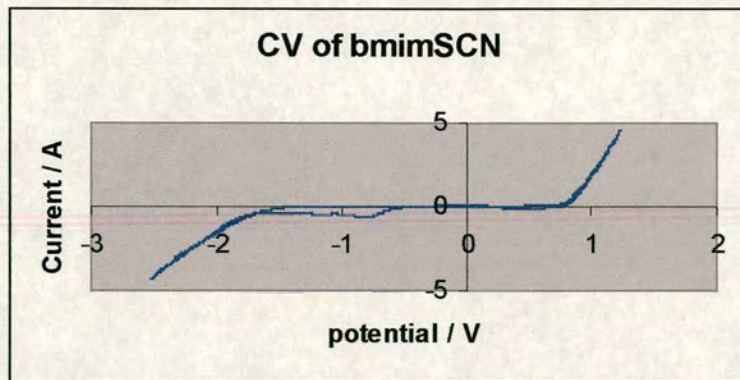


Figure 3.3. Cyclic voltammogram of 1-butyl-3-methyl imidazolium thiocyanate.

The conductivity of bmimSCN was measured at 30 °C using AC impedance Spectroscopy and was found to be 0.007 S cm^{-1} .

3.6 Conclusions.

It is important, given the wide potential applications of these air and water stable ionic liquids on an industrial level, that the synthetic procedures required to make these species do not necessitate the use of expensive or hazardous materials. The synthetic routes to the three ionic liquids outlined above all utilise cheap and commercially available reagents hence are suitable for easy laboratory-scale preparation and the possibility of larger scale synthesis.

3.7 Experimental.

1-butyl-3-methyl imidazolium chloride (**1**). 1-methyl imidazole (100 cm³, 1.25 mole) was dried by distillation over KOH under a nitrogen atmosphere and was then further dried by standing over 4A molecular sieves that had been previously baked out at 200°C under vacuum and was added to 1-chlorobutane (157 cm³, 1.49 mole, washed with sulfuric acid and distilled under nitrogen onto molecular sieves) and the mixture refluxed under nitrogen for 24 hours at 90 °C. The excess 1-chlorobutane was then removed *in vacuo* yielding a white crystalline solid at room temperature. m.p. 35 °C.

¹H NMR (CDCl₃) δ: 9.9 (s, 1H, H2), 7.2 (dd, 2H, H4 H5), 3.9 (t, 2H H6), 3.6 (s, 3H, Me), 1.5 (m, 2H, H7), 0.9 (m, 2H, H8), 0.5 (t, 3H, H9).

IR: (cm⁻¹, neat liquid) ν: 3150 (νC-H aromatic), 2924 (νCH₂ aliphatic), 1564 (νC=C), 1468.

Elemental analysis. C₈H₁₅N₂Cl requires C 55.1, H 8.67, N 16.0. Found: C 54.3, H 9.20, N 16.9.

1-butyl-3-methyl imidazole hexafluorophosphate (**2**). (**1**) (174.67g, 1 mole) was added to a saturated aqueous solution of potassium hexafluorophosphate (184.07g, 1 mole) in a separating funnel. The lower organic layer was separated and washed with water, dried over molecular sieves and filtered to remove the insoluble salts, producing a clear liquid of 1-butyl-3-methyl imidazolium hexafluorophosphate.

¹H NMR (CD₃OD) δ: 8.8 (d, 1H, H2), 7.6 (d, 1H, H4), 7.5 (d, 1H, H5), 4.8 (s, CH₃OH), 4.3 (m, 2H, H6), 4.0 (m, 3H, H10), 1.0 (m, 3H, H2), 1.9 (m, 2H, H7), 1.4 (m, 2H, H8).

¹³C NMR (CD₃OD) δ: 11.67 (C9), 18.26 (C8), 30.83 (C7), 34.28 (C10), 48.51 (C6), 121.33 (C5), 122.49 (C4), 135.56 (C2).

¹⁹F NMR (CD₃OD) δ: -69.5 (d, J_{F-F} = 709 Hz).

IR (cm⁻¹ neat liquid) ν: 3170 (ν aromatic C-H stretch), 2965, 2938, 2878 (ν aliphatic C-H stretch), 1574, 1468, 840 (ν P-F).

Elemental analysis. C₈H₁₅N₂PF₆ requires C 33.8 H 5.32 N 9.86. Found C 33.6, H 5.32, N 9.46.

1-butyl-3-methyl imidazolium tetrafluoroborate (**3**). A solution of (**1**) (24.35 g, 0.139 mole) and sodium tetrafluoroborate (15.31 g, 0.139 mole) in acetone (75 cm³) was refluxed under nitrogen for 24 hours at 80 °C. The solution was then filtered under suction to remove the white precipitate and the filtrate dried under vacuum giving a pale brown liquid. Yield = 80% based on quantity of (**1**) taken.

¹H NMR (CD₃OD) δ: 8.85 (s, 1H, H2), 7.7 (dd, 2H, H4 H5), 4.3 (t, 2H, H6), 4.0 (s, 3H, Me), 2.0 (m, 2H, H7), 1.5 (m, 2H, H8), 1.0 (t, 3H, H9).

¹H NMR δ (neat liquid) 8.4 (s, 1H, H2), 7.3 (d, 2H, H4 H5), 4.0 (d, 2H, H6), 3.7 (s, 3H, Me), 1.6 (m, 2H, H7), 1.0 (2H, H8), 0.6 (m, 3H, H9). All peaks in spectrum are broad due to high viscosity and concentration of sample.

Elemental analysis. C₈H₁₅N₂BF₄ requires C 42.5, H 66.70, N 12.39. Found C 39.79, H 6.67, N 13.9.

IR (cm⁻¹ neat liquid) ν: 3163, 3123 (ν aromatic C-H stretch), 2965, 2939, 2878 (ν aliphatic C-H stretch), 1576, 1467, 1058 (ν B-F).

FAB-MS *m/z* 139 (M⁺), 83 (loss of butyl), 29 (C₂H₇).

1-butyl-3-methyl imidazolium thiocyanate (**4**).

From the melt: Potassium thiocyanate (22.8 g, 0.235 mole) and (**1**) (40.92 g, 0.235 mole) were heated together at approximately 150 °C under nitrogen. After ten minutes the melt was observed to change consistency and became gel-like. The gel was heated for a further ten minutes and then dichloromethane (100 cm³) was added, producing a white precipitate. The precipitate was removed by filtration and the dichloromethane removed under vacuum. The filtrate was washed with more dichloromethane (50 cm³), more precipitate was removed by filtration and the solvent then removed under vacuum. This was repeated using chloroform (50 cm³) to ensure the removal of all the potassium chloride by-product. The product was collected as a brown liquid.

¹H NMR (CDCl₃) δ: 9.0 (s, 1H, H2), 7.1 (m, 2H, H4 H5), 3.8 (t, 2H, H6), 3.5 (s, 3H, Me), 1.4 (m, 2H, H7), 0.8 (m, 2H, H8), 0.3 (m, 3H, H9).

IR: (cm⁻¹, neat liquid) ν: 3144, 3090 (ν aromatic C-H stretch), 2960, 2935 (ν aliphatic C-H stretch), 2053 (ν N=C=S), 1573.7 (ν C=C), 1464.4.

Elemental analysis. $C_8H_{15}N_2SCN$ requires C 54.8, H 7.66, N 21.3. Found C 52.6, H 5.51, N21.44.

A chemical test for chloride in the presence of thiocyanate was performed. 1 g of the product was dissolved in a little water and added to aqueous silver nitrate producing a precipitate (of silver thiocyanate and silver chloride, if chloride is present). The precipitate was removed by filtration, dried and heated vigorously to remove the sulfur (evolution of yellow smoke was observed). Zinc powder and sulfuric acid were then added to the solid resulting in gas evolution. A sample of the solution was added to aqueous silver nitrate but no white precipitate was formed. Thus, it was concluded that the product contained no chloride ions indicating complete metathesis from the chloride precursor.

From an acetonitrile solution: A solution of KSCN (6.45 g, 0.066 mole) and (1) (11.60 g, 0.066 mole) in acetonitrile (30 cm³) was refluxed for 48 hours under nitrogen. The solution was then filtered and the product dried under vacuum leaving an orange liquid. Yield = 88%.

¹H NMR δ (neat liquid) 8.9 (s, 1H, H2), 7.5 (d, 2H, H4 H5), 4.1 (d, 2H, H6), 3.7 (s, 3H, Me), 1.6 (m, 2H, H7), 1.0 (2H, H8), 0.6 (m, 3H, H9). All peaks in spectrum are broad due to high viscosity and concentration of sample.

IR: (cm⁻¹, neat liquid) ν : 3144, 3092 (ν C – H aromatic stretch), 2959, 2933 (ν C – H aliphatic stretch), 2054 (ν S=C=N), 1573 (ν C=C), 1465.

IR spectrum of precipitate shows no features indicating that it is KCl and not excess KSCN.

FAB-MS m/z 139 (M⁺), 83 (loss of butyl), 29 (C₂H₇).

Elemental analysis. $C_8H_{15}N_2SCN$ requires C 54.8, H 7.66, N 21.3. Found C 54.4, H 7.64, N 21.9.

Chemical test for chloride in the presence of thiocyanate was negative indicating complete metathesis.

Elemental analysis results indicate that the product produced *via* the acetonitrile solution is cleaner than that by the high temperature route, probably as result of the incomplete metathesis of the chloride salt *via* the latter route.

4 Uses of bmimPF₆ in Synthesis.

4.1 Fluorination Reactions in Ionic Liquids.

4.1.1 Introduction - Halogen Exchange Reactions.

Organofluorine compounds are used as aerosol propellants, coatings for cooking utensils, lubricants, inhalation anaesthetics, refrigerants, drugs, blood substitutes, surfactants, dyes and in the production of agrochemicals.¹ Such widespread use means that the demand for effective synthetic routes to fluorinated organics is intense. Synthesis of such compounds, however, is complicated by the reactivity of fluorine itself, necessitating the use of other materials for the synthesis of the C-F bond.

The synthesis of organic fluorine compounds is most conveniently and easily effected by halogen exchange, driven by the formation of the thermodynamically favourable C-F bond (552 kJ mol⁻¹ compared to 397 kJmol⁻¹ for C-Cl)². Fluorination by halogen exchange has been utilised since the mid-1880's and the majority of the early work centred on the use of antimony trifluoride as the fluorinating agent. This method has since been heavily researched, with a number of other successful reagents identified and is now a wide-spread technique for the synthesis of a variety of organic fluorine compounds.³ Fluorine exchange cannot be used for the fluorination of compounds that have a functional group already containing an alkyl

¹ J. A. Wilkinson, *Chem Rev.*, **92**, 505-519, 1992.

² D. R Lide, *CRC Handbook of Chemistry and Physics*, 74th edition.

³ A. K. Barbour, L. J. Belf and M. W. Buxton, *Advances in Fluorine Chemistry*, Vol.3, 1963.

chain with poly-halogenated hydrocarbons, but the presence of only one halogen atom on the alkyl chain does not prohibit use of this synthetic technique.

Reagents now commonly used for halogen exchange include SbF₃, AgF, HgF₂, Hg₂F₂, SbClF₂ and anhydrous HF. Alkali metal fluorides are common fluorinating agents, but the use of these reagents is generally restricted to exchange of the more activated halogens. Potassium fluoride is the most widely used and has been utilised for the replacement of isolated halogen atoms in alkanes and for the preparation of α,ω -difluoro-alkanes and monofluoro-esters. These reactions can be effected either by use of an autoclave at high temperatures or by utilisation of an appropriate solvent for milder conditions. The solvents used for these reactions are generally high-boiling and include acetylacetone, nitrobenzene, dimethyl formamide and dimethyl sulfoxide, as well as a range of glycols. In all of these reactions the salts must be efficiently agitated to avoid coating of the fluoride salt by the chloride, which renders it inactive.

Sodium and lithium fluoride can be used as agents for halogen exchange, although their use is not as widespread as that of the potassium salt. There are few reports of the use of calcium fluoride for halogen exchange reactions, and those that exist centre on its use as a solid support for potassium fluoride.⁴ This helps to disperse the potassium fluoride and leads to enhanced yields and reactivity.

The major problems associated with halogen exchange by alkali metal halides are the long reaction times and high temperatures necessitated by the poor solubility of the salts in polar aprotic solvents. This solubility problem is the most severe for calcium fluoride which show negligible solubility in all solvents (0.0168 g dm⁻³ in water at 18 °C, sparingly soluble in mineral acids)². However, the ionic liquid 1-butyl-3-methyl imidazolium hexafluorophosphate (bmimPF₆) was observed to dissolve calcium fluoride in significant quantities (up to 0.4 mol dm⁻³) with gentle heating.⁵ Calcium fluoride is the cheapest and most readily available of the group 1 and group 2 metal halides and as such is potentially a very attractive fluorinating agent. Hence, calcium fluoride in bmimPF₆ potentially represents a cheap, easy to handle and safe medium

⁴ J. Ichihara, T. Matsuo, T. Hanafusa and T. Ando, *J. Chem. Soc., Chem. Comm.*, 1986, 793-794. T. Ando, D. G. Cork, M. Fujita, T. Kimura and T. Tatsuno, *Chem. Lett.*, 1988, **11**, 1877-1878.

⁵ Observation by co-worker D. Sanders, Department of Chemistry, University of Edinburgh.

for halogen exchange reactions and so it was decided to assess the fluorinating potential of this system for both inorganic and organic compounds.

4.1.2 Fluorination Reactions in Ionic Liquids.

To date, there is only one fluorination reaction in ionic liquids reported in the literature. The ionic liquids 8-ethyl-1,8-diazabicyclo[5,4,0]-7-undecene trifluoromethanesulfonate and 8-methyl-1,8-diazabicyclo[5,4,0]-7-undecene trifluoromethanesulfonate were reported as media for the synthesis of α -fluoro- α,β -unsaturated esters.⁶

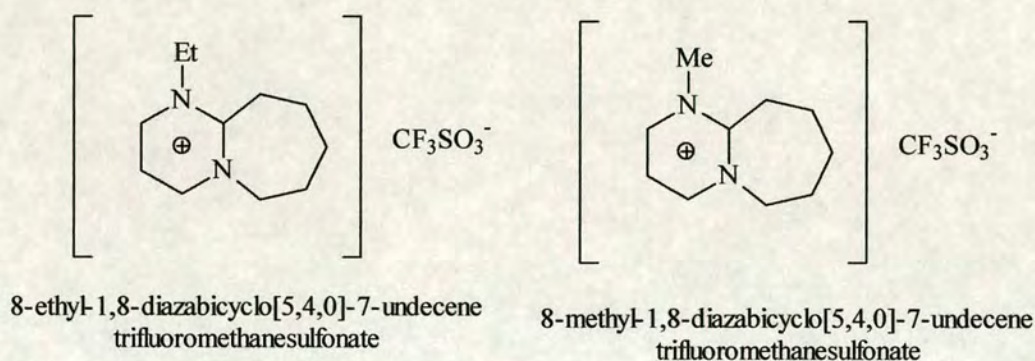
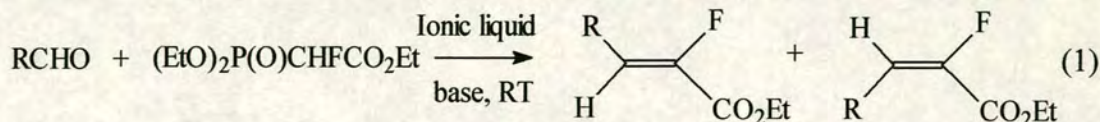


Figure 4.1. Ionic liquids previously used for fluorination reactions.

The fluorinated esters were prepared in these ionic liquids *via* the Horner-Wadsworth-Emmons reaction by combination of two aldehydes in the presence of a base. The use of ionic liquids allowed the reaction to proceed at room temperature, whereas the reaction conventionally uses diethyl ether as the solvent and either refluxing temperatures, when sodium hydride is used as the base, or at -78°C with butyl lithium. The products of the reaction in the ionic liquid were then extracted using diethyl ether.



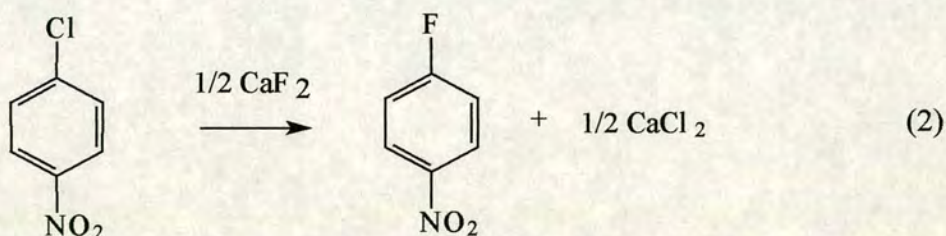
⁶ T. Kitazume and G. Tanaka, *Journal of Fluorine Chemistry*, 2000, **106**, 211-215.

The use of 1-ethyl-3-methyl imidazolium tetrafluoroborate or hexafluorophosphate as a solvent is reported to decrease both the yield and the amount of product recoverable by extraction. The difficulty in removing the fluorinated product from these ionic liquids suggests that these species are more strongly bound in these ionic liquids than in the fluorinated ionic liquids detailed above. This may be due to interactions of the fluorine with the imidazolium cation and our work indicates a similar affinity of 1-fluoro-2,4-dinitrobenzene for the bmimPF₆ ionic liquid (see section 4.1.3.2).

4.1.3 Organic Fluorinations using Calcium Fluoride.

4.1.3.1 Fluorination of *p*-chloronitrobenzene.

The fluorination of *p*-chloronitrobenzene using potassium fluoride was reported by Finger *et al.* in 1956.⁷ The authors report having to use a solution of dimethyl sulfoxide at 190 °C for fourteen hours, reflecting the fact that the chloride group in this compound is only moderately activated by the nitro group.

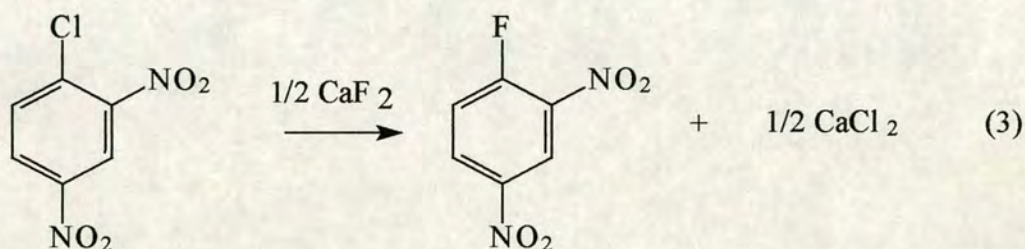


This reaction was attempted using calcium fluoride as a fluorinating agent by heating a mixture of *p*-chloronitrobenzene (0.6 g, 3.8 mmole) and calcium fluoride (0.148 g, 3.8 mmole) in bmimPF₆ (20 cm³) at 160 °C for twenty four hours. Work up of the reaction mixture either by vacuum distillation or extraction with diethyl ether (50 cm³) and hexane (25 cm³) yielded no fluorinated product. Repetition of this experiment in the presence of dimethyl sulfoxide (7 cm³) was also unsuccessful.

⁷ G. C. Finger and C. W. Kruse, *J. Am. Chem. Soc.*, 1956, **78**, 6034 - 6037.

4.1.3.2 Fluorination of 1-chloro-2,4-dinitrobenzene.

This reaction has also been reported by Finger *et al.*⁷ and can be carried out under less harsh conditions than those utilised in the previous reaction because the activity of the chloride is increased by the presence of the second nitro group. Finger reported the successful fluorination of this compound in dimethyl sulfoxide, dimethyl formamide and nitrobenzene. This reaction has never been reported using calcium fluoride as the fluorinating agent.



This reaction was first attempted by heating a mixture of calcium fluoride (0.125 g, 1.6 mmole) and 1-chloro-2,4-dinitrobenzene (0.162 g, 0.8 mmole) in bmimPF₆ (20 cm³) at 150 °C for 24h under nitrogen, but isolation of the product by vacuum distillation yielded none of the desired product. The reaction was repeated and worked up by extraction into diethyl ether (50 cm³) and hexane (25 cm³), but again this yielded only the unreacted 1-chloro-2,4-dinitrobenzene.

It was proposed that the addition of a small amount of co-solvent, of the type proven to be a suitable solvent as reported by Finger *et al.* might assist in the fluorination using calcium fluoride.

The fluorination of 1-chloro-2,4-dinitrobenzene was attempted by heating calcium fluoride (2.5g, 0.032 mole) and 1-chloro-2,4-dinitrobenzene (3.13g, 0.0154 mole) in bmimPF₆ (15 cm³) with dimethyl sulfoxide (7 cm³, 50 % by weight) for 18 hours at 130 °C. Extraction of the reaction mixture with diethyl ether (50 cm³) and hexane (25 cm³) gave an approximately equimolar mixture of chloro and fluoro-2,4-dinitrobenzene.

¹H NMR (CDCl₃) δ: 8.95 (d, 1H, 1-fluoro-2,4-dinitrobenzene), 8.7 (d, 1H, 1-chloro-2,4-dinitrobenzene), 8.35 (m, 2H, 1-fluoro and 1-chloro-2,4-dinitrobenzene), 7.85 (d, 1H, 1-chloro-2,4-dinitrobenzene), 7.6 (d, 1H, 1-fluoro-2,4-dinitrobenzene).

Literature value for 1-fluoro-2,4-dinitrobenzene ¹H NMR δ: (CDCl₃) δ: 8.95, 8.55, 7.6.

¹⁹F NMR (CDCl₃) δ: -151.26 (s, unknown), -106.80 (s, 1-fluoro-2,4-dinitrobenzene).

Literature value for 1-fluoro-2,4-dinitrobenzene⁸ ¹⁹F NMR δ: (d₈-toluene) -108.12.

The successful fluorination of 1-chloro-2,4-dinitrobenzene represents a significant step forward in the drive to use calcium fluoride as a fluorinating agent. However, this reaction has a number of idiosyncrasies, as outlined below, and these require further investigation to aid understanding in the use of calcium fluoride in bmimPF₆ as a viable fluorinating medium.

(i) Driving the reaction to completion.

The reaction as described above does not go to completion.

The reaction was repeated using temperatures of 180 °C for 20 hours but no further fluorination was observed. Using double the amount of dimethyl sulfoxide or three times the amount of calcium fluoride also made no observable difference to the amount of fluorinated product recovered. It was proposed that the calcium fluoride was becoming coated in the calcium chloride by-product and hence was being rendered inactive.

To test this hypothesis 1-chloro-2,4-dinitrobenzene (0.324 g, 1.6 mmole) was added to calcium fluoride (0.25 g, 3.2 mmole) in bmimPF₆ (10 cm³) and dimethyl sulfoxide (4 cm³) and the mixture heated at 130 °C for 24 hours under nitrogen. The reaction mixture was then washed with deionised water (50 cm³) and more dimethyl sulfoxide (4 cm³) and calcium fluoride (0.25 g, 3.2 mmole) added. The reaction mixture was heated for a further 4 hours at 140 °C under nitrogen and then extracted with diethyl ether (50 cm³) and hexane (25 cm³) leaving a yellow oil. However, ¹H NMR analysis

⁸ The Aldrich library of ¹³C and ¹H FT NMR spectra / [Milwaukee] : Aldrich Chemical Co., c1993.

of the product again showed a 50/50 mix of chloro and fluoro-dinitrobenzene. It is believed that shaking with water resulted in the presence of significant amounts of water in the reaction mixture and this may have hindered any further reaction that might have occurred on the addition of more reactants.

(ii) Identifying the by-products.

During the reaction, copious amounts of a white solid sublimed from the bmimPF₆ and collected on the walls of the reaction vessel and the reflux condenser. This solid had an unpleasant odour and identification of this compound by NMR analysis proved troublesome owing to its low solubility in all solvents. The mass spectra have been inconsistent using a variety of techniques and no peak attributable to the molecular ion has so far been definitely identified. Using fast atom bombardment mass spectrometry a spectrum was obtained that shows sequential loss of alternating 78 and 75 mass units from m/z 997 to 79.

Chemical analysis for carbon, hydrogen and nitrogen have also proved inconsistent. The first analysis indicated carbon and hydrogen percentages of 17.4 and 4.70 respectively, but the second analysis of a different sample of powder gave these percentages as 32.5 % and 5.62 % and a third analysis gave 10.5 % C and 1.33 % H. However, all analyses were in agreement with the fact that the solid contained no nitrogen.

The unknown solid was found to dissolve in sulfuric acid, but no precipitate was observed. If the by-product contained significant amounts of calcium a precipitate of calcium sulfate would be expected. Addition of the solid to a solution of ammonium carbonate did not dissolve the solid or appear to form any new precipitate. The solid did not dissolve in acetic acid, as would be expected if a new precipitate of calcium carbonate were present hence it was concluded that the by-product contained no calcium.

It is considered likely that the inconsistency in these analytical results is due to the unknown white solid being a polymer or oligomer. The poor solubility that it displays also suggests this.

It is proposed that this polymer is composed of carbon, hydrogen, sulfur, oxygen and fluorine and is formed by the reaction of dimethyl sulfoxide and the fluoride ions from calcium fluoride. The dissolution of the calcium fluoride by the bmimPF₆ enables this reaction to take place hence it is not observed in conventional molecular solvents. However, it is interesting to note that in the original report of this reaction by Finger *et al.*⁷ it is reported that “some –SCH₃ substituted products have been isolated from reactions in DMSO” but no further information is given.

Analysis by X-ray powder diffraction failed to produce any match with the diffraction patterns on the database.

The infrared spectrum of the compound shows few features: ν cm⁻¹ 2983, 2924 (ν CH₃, CH₂), 1384 (ν CH₃), 1239 (ν C-F), 1094, 934 (ν S=O), 638 (ν C-F) and is inconclusive.

It was thought initially that this white solid might be the product of a reaction in competition with the fluorination. However, when the reaction mixture of calcium fluoride, 1-chloro-2,4-dinitrobenzene and dmsol in bmimPF₆ is heated at just 70°C for 72 hours, no fluorination is observed, which would be expected due to the low temperatures, but additionally no white solid is produced. The synthesis of the 1-fluoro-2,4-dinitrobenzene and the white solid appear to occur simultaneously. It is possible that it is the decomposition product of dimethyl sulfoxide that initiates the fluorination reaction. However, the unknown by-product alone was found not to act as a fluorinating agent.

Heating only a mixture of calcium fluoride, dmsol and bmimPF₆ appeared to yield no white solid, and likewise a heated mixture of 1-chloro-2,4-dinitrobenzene in dimethyl sulfoxide and bmimPF₆, with no calcium fluoride, produced none of the unknown product. However, this might only be due to the increased solubility of the by-product in the bmimPF₆ in the absence of these reagents.

(ii) Removing the 1-fluoro-2,4-dinitrobenzene from the bmimPF₆.

One of the advantageous properties of bmimPF₆, as with all ionic liquids, is that it has negligible effective vapour pressure even at temperatures up to 100 °C. This

means that, in theory, the volatile product of a reaction can be removed under vacuum, avoiding the necessity for lengthy extractions.

The initial attempts to fluorinate 1-chloro-2,4-dinitrobenzene were followed by attempts to remove the products by vacuum distillation. However, this resulted only in the sublimation of the 1-chloro-2,4-dinitrobenzene starting material and, in the case of the reaction with dimethyl sulfoxide, the unknown white solid. Collection of the 1-fluoro-2,4-dinitrobenzene could only be achieved by extraction of the reaction mixture with organic solvents such as diethyl ether and hexane, despite the fact that the boiling point of this compound is lower than the chloride analogue.⁹ This suggests that 1-fluoro-2,4-dinitrobenzene interacts strongly with bmimPF₆. This could be caused by hydrogen bonding between the fluorine of the aromatic ring and the ionic liquid, which makes it harder to remove under vacuum. The observation of intra-molecular hydrogen bonds within the crystal structures of these ionic liquids (see Chapter 8) suggests that inter-molecular hydrogen bonding within these species is also probable. The crystal structure of 1-fluoro-2,4-dinitrobenzene shows two close contacts between the fluorine and the carbon atoms of adjacent benzene rings indicating that such interactions can take place.¹⁰ By contrast, the only close contact involving chlorine atoms with neighbouring groups evident in the crystal structure of 1-chloro-2,4-dinitrobenzene crystal structure is a hydrogen bond to a proton on the benzene ring.¹¹ The difference in the interactions of the chlorine and fluorine groups points to a possible explanation for the retention of the 1-fluoro-2,4-dinitrobenzene in the ionic liquid.

(iii) Use of other co-solvents.

The fluorination of 1-chloro-2,4-dinitrobenzene has also been reported using potassium fluoride in dimethyl formamide and nitrobenzene. Hence it was decided to use a small amount of these as co-solvents in an attempt to drive the reaction to completion.

⁹ 1-chloro-2,4-dinitrobenzene; b.p. 315 °C. 1-fluoro-2,4-dinitrobenzene; b.p. 296 °C.

¹⁰ A. Wilkins and R. W. H. Small, *Acta Cryst.* 1991, C47, 221 – 222.

¹¹ H. Takazawa, S. Ohba and Y. Saito, *Acta Cryst.* 1989, B45, 432 – 437.

1-chloro-2,4-dinitrobenzene (0.324 g, 1.6 mmole) was added to calcium fluoride (0.25 g, 3.2 mmoles) in bmimPF₆ (20 cm³) and dimethyl formamide (5 cm³) and the solution heated for 20 hours at 130 °C under nitrogen. The mixture was then extracted with diethyl ether (50 cm³) and hexane (25 cm³) yielding a yellow solid that was found to be unreacted 1-chloro-2,4-dinitrobenzene on the basis of its NMR spectrum.

1-chloro-2,4-dinitrobenzene (1.21 g, 7.68 mmole) was added to calcium fluoride (2.4 g, 0.03 mole) in bmimPF₆ (15 cm³) and nitrobenzene (7 cm³) and the mixture heated at 140°C for 24 hours under nitrogen. However, extraction with diethyl ether (50 cm³) and hexane (25 cm³) again isolated only unreacted 1-chloro-2,4-dinitrobenzene. Hence, the presence of these compounds as co-solvents did not effect any fluorination of the 1-chloro-2,4-dinitrobenzene.

Acetone, ethyl acetate and ethyl benzoate were also unsuccessful as co-solvents under the same conditions. However, it is worth noting that the presence of some solvents in the reaction mixture reduced the temperature at which the mixture could be heated, which may be a significant deterrent to fluorination.

(iv) Use of other ionic liquids.

Calcium fluoride (2.5g, 0.032 mole) and 1-chloro-2,4-dinitrobenzene (3.13g, 0.0154 mole) were heated together in bmimBF₄ (10 cm³) with dimethyl sulfoxide (4 cm³) for 24 hours at 130 °C. The reaction mixture was then extracted with diethyl ether (50 cm³) and hexane (25 cm³) but ¹H NMR analysis of the product showed only unreacted 1-chloro-2,4-dinitrobenzene.

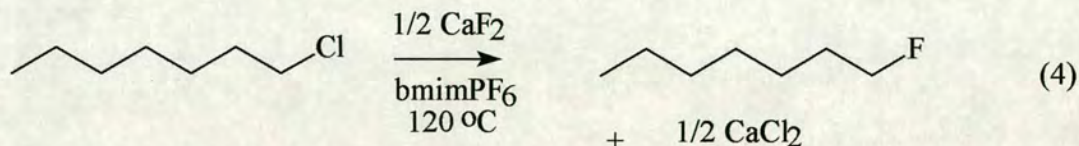
The reaction was repeated using the 1-butyl-2,3-dimethyl imidazolium hexafluorophosphate ionic liquid, under the same conditions, but again no fluorination was observed.

The failure of this reaction in ionic liquids other than 1-butyl-3-methyl imidazolium hexafluorophosphate is surprising, but is possibly due to the lower solubility of calcium fluoride in these ionic liquids.

4.1.4 Fluorination of Other Organic Compounds.

4.1.4.1 1-chloroheptane.

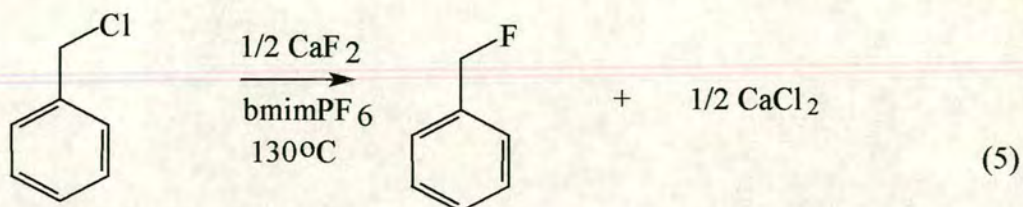
Following the successful fluorination of an aromatic compound, it was decided to attempt the fluorination of a straight-chain organic alkyl chloride with calcium fluoride. 1-chloroheptane was chosen for its availability and relatively low toxicity compared to that of many other straight-chained alkanes.¹²



1-chloroheptane (1.346 g, 0.01 mole) and calcium fluoride (0.78 g, 0.01 mole) were heated together in bmimPF₆ (10 cm³) for 24 hours at 120 °C under nitrogen. Removal of the product by vacuum distillation yielded only 1-chloroheptane, based on the ¹H and ¹⁹F NMR spectra. To eliminate the possibility that any fluorinated product was being retained in the reaction mixture the reaction was repeated and a sample of the supernatant product was removed directly from the reaction mixture. However, ¹H NMR analysis revealed this to be only unreacted chloroheptane. Repetition of this experiment followed by extraction with diethyl ether (50 cm³) and hexane (25 cm³) also failed to yield any fluorinated product.

¹² Namavari, N Satyamurthy and J. R. Barrio, *J. Fluorine Chem.*, 1995, **72**, 83 - 93. F. L. M. Pattison and J. J. Norman, *J. Am. Chem. Soc.*, **79**, 2311-2315, 1957.

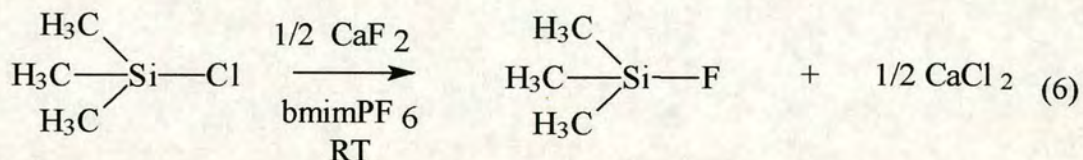
4.1.4.2 Benzyl chloride.



Benzyl chloride (11.35 cm³, 0.1 mole) and calcium fluoride (5.85 cm³, 0.75 mole) were heated together in bmimPF₆ (10 cm³) at 130 °C for 24 hours under nitrogen and the product removed under extraction with diethyl ether (50 cm³) and hexane (25 cm³). ¹⁹F NMR spectroscopy showed no fluorinated product.

4.1.5 Fluorination of Inorganic Compounds – Chlorotrimethylsilane.

The ability of calcium fluoride in bmimPF₆ to fluorinate inorganic compounds was tested by the fluorination of chlorotrimethylsilane.



Chlorotrimethylsilane can be conventionally fluorinated by passing the vapour, at a pressure of 700 – 750 mm Hg, over solid calcium fluoride, at 200 °C, but this has not been reported using milder conditions.¹³

The fluorination of chlorotrimethylsilane was attempted by addition of chlorotrimethylsilane (1.27 cm³, 0.01 mole) under nitrogen to a mixture of calcium fluoride (0.78 g, 0.01 mole) in bmimPF₆ (10 cm³) and the mixture stirred at room temperature for 24 hours. The products were removed under vacuum and trapped out at -196 °C.

¹H NMR analysis of the products in CDCl₃ revealed the presence of fluorotrimethylsilane at a peak intensity ratio of

¹³ M. C. Sheed, L. J. Maynard and R. C. Brasted, *Comprehensive Inorganic Chemistry*, Vol III, 41-42.

fluorotrimethylsilane:chlorotrimethylsilane of 1:7.¹⁴ ¹H NMR (CDCl₃) δ: 0.443 (s, 7H, TMSCl), 0.22 (d, 1H, TMSF).

It was proposed that repetition of this reaction using a complexing agent to complex the calcium might increase the concentration of free fluoride ions and thus enhance the yield of fluorotrimethylsilane.

Chlorotrimethylsilane (1.2 cm³, 9.46 mmole) was added under nitrogen to a mixture of calcium fluoride (0.86 g, 9.46 mmole) in bmimPF₆ (10 cm³) and 15-crown-5 (0.7 cm³, 5 mmole) and the mixture stirred at room temperature for 45 hours. The product was then collected by distillation under high vacuum. ¹H NMR (CDCl₃) δ: 0.45 (s, 7H, TMSCl), 0.25 (d, 1H, TMSF).

The reaction was repeated as above using double the quantity of 15-crown-5 and reaction times of 36 hours. Again the product was isolated by distillation under high vacuum. ¹H NMR (CDCl₃) δ: 0.48 (s, 3H, TMSCl), 0.28 (d, 4H, TMSF, J_{H-F} 7.2 Hz). The increase in the ratio of fluoro- to chlorotrimethylsilane from 1:7 to 4:3 indicates the value of using a complexing agent in this reaction.

¹⁴ ¹H NMR of TMSF: G. A. Olah, D. O'Brien and C. Lui, *J. Am. Chem. Soc.*, **91**, 701, 1969.

4.2 Reduction Reactions in 1-butyl-3-methyl imidazolium hexafluorophosphate.

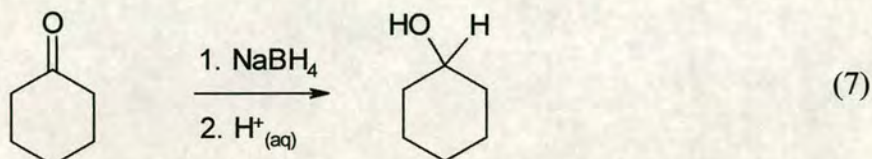
One potentially valuable use of ionic liquids is their use as solvents for the reduction of organic compounds. Again, the ability to be able to remove products simply by distillation makes them ideal solvents, but it was also hoped that their unique ionic character may result in the reduction of organic compounds with common reducing agents that cannot be used with conventional molecular solvents.

One such reducing agent is sodium tetrahydroborate.¹⁵ This is a widely used and relatively cheap reagent and has been observed to be sparingly soluble (*ca.* 0.2 mol dm⁻³) in 1-butyl-3-methyl imidazolium hexafluorophosphate. It was decided to investigate the potential of sodium tetrahydroborate in bmimPF₆ as a medium for the reduction of both organic and inorganic compounds.

¹⁵ Sodium Borohydride Digest, Morton, 3rd edition.

4.2.1 Reduction of Cyclohexanone.

The use of sodium tetrahydroborate in bmimPF₆ as a reducing medium was first tested by the reduction of cyclohexanone. This reduction can be effected with sodium tetrahydroborate in molecular solvents such as methanol or ethanol stabilised with a base to prevent hydrogen evolution.¹⁶



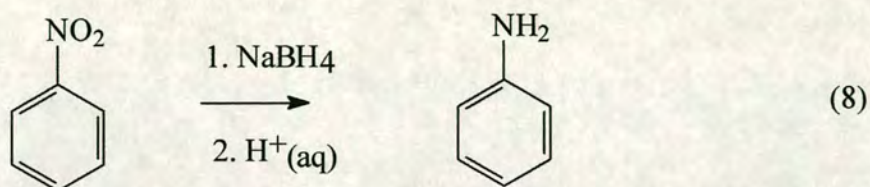
Sodium tetrahydroborate (0.567g, 0.015 mole) was added to bmimPF₆ (10 cm³) and the mixture warmed gently then filtered through a Buchner filter funnel to remove any undissolved sodium tetrahydroborate. Cyclohexanone (1.56 cm³, 0.015 mole, distilled under nitrogen) was then added and the mixture stirred at room temperature for 72 hours under nitrogen. Deionised water (0.27 cm³) and hydrochloric acid (1.5 cm³) were then added to the mixture because any cyclohexanol synthesised would be present in the deprotonated form and hence could not be removed by vacuum distillation. Removal of the products by vacuum distillation yielded a mixture of cyclohexanone and cyclohexanol in a ratio of 9:1, as determined by ¹H NMR, indicating the successful, although incomplete, reduction of cyclohexanone. ¹H NMR (CD₃OD) δ: 3.6 (m, 1H, cyclohexanol), 2.4 (m, 18H, cyclohexanone), 2.3 (s, 1H, cyclohexanol), 1.9 (m, 27H, cyclohexanone), 1.7 (m, 2H, cyclohexanol), 1.6 (m, 1H, cyclohexanol), 1.5 (m, 1H, cyclohexanol), 1.3 (d, 5H, cyclohexanol).

This result led to the expectation that a solution of sodium tetrahydroborate in bmimPF₆ could be used to achieve reductions of organic compounds previously unreported using sodium tetrahydroborate.

¹⁶ N. J. Hudak and A. H. Sholes, *J. Chemical Education*, 1986, **63**, 161.

4.2.2 Reduction of Nitrobenzene.

This reaction has not been previously reported with sodium tetrahydroborate, but has been achieved using the sulfurated species NaBH₂S₃ by refluxing for 24h in tetrahydrofuran.¹⁷



Nitrobenzene (0.77 cm³, 7.5 mmole) was heated in a filtered solution of sodium tetrahydroborate (0.33 g, 8.7 mmole before filtration) in bmimPF₆ (10 cm³) at 50 °C for 48 hours under nitrogen. Removal of the product by vacuum distillation produced only nitrobenzene. ¹H NMR (CDCl₃) δ: 8.2 (m, 2H, nitrobenzene), 7.7 (m, 1H, nitrobenzene), 7.5 (m, 2H, nitrobenzene).

4.2.3 Reduction of other Organic Compounds.

Ethyl acetate (2 cm³) was heated in a filtered solution of sodium tetrahydroborate (0.5 g, before filtration) in bmimPF₆ (25 cm³) at 75 °C for 24 hours under nitrogen. Water (1 cm³) and hydrochloric acid (1 cm³) were then added and the product isolated by vacuum distillation but no ethanol was detected, which would be present after the successful reduction of ethyl acetate. ¹H NMR δ: (CD₃OD) 3.7 (q, 2H, ethyl acetate), 2.2 (s, 3H, ethyl acetate), 1.3 (m, 3H, ethyl acetate).

The reduction of benzophenone to benzhydrol was attempted using the same reaction conditions as above, using benzophenone (1.37 g, 7.5 mmole) and temperatures of 120 °C. ¹H NMR δ: (CDCl₃) 7.3 (m, 10 H, benzophenone), 5.4 (s, 1H). The presence

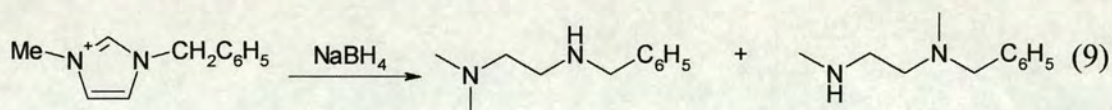
¹⁷ J. M. Lancette and J. R. Brindle, *Canadian Journal of Chem.*, 1971, **49**, 2990 - 2995.

of any benzhydrol would be expected to give peaks at 5.9 and 5.7 ppm which are absent in this spectrum indicating no reduction had taken place.

The reduction of ethyl benzoate to ethanol and benzyl alcohol proved similarly unsuccessful using the same reaction conditions with ethyl benzoate (2.15 cm³, 0.015 mole) and temperatures of 80 °C. ¹H NMR δ: (CD₃OD): 8.0 (m, 2H, ethyl benzoate), 7.6 (m, 1H, ethyl benzoate), 7.5 (m, 2H, ethyl benzoate), 4.4 (m, 2H, ethyl benzoate), 1.4 (t, 3H, ethyl benzoate).

4.2.4 Reaction of Imidazoles with Sodium Tetrahydroborate.

A report published in 1968 by Godefroi highlights one possible complication in the use of sodium tetrahydroborate in bmimPF₆.¹⁸ He reported the reductive ring cleavage of a number of different disubstituted imidazolium iodides by sodium tetrahydroborate, albeit under harsh conditions.



This was achieved by refluxing a 5:1 solution of sodium tetrahydroborate and the imidazole compound in ethanol at 55 °C for an hour. Whilst these are more extreme conditions than those utilised for the reduction reactions described above it is worth noting that sodium tetrahydroborate can and will react with imidazole rings.

¹⁸ E. F. Godefroi, *J. Organic Chem.*, 1968, 33, 2, 860 - 861.

4.3 Synthesis of Tin Compounds in Ionic Liquids.

Another potential use for air and water stable ionic liquids that has been identified is their use in the reaction and synthesis of volatile main group compounds. The negligible vapour pressure of bmimPF₆ makes it ideal for use under the high vacuum conditions necessary for the manipulation of many volatile main group compounds.

To date, reports of investigations into the use of ionic liquids with tin compounds are extremely limited. The first report appeared in 1972 and described the synthesis of the tetrabutylammonium trichlorostannate(II) ionic liquid from a combination of acidified SnCl₂.H₂O and tetrabutyl ammonium chloride.¹⁹ This compound is a solid at room temperature (mp 58-59 °C) and can be used for hydrogenations and hydroformylations in combination with a PdCl₂ catalyst. This reaction is similar to that observed using more conventional solvents, but even thirty years ago the advantages of ionic liquids as a new solvent medium were recognised.

Despite this encouraging report, however, the only subsequent paper on this subject was published in March 2000, after the work detailed below was completed. Wassercheid *et al.* described the synthesis of both bmim⁺SnCl₃⁻ and bmim⁺Sn₂Cl₅⁻ and the use of these slightly acidified ionic liquids for the hydroformylations of 1-octene and methyl-3-pentenoate with a (PPh₃)₂PtCl₂ catalyst.²⁰ There are no reports of the synthesis of any dicationic tin species for use as ionic liquids.

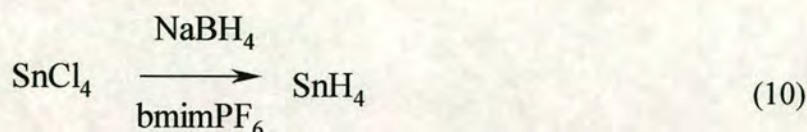
4.3.1 Stannane.

The first reaction attempted was the preparation of stannane, SnH₄. The original impetus behind this area of research was the observation of the solubility of sodium borohydride in bmimPF₆. This highlighted the possibility of using bmimPF₆ and sodium borohydride, not only for the reduction of organic compounds, but also for the synthesis of main group hydrides that are more difficult to handle on account of their air- and moisture-sensitivity and often low thermal stability.

¹⁹ G. W. Parshall, *J. Am. Chem. Soc.*, 1972, **94**, 8716-8719.

²⁰ P. Wassercheid and H. Waffenschmidt, *J. Mol. Cat. A: Chemical*, 2000, **164**, 61-67.

The conventional synthesis of stannane involves the reaction between lithium aluminium hydride and tin (IV) chloride.²¹ The two reagents are mixed as an ethereal slurry at low temperature and the stannane removed under high vacuum. One drawback of this route is the co-distillation of diethyl ether with stannane. The possibility of avoiding this synthetic route and preparing stannane directly in bmimPF₆ was a major incentive for the study of this reaction.



Tin(IV) chloride was condensed onto a sample of bmimPF₆ (8 cm³) held at -196 °C on the high vacuum line. The reaction mixture was then warmed to room temperature. Upon warming, two layers were observed, presumed to be unreacted tin tetrachloride and the solution of sodium borohydride in bmimPF₆. The apparatus was isolated from the pump and an attempt was made to trap out any tin hydride into an adjacent trap at -196 °C. No tin mirror was observed upon heating the top of the trap. This would have indicated the presence of any stannane that had decomposed to elemental tin.

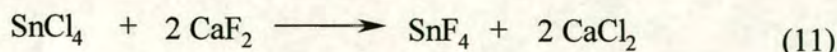
No increase in pressure was recorded by the pressure gauge, which would have indicated the presence of the volatile tin hydride. It is postulated that the synthesis of tin hydride was unsuccessful because the two reactants are present in different phases and as a result insufficient mixing occurs. Longer reaction times and more vigorous stirring may help to effect this synthesis.

4.3.2 Tin(IV) fluoride.

It was proposed that in addition to the fluorination of organic compounds using calcium fluoride, the fluorination of inorganic materials should also be investigated. Tin(IV) fluoride was identified as a target product, again utilising tin(IV) chloride as the starting material.

²¹ A. E. Finholt, A. C. Bond, Jr., K. E. Wolzbach and H. I. Schlesinger, *J. Am. Chem. Soc.*, 1947, **69**, 2692.

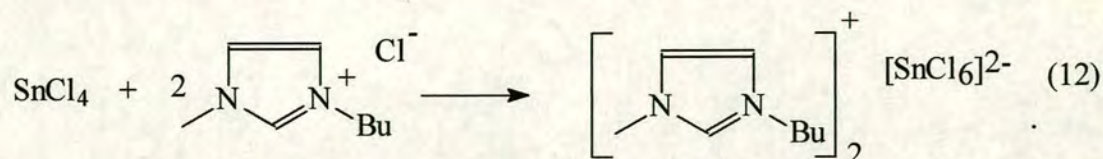
Tin(IV) fluoride is conventionally synthesised from the fluorination of tin oxide, SnO,²² but it has also been synthesised by reaction of elemental tin with NF₃O.²³ In an attempt at the fluorination, tin(IV) chloride was condensed into a mixture of calcium fluoride in bmimPF₆ *via* the vacuum line.



Tin(IV) chloride (4.464 g, 0.0171 mole) was condensed into a mixture of calcium fluoride (2.67 g, 0.342 mole) in bmimPF₆ (15 cm³) at -196 °C. The mixture was then warmed to room temperature and resulted in the production of two layers, assumed to be the unreacted reagents on the basis that tin(IV) fluoride exists as a white solid at room temperature. Synthesis of a tin(IV) chloride – diethyl ether complex was achieved by addition of some of the mixture to diethyl ether. Addition of water to this mixture yielded a layer of unchanged ionic liquid. It was thus concluded that the synthesis of tin(IV) fluoride had been unsuccessful.

4.3.3 Hexachlorostannate (IV) derivative

There are a number of salts of SnCl₆²⁻ known and these are generally prepared by mixing solutions of metal chlorides with tin(IV) chloride. It was therefore proposed that combination of tin(IV) chloride and two equivalents of bmimCl would result in the formation of (bmim⁺)₂SnCl₆²⁻. This was performed by condensing, *via* the vacuum line, tin (IV) chloride (10.04 g, 0.0385 mole) into a sample of bmimCl (13.46 g, 0077 mole) at -196 °C and then warming to room temperature.



²² H. M. Haendler, S. F. Bartram, W. J. Bernard and D. Kippax, *J. Am. Chem. Soc.*, 1954, 2179 - 2180.

²³ O. D. Gupta, L. Kirchmeier and J. M. Shreeve, *Inorg. Chem.*, 1990, **29**, 573 - 574.

The mixture was heated to melt the bmimCl and this resulted in the production of a light yellow solid (mp 125 °C) which appeared to be stable in air. Chemical analysis of the product revealed carbon, hydrogen and nitrogen content of 28.2, 4.54 and 8.51 %, respectively. The values expected for (bmim⁺)₂SnCl₆²⁻ are 31.5, 4.96 and 9.19 %. (Carbon, hydrogen and nitrogen values expected for bmim⁺Sn₂Cl₅⁻ are 17.3, 2.73 and 5.06 %, respectively). It was concluded from these results that the synthesis had been successful and attempts to determine the crystal structure of this compound are ongoing.

4.4 Future Work.

The solubility of calcium fluoride in bmimPF₆ makes the utilisation of calcium fluoride as a fluorinating agent a real possibility. Use of this new fluorinating medium has been investigated both for the fluorination of organic and inorganic compounds, but more work needs to be done in this area. The successful fluorination of 1-chloro-2,4-dinitrobenzene is encouraging, although there are clearly aspects of this reaction that are poorly understood. It is suggested that use of other ionic liquids and co-solvents should be investigated and the fluorination of other organic and inorganic compounds should be attempted. It is also proposed that the use of microwave heating could allow the fast and efficient heating of these systems and that this may drive some reactions more effectively than using conventional heating methods.

Utilisation of bmimPF₆ for the synthesis of air sensitive materials, such as stannane, is a further interesting area of work. The negligible vapour pressure of the imidazolium-based ionic liquids make them ideally suited for use under the high vacuum conditions required for the synthesis of a number of main group compounds. It is possible that utilisation of an ionic liquid could effect the synthesis of materials that are otherwise troublesome under the solvent-free conditions that are normally used.

5 Hydrogenation Reactions in Chiral Ionic Liquids.

5.1 Heterogeneous Hydrogenation.

5.1.1 Introduction.

To date there has been only one report of the use of an ionic liquid as a medium for heterogeneous hydrogenation. *Carlin et al.*¹ report the use of a membrane composed of bmimPF₆ and poly(vinylidene fluoride)-hexafluoropropylene impregnated with palladium to effect the heterogeneous hydrogenation of propene. *Carlin et al.* have also reported the use of a similar membrane containing a rhodium catalyst for the hydrogenation of propene and ethene, but because of the catalysts involved they describe these processes as homogeneous not heterogeneous.² There have been no reports of the use of Raney nickel in an ionic liquid.

¹ R. T. Carlin and J. Fuller, *Chem. Commun.*, 1997, 1345 – 1346.

² T. H. Cho, J. Fuller and R. T. Carlin, *High Temp. Material Processes*, 1998, **2**, 4, 543 – 558.

5.1.2 Raney Nickel.

Raney nickel is a versatile heterogeneous catalyst used in a wide range of organic reactions. It can be prepared by a variety of methods that result in a number of different forms of catalyst, with varying hydrogen content and reactivity.³ The Raney nickel used in this investigation was obtained commercially as a water slurry and dried under vacuum before use. It is essential that the reagent is never exposed to air when dry to avoid spontaneous ignition.

Raney nickel can be used for a range of reactions, most commonly desulfurisations, but it has also found widespread applications in deoxygenation, deamination and deselenation reactions, as well as the reductive amination of carbonyl groups and the cleavage of heteroatom to heteroatom bonds.⁴

Raney nickel is rarely the first choice of catalyst for the hydrogenation of organic compounds, often being overlooked in favour of platinum and palladium compounds. However, studies have shown that whilst the amount of catalyst required for a specific rate of hydrogenation might be higher for Raney nickel, under the same mild conditions the most active forms of Raney nickel can be just as effective and often more selective than the platinum or palladium alternative. The use of Raney nickel for hydrogenation has, in fact, become the focus of much attention in recent years with interest centring on its use in asymmetric hydrogenation.

Enantioselective synthesis is a vast area of research and the drive to produce enantiomerically pure compounds cannot be overestimated, particularly in the area of medicinal chemistry where the presence of any undesirable isomers can have devastating effects. Synthesis of chiral products by asymmetric catalysis requires the introduction of asymmetry into the reaction. The strategy of using enantio-differentiating hydrogenation over a heterogeneous catalyst to produce optically pure

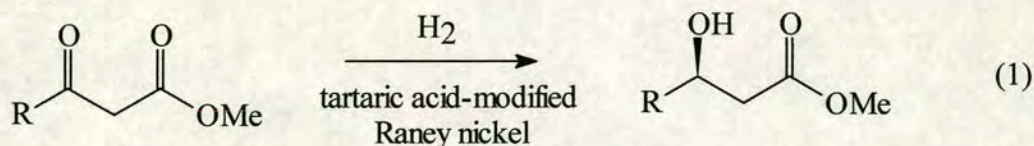
³ S. J. Thomson and G. Webb, *Heterogeneous Catalysis*, Oliver and Boyd.

⁴ *Handbook of Reagents for Organic Synthesis; Oxidising and Reducing Agents*, p335 – 339. Ed. S. D. Burke and R. L. Danheiser. J. Wiley and Sons.

compounds has found success at an industrially useful level using two reagents (i) cinchona-modified platinum catalysts and (ii) tartaric acid-modified Raney nickel.⁵ Raney nickel can be used in its untreated state for asymmetric reductive amination, as detailed by Blacklock *et al.*⁶, but the chirality must be introduced by the use of a chiral reagent, in this case a chiral amine.

The use of modified Raney nickel was first described by Isumi *et al.* in 1963 and centres on the use of tartaric acid to bind to the surface of the nickel to produce enantio-differentiating sites which thereby introduce asymmetry.⁷ The hydrogenation activity and the enantio-differentiating ability of the catalyst were both reported to improve on ultrasound irradiation of the Raney nickel during the preparation. The preparative procedure to coat the Raney nickel surface with the tartaric acid has a significant effect on the performance of the catalyst and can vary in temperature and pH, source of nickel and co-modifier (usually sodium bromide). The modifier itself, tartaric acid, was initially chosen from over a hundred other compounds tested.⁵ The hydrogenation of a range of prochiral ketones, including cyclic and acyclic β -ketoesters,⁸ using modified Raney nickel has been successful in producing the respective alcohol in greater than 70% enantiomeric excess.

The use of the tartaric acid-modified Raney nickel for asymmetric reduction has been illustrated by the hydrogenation of a range of methyl-3-oxoalkanoates. The enantiomeric excess obtained in each case exceeded 60%. The highest enantiomeric excess observed was for the methyl-3-oxopentanoate species, at 92%.



R = Me, Et, Hept, Nonyl, Undecyl.

⁵ T. Osawa, T. Harada and O. Takayasu, *Topics in Catalysis*, 2000, **13**, 155 – 168.

⁶ T. J. Blacklock, R. F. Shuman, J. W. B. Butcher, W. E. Shearin Jr., J. Budavari and V. J. Grenda, *J. Org. Chem.*, 1998, **53**, 836 – 844.

⁷ Y. Izumi, M. Imaida, H. Fukawa and S. Akabore, *Bull. Chem. Soc. Jpn.*, 1963, **36**, 21 – 22.

⁸ G. Wittmann, G. Gondos and M. Bartok, *Helv. Chimica Acta.*, 1990, **73**, 635 – 639.

The successful use of surface-modified Raney nickel to introduce asymmetry and thus effect asymmetric hydrogenation led us to investigate whether similar success could be achieved using Raney nickel in a chiral ionic liquid, where the asymmetry is supplied by the ionic liquid. It was believed that if sufficient co-ordination occurred between the Raney nickel and the chiral solvent, then enantio-differentiating sites could be produced thus enabling asymmetric hydrogenation to take place without the need for the complicated procedure for coating the Raney nickel.

To test this hypothesis it was necessary to address three issues. The primary objective was the synthesis of a chiral ionic liquid, with a suitably low melting point and ideally possessing air- and water-stability. Secondly, there was a need to establish the suitability of this new ionic liquid as a solvent for hydrogenation. Only then could the binding of this liquid to Raney nickel and thus the suitability of this compound as a solvent for asymmetric hydrogenation be assessed.

5.1.3 Synthesis of a Chiral Ionic Liquid.

5.1.3.1 Synthesis of *bis*-(1-butyl-3-methyl imidazolium) tartrate.

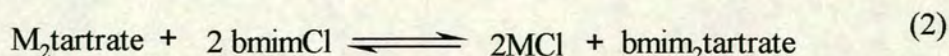
The first ionic liquid chosen for synthesis was the (bmim)₂tartrate, so as to allow direct comparison with the tartaric acid-modified Raney nickel. Metathesis from the bmimCl species was attempted using a variety of reaction conditions, as shown in Table 5.1, but none of these were successful.

Chloride	Tartrate salt	Solvent	Temperature / °C	Time / hours
BmimCl	Sodium tartrate	water	100	36
BmimCl	Sodium tartrate	methanol	80	72
BmimCl	Ammonium tartrate	none	150	1
BmimCl	Ammonium tartrate	none	150	10
BmimCl	Ammonium tartrate	water	100	24
BmmimCl	Sodium tartrate	water	100	72

Table 5.1. Attempted synthesis of *bis*-(1-butyl-3-methyl imidazolium) tartrate.

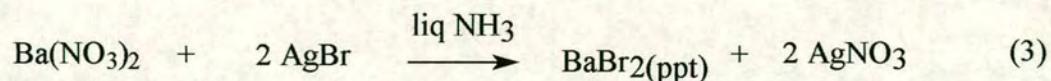
At the conclusion of each of these reactions only unreacted bmimCl and tartrate salt were recovered.

This suggests that the equilibrium position of the reaction (2) lies well over to the left and is presumably dominated by the higher lattice energy of M₂tartrate compared with bmim₂tartrate.



It is evident from the synthetic attempts that heating the reaction has no effect on the position of this equilibrium. However, it is possible that the use of a different solvent system might change the equilibrium position. Metathesis reactions are known to be highly solvent dependent, as the position of the equilibrium depends on the relative solubilities of each of the components in the solvent system chosen. An excellent

example of this is the metathesis reaction between silver bromide and barium nitrate that proceeds in liquid ammonium, according to (3), owing to the high solubility of the $[\text{Ag}(\text{NH}_3)_2]^+$ complex and the insolubility of BaBr_2 . This is the reverse of the aqueous reaction.

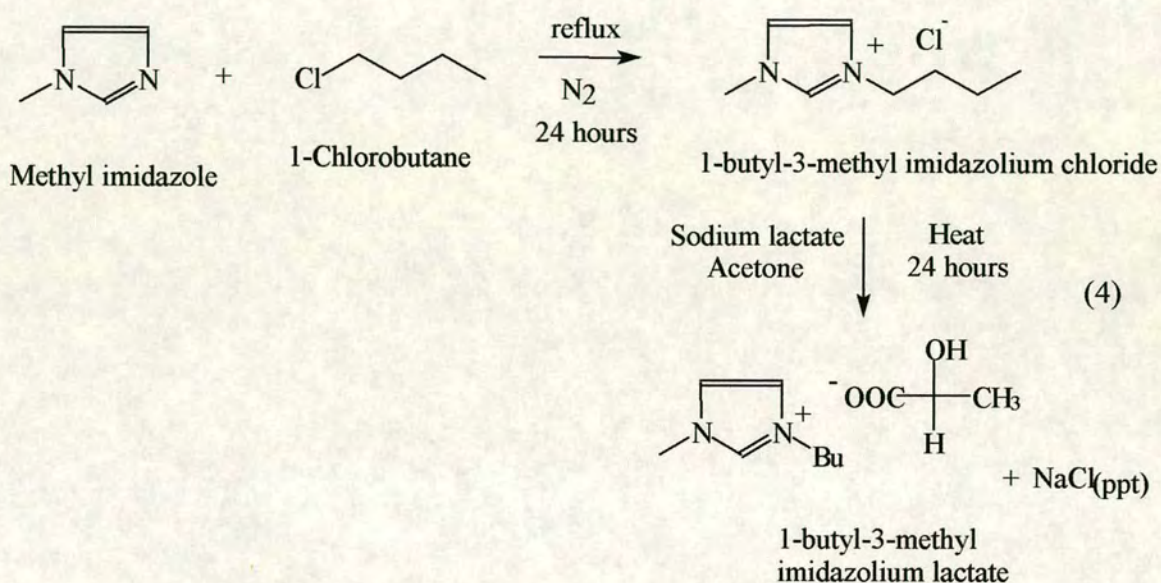


Clearly, for the synthesis of significant quantities of an ionic liquid, liquid ammonia may not be a suitable solvent, but it is suggested as an area of future work that alternative solvent systems be investigated.

It was proposed that the preparation of chiral ionic liquids containing uni-positive and uni-negative ions would be easier than for ionic liquids containing di-positive species, hence synthesis of a chiral ionic liquid was investigated using an alternative chiral anion.

5.1.3.2 Synthesis of 1-butyl-3-methyl imidazolium lactate.

Like the other 1-butyl-3-methyl imidazolium-based ionic liquids, the lactate can be prepared by metathesis from bmimCl. This was achieved by refluxing with L (+) sodium lactate in acetone for 24 hours under nitrogen to give a solution of the 1-butyl-3-methyl imidazolium lactate and a precipitate of sodium chloride, which was easily removed by filtration.

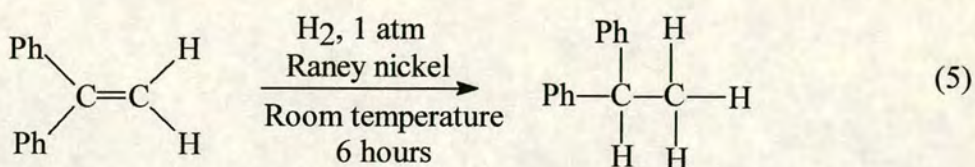


Removal of the acetone under vacuum gave a pale yellow, highly viscous liquid at room temperature. This liquid rotated the plane of optically polarised light, hence contained one enantiomer of a species with a chiral centre. This suggested the presence of the lactate anion. ^1H NMR, IR and elemental analysis confirmed the successful synthesis of this ionic liquid.

5.1.4 Suitability of 1-butyl-3-methyl imidazolium lactate as a Hydrogenation Solvent.

5.1.4.1 Hydrogenations using Hydrogen Gas.

The hydrogenation preference of Raney nickel is known to increase in the order alkenes \approx alkynes \approx nitro groups $>$ imines $>$ aldehydes \approx ketones \approx nitriles. Thus, the activity of the Raney nickel used in the study was confirmed by the hydrogenation of the simple alkene *cis*-stilbene (1,1-diphenyl ethene).



The *cis*-stilbene was successfully hydrogenated to 1,1-diphenyl ethane using the Raney nickel, dried as described and using tetrahydrofuran as the solvent. The hydrogen was supplied at atmospheric pressure by bubbling hydrogen gas through the reaction mixture *via* a syringe needle. The hydrogenation was complete within 6h at room temperature, which confirmed the catalytic activity of the Raney nickel.

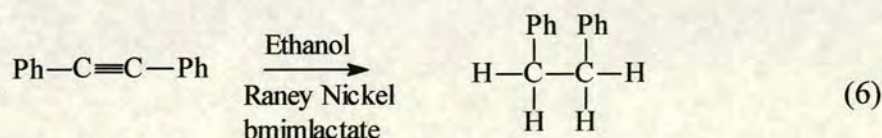
This procedure was then extended to 1-butyl-3-methyl imidazolium lactate as the solvent for hydrogenation. The hydrogenation of *cis*-stilbene was repeated as before, over 7h at room temperature, using bmim lactate as the solvent. *Cis-stilbene* is immiscible with the bmim lactate ionic liquid, but the two layers can be emulsified by stirring during the reaction. Allowing the mixture to settle produced two layers, thus enabling a sample of the upper layer to be easily removed. Analysis of the reaction product showed that no hydrogenation of the *cis*-stilbene had taken place. This suggests that when utilising bmim lactate as a solvent for alkene hydrogenation harsher conditions are required.

5.1.4.2 Hydrogenation using a Hydride Donor.

Transfer hydrogenation (or hydrogen-transfer reaction) is the reduction of multiple bonds using a hydrogen donor in place of hydrogen gas. This involves the abstraction of a hydrogen atom from a donor, by a catalyst, followed by addition to the functional group of a substrate (the hydrogen acceptor). The donors are commonly primary or secondary alcohols, including methanol, ethanol, benzyl alcohol or isopropanol, or unsaturated hydrocarbons such as cyclohexene or cyclohexadiene. Formic acid and its salts are also commonly used and, occasionally, inorganic reagents such as hydrazine. This method can be used to hydrogenate a large number of different substrates including ketones, imines, nitro groups and α,β -unsaturated carbonyl compounds, acids and esters. Transfer hydrogenation has been successfully utilised in both heterogeneous and homogeneous catalysis.⁹

The combination of Raney nickel and a hydride donor can be used to reduce unhindered alkenes and alkynes at room temperature, some hindered alkenes at higher temperatures and aromatic compounds at elevated temperatures and extended reaction times.¹⁰ Carbonyl groups in both aryl ketones and aryl aldehydes can be reduced to their respective methylene derivatives.¹¹

The hydrogenation of a substrate using a hydride donor in a sample of bmim lactate was tested using diphenyl acetylene as the substrate. This reaction has been reported previously using ethanol as both the solvent and the hydride donor.¹² The hydrogenation of the alkene, *cis*-stilbene, used above, has also been reported using this method, with both species giving the fully saturated dibenzyl product. However, it was decided to study the alkyne first as this species shows a higher preference for hydrogenation.



⁹ G. Zassinovich and G. Mestroni, *Chem. Rev.*, 1992, 92, 1051 – 1069.

¹⁰ P. M. Pojer, *Chemistry and Industry*, March 1986.

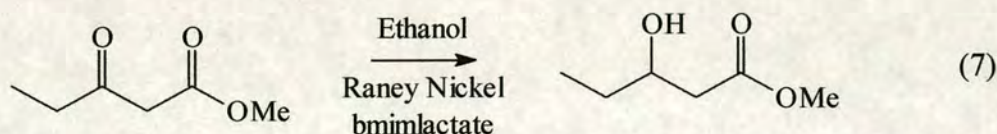
¹¹ R. H. Mitchell and Y. Lai, *Tet. Lett.*, 1980, 21, 2637 - 2638.

A suspension of Raney nickel, prepared as before, containing diphenyl acetylene in bmim lactate and a small quantity of ethanol was refluxed for eight hours under an inert atmosphere. The Raney nickel was then removed by filtration and the ethanol removed by distillation. Diethyl ether extraction of the bmim lactate solution gave a mixture of unreacted diphenyl acetylene and the fully hydrogenated bibenzyl product in a ratio of approximately 1:4. The successful hydrogenation of diphenyl acetylene indicates the suitability of bmim lactate as a heterogeneous hydrogenation solvent.

5.1.5 Use of a Chiral Ionic Liquid as an Asymmetric Hydrogenation Solvent.

Following the successful demonstration of bmim lactate as a solvent for heterogeneous hydrogenation, the next area of investigation was its extension to asymmetric heterogeneous hydrogenation.

The hydrogenation of the diketone methyl-3-oxopentanoate, as described previously (section 5.1.2),¹³ was attempted in bmim lactate.

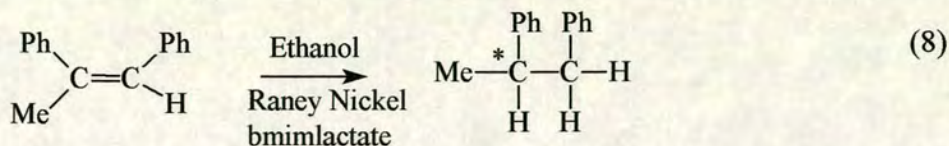


The diketone was refluxed with a solution of Raney nickel and ethanol in bmim lactate for 48 hours under nitrogen. However, attempts to isolate the product by both distillation and extraction with diethyl ether failed to give the desired product, and resulted only in the isolation of a number of aliphatic compounds, as indicated by the ¹H NMR spectrum.

The hydrogenation of a pro-chiral alkene was attempted as this species should exhibit higher activity towards hydrogenation than the pro-chiral ketone, and the successful hydrogenation of a related system, diphenyl acetylene, in bmim lactate had been demonstrated.

¹² E. C. Kleiderer and E. C. Kornfeld, *J. Org. Chem.*, 1948, 13, 455.

¹³ S. Nakagawa, T. Sugimura and A. Tai, *Chem. Lett.*, 1998, 1257 – 1258.



α -Methyl stilbene was refluxed in a solution of ethanol and bmim lactate with Raney nickel for 7h and then extracted with diethyl ether and hexane, but no hydrogenated product was observed. The reaction was repeated using isopropanol as the hydride donor, with a reaction time of 12h, but again no hydrogenated product was formed. It is proposed that unsuccessful hydrogenation of this compound may be due to steric hindrance. Hydrogenation of a less sterically hindered pro-chiral alkene is suggested as an area of future work.

5.1.6 Decomposition of bmim lactate with Raney Nickel.

It was observed throughout these investigations that isolation of the products of each reaction by vacuum distillation gave ^1H NMR spectra with similar features for each reaction. It was common to observe a number of unidentified aliphatic peaks in each spectrum and also three unidentified signals in the aromatic region of the spectrum. It was postulated that these peaks were due to the decomposition of the bmim lactate during the hydrogenation reactions. This was confirmed by refluxing a slurry of Raney nickel in bmim lactate and ethanol for 72 hours under nitrogen. The Raney nickel was removed by filtration and then the ethanol and any decomposition product removed by vacuum distillation. ^1H NMR analysis of the distillate revealed the same peaks as observed in previous reactions. These were identified as methyl imidazole and butanol, indicating that the substituted imidazolium ring had been dealkylated.

5.1.7 Conclusions.

The chiral room temperature ionic liquid 1-butyl-3-methyl imidazolium lactate has been successfully prepared. Heterogeneous hydrogenation was found to proceed in this new solvent using Raney nickel, with the hydrogen atoms supplied by a hydride donor, at moderate temperatures and ambient pressures. However, the identification of a significant quantity of decomposition products produced on heating bmim lactate with Raney nickel indicates that this particular ionic liquid is unsuitable for heterogeneous hydrogenations of this type. However, it is proposed that use of a different cation, such as the tetrabutyl ammonium cation, in combination with the chiral anion might give a chiral ionic liquid more stable towards hydrogenation or decomposition. It is expected that such an ionic liquid could then be used for the enantioselective hydrogenation of organic compounds.

5.2 Homogeneous Hydrogenation.

5.2.1 Introduction.

Although the use of homogeneous catalysis for hydrogenation is a relatively new field, and significantly newer than that of heterogeneous catalysis, the success of this technique has made it a very widely studied area over the last twenty years. The first truly successful system for the hydrogenation of alkenes, alkynes and other unsaturated double bonds came with the discovery of $\text{RhCl}(\text{PPh}_3)_3$ - Wilkinson's catalyst, which can be used at ambient temperatures and pressures. This has since been followed by the discovery of a wide range of catalysts that dissolve in organic solvents and hence catalyse the hydrogenation reactions in a single phase in solution. Homogeneous catalysts fall into three categories: those with a metal-hydrogen bond e.g. $\text{RuHCl}(\text{PPh}_3)_3$; those without, such as Wilkinson's catalyst; and hydrides of the f-block elements.

The advantages of homogeneous catalysis over heterogeneous lie in the enhancement of the rate of reaction, and the potential for greatly enhanced selectivity. The disadvantage is the difficulty in separating the products from the solution on completion of the reaction. Steps to overcome this problem have recently involved the use of solid supports for the catalyst that can be filtered off at the end of the reaction. Although this technically defines the reaction as heterogeneous, the hydrogenations still follow a homogeneous mechanism,¹⁴ thus retaining the advantages of high rate and selectivity.

The high selectivity of homogeneous catalysis stems from the wide variety of ligands available for use with the metal catalyst. These can be tailored to maximise rate and / or selectivity for each reaction individually. The use of chiral ligands can be used to introduce asymmetry into the reaction site and thus effect enantioselective hydrogenation. In all cases the role of the catalyst is to lower the energy of activation of the hydrogenation reaction to allow the reaction to proceed at moderate temperatures. It does this by binding the reactants to the metal atom, allowing the reaction to proceed *via* a different mechanism, as shown in Figure 5.1.

¹⁴ R. T. Morrison and R. N. Boyd, *Organic Chemistry*, 5th Ed, Allyn and Bacon, Inc.

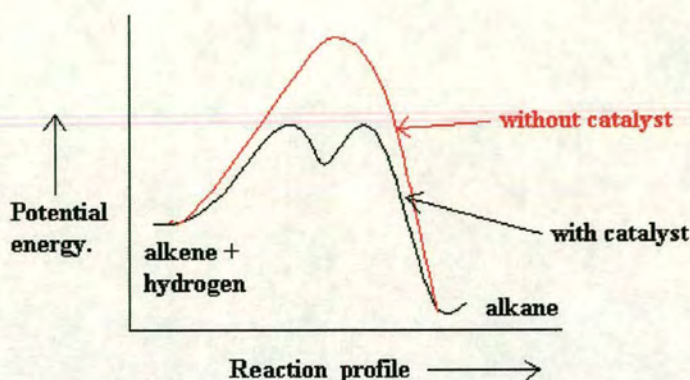


Figure 5.1 The effect of a catalyst on the energetics of a reaction.

In homogeneous catalysis the hydrogen-hydrogen bond of H_2 is broken and the hydrogen atoms transferred one at a time to the substrate. An example of this mechanism for Wilkinson's catalyst is shown in Figure 5.3.

5.2.2 Homogeneous Hydrogenations in Ionic Liquids.

The use of ionic liquids as media for homogeneous hydrogenation has significant advantages over molecular solvent systems. The main advantage lies in the easy separation of the products from the reaction. The ionic liquid is immiscible with the organic reactants and so the reaction mixture exists in two phases, as shown in Figure 5.2. The transition metal catalyst is dissolved in the lower ionic liquid layer and vigorous stirring of the solution allows sufficient mixing for catalysis to occur. On completion of the reaction the product now forms the upper layer and can simply be decanted off.

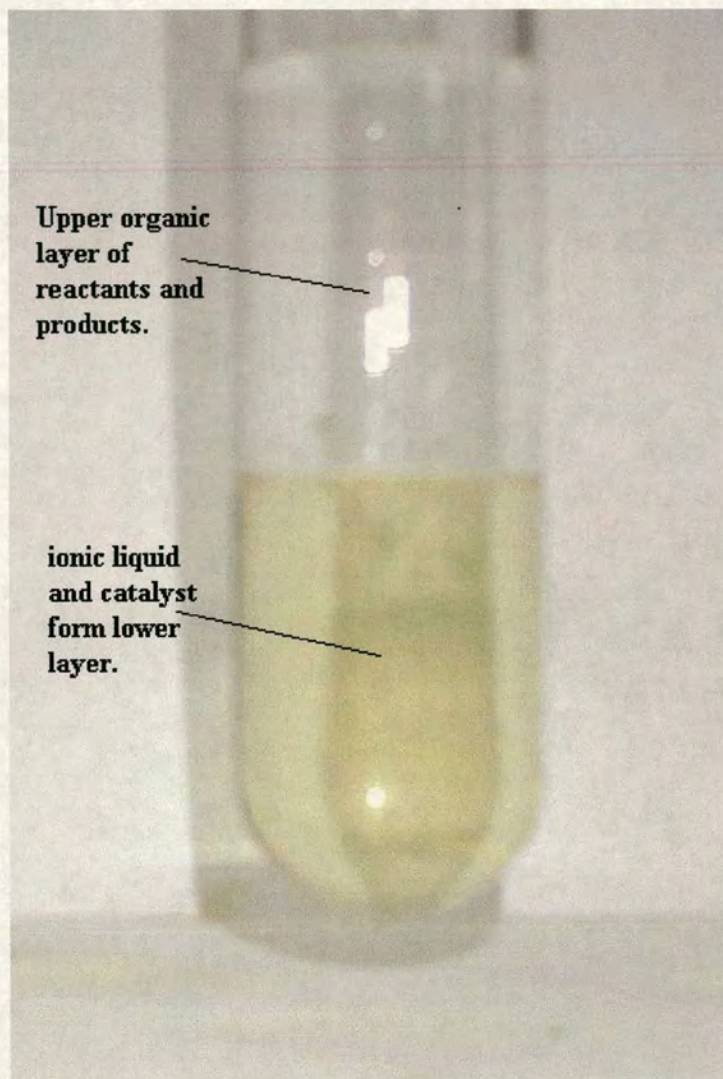


Figure 5.2. The immiscibility of bmimPF_6 and organic compounds utilised in biphasic catalysis.

This technique is commonly referred to as biphasic catalysis and avoids the need for any extraction or distillation. The use of any volatile organic compounds (VOCs) is also avoided. Use of this technique also means that the reaction can potentially be performed as a continuous stream process as the catalyst normally exhibits only a small loss of activity after each reaction and leaching into the upper layer is negligible. It is this potential of the ionic liquid-biphasic catalysis to form a recyclable and VOC-free system that has driven much of the research in this field,

particularly with respect to the development of processes that have a reduced environmental impact.

The first report of the use of an ionic liquid for biphasic homogeneous hydrogenation appeared in 1995 and was based on the use of 1-butyl-3-methyl imidazolium ionic liquids and rhodium catalysts.¹⁵ The catalyst $[\text{Rh}(\text{norbornadiene})(\text{PPh}_3)_2]^+\text{PF}_6^-$ was successfully dissolved in bmimPF_6 and bmimSbF_6 and found to catalyse the hydrogenation of pent-1-ene at a higher conversion and a higher rate than when acetone was used as a solvent. The observed rate and conversion with bmimBF_4 was poor by comparison, and Chauvin *et al.* postulated that chloride poisoning of the catalyst from impurities in the ionic liquid was responsible.

Conjugated diolefins are more soluble in ionic liquids than the monoalkenes and these can also be hydrogenated using the same catalyst and conditions (0.1MPa of hydrogen, 30 °C). The active species in these hydrogenations is believed to be a cationic unsolvated dihydrido-rhodium species with two coordination sites available for the binding of the alkene. This rhodium norbornadiene catalyst has also been studied by Cho *et al.*¹⁶ as a catalyst for the hydrogenation of propene and ethene by incorporation of the catalyst and ionic liquid into a membrane of poly(vinylidene fluoride) filter membranes. This method was successful for such hydrogenations, but the mechanism and advantages of such a process differ from the use of ionic liquids as solvents for biphasic homogeneous catalysis.

Ruthenium catalysts dissolved in ionic liquids have also found success in the homogeneous hydrogenation of unsaturated compounds. Catalysts studied include $\text{RuCl}_2(\text{PPh}_3)_3$ for the hydrogenation of olefins,¹⁷ and $[\text{Ru}_4(\eta^6\text{C}_6\text{H}_6)_4][\text{BF}_4]$ in bmimBF_4 for the hydrogenation of arenes.¹⁸

1-butyl-3-methyl imidazolium ionic liquids will also dissolve palladium catalysts and studies have been performed on the use of palladium acetate in bmimBF_4 for the selective two-phase hydrogenation of dienes into monoenes.¹⁹

¹⁵ Y. Chauvin, L. Mussmann and H. Olivier., *Angew. Chem. Int. Ed. Engl.*, 1995, **34**, 2698 - 2700.

¹⁶ T. H. Cho, J. Fuller and R. T. Carlin, *High Temperature Material Process*, 1998, **2** (4), 543 – 558..

¹⁷ P. A. Z. Suarez, J. E. L. Dullius, S. Einloft, R. F. deSouza and J. Dupont, *Inorg. Chimica Acta*, 1997, **255**, (1), 207 – 209.

¹⁸ P. J. Dyson, D. J. Ellis, D. J. Parker and T. Welton, *Chem. Comm.*, 1999, **1**, 35 – 36..

¹⁹ J. Dupont, P. A. Z. Suarez, A. P. Umpierre and R. F. de Souza, *J. Brazilian Chem. Soc.*, 2000, **11**, 293 - 297.

The most recent reports of the use of ionic liquids for hydrogenation reactions focus on the use of supercritical carbon dioxide as the second layer in the biphasic reaction. The principal of biphasic catalysis remains the same but with the added advantage that reducing the pressure converts the supercritical CO₂ back into the gaseous form for recovery and re-use and allows effective isolation of the reaction products. CO₂ dissolves in up to 0.6 mole fraction in bmimPF₆, but none of the bmimPF₆ dissolves in the scCO₂.²⁰

Hydrogenation reactions using Wilkinson's catalyst in the bmimPF₆/scCO₂ system is reported by Liu *et al.*²¹ to proceed effectively for the hydrogenation of alkenes. Dec-1-ene is hydrogenated to n-decane with 98 % conversion after one hour using 48 bar of hydrogen. The product was recovered by transferring the scCO₂ phase under high pressure. The ionic liquid phase was then recharged with dec-1-ene, hydrogen and carbon monoxide. The hydrogenation reaction proceeded four times with the same catalyst system with conversions of approximately 98 %. However, this activity is the same as that observed for the bmimPF₆/n-hexane system indicating no reactivity advantage of scCO₂ over more conventional biphasic systems. The advantages of this system are capitalised more effectively for reactions that proceed through polar intermediates that are soluble in the bmimPF₆ and not in the scCO₂. For example, the catalytic hydrogenation of CO₂ to formamides in the presence of dialkylamines proceeds with increased activity and selectivity (i.e. formic acid versus formamide production) compared to the reaction in neat scCO₂.

²⁰ L. A. Blanchard, Z. Gu and J. F. Brennecke, *J. Phys. Chem. B*, 2001, **105**, 2437 – 2444.

²¹ F. Liu, M. B. Abrams, R. T. Baker and W. Tumas, *Chem. Commun.*, 2001, 433 – 434.

5.2.3 Asymmetric Homogeneous Hydrogenation in Ionic Liquids.

Studies involving the use of ionic liquids for asymmetric homogeneous hydrogenation are scarce amongst the literature, and all rely on the introduction of asymmetry into the reaction through use of a chiral catalyst. Montiero *et al.*²² reported the use of a chiral ruthenium compound, $[\text{RuCl}_2\text{-(S)-BINAP}]_2\cdot\text{NEt}_3$ to hydrogenate 2-phenylacrylic acid in bmimBF_4 , to give 2-phenylpropionic acid in more than 60% enantiomeric excess. This is an equivalent or higher enantiomeric excess compared to the use of conventional solvents, but with all the advantages of biphasic catalysis afforded by the use of an ionic liquid.

In a recent publication, Brown *et al.*²³ described the use of bmimPF_6 and a chiral ruthenium catalyst for the enantioselective hydrogenation of 2-methyl-2-butenoic acid (tiglic acid) to 2-methyl-2-butanoic acid, where the product is removed from the reaction using supercritical carbon dioxide. Similarly, they describe the asymmetric hydrogenation of isobutylatropic acid to give the anti-inflammatory ibuprofen. The former hydrogenation proceeded readily in wet bmimPF_6 with the hydrogen pressure dictating the enantioselectivity of the reaction. The synthesis of ibuprofen proceeded with poor enantioselectivity in wet bmimPF_6 but with good enantioselectivity (85 % at 100 bar H_2) with methanol added to the ionic liquid. This selectivity was better than that observed for the aqueous/organic biphasic system.

In a drive to retain the benefits of using an ionic liquid for hydrogenation, but avoid the use of costly chiral catalysts, it was decided that the use of an asymmetric catalyst in a chiral ionic liquid should be investigated and the hydrogenation properties of the catalyst investigated. It was postulated that use of the chiral ionic liquid would provide the necessary introduction of asymmetry for enantioselective hydrogenation, provided sufficient coordination of the ionic liquid and the catalyst occurred. It was decided to use Wilkinson's catalyst to study the feasibility of asymmetric hydrogenation in chiral ionic liquids.

²² A. L. Monteiro, F. K. Zinn, R. F. deSouza and J. Dupont, *Tet. Asymm.*, 1997, **8** (2), 177 - 179.

5.2.4 Wilkinson's Catalyst.

Chloro-*tris*(triphenylphosphine)rhodium(I), commonly known as Wilkinson's catalyst, was discovered in 1966²⁴ and was one of the first catalysts to be used for the homogeneous hydrogenation of a variety of carbon-carbon double and triple bonds. It can be conveniently prepared by the reaction of triphenyl phosphine and rhodium(III) chloride in ethanol, with the rigorous exclusion of oxygen from the reaction.²⁵ The catalyst itself is air sensitive, but can be purchased commercially from Sigma-Aldrich in a suitably pure form.

Wilkinson's catalyst can be used for the hydrogenation of unconjugated alkenes at ambient temperatures and pressures, although the steric environment of the alkene affects the reactivity - unhindered alkenes react quickly whereas sterically crowded species may not react at all.

The compound chloro-*tris*(triphenylphosphine)rhodium is not a catalyst in the strictest sense, but is actually a catalyst precursor. The active species forms on exchange of one of the triphenyl phosphine groups with a solvent molecule. This species then comes into contact with molecular hydrogen and the alkene, and the hydrogenation takes place in a step-wise fashion as shown in Figure 5.3.

²³ R. A. Brown, P. Pollet, E. M^cKoon, C. A. Eckert, C. L. Liotta and P. G. Jessop, *J. Am. Chem. Soc.*, 2001, **123**, 1254 – 1255.

²⁴ J. A. Osborn, F. H. Jardine, F. H. Young and G. Wilkinson, *J. Chem. Soc. A*, 1966, 171-172.

²⁵ J. A. Osborn and G. Wilkinson, *Inorg. Synth.*, 1990, **28**, 77 - 78.

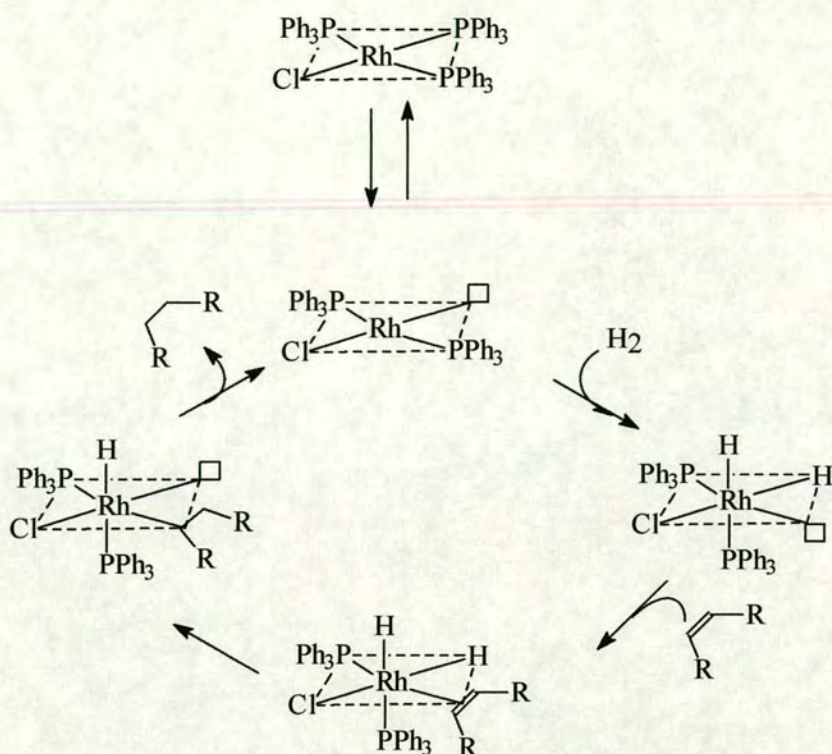


Figure 5.3. The mechanism of hydrogenation using Wilkinson's catalyst.

The addition of di-hydrogen to the alkene is always stereospecifically *cis*. Each hydrogen atom bonds separately to the rhodium thus oxidising rhodium(I) to rhodium(III). The metal is returned to the original oxidation state on the reductive elimination of the alkyl species.

^{31}P NMR can easily monitor the purity of the catalyst prior to reaction where the *cis* and *trans* phosphine groups exhibit characteristic chemical shifts at 31.8 and 48.0 ppm, respectively (CDCl_3). Any phosphine oxide contaminant displays a resonance at 29.2 ppm, and any free triphenyl phosphine is observed at $\delta -6.3$ ppm.²⁶

²⁶ A. B. Shortt, L. J. Durham and H. S. Mosher, *J. Org. Chem.*, 1983, **48** (18), 3215 – 3216.

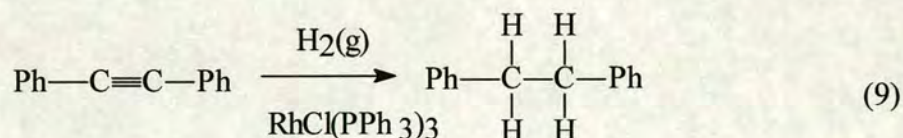
5.2.5 1-butyl-3-methyl imidazolium Lactate as a Solvent for Hydrogenation.

5.2.5.1 Using Hydrogen Gas.

The suitability of the new ionic liquid, 1-butyl-3-methyl imidazolium lactate as a solvent for homogeneous hydrogenation was first assessed using the hydrogenation of cyclohexene as a test reaction. Wilkinson's catalyst is effective for the hydrogenation of less-hindered alkenes at room temperature using hydrogen gas.²⁷ This catalyst has also been successfully utilised in the hydrogenation of cyclohexene in bmimPF₆, although high temperatures and pressures were used.²⁸

Hydrogen was bubbled through a solution of cyclohexene in bmim lactate and RhCl(PPh₃)₃ for five hours at room temperature during which time the cyclohexene remained as an upper layer. The two layers were mixed during reaction by vigorous stirring. At the end of the reaction a sample of the upper layer was removed and found to contain only the unsaturated cyclohexene, indicating no hydrogenation had taken place. It was decided to repeat the experiment using a less-hindered alkene to encourage hydrogenation.

The hydrogenation of diphenyl acetylene was attempted in the same manner at room temperature.



After four hours a sample of the upper organic layer was removed and again found to contain no hydrogenated product. It was concluded from these reactions that to utilise the ionic liquid as a successful hydrogenation solvent for these reactions higher temperatures and pressures would be required. However, the use of high-pressure hydrogen is undesirable owing to the hazards and expense involved in using

²⁷ S. D. Burke and R. L. Danheiser, *Handbook of Reagents for Organic Synthesis*; F. Albert Cotton and G. Wilkinson, *Advanced Inorganic Chemistry*.

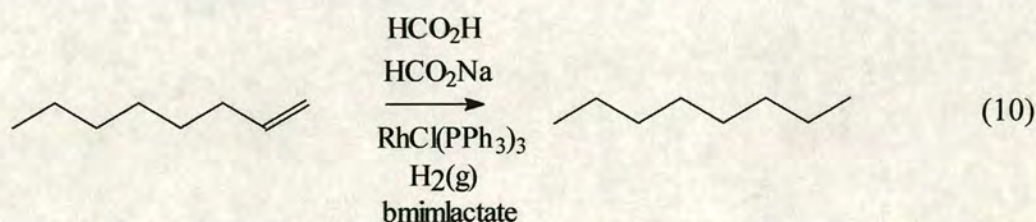
²⁸ P. A. Z. Suarez, J. E. L. Dullius, S. Einloft, R. F. De Souza and J. Dupont, *Polyhedron*, 1996, **15** (7), 1217 – 1219.

high-pressure apparatus. It was decided to use a hydride donor to supply the necessary hydrogen in the hope of effecting the hydrogenation without the need for forcing conditions.

5.2.5.2 Using a Hydride Donor.

For homogeneous hydrogenation the most active hydride donors have been found to be alcohols, cyclic ethers and formic acid. Use of formic acid is particularly advantageous as the release of carbon dioxide on decomposition of this donor is an added driving force in the reaction and prevents the achievement of an equilibrium by prohibiting any back reaction.

Homogeneous hydrogenation using a hydride donor in 1-butyl-3-methyl imidazolium lactate was tested using formic acid as the hydride donor. This is commonly used in conjunction with some sodium formate to increase the degree of reduction.²⁹ Vol'pin *et al.* reported the use of Wilkinson's catalyst to reduce oct-1-ene to octane at 40 °C using a mixture of formic acid and sodium formate at a ratio of octene : formic acid : sodium formate : catalyst of 30 : 100 : 30 : 1. The same ratio was used in an attempt to effect this hydrogenation using bmimlactate as the solvent.



The mixture was heated with a catalytic amount of DMF for 3h but after this time no hydrogenation was observed. Extension of the reaction time to six hours failed to produce any observable hydrogenation.

The hydrogenation of cyclohexene was also attempted under the same conditions but using ten times the previous amount of catalyst, but no hydrogenation was observed after refluxing for seven hours. It was decided to try an alternative hydride donor to effect hydrogenation.

²⁹ M. E. Vol'pin, V. P. Kukolev, V. O. Chernyshev and I. S. Kolomnikov, *Tet. Lett.*, 1971, **46**, 4435 – 4438.

The hydrogenation of octene was attempted using ethanol as the hydride donor. A solution of ethanol, octene and $\text{RhCl}(\text{PPh}_3)_3$ was refluxed for three hours after which time the product was removed by distillation, but only unreacted octene was recovered. The hydrogenation of cyclohexanone using 2-propanol was similarly unsuccessful using bmim lactate as the solvent.

The results of all the hydrogenations attempted in bmim lactate using hydride donors and Wilkinson's catalyst are given in Table 5.2.

Substrate.	Hydride donor.	Temperature/ $^{\circ}\text{C}$	Time / hours.	Hydrogenation?
Oct-1-ene	Formic acid	90	3	No
Oct-1-ene	Formic acid	90	6	No
Cyclohexene	Formic acid	70	7	No
Octene	Ethanol	80	3	No
Cyclohexanone	2-propanol	80	4	No

Table 5.2. Hydrogenation reactions using hydride donors with Wilkinson's catalyst.

5.2.6 Decomposition of the Ionic Liquid.

Following the attempted hydrogenations outlined above, the product was removed directly from the upper layer whenever possible, otherwise distillation was used. ^1H NMR analysis of the distillate revealed not only the absence of any hydrogenated product, but also the presence of significant amounts of other material. The ^1H NMR shifts of these species correspond to butanol and methyl imidazole, indicating the decomposition of the 1-butyl-3-methyl imidazolium cation. The same species were identified on analysis of both distillate and any product collected by ether extraction of the reaction mixtures.

The decomposition of the bmim lactate under these conditions was studied by heating a mixture of sodium formate, formic acid and Wilkinson's catalyst for 24 hours at 100°C , after which time a significant amount of decomposition product was collected. The ^1H NMR spectrum exhibited the same features as observed previously and the spectrum of the remaining ionic liquid showed significantly reduced intensities in the butyl-region.

5.2.7 Interaction of the Ionic Liquid with Wilkinson's Catalyst.

As outlined above, the use of Wilkinson's catalyst for hydrogenation involves the formation of an active species by the displacement of the phosphine group from the metal followed by weak coordination of the solvent species. It is this solvent-coordinated species that is believed to effect the hydrogenation of the unsaturated compound. In an attempt to understand the lack of activity observed during use of Wilkinson's catalyst in the lactate ionic liquid, the ^{31}P NMR of the catalyst dissolved in 1-butyl-3-methyl imidazolium lactate was recorded.

It is possible to perform NMR analysis on a neat sample of ionic liquid, in the absence of any deuterated solvent, by locking the signal to a deuterated solvent immediately prior to running the sample. The high stability of the NMR instrumentation ensures very little shimming between samples, thus the chemical shifts observed can be assumed to be significantly accurate to allow accurate comparison of the ionic samples with those obtained using an internal lock.

The ^{31}P NMR spectrum of the $\text{RhCl}(\text{PPh}_3)_3$ dissolved in the neat lactate ionic liquid showed only one peak, at -6 ppm corresponding to free triphenyl phosphine. This indicates that the phosphine groups have been displaced from the metal, either by the lactate group of the ionic liquid or by the presence of trace chloride impurities present as a result of incomplete metathesis during synthesis, thus rendering the catalyst inactive.

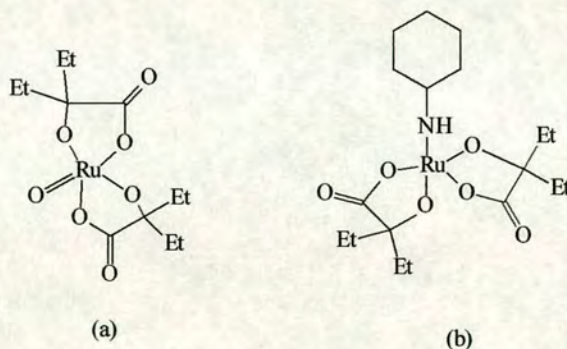
5.2.8 Conclusions.

Attempts to hydrogenate simple alkenes using Wilkinson's catalyst were unsuccessful using both hydrogen gas and a range of hydride donors. Analysis of the products from these reactions indicated decomposition of the imidazolium group of the ionic liquid into methyl imidazole and aliphatic species.

The inactivity of the catalyst in this ionic liquid can be attributed to the displacement of the phosphine groups, from the metal of the catalyst, by the lactate group of the ionic liquid.

5.2.9 Future Work.

An important area of future investigation involves the prevention of displacement of the catalyst ligands by the chiral ionic liquid. One way of doing this may be by utilising an alternative homogeneous catalyst that is not so prone to ligand displacement as Wilkinson's catalyst appears to be. Alternatively, a chiral ionic liquid with a less co-ordinating anion could be used in place of the lactate. The ease of displacement of the triphenyl phosphine groups of the catalyst by the lactate ion may be in part due to the ability of the lactate group to bind in a bidentate fashion. The replacement of a monodentate ligand with a bidentate species on a metal centre has a strong driving force energetically. Removal of this driving force may be sufficient to prevent ligand displacement and deactivation of the catalyst. There are no examples of lactate ions bound to rhodium in the literature, but there are two ruthenium complexes with similar groups bound in a bidentate fashion, analogous to that postulated for the rhodium lactate species.³⁰



³⁰ (a) A. C. Dengel, W. P. Griffith, C. A. O'Mahoney and D. J. Williams, *J. Chem. Soc., Chem. Commun.*, 1989, 1720 – 1721. (b) C. Redshaw, W. Clegg and G. Wilkinson, *J. Chem. Soc., Dalton Trans.*, 1992, 2059 – 2062.

5.2.10 Experimental.

(i) Heterogeneous Hydrogenation.

Potassium lactate: L (+) lactic acid (30 g, 0.33 mole) was neutralised by the dropwise addition of aqueous potassium hydroxide (18.69 g, 0.333 mole). The water was then removed under vacuum giving the product as a colourless solid.

1-butyl-3-methyl imidazolium lactate: 1-butyl-3-methyl imidazolium chloride (46.8 g, 0.268 mole) and potassium lactate (34.3 g, 0.268 mole) were refluxed together in acetone (75 cm³) for twenty four hours under nitrogen. The white precipitate produced was removed by filtration and the acetone removed from the filtrate under vacuum giving a light yellow liquid.

¹H NMR (D₂O) δ : 8.6 (s, 1H, H2), 7.4 (dd, 2H, H4 H5), 4.1 (m, 3H, H6 + lactate OH), 3.8 (s, 3H, Me), 1.8 (m, 2H, H7), 1.3 (m, 5H, H8 + lactate CH₃), 0.85 (3H, t, H9).

$[\alpha]_D = -6.1$ (5893 Å).

IR ν cm⁻¹: 3384 (O-H), 2962 (CH₃), 1599 (CO₂⁻), 1374 (OH).

Precipitate: $[\alpha]_D = 0$. Infrared spectrum shows no features indicating it to be potassium chloride and not potassium lactate.

Elemental analysis. C₁₁H₂₀N₂O₃ requires C 57.9, H 8.83, N 12.3. Found C 57.8, H 9.00, N 12.2.

Hydrogenation of 1,1-diphenyl ethylene in THF and H₂ gas. Raney nickel (3 cm³, water slurry) was dried under vacuum with heating to remove all traces of water. Tetrahydrofuran (8 cm³) was added *via* cannula under nitrogen and 1,1-diphenyl ethylene (*cis*-stilbene, 3 cm³, 0.017 mole) added *via* syringe. Hydrogen was bubbled through the reaction mixture *via* a syringe needle for six hours. The Raney nickel was removed by filtration under suction and the tetrahydrofuran removed by distillation leaving the fully hydrogenated product.

^1H NMR (CDCl_3) δ : 7.3 (m, 10H, Phenyl), 4.2 (m, 1H, CH), 3.8 (THF), 1.9 (THF), 0.7 (3H, d, CH_3).

Hydrogenation of 1,1-diphenyl ethylene in bmimlactate with H_2 gas. Raney nickel (3 cm^3 , water slurry) was dried under vacuum with moderate heating and the bmimlactate (5 cm^3) added *via* cannula. 1,1-diphenyl ethylene (2 cm^3 , 0.011 moles) was added *via* syringe and hydrogen gas bubbled through the slurry for seven hours. The mixture was then left to settle overnight and a sample of the supernatant removed for NMR analysis.

^1H NMR (CDCl_3) δ : 11.2 (bs, 1H, H2), 7.4 (s, *cis*-stilbene), 7.2 (m, 2H, H4 H5), 5.5 (s, *cis*-stilbene), 4.3 (m, H6, 2H), 4.0 (3H, s, Me), 3.7 (bs, 1H, lactate), 1.9 (m, 2H, H7), 1.4 (5H, m, H8 + lactate), 1.0 (3H, m, H9).

Reduction of diphenyl acetylene with Raney nickel and ethanol. Raney nickel (5 cm^3 , water slurry) was dried under vacuum with heating to remove all traces of water. 1-butyl-3-methyl imidazolium lactate (10 cm^3) was dried under vacuum and transferred onto the Raney nickel *via* cannula under nitrogen. This slurry was transferred *via* cannula into a solution of diphenyl acetylene (1 g, 5.6 mmole) and ethanol (5 cm^3). This solution was refluxed for eight hours under nitrogen and then the Raney nickel removed by filtration under suction. The ethanol was removed by distillation and the bmimlactate solution extracted with diethyl ether (60 cm^3). Removal of the diethyl ether under vacuum yielded a yellow oil.

^1H NMR of extracted product: (CDCl_3) δ : 7.5 (m, 5H, diphenyl acetylene), 7.4 (m, 5H, diphenyl acetylene), 7.2 (m, 80H, bibenzyl), 6.6 (s, 15H, aromatic), 2.9 (s, 1H, bibenzyl).

^1H NMR of distillate: (CDCl_3) δ : 7.5 (m, 8H, diphenyl acetylene), 7.3 (m, 8H, diphenyl acetylene), 7.2 (m, 85H, bibenzyl), 7.1 (s, 3H, methyl imidazole), 6.9 (s, 3H, methyl imidazole), 6.6 (s, 13H), 2.9 (s, 3H, bibenzyl), 1.9 (m, 4H, butanol), 1.4 (m, 10H, butanol), 0.9 (m, 6H, butanol). The spectra of both the distillate and the extractant show the presence of diphenyl acetylene and the hydrogenated product, bibenzyl, at a ratio of approximately 1:4.

Hydrogenation of methyl-3-oxopentanoate. Raney nickel (5 cm³, water slurry) was dried under vacuum with gentle warming. Bmim lactate (5 cm³) was added *via* cannula and ethanol (3 cm³) and methyl-3-oxopentanoate (methyl propionyl acetate, 3 cm³, 0.024 mole) added *via* syringe. The mixture was refluxed for 48 hours under nitrogen with vigorous stirring. The Raney nickel was then removed by filtration and the products removed by vacuum distillation.

¹H NMR (CDCl₃) δ: 7.4 (s, 1H, methyl imidazole), 7.0 (s, 1H, methyl imidazole), 6.8 (s, 1H, methyl imidazole), 3.9 (t, 3H, decomposition product), 3.6 (s, 1H, butanol), 3.3 (bs, 3H, butanol), 1.7 (m, 3H, butanol), 1.4 (m, 6H, butanol), 0.9 (m, 9H, butanol). Spectrum shows only the presence of methyl imidazole and butanol indicating decomposition of the bmimlactate.

Hydrogenation of α-methyl stilbene. Raney nickel (5 cm³, water slurry) was dried under vacuum with gentle warming. Bmim lactate (10 cm³) was added *via* cannula and ethanol (3 cm³) and α-methyl stilbene (1g, 5.15 mmole) added. The mixture was refluxed for 7 hours under nitrogen with vigorous stirring. The Raney nickel was then removed by filtration and the reaction mixture extracted with diethyl ether (50 cm³) and hexane (25 cm³).

¹H NMR (CDCl₃) δ: 7.4 (m, 10H, Ph), 6.9 (s, 1H, CH), 2.3 (s, 3H, Me).

The reaction was repeated using the same conditions as above using isopropanol (3 cm³) and a reaction time of 12 hours. The Raney nickel was then removed by filtration and the reaction mixture extracted with diethyl ether (50 cm³) and hexane (25 cm³).

¹H NMR (CDCl₃) δ: 7.4 (m, 10H, Ph), 6.9 (s, 1H, CH), 2.3 (s, 3H, Me).

Degradation of bmimlactate by Raney nickel and ethanol. Raney nickel (4 cm³, water slurry) was dried under vacuum with gentle warming. Bmim lactate (8 cm³) and ethanol (3 cm³) were then added *via* cannula and the slurry heated under nitrogen for 72 hours at 100 °C. The Raney nickel was then removed by filtration and the products removed by vacuum distillation.

^1H NMR (CDCl_3) δ : 7.4 (s, 1H, methyl imidazole), 7.0 (s, 1H, methyl imidazole), 6.9 (s, 1H, methyl imidazole), 3.9 (t, 1H, H6), 3.8 (s, Me, 0.5H), 3.7 (s, 0.5H), 3.4 (s, 0.5H, butanol), 1.8 (m 2H, butanol), 1.3 (m, 3H, butanol + lactate), 0.9 (m, 3H, butanol).

(ii) Homogeneous Hydrogenation.

Hydrogenation of cyclohexene. $\text{RhCl}(\text{PPh}_3)_3$ (0.0167g, 83.5 μmole) was dissolved in bmim lactate (8 cm^3) under nitrogen with a little heating and cyclohexene (5 cm^3) added *via* syringe. Hydrogen was bubbled through the reaction, *via* a syringe needle, for five hours at room temperature with stirring. After this time a sample of the upper layer was removed by syringe and submitted for NMR analysis.

^1H NMR (CDCl_3) δ : 5.6 (s, 2H, cyclohexene), 2.0 (m, 4H, cyclohexene), 1.6 (m, 4H, cyclohexene).

Hydrogenation of diphenyl acetylene. $\text{RhCl}(\text{PPh}_3)_3$ (0.0167g, 83.5 μmole) was dissolved in bmim lactate (8 cm^3) under nitrogen with a little heating and *cis*-diphenyl ethylene (3 cm^3) added *via* syringe. Hydrogen was bubbled through the reaction, *via* a syringe needle, for four hours at room temperature with stirring. After this time a sample of the reaction mixture was removed by syringe and submitted for NMR analysis. It was necessary to leave the reaction mixture to settle for twenty-four hours before removal of the supernatant *via* syringe was possible. A sample of this supernatant was also submitted for NMR analysis.

^1H NMR of reaction mixture (CDCl_3) δ : 10.9 (s, 1H, H2, bmim lactate), 7.4 (m, 5H, *cis*-diphenyl acetylene), 7.3 (m, 7H, H4, H5, bmim lactate + *cis*-diphenyl acetylene), 5.4 (s, 1H, *cis*-diphenyl acetylene), 4.2 (m, 3H, H6, bmim lactate + lactate OH), 4.0 (4H, Me, bmim lactate), 1.8 (m, 2H, H7), 1.3 (m, 5H, H8, bmim lactate + lactate CH_3), 0.9 (3H, t, H9, bmim lactate).

^1H NMR supernatant: (CDCl_3) δ : 5.5 (s, 1H, *cis*-diphenyl acetylene),.

Hydrogenation of oct-1-ene using formic acid. $\text{RhCl}(\text{PPh}_3)_3$ (0.1 g, 0.5 μmole) was dissolved in bmim lactate under nitrogen and formic acid (2.1 cm^3 , 0.055 mole), sodium formate (1.103 g, 0.015 mole) and oct-1-ene (2.5 cm^3 , 0.0146 mole) added.

The mixture was heated at 90 °C for seven hours under nitrogen then stirred overnight at room temperature. The reaction mixture was extracted with diethyl ether (40 cm³). Removal of the diethyl ether under vacuum left a dark brown liquid.

¹H NMR (CDCl₃) δ: 5.8 (m, 1H, octene), 5.0 (m, 2H, octene), 2.0 (m, 2H, octene), 1.3 (m, 8H, octene), 0.9 (m, 3H, octene).

Hydrogenation of cyclohexene using formic acid. RhCl(PPh₃)₃ (0.1 g, 0.5 mmole) was dissolved in bmim lactate under nitrogen and formic acid (2.1 cm³, 0.055 mole), sodium formate (1.103 g, 0.015 mole) and cyclohexene (1.6 cm³, 0.016 mole) added. The mixture was heated at 70 °C for seven hours under nitrogen then distilled under nitrogen to remove the products.

¹H NMR (CDCl₃)₃ δ: 5.6 (s, 2H, cyclohexene), 2.0 (m, 4H, cyclohexene), 1.6 (m, 4H, cyclohexene).

Hydrogenation of oct-1-ene with ethanol. Oct-1-ene (1 cm³) and ethanol (5 cm³) were added to RhCl(PPh₃)₃ (0.004 g, 0.43 mmole) in bmim lactate (10 cm³) and the solution refluxed for 3 hours at 80 °C under nitrogen. The product was then removed by distillation under nitrogen.

¹H NMR (CDCl₃) δ: 5.8 (m, 1H, octene CH=), 4.9 (m, 2H, octene =CH₂), 3.7 (m, 2H, ethanol), 2.7 (bs, 1H, ethanol), 2.1 (m, 2H, octene), 1.4 (m, 8H, octene), 1.2 (3H, t, ethanol), 0.8 (m, 3H, octene CH₃).

Hydrogenation of cyclohexanone with isopropanol. Dried and degasses 2-propanol (5 cm³) and cyclohexanone (2 cm³) were added *via* syringe to RhCl(PPh₃)₃ (0.004 g, 0.43 mmole) in bmim lactate (10 cm³) and the solution refluxed under nitrogen for four hours at 80 °C. The products were then isolated from the reaction mixture by distillation under nitrogen, giving two fractions. 1st fraction, b.p. 80 °C = 2-propanol. 2nd fraction ¹H NMR (CDCl₃) δ: 3.9 (m, isopropanol), 2.3 (m, cyclohexanone), 1.8 (m, cyclohexanone), 1.15 (d, isopropanol).

6 Substituted Imidazolium Ionic Liquids.

6.1 Introduction.

The preparation and widespread use of 1-butyl-3-methyl imidazolium ionic liquids was discussed in Chapters 1 and 3 and the importance of these new compounds as solvents in a variety of reactions was highlighted. The intense interest in these novel solvents is clearly evident from the abundance of recent publications in this area.¹ However, despite this interest, the number of investigations that have probed the exact nature of these unusual compounds is surprisingly small. For example, although a number of different anions have been utilised in combination with the imidazolium cation, there is little understanding about the relationship between the nature of the anion and the physical properties of the resultant ionic liquid. Similarly, although imidazolium cations with a variety of alkyl chain substituents have been investigated, the effects of changes to this ion with respect to properties, such as melting point, are poorly understood.

The latter part of this investigation is concerned with probing the relationship between the structures and physical properties of imidazolium-based ionic liquids. This chapter outlines the attempts undertaken to prepare ionic liquids with a range of substituted imidazolium cations, and the changes in physical properties observed as a result of these substitutions.

¹ M. Freemantle, *Chemical and Engineering News*, 2001, May 28th, 30 – 34.

6.2 Methyl-Substituted Imidazolium Ionic Liquids.

The extent of hydrogen bonding within 1-butyl-3-methyl imidazolium ionic liquids has been a subject of considerable debate since their inception in the early 1980s. It was initially suggested that the extent of hydrogen bonding could be directly inferred from the ^1H NMR spectra of the liquids.² However, this has since been dismissed as too simplistic on account of the fact that the chemical shifts of the ring protons show both a dependence on concentration and on the extent of the interactions between the cations, which varies between ionic liquids.³ What has always been assumed, however, is that the most significant hydrogen bonding that exists in these compounds takes place between the anion and the hydrogen at the 2-position of the cation. This assumption is based on the nature of this hydrogen as the most acidic of all the ring hydrogens. The validity of this assumption is discussed in more detail in Chapter 8, with reference to the crystal structures of some ionic liquids.

It was proposed that the extent of the hydrogen bonding within the 1-butyl-3-methyl imidazolium ionic liquids could be probed experimentally by observing the effect of methylation at the 2-position of the cation. The melting point of a compound is an excellent indication of the relative strength of interactions within the structure. A species that is held together in the solid phase with strong interactions requires more thermal energy to effect the phase change to a liquid than a compound held together with weaker interactions. It was proposed that by methylating the imidazolium ring at the position of greatest acidity the propensity for hydrogen bonding would be severely reduced. This, in turn, would be expected to reduce the strength of interactions within the compound and thus reduce the melting point.

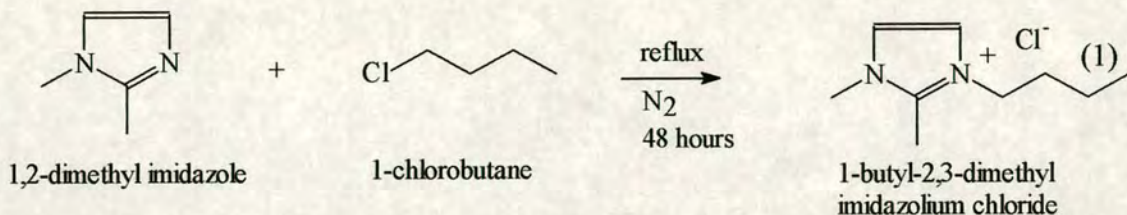
Four imidazolium ionic liquids were substituted with methyl groups at the 2-position and the effect on melting point assessed.

² P. A. Z. Suarez, S. Einloft, J. E. L. Dullius, R. F. De Souza and J. Dupont, *J. Chim. Phys.*, 1998, **95**, 1626 - 1639.

³ J. Holbrey and K. R. Seddon, *J. Chem. Soc., Dalton Trans.*, 1999, 2133 – 2139. P. Bonhôte, A. Dias, N. Papageorgiou, K. Kalyanasundaram and M. Grätzel, *Inorg. Chem.*, 1996, **35**, 1168 – 1178.

6.2.1 1-butyl-2,3-dimethyl imidazolium chloride.

As for the 1-butyl-3-methyl imidazolium ionic liquids, the chloride species was used as the precursor for the synthesis of the PF₆ and BF₄ analogues of the dimethylated imidazolium ionic liquids. The chloride species was synthesised by the reaction of 1,2-dimethyl imidazole, which is commercially available, and 1-chlorobutane.



The excess 1-chlorobutane was then be removed by drying under vacuum and the product recrystallised from acetonitrile and ethyl acetate. As for the mono-methylated species, this chloride ionic liquid is extremely hygroscopic and will take on significant amounts of moisture from the air.

The electrochemical behaviour of the compound was assessed using cyclic voltammetry. Platinum wire was used for the reference electrode, a platinum sheet for the working electrode and platinum gauze for the counter electrode. The CV is shown in Figure 6.1. The species has a large electrochemical window and contains no electro-active impurities. The compound was also characterised by NMR, IR, mass-spectrometry and elemental analysis (detailed in section 6.6) and again no impurities were detected.

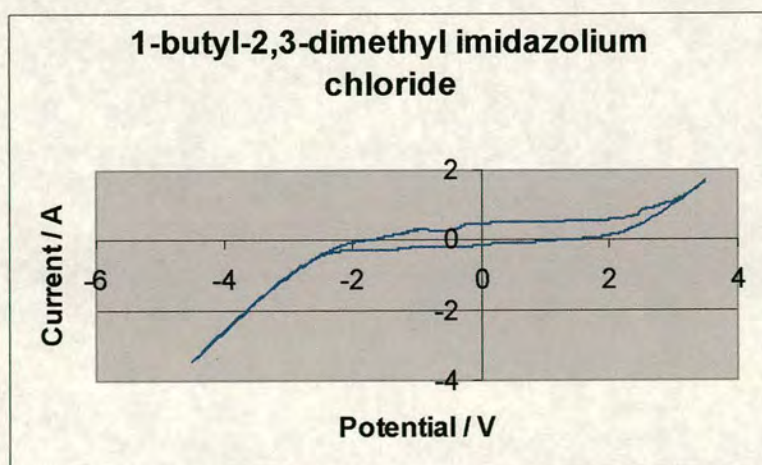
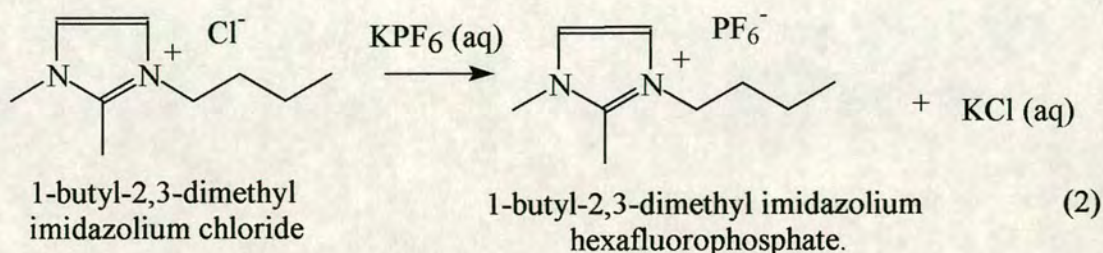


Figure 6.1. Cyclic voltammogram of 1-butyl-2,3-dimethyl imidazolium chloride, recorded under nitrogen.

6.2.2 1-butyl-2,3-dimethyl imidazolium hexafluorophosphate.

The hexafluorophosphate ionic liquid was prepared by metathesis from the chloride using the new aqueous route developed previously for the 1-butyl-3-methyl imidazolium species (see section 3.3). Addition of the chloride ionic liquid to an aqueous solution of potassium hexafluorophosphate gave the hexafluorophosphate ionic liquid as a lower layer.



The product was then separated from the aqueous layer, containing the KCl by-product, washed repeatedly with warm water and dried under vacuum. It is interesting to note that methylation of the imidazolium ring has no apparent effect on the hydrophobicity of the ionic liquid.

The cyclic voltammogram of the hexafluorophosphate ionic liquid was recorded under the same conditions as before and again showed an extremely large electrochemical window, shown in Figure 6.2.

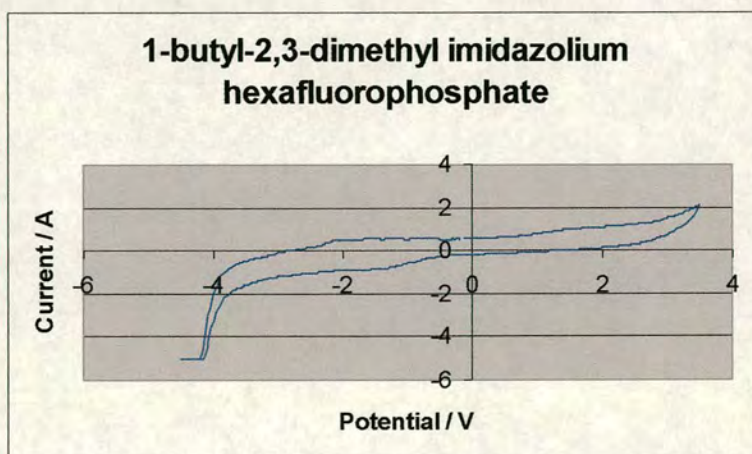


Figure 6.2. Cyclic voltammogram of 1-butyl-2,3-dimethyl imidazolium hexafluorophosphate, recorded under nitrogen. Sweep rate = 0.05 Vs^{-1} .

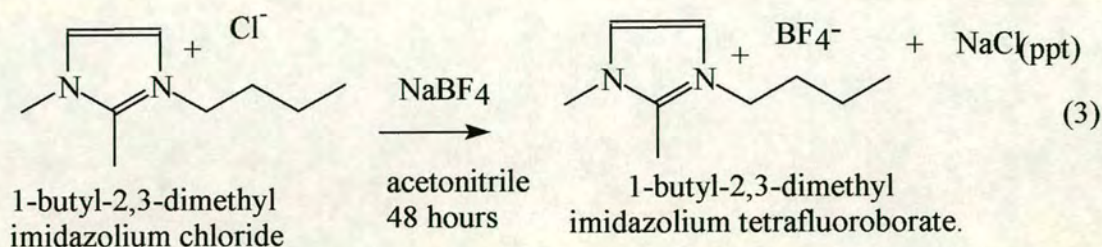
The electrochemical window of the dimethylated species is larger than that observed for the mono-methylated species, shown in Chapter 3, under the same conditions. While the upper limit is relatively unchanged at approximately 3 V, the lower limit has decreased from -1.6 V to -3.6 V on methylation. This may indicate an increase in the electrochemical stability of the cation, consistent with an increase in the delocalisation of the positive charge on methylation. 1,3-dialkyl imidazolium cations can form relatively stable carbenes,⁴ and it is suggested that methylation makes this formation by electrochemical reduction more difficult. A small increase in the electrochemical window of the 1-ethyl-3-methyl-imidazolium bis((trifluoromethyl)sulfonyl)amide ionic liquid upon 2-methylation was observed by Bonhôte *et al.*⁵ and attributed to a decrease in the acidity of the cation.

⁴ W. A. Herman and C. Kocher, *Angew. Chem. Int. Ed. Engl.*, 1997, **36**, 2162 – 2187.

⁵ P. Bonhôte, A. Dias, N. Papageorgiou, K. Kalyanasundaram and M. Grätzel, *Inorg. Chem.*, 1996, **35**, 1168 – 1178.

6.2.3 1-butyl-2,3-dimethyl imidazolium tetrafluoroborate.

The tetrafluoroborate analogue was also prepared *via* metathesis of the chloride salt. The chloride species was refluxed in a solution of sodium tetrafluoroborate in acetonitrile for 48 hours under nitrogen. The sodium chloride by-product precipitated out of solution and was easily removed by filtration.



The acetonitrile was then be removed under vacuum and the product purified by washing with dichloromethane.

The cyclic voltammogram of this new ionic liquid, shown in Figure 6.3, again indicates a dramatically increased electrochemical window on methylation, with the lower limit decreasing from -2.6 to -4.0 V.

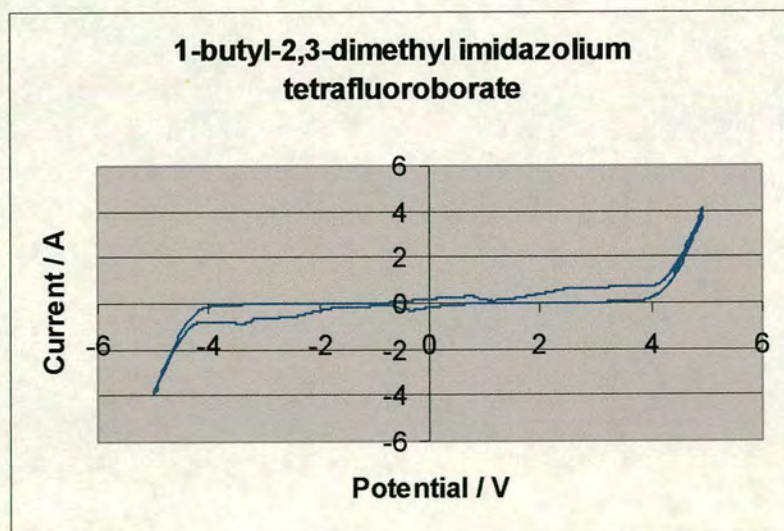
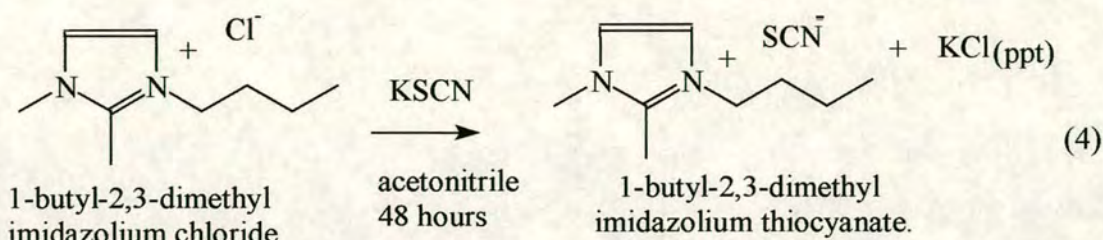


Figure 6.3. Cyclic voltammogram of 1-butyl-2,3-dimethyl imidazolium tetrafluoroborate, recorded under nitrogen. Sweep rate = 0.05 Vs^{-1} .

6.2.4 1-butyl-2,3-dimethyl imidazolium thiocyanate.

Refluxing 1-butyl-3-methyl imidazolium chloride with potassium thiocyanate in acetonitrile for 48 hours effected the metathesis to the corresponding thiocyanate ionic liquid.



The potassium chloride by-product was again removed by filtration and the acetonitrile removed under vacuum. The product was then washed with dichloromethane to ensure removal of all impurities.

As for the mono-methylated species, the electrochemical window of the thiocyanate ionic liquid is smaller than that of the tetrafluoroborate and hexafluorophosphate analogues. This suggests that it is the oxidation and reduction of thiocyanate that is responsible for the solvent limits. This is perhaps unsurprising as thiocyanate can be chemically oxidised by mild oxidising agents such as iodine.

The electrochemical window of 1-butyl-2,3-dimethyl imidazolium thiocyanate, shown in Figure 6.4, does not appear significantly altered from that of the 1-butyl-3-methyl analogue.

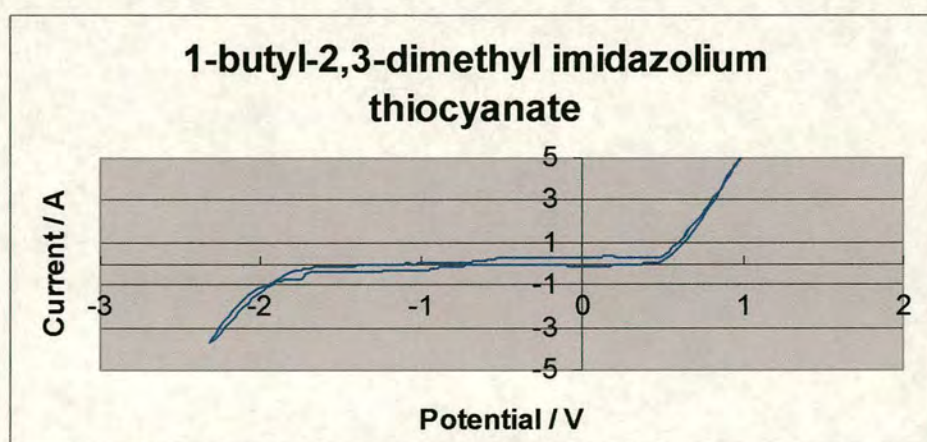


Figure 6.4. Cyclic voltammogram of 1-butyl-2,3-dimethyl imidazolium thiocyanate. Sweep rate = 0.05 Vs^{-1} .

6.2.5 The Effect of Methylation on Melting Point.

The primary aim of preparing this range of dimethylated imidazolium ionic liquids was to assess the effect of methylation on the physical properties of the compounds. It was expected that methylation at the 2-position of the imidazolium ring would decrease the extent of hydrogen bonding within these species and thus result in a corresponding decrease in melting point.

Surprisingly, it was immediately apparent on synthesis of these new ionic liquids that the reverse was true. Addition of an extra methyl group to the cation resulted in the formation of compounds that formed solids at room temperature. This unexpected result further highlighted the poor understanding of the relationship between the structure and physical properties of these species.

The exact melting points of the three dimethylated ionic liquids were measured using differential thermal analysis (DTA) and are shown in Table 6.1. The glass transition temperatures of the 1-butyl-3-methyl imidazolium analogues are included for comparison.

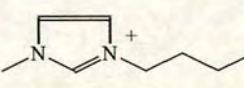
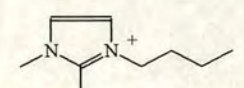
Cation	Melting point / °C			
	Cl	BF ₄	PF ₆	SCN
	35	-81 ²	-61 ²	-
	81	32	36	35 [†]

Table 6.1. The melting points of the mono- and dimethylated ionic liquids, determined by DTA. [†] Measured using Gallenkamp melting point apparatus.

It is clear from the melting points of these compounds that contrary to expectation, methylation of the imidazolium ring of 1-butyl-2-methyl imidazolium ionic liquids results in significant increase in melting point. An explanation for this is presented in section 8.2.

6.2.6 The Effect of Methylation on Viscosity.

The viscosity of each of the ionic liquids from room temperature, or their melting point, to 80 °C was measured using a Haake VT 550 cone and plate viscometer to determine the effect of methylation on viscosity. The results are shown in Figure 6.5.

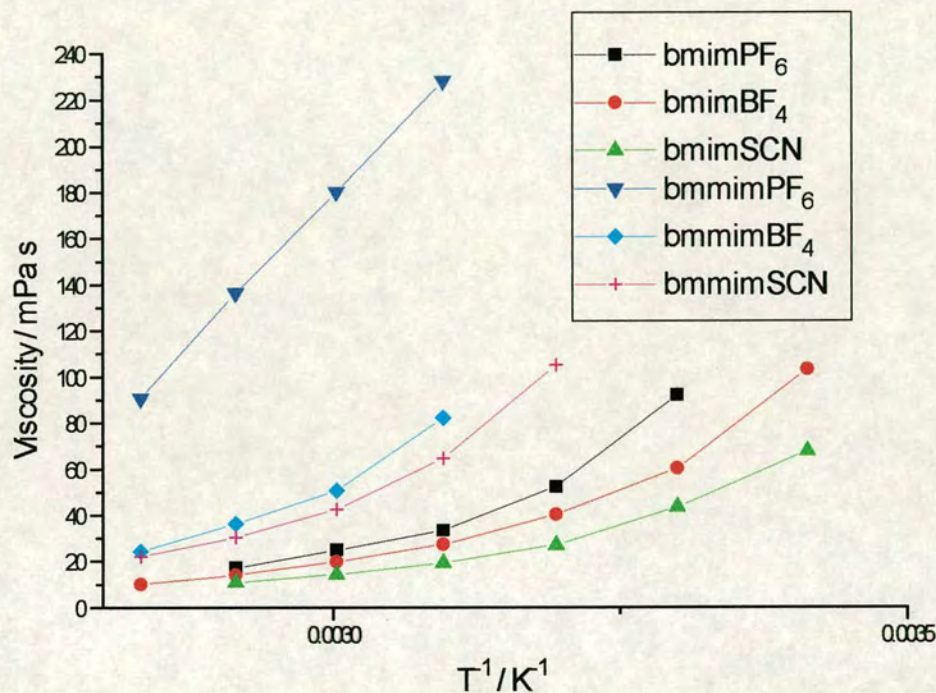
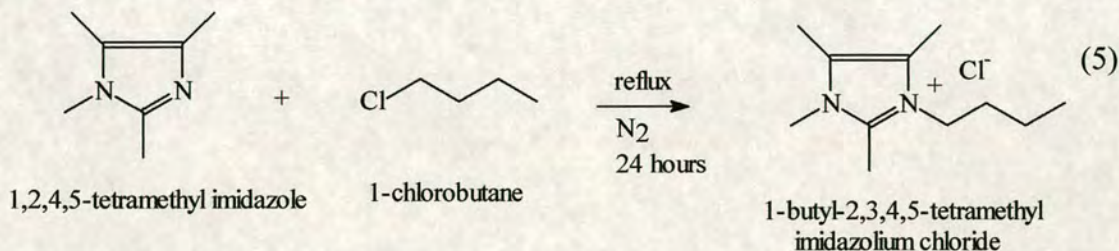


Figure 6.5. The change of viscosity with temperature for the mono- and dimethylated ionic liquids.

The results are consistent with those reported for other imidazolium ionic liquids in showing a relationship between the viscosity and temperature that is not quite linear. What is clear from the results, however, is that methylation of the imidazolium ring results in a significant increase in viscosity for all three of the ionic liquids studied.

6.2.7 1-butyl-2,3,4,5-tetramethyl imidazolium chloride.

Following the unexpected observation that removal of the H₂ proton from the imidazolium ring results in an increase in melting point, it was decided to investigate the effect of removing all of the ring hydrogens by methylation at the 2,4 and 5 positions. 1-butyl-2,3,4,5-tetramethyl imidazolium chloride was prepared by alkylation of 1,2,4,5-tetramethyl imidazole, which is commercially available.



The melting point of the tetramethylated species is 97 °C. Thus, increased methylation of the imidazolium ring results in a further increase in the melting point. Again this is counter to the accepted wisdom that the hydrogen atoms on the imidazolium ring dominate the hydrogen bonding in the structure.

It interesting to note that the symmetrical isomer of this compound, 1,3-dibutyl imidazolium chloride, melts at 58 – 61 °C.⁶ Thus, the melting point increase is not purely a result of increased mass. This result also appears to contradict the widely held belief that it is the asymmetry of the cation in imidazolium-based room temperature ionic liquids that accounts for the low melting points of these compounds.

⁶ K. J. Harlow, A. F. Hill and T. Welton, *Synthesis*, 1996, 697 – 698.

6.2.8 Conclusions.

The unexpected result of the methylation of room temperature imidazolium ionic liquids on their melting points serves to highlight the fundamental lack of understanding about the relationship between the structures of these compounds and the physical properties that they display.

The effect of methylation on the hydrogen bonding within these species has been studied in more detail using x-ray crystallography, and the results of these investigations will follow in Chapter 8.

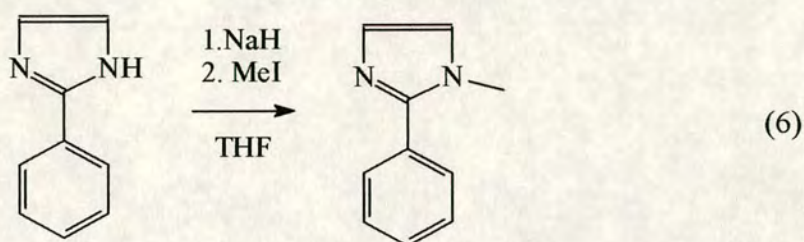
It was proposed that much better understanding of the structure-property relationships of imidazolium ionic liquids would be gained by the synthesis of a range of compounds with different substituents in the 2-position of the imidazolium ring. The further work in this chapter describes the synthesis and analysis of a range of these compounds.

6.3 Phenyl-Substituted Imidazolium Ionic Liquids.

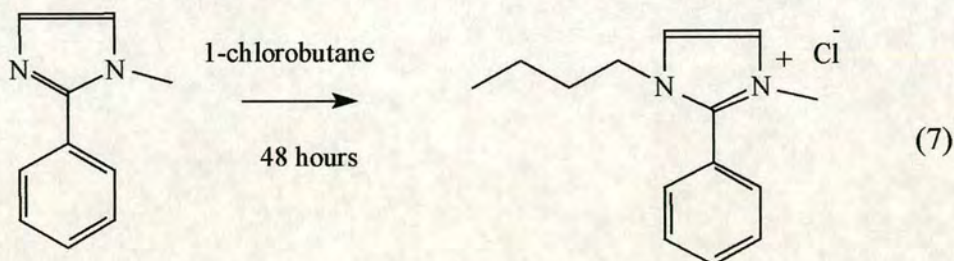
6.3.1 1-butyl-2-phenyl-3-methyl imidazolium chloride, I.

The first target compound identified was the 2-phenyl substituted species. It was decided to prepare first the chloride species and to use this subsequently as the precursor for metathesis into the hexafluorophosphate and tetrafluoroborate analogues.

The chloride was prepared in two steps from the commercially available 2-phenyl imidazole. This was deprotonated using sodium hydride and then methylated using iodomethane.

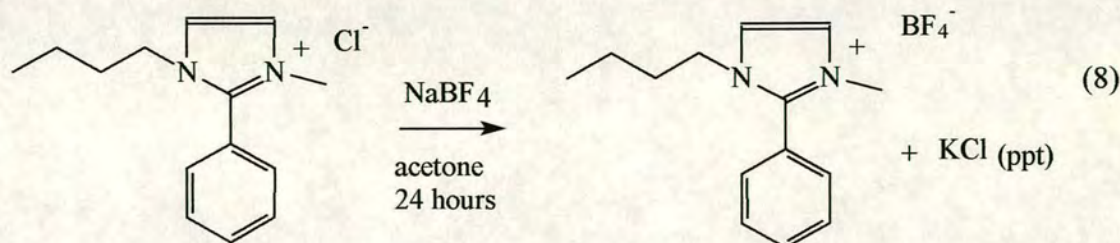


Refluxing the substituted imidazole with 1-chlorobutane for 24 hours under nitrogen then produced the ionic liquid, I.



6.3.2 1-butyl-2-phenyl-3-methyl imidazolium tetrafluoroborate.

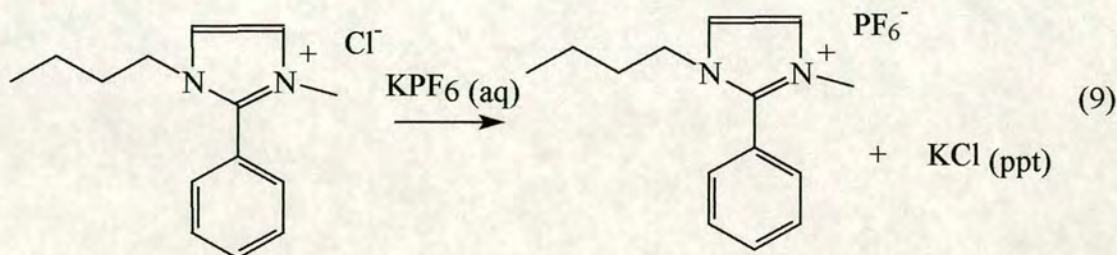
Metathesis of the chloride derivative, I, to the tetrafluoroborate analogue was achieved by refluxing I with sodium tetrafluoroborate in acetone.



The KCl by-product was removed by filtration and the product dried under vacuum.

6.3.3 1-butyl-2-phenyl-3-methyl imidazolium hexafluorophosphate.

The new aqueous route developed for the 1-butyl-3-methyl-imidazolium hexafluorophosphate species was used to prepare 1-butyl-2-phenyl-3-methyl imidazolium hexafluorophosphate. Again it is interesting to note that, as for the other ionic liquids studied, the hexafluorophosphate salt of 1-butyl-2-phenyl-3-methyl imidazole is hydrophobic, whilst the tetrafluoroborate analogue is hydrophilic.



The product was purified by washing with dichloromethane and drying under vacuum to give a solid at ambient temperature.

The melting point of the 1-butyl-2-phenyl-3-methyl imidazolium hexafluorophosphate was measured by differential thermal analysis to be 43 °C, which represents a substantial increase in melting point compared with the unsubstituted derivative.

In addition to studying the effect of phenyl substitution on melting point it was proposed that incorporation of a phenyl group into the ionic liquid would enhance crystallisation thereby facilitating the growth of single crystals suitable for study by x-ray diffraction. This is a strategy commonly employed in organic and organometallic chemistry.

A single crystal of 1-butyl-2-phenyl-3-methyl imidazolium hexafluorophosphate suitable for study by x-ray diffraction was grown by solidification of the neat liquid on the flat inner wall of a schlenk tube under nitrogen. The crystal structure of this species is detailed in Chapter 8.

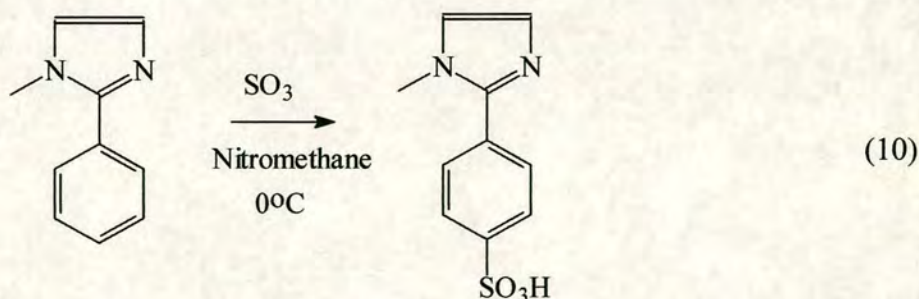
6.4 Reaction of Phenyl-Substituted Imidazolium Ionic Liquids

Although phenyl substitution of the imidazolium ring increases the melting point of these derivatives, melting points are not so high as to prohibit the use of the compounds as solvents at slightly elevated temperatures. Furthermore, the presence of the phenyl ring allows the possibility of tuning the properties of the ionic liquids by electrophilic substitution of the ring.

6.4.1 Sulfonation.

The susceptibility of the phenyl ring to sulfonation was studied using sulfur trioxide as the sulfonating agent. This is a highly reactive electrophilic reagent and can be used for the replacement of a hydrogen with an SO_3H group in many aromatic compounds.⁷ Initially the reaction forms a pyrosulfonic acid of the aromatic compound ($\text{ArS}_2\text{O}_6\text{H}$) but addition of water followed by moderate heating hydrolyses this to the desired arene sulfonic acid. Sulfur trioxide is a particularly hazardous material and must be handled under an inert atmosphere at all times as reaction with air results in the evolution of a sulfur trioxide-sulfuric acid spray.

Sulfonation of 1-methyl-2-phenyl imidazole was achieved by reaction with sulfur trioxide in a nitromethane solution.⁸



The SO_3 was dissolved in nitromethane and added dropwise over 15 minutes to a solution of 1-methyl-2-phenyl imidazole, also in nitromethane, at 0°C . The low temperature and long reaction times were used in an attempt to avoid any multiple substitution of the phenyl ring. However, although analysis of the products by mass

⁷ L. F. Fieser, *Reagents for Organic Synthesis. Acidic and Basic Reagents*, Wiley, New York.

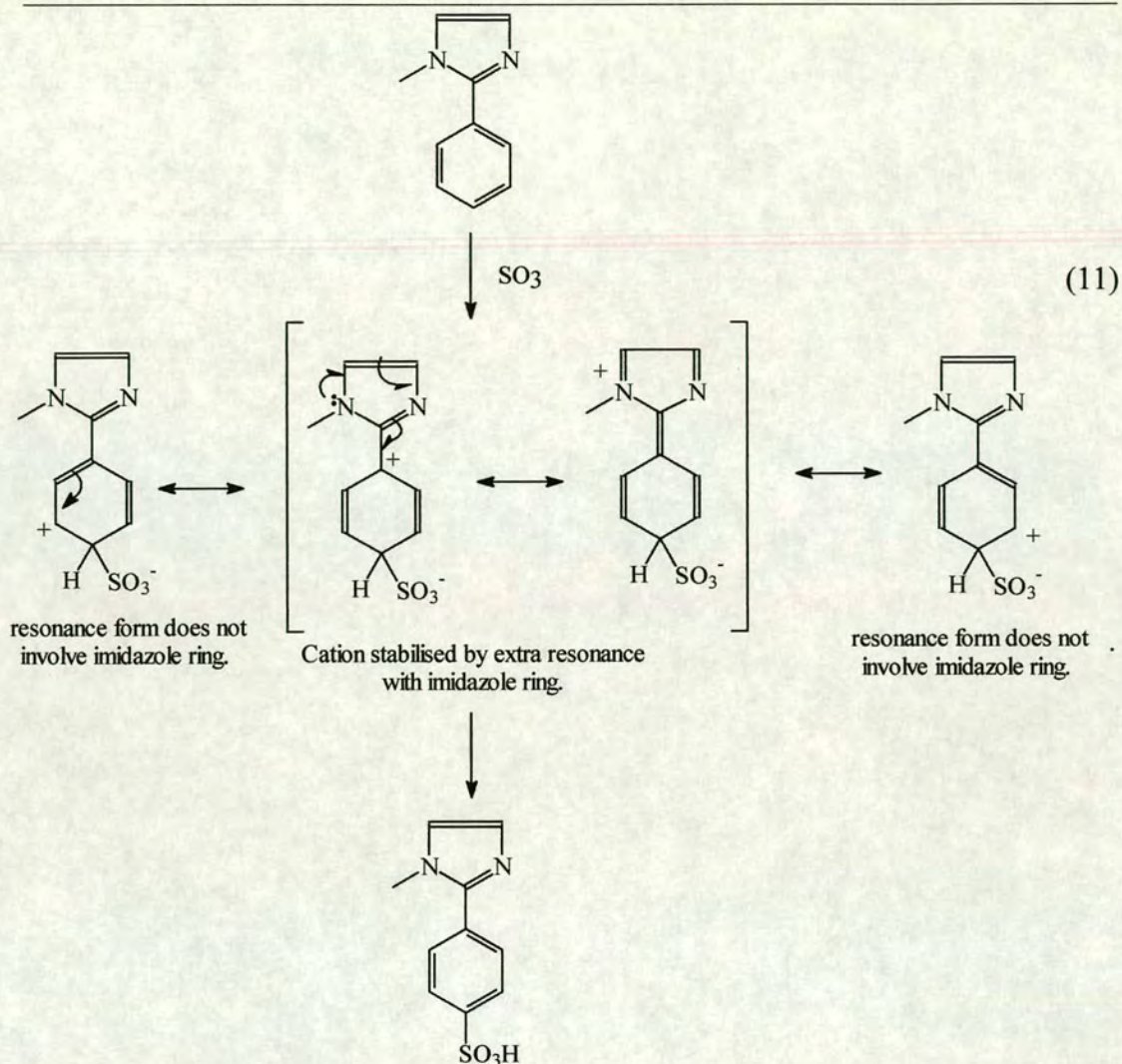
⁸ K. Lammertsma, H. Cerfontain, *Tetrahedron*, 1982, **38**, 1667 – 1671.

spectrometry indicated that the sulfonation had been successful, some multiple substitution was evident, even on repetition of the reaction with longer reaction times and more dilute solutions.

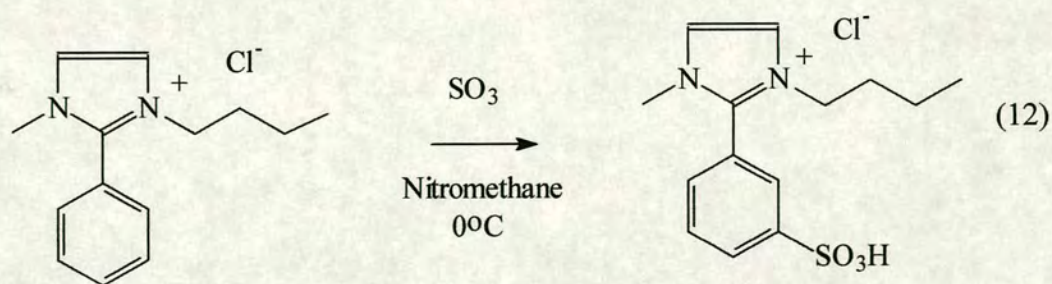
It is evident from the ease of substitution of the phenyl ring that the imidazole ring acts as an activating group in this reaction, activating the phenyl ring to electrophilic substitution. This is consistent with the imidazole group releasing electron density into the phenyl ring thereby stabilising the intermediate carbocation formed during substitution of the sulfonyl group.

The activating nature of the imidazole also affects the position of substitution of the phenyl ring. Activating groups increase the rate of substitution at the *ortho* and *para* positions of the phenyl ring in comparison to the *meta* position. This is because with the substituent in this position the intermediate carbocation has an additional stable canonical form through resonance interaction with the imidazole ring, as shown in equation (10). This resonance stability is not possible when substitution occurs at the *meta* position. In 1-methyl-2-phenyl imidazole the *ortho* position is heavily sterically hindered thus sulfonation would be expected to take place almost exclusively in the *para* position.

The ^1H NMR spectrum of the product shows two multiplets of equal intensity in the aromatic region indicating predominantly *para*-substitution, with some multiple substitution of the phenyl ring resulting in a slight complication of the aromatic signals compared to the AB quartet that would be expected.



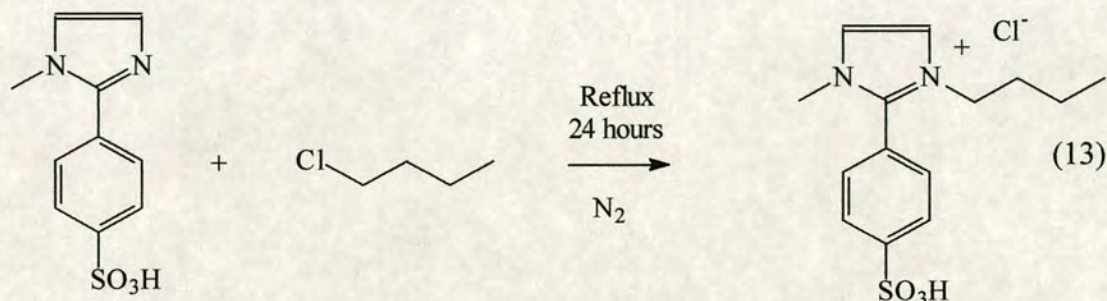
By comparison, the sulfonation of the ionic liquid 1-butyl-2-phenyl-3-methylimidazolium chloride was unsuccessful under the same conditions.



The positive charge on the imidazole ring has a deactivating effect of the phenyl ring with respect to electrophilic substitution. If the sulfonation were successful, addition would be expected to take place at the *meta* position on the phenyl ring. Substitution at this position, in the presence of a deactivating group, results in the maximum

stabilisation of the intermediate carbocation. However, analysis of the product showed that no sulfonation had occurred.

It was evident from these results that synthesis of the sulfonated ionic liquid 1-butyl-2-(phenyl sulfonyl)-3-methyl imidazolium chloride would have to be achieved by sulfonation prior to addition of the butyl group. Addition of a butyl group to the sulfonated species was attempted by refluxing with 1-chlorobutane for 24 hours.



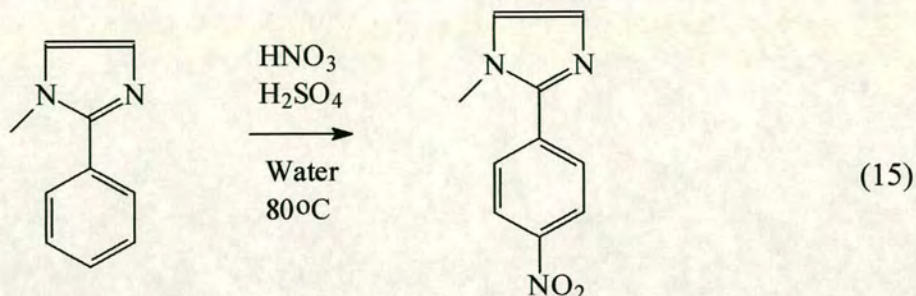
These are the same conditions as used to synthesise all the previous ionic liquids from the neutral species. However, under these conditions, no alkylation was observed, hence the presence of the sulfonyl group on the phenyl ring prevents the butylation of the imidazole ring. It is proposed that this is a result of the formation of the zwitterion of the compound. If the amine group is a stronger base than the SO_3^- then the hydrogen ion attaches to the nitrogen and a zwitterion (14) is formed, preventing alkyl substitution.



The protection of the sulfonyl group would prevent the formation of the zwitterion, thus this may be necessary to effect the butylation of the compound, with the subsequent removal of the protecting group after substitution.

6.4.2 Nitration.

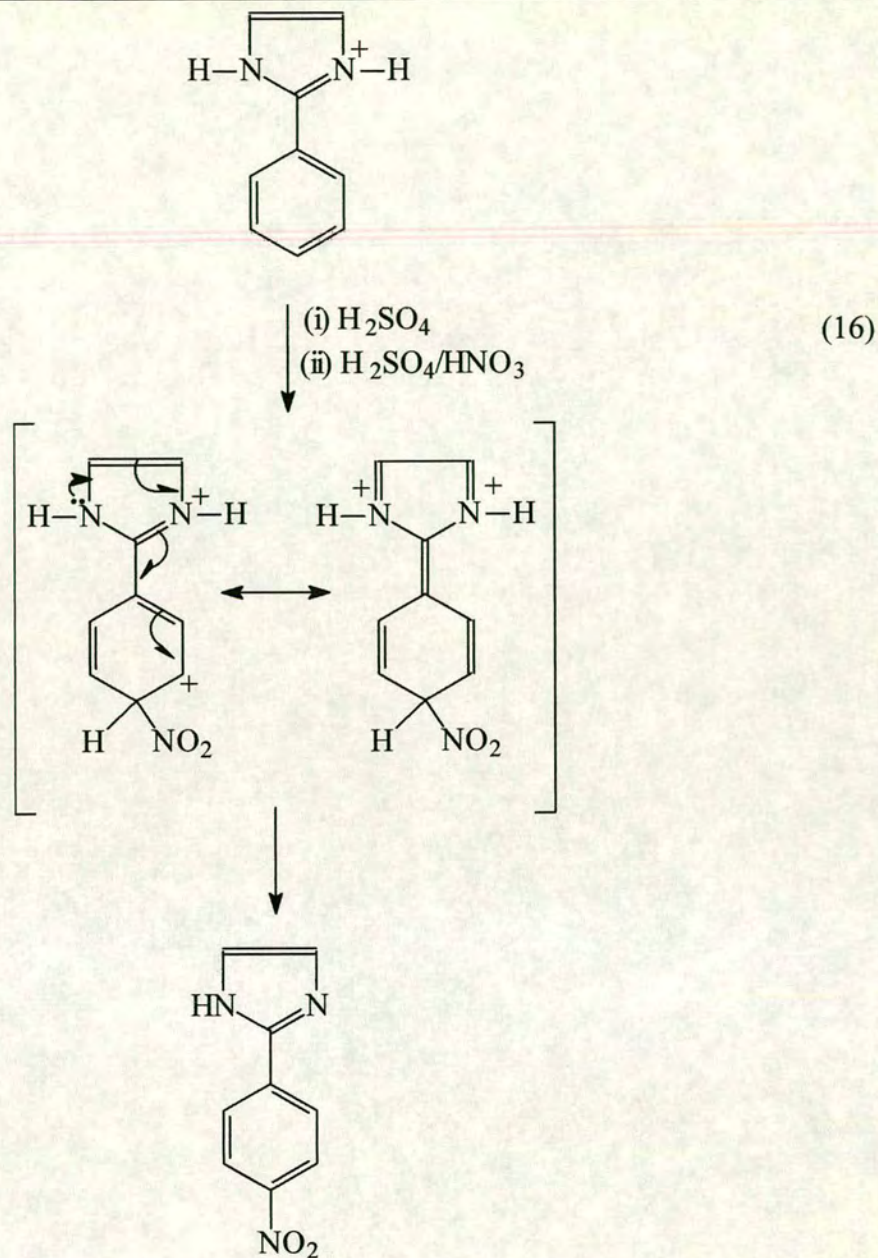
Nitration of 1-methyl-2-phenyl imidazole was attempted by addition of a mixture of nitric and sulfuric acids to 1-methyl-2-phenylimidazole in water. The solution was heated at 80 °C for 24 hours and the product extracted with chloroform.



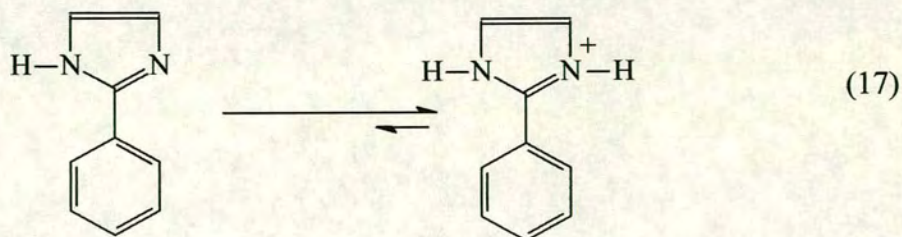
Analysis of the product by mass spectrometry indicated that some nitration of the phenyl ring had taken place, but ^1H NMR analysis showed the product to be impure, even after recrystallisation, making it difficult to assess the nature or extent of the substitution.

The nitration of 2-phenyl imidazole has been reported in the literature, although authors disagree on the relative ratios of *ortho*, *meta* and *para* substitution observed.⁹ Substitution would be expected to occur almost exclusively at the *para* position because substitution at this position, in an acidic solution, results in the formation of a more resonance stabilised intermediate.

⁹ (a) F. L. Pyman and E. Stanley, *J. Chem. Soc.*, 1924, **125**, 2484–2488. (b) R. Forsyth and F. L. Pyman, *J. Chem. Soc.*, 1930, 397–408. (c) D. T. Hurst, *Heterocycles*, 1988, **27**, 2, 371–376.



It is also proposed that a very small amount of the basic species could be present in the reaction mixture, in equilibrium with the acidic form, and this would be nitrated in the para position.



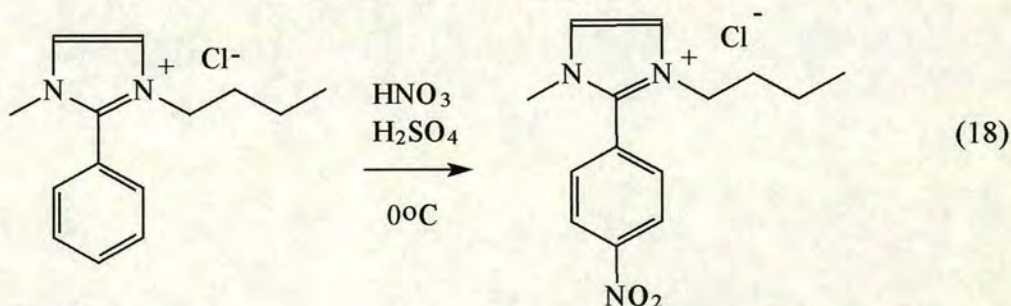
Although there may be only a very small quantity of this species present at any one time, removal of the unprotonated form by nitration would shift the equilibrium position and result in the formation of more of the unprotonated form.

It was decided to attempt the nitration of phenyl imidazole both to determine the exact position of the substitution of the nitro group and also to use the product for the subsequent synthesis of the nitrated ionic liquid.

2-phenyl imidazole was dissolved in sulfuric and a solution of nitric acid in sulfuric acid added slowly at 0 °C. The solution was stirred at 0 °C for two hours and at room temperature overnight then poured into iced water. Sodium hydroxide was added to give a pH of 9 at which point a yellow precipitate was produced. This was then washed with water and diethyl ether.

The melting points of the *ortho*, *meta* and *para* derivatives are reported to be 188-189 °C, 193 – 194 °C and 310 - 315 °C respectively.^{9(a)} The product obtained from the above reaction exhibited a melting point of 305 – 307 °C, clearly indicating it to be the *para*-substituted derivative.

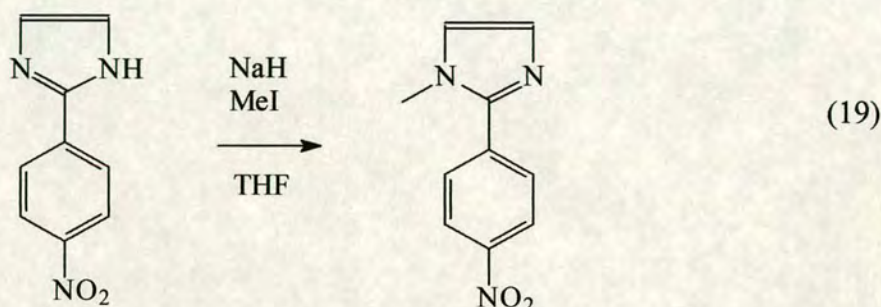
Nitration of 1-butyl-2-phenyl-3-methyl imidazolium chloride was attempted using the same conditions as above in order to compare the reactivity of the two species and to attempt the synthesis of the nitrated ionic liquid.



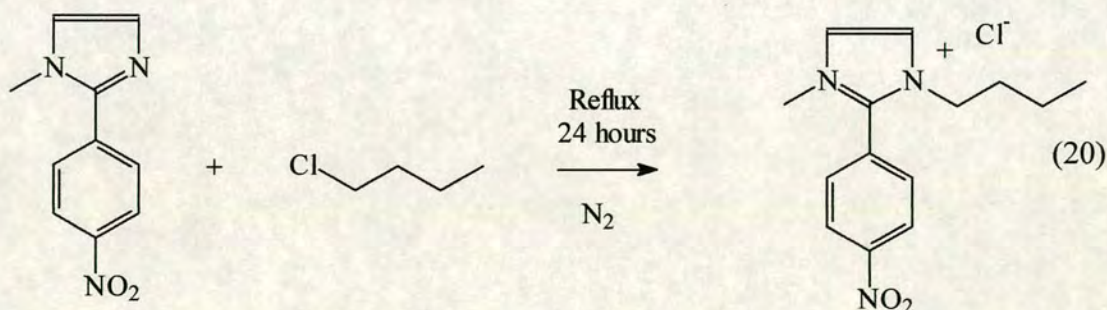
However, as observed for sulfonation, this direct route to a substituted phenyl imidazolium ionic liquid does not appear to be viable. Unlike the sulfonation, mass spectral analysis of the product indicated that some substitution had taken place, but ¹H NMR analysis indicated that the product was extremely impure and suggested that significant decomposition had taken place. It may be that decomposition of the starting product is the penalty for the severe acidic conditions required to overcome

the strong deactivating effect of the positively charged imidazole ring and effect nitration. It is possible that careful optimisation of the reaction conditions could achieve clean nitration, but it was decided to attempt first the preparation of the ionic liquid starting from the 2-nitrophenyl imidazole.

2-nitrophenyl imidazole was successfully methylated by reaction with iodomethane in tetrahydrofuran, using the same conditions as used for the methylation of the unsubstituted 2-phenyl imidazole.



The methylated product was isolated in a pure form and an attempt was then made to butylate the compound to give an ionic liquid.



The 1-methyl-2-nitrophenyl imidazole was heated with 1-chlorobutane for 24 hours, both in a tetrahydrofuran solution and as a neat mixture, but no alkylation was observed.

It was concluded that the presence of the strongly electron withdrawing nitro-group on the phenyl ring reduces the electron density of the imidazole ring thereby preventing the alkylation under these conditions.

It should be noted, however, that the successful addition of the nitro-group to the phenyl ring would allow the possibility of substituting this group for other functional

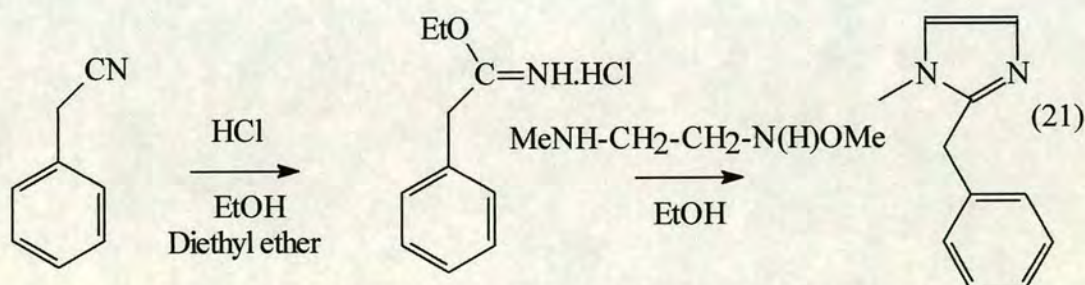
groups. For example, the nitro-group could be reduced to an amine.¹⁰ This, in turn, could be substituted for a range of halides *via* the diazonium salt. Alkylation of the imidazole ring to form an ionic liquid with an amine substituent on the phenyl ring should be straightforward. This is an area that requires further investigation.

¹⁰ I. E. Balaban and H. King, *J. Chem. Soc.*, 1925, **127**, 2701 – 2714. M. Slavica, L. Lei, P. N. Patil, D. R. Feller and D. D. Miller, *J. Med. Chem.*, 1994, **37**, 1874 – 1881.

6.5 Future work - Benzyl-Substituted Ionic Liquids.

Following the successful synthesis of 1-butyl-2-phenyl-3-methyl imidazolium ionic liquids, it is proposed that synthesis of ionic liquids with a benzyl group substituted at the 2-position of the imidazole ring would be of particular interest. This difference between the phenyl and benzyl-substituted cation is significant in that the latter structure is not stabilised by resonance interactions between the phenyl ring and the imidazole. The addition of a CH₂ linker between the phenyl ring and the imidazole increases the steric bulk of the cation but potentially allows more flexibility for the large phenyl ring to orientate itself into a more energetically favourable orientation within the solid phase. It is hoped that analysis of these new species and their crystal structures would provide insight into the effect of changing the cation in this way and allow comparison of the physical properties of the corresponding ionic liquids.

Synthesis of 2-benzyl imidazole was reported in 1996, although work on similar compounds had been described previously. Abbotto *et al.* described the synthesis of 2-benzyl imidazole,¹¹ utilising the synthesis of a hydrochloride salt of benzyl cyanide reported in a previous publication.¹²



The synthesis involves bubbling HCl gas into a solution of benzyl cyanide in the presence of one equivalent of ethanol until one equivalent of the gas has been absorbed. Cooling the solution is then reported to produce the phenylacetimidoyl ethyl ether hydrochloride as a precipitate that can be isolated and reacted with the (methylamino)acetaldehyde dimethyl acetal to form the imidazole ring.

¹¹ A. Abbotto, S. Bradamante and G. A. Pagani, *J. Org. Chem.*, 1996, **61**, 1761 – 1769.

¹² S. M. McElvain and J. W. Nelson., *J. Am. Chem. Soc.*, 1942, **64**, 1825 – 1828.

There are a large number of substituted phenyl and benzyl cyanides commercially available and utilisation of these as starting materials should result in a range of substituted phenyl and benzyl imidazole compounds. For example, this technique has been reported for the synthesis of *p*-aminophenyl imidazole,¹⁰ *p*-hydroxyphenyl imidazole¹³ and a range of halogenated phenyl imidazoles,¹⁴ as well as *p*-hydroxybenzyl imidazole¹⁵ and *o*-nitrobenzyl imidazole.¹⁶ Synthesis of a range of these compounds could provide valuable insight into the relationship between the structure and physical properties of these compounds.

¹³ E. I. Du Pont de Nemours, *Chem. Abs.*, 1968, **69**, 60054C.

¹⁴ Merck & Co., *Chem. Abs.*, 1965, **63**, 18097, L. H. Sarett, D. R. Hoff and D. W. Henry, *Chem. Abs.*, 1972, **77**, 140080r.

¹⁵ H. Jones, M. W. Fordice, R. B. Greenwald, J. Hannah, A. Jacobs, W. V. Ruyle, G. L. Walford and T. Y. Shen, *J. Med. Chem.*, 1978, **21**, 11, 1100 – 1104.

¹⁶ Merck & Co., Inc. *Chem. Abs.*, 1967, **66**, 37928x,

6.6 Experimental

2-methyl substituted ionic liquids.

1-butyl-2,3-dimethyl imidazolium chloride. 1,2-dimethyl imidazole (36 g, 0.37 mole) and 1-chlorobutane (42 cm³, 0.41 mole, washed with sulfuric acid and distilled under nitrogen onto molecular sieves) were refluxed together for 48 hours at 80 °C under nitrogen. Removal of the excess 1-chlorobutane under vacuum resulted in the formation of a crystalline, cream coloured solid at room temperature. M.P. 81 °C

¹H NMR (CDCl₃) δ: 7.7 (d, 1H, H4), 7.5 (d, 1H, H5), 6.7 (d, unknown), 4.15 (t, 2H, H6), 3.9 (s, 3H, Me1), 3.5 (s, unknown), 2.7 (s, 3H, Me2), 2.2 (s, unknown), 1.7 (m, 2H, H7), 1.3 (m, 2H, H8), 0.8 (t, 3H, H9).

IR: (cm⁻¹, neat liquid) ν: 3060 (CH aromatic), 2960 (CH₂ aliphatic), 1563 (C=C).

FABMS *m/z* 153 (M⁺), 97 (dimethyl imidazole), 29 (CH₂CH₃).

Elemental analysis. C₉H₁₉N₂Cl requires C 57.3, H 9.08, N 14.8. Found C 57.2, H 9.00, N 15.0.

1-butyl-2,3-dimethyl imidazolium tetrafluoroborate. 1-butyl-2,3-dimethyl imidazolium chloride (13.56 g, 0.072 mole) and sodium tetrafluoroborate (7.89 g, 0.072 mole) were refluxed together in acetonitrile (50 cm³) for 48 hours under nitrogen. The white precipitate produced was removed by filtration and the filtrate dried under vacuum. Dichloromethane (50 cm³) was then added and the solution filtered and dried giving the product as a brown solid. Yield = 81 %.

¹H NMR (CD₃OD) δ: 7.5 (dd, 2H, H4 and H5), 4.2 (t, 2H, H6), 3.9 (s, 3H, Me1), 2.7 (s, 3H, Me2), 1.9 (m, 2H, H8), 1.5 (m, 2H, H8), 1.1 (t, 3H, H9).

¹⁹F NMR (CD₃OD) δ: -155.8 (s, BF₄).

IR (cm⁻¹ neat liquid) ν: 3151, (ν aromatic C-H stretch), 2964, 2878 (ν aliphatic C-H stretch), 1590, 1466, 1057 (ν B-F).

FAB-MS *m/z* 153 (M⁺), 97 (loss of butyl), 29 (C₂H₅).

Elemental analysis C₉H₁₇N₂BF₄ requires C 45.0, H 7.14, N 11.7. Found C 44.9, H 7.30, N 11.6.

1-butyl-2,3-dimethyl imidazolium hexafluorophosphate. 1-butyl-2,3-dimethyl imidazolium chloride (40.0 g, 0.212 mole) was added to aqueous potassium hexafluorophosphate (39.07 g, 0.212 mole) producing the product as a lower layer. This layer was separated, washed with deionised water and dried under high vacuum giving a cream coloured solid. M.P. 36 °C.

$^1\text{H NMR } \delta$: (CD_3OD) 7.5 (dd, 2H, H4 H5), 4.2 (t, 2H, H6), 3.9 (s, 3H, Me1), 2.7 (s, 3H, Me2), 1.9 (m, 2H, H7), 1.5 (m, 2H, H8), 1.1 (t, 3H, H9).

FABMS m/z 153 (M^+), 97 (dimethyl imidazole), 29 (CH_2CH_3).

IR (cm^{-1} nujol mull) ν : 3156 (ν aromatic C-H stretch), 2853 (ν aliphatic C-H stretch), 1465, 841 (ν P-F).

Elemental analysis. $\text{C}_9\text{H}_{17}\text{N}_2\text{PF}_6$ requires C 36.3, H 5.75, N 9.39. Found C 36.6, H 6.14, N 10.3.

1-butyl-2,3-dimethyl imidazolium thiocyanate. 1-butyl-2,3-dimethyl imidazolium chloride (34.27 g, 0.182 mole) and potassium thiocyanate (17.96 g, 0.182 mole) were heated together in acetonitrile (50 cm^3) for 48 hours under nitrogen. The precipitate was then removed under vacuum and the product washed with dichloromethane (50 cm^3). Yield 78%.

$^1\text{H NMR } \delta$: (CD_3OD) 7.6 (dd, 2H, H4 H5), 4.3 (t, 2H, H6), 3.95 (s, 3H, Me1), 2.8 (s, 3H, Me2), 1.95 (m, 2H, H7), 1.5 (m, 2H, H8), 1.1 (t, 3H, H9).

IR: (cm^{-1} , neat liquid) ν : 3135 (CH aromatic), 2961, 2935 (CH_2 aliphatic), 2057 ($\text{N}=\text{C}=\text{S}$), 1588 ($\text{C}=\text{C}$), 1466 ($\text{C}=\text{C}$).

Elemental analysis. $\text{C}_9\text{H}_{17}\text{N}_2\text{SCN}$ requires C 56.8, H 8.10, N 19.9. Found C 57.2, H 8.01, N 19.8.

1-butyl-2,3,4,5-tetramethyl imidazolium chloride. 1,2,4,5-tetramethyl imidazole (5.30 g, 0.043 mole) and 1-chlorobutane (4.5 cm^3 , 0.043 mole) were refluxed together under nitrogen for 24 hours and then any unreacted 1-chlorobutane removed under vacuum. The product was recrystallised from acetonitrile and ethyl acetate.

$^1\text{H NMR}$ (CDCl_3) δ : 4.0 (t, 2H, H6), 3.8 (s, 3H, Me), 2.8 (s, 3H, Me), 2.2 (s, 6H, 2x Me), 1.6 (m, 2H, H7), 1.3 (m, 2H, H8), 0.9 (t, 3H, H9).

FAB-MS m/z 181 (M⁺), 124 (loss of butyl), 56 (butyl).

Elemental Analysis. C₁₁H₂₁N₂Cl requires C 61.0, H 9.77, N 12.9. Found C 60.5, H 9.83, N 13.1.

2-phenyl substituted ionic liquids.

1-methyl-2-phenyl imidazole. 2-phenyl imidazole (4.32 g, 0.03 mole) in tetrahydrofuran (50 cm³) was added to a slurry of sodium hydride (3.60 g, 0.09 mole, 60 % slurry in oil, cleaned by washing with pentane) in tetrahydrofuran (20 cm³) under nitrogen. Iodomethane (1.87 cm³, 0.03 mole) was added *via* syringe under nitrogen causing effervescence and heat release. The solution was stirred for 2 hours at 50 °C and then the tetrahydrofuran removed under vacuum. Dichloromethane (50 cm³) and water (50 cm³) were added and the solution neutralised by addition of hydrochloric acid. The dichloromethane layer was removed by separation and dried under vacuum.

¹H NMR (CDCl₃) δ : 7.5 (m, 5H, phenyl), 7.1 (s, 1H, H5), 6.9 (s, 1H, H4), 3.7 (s, 3H, Me).

1-butyl-2-phenyl-3-methyl imidazolium chloride. 1-methyl-2-phenyl imidazole (1.67 g, 0.01 mole) and 1-chlorobutane (1.3 cm³, 0.012 mole) were refluxed together under nitrogen for 24 hours. The excess 1-chlorobutane was then removed under vacuum leaving the product as a brown solid. Yield 86%.

¹H NMR (CDCl₃) δ : 8.2 (m, 5H, Ph), 7.9 (dd, 2H, H4 H5), 4.0 (t, 2H, H6), 3.8 (s, 3H, Me), 1.7 (m, 2H, H7), 1.2 (m, 2H, H8), 0.8 (t, 3H, H9).

Elemental analysis: C₁₄H₁₉N₂Cl expects C 67.1, H 7.64, N 11.2. Found C 67.1, H 7.53, N 12.1.

FAB-MS m/z 215 (M⁺), 159 (loss of butyl).

1-butyl-2-phenyl-3-methyl imidazolium tetrafluoroborate. 1-butyl-2-phenyl-3-methyl imidazolium chloride (5.92 g, 0.024 mole) and sodium tetrafluoroborate (2.60 g, 0.024 mole) were refluxed together in acetone (25 cm³) for 24 hours under nitrogen.

The precipitated potassium chloride was removed by filtration and the acetone removed under vacuum. Dichloromethane (50 cm³) and water (50 cm³) were added and the dichloromethane layer separated and dried under vacuum leaving a brown liquid. Yield 71 %.

¹H NMR (CDCl₃) δ: 7.6 (m, 5H, Ph), 7.1 (s, 1H, H4), 6.9 (s, 1H, H5), 4.0 (t, 2H, H6), 3.7 (s, 3H, Me), 1.7 (m, 2H, H7), 1.2 (m, 2H, H8), 0.8 (t, 3H, H9).

¹⁹F NMR (CDCl₃) δ: -153.4 (q, 4H, BF₄).

FAB-MS *m/z* 215 (M⁺), 159 (loss of butyl).

Elemental analysis. C₁₄H₁₉N₂BF₄ expects C 55.7, H 6.30, N 9.28. Found C 57.1, H 6.28, N 10.9.

1-butyl-2-phenyl-3-methyl imidazolium hexafluorophosphate. 1-butyl-2-phenyl-3-methyl imidazolium chloride (5.00 g, 0.02 mole) was added to an aqueous solution of potassium hexafluorophosphate (3.67 g, 0.02 mole) and the hexafluorophosphate product separated as a lower layer. This was washed with water and dried under vacuum. Dichloromethane (50 cm³) was added and the solution filtered and dried leaving the product as an orange solid. Yield 75%.

¹H NMR (CDCl₃) δ: 7.4 (m, 5H, Ph), 7.1 (s, 1H, H4), 6.9 (s, 1H, H5), 4.0 (t, 2H, H6), 3.7 (s, 3H, Me), 1.7 (m, 2H, H7), 1.2 (m, 2H, H8), 0.8 (t, 3H, H9).

¹⁹F NMR (CDCl₃) δ: -73 (d, PF₆).

FAB-MS *m/z* 215 (M⁺), 159 (loss of butyl).

Elemental analysis. C₁₄H₁₉N₂PF₆ expects C 46.7, H 5.28, N 7.78. Found C 48.9, H 5.32, N 8.90.

Sulfonation reactions.

Sulfonation of 1-methyl-2-phenyl imidazolium. SO₃ (0.75 g, 9.4 mmole) in nitromethane (20 cm³) was added dropwise over 15 minutes to a solution of 1-methyl-2-phenyl imidazole (1.48 g, 9.4 mmole) in nitromethane (20 cm³) at 0 °C under nitrogen and the solution stirred for a further 15 minutes at 0 °C. Water (20 cm³) was then added and the solution heated to 50 °C for 20 minutes. The lower

organic layer was then separated and the aqueous layer washed with dichloromethane (30 cm³). The washings were added to the nitromethane solution and the solvents removed under vacuum leaving an orange solid.

FAB-MS *m/z* 397 (C₁₀H₇N₂(SO₃H)₃), 317 (C₁₀H₈N₂(SO₃H)₂), 239 (C₁₀H₉N₂SO₃H), 159 (C₁₀H₉N₂).

Sulfonation of 1-methyl-2-phenyl imidazolium at high dilution. SO₃ (1.0 g, 0.0125 mole) in nitromethane (30 cm³) was added dropwise over 45 minutes to a solution of 1-methyl-2-phenyl imidazole (1.976 g, 0.0125 mole) in nitromethane (40 cm³) at 0 °C under nitrogen and the solution stirred for a further 45 minutes at 0 °C. Water (30 cm³) was then added and the solution heated to 50 °C for 20 minutes. The lower organic layer was then separated and the aqueous layer washed with dichloromethane (30 cm³). The washings were added to the nitromethane solution and the solvents removed under vacuum leaving an orange solid.

FAB-MS *m/z* 397 (C₁₀H₇N₂(SO₃H)₃), 317 (C₁₀H₈N₂(SO₃H)₂), 239 (C₁₀H₉N₂SO₃H), 159 (C₁₀H₉N₂).

¹H NMR (CDCl₃) δ: 7.6 (m, 2H, Ph), 7.5 (m, 2H, Ph), 7.1 (s, 1H, H5), 7.0 (s, 1H, H4), 3.8 (s, 3H, Me).

Sulfonation of 1-butyl-2-phenyl-3-butyl imidazolium chloride. SO₃ (1.00 g, 0.0125 mole) was dissolved in nitromethane (20 cm³) and added dropwise over 15 minutes to a solution of 1-butyl-2-phenyl-3-methyl imidazolium chloride (3.13 g, 0.0125 mole) in nitromethane (20 cm³) at 0 °C under nitrogen. The solution was stirred at 0 °C for a further 15 minutes then water (20 cm³) added. The solution was heated at 50 °C for 20 minutes to hydrolyse any sulfonic anhydride present. The organic layer was then separated and the aqueous layer washed with dichloromethane (30 cm³). The washings were added to the nitromethane solution and the solvents removed under vacuum leaving an orange solid.

FAB – MS *m/z* 215 (1-butyl-2-phenyl-3-methyl imidazolium chloride), 159 (loss of butyl).

^1H NMR (CDCl_3) δ : 8.1 (d, 1H, H5), 7.9 (d, 1H, H4), 7.6 (m, 5H, Ph), 4.1 (t, 2H, H6), 3.8 (s, 3H, Me), 1.7 (t, 2H, H7), 1.2 (m, 2H, H8), 0.8 (m, 3H, H9).

Alkylation of 1-methyl-2-(phenyl sulfonyl) imidazole. 1-methyl-2-(phenyl sulfonyl) imidazole (1.00 g, 4.2 mmole) and 1-chlorobutane (5 cm³, 0.047 mole) were refluxed together under nitrogen for 24 hours. The excess 1-chlorobutane was removed under vacuum leaving a brown solid.

FAB-MS m/z 397 ($\text{C}_{10}\text{H}_7\text{N}_2(\text{SO}_3\text{H})_3$), 317 ($\text{C}_{10}\text{H}_8\text{N}_2(\text{SO}_3\text{H})_2$), 239 ($\text{C}_{10}\text{H}_9\text{N}_2\text{SO}_3\text{H}$), 159 ($\text{C}_{10}\text{H}_9\text{N}_2$).

^1H NMR (CDCl_3) δ : 7.7 (m, 2H, Ph), 7.5 (m, 2H, Ph), 7.1 (s, 1H, H5), 7.0 (s, 1H, H4), 3.8 (s, 3H, Me).

Nitration reactions.

Nitration of 1-methyl-2-phenyl imidazole. A solution of nitric acid (70 %, 11.44 cm³, 8 mmole) and sulfuric acid (98 %, 10 cm³, 0.187 mole) was slowly added to a solution of 1-methyl-2-phenyl imidazole in water (20 cm³) and the solution heated at 80 °C for 24 hours. The solution was stirred overnight at room temperature then neutralised by addition of potassium carbonate (52.79 g, 0.382 mole). The solution was extracted twice with chloroform (50 cm³) and the solvent removed under vacuum leaving an orange oil, recrystallised from diethyl ether to give a yellow solid. FAB-MS m/z 204 ($\text{C}_{10}\text{H}_9\text{N}_2\text{NO}_3$), 158 (1-methyl-2-phenyl imidazole).

^1H NMR (CDCl_3) δ : 8.5 – 7.5 (m, 9H, Ar), 7.1 (m, 1H, H5), 7.0 (m, 1H, H4), 3.8 (d, 3H, Me).

Nitration of 2-phenyl imidazole. 2-phenyl imidazole (4.0 g, 0.028 mole) was dissolved in sulfuric acid (98 %, 20 cm³) and a solution of nitric acid (70 %, 1.76 cm³, 0.028 mole) in sulfuric acid (40 cm³) added slowly with stirring at 0 °C. The solution was stirred at 0 °C for two hours and at room temperature overnight then poured into iced water. Sodium hydroxide was added until pH9 was achieved producing a yellow precipitate. This was removed by filtration, washed three times

with hot water (50 cm³) and then diethyl ether (50 cm³) then dried under vacuum. M.p. 305 – 307 °C.

FAB-MS 190 (nitrophenyl imidazole), 145 (phenyl imidazole).

¹H NMR (d₆-dmsO) δ: 8.3 (dd, 4H, Ph), 7.4 (s, 1H, H5), 7.2 (s, 1H, H4).

Nitration of 1-butyl-2-phenyl-3-methyl imidazolium chloride. 1-butyl-2-phenyl-3-methyl imidazolium chloride (3.47 g, 0.014 mole) was dissolved in sulfuric acid (10 cm³) and a solution of nitric acid (70 %, 0.88 cm³, 0.014 mole) in sulfuric acid (98 %, 10 cm³) added dropwise with stirring at 0 °C. The mixture was stirred at 0 °C for 2 hours and then at room temperature overnight. The solution was poured into iced water and neutralised with sodium hydroxide. Extraction with dichloromethane (50 cm³) followed by drying under vacuum left a brown oil.

FAB-MS *m/z* 257 (1-butyl-2-nitrophenyl-3-methyl imidazolium), 215 (1-butyl-2-phenyl-3-methyl imidazolium), 215 (1-methyl-2-phenyl imidazole).

¹H NMR (CDCl₃) contains large numbers of peaks in both the aromatic and aliphatic region of the spectrum indicating the probable decomposition of the 1-butyl-2-phenyl-3-methyl imidazolium chloride.

Methylation of 2-(nitrophenyl) imidazole. 2-(nitro phenyl) imidazole (3.00 g, 0.016 mole) in tetrahydrofuran (50 cm³) was added to a slurry of sodium hydride (1.9 g, 0.048 mole of 60 % slurry in oil, cleaned with pentane) in tetrahydrofuran (20 cm³) and iodomethane (1 cm³, 0.016 mole) added *via* syringe. The solution was stirred overnight at room temperature then at 50 °C for 3 hours. The tetrahydrofuran was removed under vacuum and dichloromethane (50 cm³) and water (50 cm³) added. The solution was neutralised by addition of hydrochloric acid and the dichloromethane layer separated off. This was dried under vacuum yielding a yellow solid. M.p. 111-113 °C.

¹H NMR (CDCl₃) δ: 8.3 (dd, 2H, Ph), 7.85 (dd, 2H, Ph), 7.2 (d, 1H, H5), 7.0 (d, H4, 1H), 3.7 (s, 3H, Me).

FAB-MS *m/z* 204 (1-methyl-2-(nitrophenyl) imidazole).

Alkylation of 1-methyl-2-nitrophenyl imidazole in tetrahydrofuran. 1-methyl-2-nitrophenyl imidazole (2.08 g, 0.01 mole) and 1-chlorobutane (2 cm³, 0.02 mole) were refluxed together in tetrahydrofuran under nitrogen for 24 hours then dried under vacuum.

¹H NMR (CDCl₃) δ: 8.3 (dd, 2H, Ph), 7.85 (dd, 2H, Ph), 7.2 (d, 1H, H5), 7.0 (d, H4, 1H), 3.7 (s, 3H, Me).

Alkylation of 1-methyl-2-nitro phenyl imidazole in neat 1-chlorobutane. 1-methyl-2-nitrophenyl imidazole (2.08 g, 0.01 mole) and 1-chlorobutane (2 cm³, 0.02 mole) were refluxed together under nitrogen for 24 hours then the excess 1-chlorobutane removed under vacuum.

¹H NMR (CDCl₃) δ: 8.3 (dd, 2H, Ph), 7.8 (dd, 2H, Ph), 7.2 (s, 1H, H5), 7.0 (s, H4, 1H), 3.8 (s, 3H, Me).

7 The Structure of Ionic Liquids in the Liquid State.

7.1 Introduction.

The composition of room temperature ionic liquids by their very nature is quite unlike that of conventional molecular solvents. As outlined in Chapter 1, the interest in ionic liquids has increased rapidly in the last decade and the potential uses of these new species have centred on their use in the liquid form. Despite this, however, very few studies have been devoted to the investigation of their liquid structure. This is a direct result of the inherent difficulties in obtaining this structural data. Some information can be gained from NMR and IR studies, as discussed in Chapter 3, and EXAFS has been used to study the structure of some dissolved species,¹ but few other analytical probes are suitable for liquid studies. Structural studies of ionic liquids have mainly been confined to investigations in their solid state using x-ray crystallography, although even in this area coverage is rather sparse (see Chapter 8).

A review of the structural determination of imidazolium ionic liquids in the liquid form highlights not only a dearth of investigations, but also suggests some significant problems in those that do exist. The use of ¹H NMR to gain some insight into the nature and extent of the hydrogen bonding within the bmimPF₆ and BF₄ species has been described in detail in Chapter 3 and these investigations have subsequently been

¹ A. J. Dent, K. R. Seddon and T. Welton, *J. Chem. Soc., Chem. Commun.*, 1990, 315–316. A. J. Carmichael, C. Hardacre, J. D. Hobrey, M. Nieuwenhuyzen and K. R. Seddon, *Anal. Chem.*, 1999, **71**, 4572–4574.

challenged by a number of authors. It is now considered unlikely that the chemical shift of the H2 proton of the imidazolium ring in the ^1H NMR spectrum can be used as a direct measure of the extent of hydrogen bonding within each species.² It is evident, therefore, that a new structural tool for the analysis of the liquid structure of room temperature ionic liquids is required.

One possibility is to use the electrochemical technique, Alternating Current (AC) Impedance Spectroscopy, to provide insight into the structural nature of these liquid species. Electrochemical analysis has previously been performed on a number of ionic liquids to determine the size of their electrochemical window (see Chapter 3) using cyclic voltammetry. Use of AC impedance spectroscopy as an alternative technique, one not previously used in the analysis of ionic liquids, gives values for the real and imaginary impedance of these species, as a function of frequency. These data can be related to the fundamental physical properties of the system giving insight into the structure and dynamics of the liquids.

² J. D. Holbrey and K. R. Seddon, *J. Chem. Soc., Dalton Trans.*, 1999, 2133 – 2139.

7.2 AC Impedance Spectroscopy.

7.2.1 Introduction.

AC impedance spectroscopy is a method of studying a chemical system using small amplitude voltage oscillations. This perturbs the system from its equilibrium position and the response is then monitored. The voltage perturbation used is often very small to prevent large-scale modification of the system, thereby simplifying the mathematical modelling. In order to understand fully the applicability of this technique to the study of ionic liquids it is useful to understand the response of a number of different systems to the application of an alternating potential.

If the system is composed only of a resistor then the response of the system to an alternating potential is an in phase alternating current, as shown in Figure 7.1. The conduction that occurs is a result of the direct transfer of electrons across the resistor.

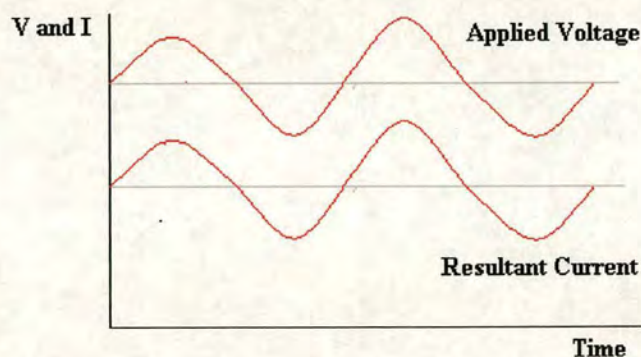


Figure 7.1. The response of a resistor to an alternating voltage.

(The applied voltage is equivalent to the potential if the potential at the reference electrode is zero, otherwise the term potential difference must be used. Throughout this investigation the potential of the reference electrode is taken as zero, hence the terms potential and voltage can be used interchangeably.)

In a capacitor, the conduction is indirect as no electrons actually cross the capacitor. Application of a voltage to a capacitor results in the capacitor becoming charged, by an amount dependant of the size of the capacitance. The conduction that occurs is due to injection of electrons into one plate of the capacitor and the removal of

electrons from the other plate. The current that results from the application of an oscillating voltage to a capacitor is 90° out of phase with the applied voltage, as shown in Figure 7.2.

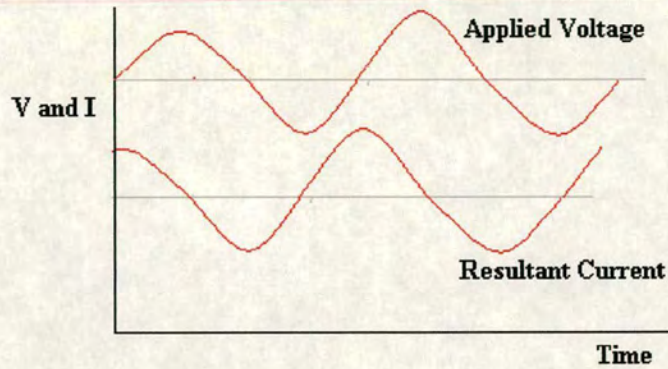


Figure 7.2. The response of a capacitor to an alternating voltage.

Hence, by measuring the response of an electrical system to an alternating voltage it is possible to deduce its composition in terms of resistance and capacitance.

7.2.2 AC Impedance Spectroscopy of Ionic Aqueous Solutions.

Of course, real systems do not consist of capacitors and resistors. However, when two parallel plate electrodes are inserted into an ionic aqueous solution and a voltage is applied, ions move towards the plate of opposite charge. Analysis by AC impedance spectroscopy is performed by measuring the response of the system to an alternating voltage over a range of frequencies.

At high frequency, the induced current is proportional to the voltage applied and is direct as the ions move or migrate under direct influence of the field. Therefore, bulk ion movement behaves in an analogous way to a resistor. The ions oscillate near their equilibrium position and the current passed is due to the ion movement. At low ionic concentration, as there is negligible interactions between the cations and anions, the total current is the sum of the contributions from the individual ions, and

$$\Lambda_{MX}^0 = \lambda_M^0 + \lambda_X^0 \quad (1)$$

where Λ_{MX}^0 is the limiting molar conductivity of the salt M^+ and X^- , and λ_X^0 and λ_M^0 are the limiting molar conductivities of the individual ions. Therefore, current is due to ion motion and the system behaves as a resistor.

As the frequency of the ac perturbation is reduced the ions travel further through solution. At the low frequency limit the electrode double layers become charged, with ions from the solution at the plates exactly balancing the charge on the electrodes, forming a double layer at each electrode. Thus, if there is no electrode redox reaction, at the low frequency limit the system behaves as two capacitors, with the parallel plates of each capacitor being an electrode and its double layer respectively.

Hence, the simplest electrical representation of an ionic aqueous solution is a resistor and two capacitors in series, as shown in Figure 7.3.

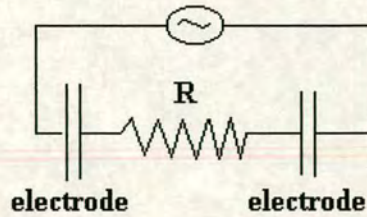


Figure 7.3. The simplest electrical representation of an ionic aqueous solution.

AC impedance spectroscopy uses alternating voltages over a range of different frequencies. The magnitude of the applied voltage, V , at any given frequency, is given by:

$$V(f) = V_0 + V_1 \sin(2\pi ft) \quad (2)$$

Where f is the frequency of the applied potential (Hz). The resulting current, i , is used to calculate the impedance, Z , of the system:

$$Z(f) = V(f) / i(f) = Z_{\text{real}} \sin(2\pi ft) - Z_{\text{im}} \cos(2\pi ft) \quad (3)$$

Impedance can be considered as analogous to resistance in that it is a measure of the amount that the system *impedes* the passage of current. Z_{real} is the real impedance, which is in phase with the applied voltage, and represents the resistive or conductive component of the system. Z_{im} is the imaginary impedance, which is out of phase with the applied voltage and this represents the capacitive component.

The response of a system to AC impedance spectroscopy is often recorded in the form of a Nyquist plot, shown in Figure 7.4. This shows the real impedance of the system plotted against the imaginary impedance at a variety of frequencies.

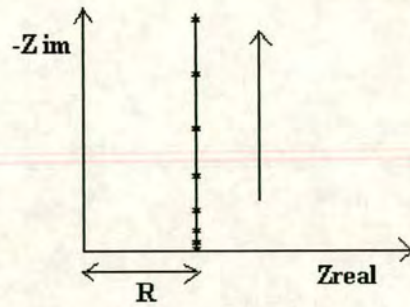


Figure 7.4. An idealised Nyquist plot for the circuit in Figure 7.3. The arrow shows the direction of scan of data points from high to low frequency.

The real impedance (or resistance) of the system is given by the high frequency intercept of the line with the Z_{real} axis. At this point the ions are oscillating around their equilibrium positions and no double layers have formed, hence the capacitive impedance is zero. At lower frequencies (the upper portion of the plot) the ions have more time to move and the double layers are formed. Thus, the vertical line gives information about the capacitance of the system. The Nyquist plot recorded for a $0.1 \text{ mol dm}^{-3} \text{ KCl}_{(\text{aq})}$ solution is shown in Figure 7.5.

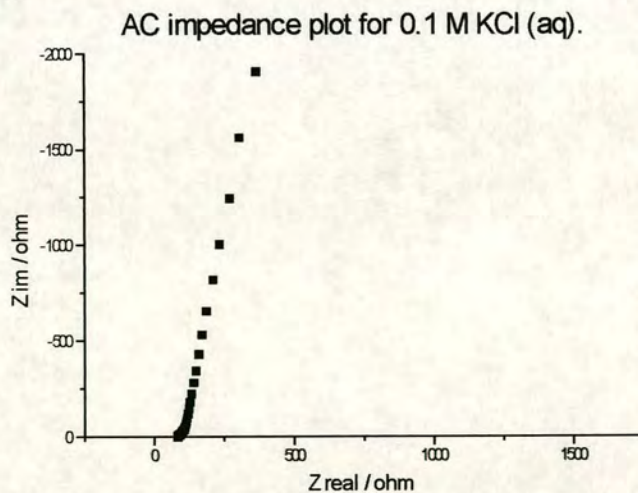


Figure 7.5. The Nyquist plot for $0.1 \text{ M KCl}_{(\text{aq})}$. For all measurements made, the frequency of the alternating potential was decreased logarithmically from $10\,000 \text{ Hz}$ to 1 Hz . The line intercepts the x-axis at the position of highest frequency and runs upward to the position of lowest frequency.

It is evident that there is a deviation of this plot from the idealised form in that it is not vertical but has a slight gradient. This is attributed to inhomogeneity of the electrode surface.³ At high frequencies the resistance is proportional to the distance between the two electrodes. As the frequency decreases all areas of the electrodes become charged including the pits and troughs present on the roughened surface. This causes an increase in the resistance hence the Nyquist plot cants slightly to increased values of Z_{real} .

Measurement of the impedance of a solution of known resistance also allows the cell constant to be determined. The measured resistance of a solution ideally depends on the area of the electrodes used, A , and the distance between them, L :

$$R = \rho \left(\frac{L}{A} \right) \quad (4)$$

Where R is the resistance and ρ is the resistivity of the solution. L/A is termed the cell constant. In practise, this cell constant is not exactly equal to L/A as the equation assumes normal field lines and no edge effects, but L/A can be determined by calibration by measuring R for the cell for a solution of known ρ . This was measured experimentally using 0.1 M KCl and 0.01 M KCl as $(1.0 \pm 0.05) \text{ cm}^{-1}$. This cell allows the direct relation of the resistance of the system, in ohms, to the resistivity, in ohm cm, with no need for the inclusion of a term for the cell constant.

³ *Research in Chemical Kinetics*, Vol. 4. Ed. R. G. Compton and G. Hancock. p1-31, A. R. Mount.

7.2.3 AC Impedance Spectroscopy of Ionic Liquids.

The Nyquist plot measured for 1-butyl-3-methyl imidazolium hexafluorophosphate at 30 °C is shown in Figure 7.6.

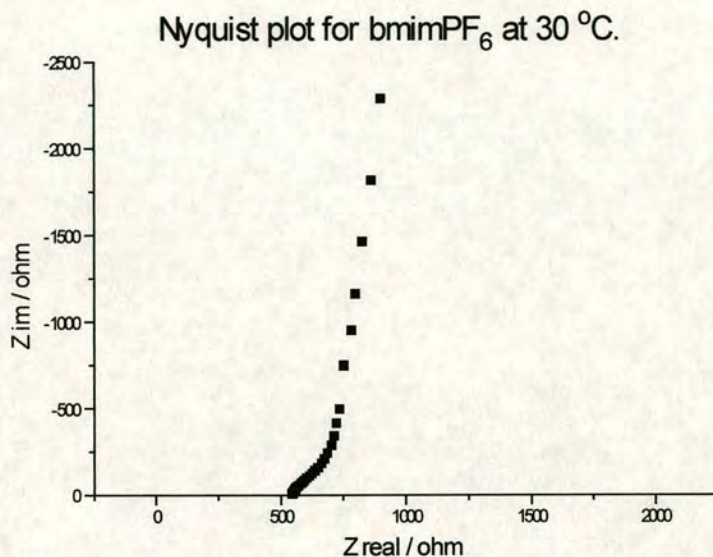


Figure 7.6. Plot of real against imaginary impedance for bmimPF₆ at 30 °C.

There are significant differences in this plot from that of the aqueous solution of KCl and these give information about the behaviour of ionic liquids under an applied voltage.

The behaviour of an ionic liquid on application of a voltage clearly differs from that of an ionic aqueous solution. The behaviour of these systems appears similar to that of the transmission line for redox active polymers and therefore the application of this model to ionic liquid systems should be considered.

Previous studies suggested that the ionic liquids show significant aggregation and effectively exist as neutral solvents (thus the observed resistance is considerably higher than might be expected for an entirely ionic medium). It was proposed that application of a voltage to the system results in the formation of double layers, which requires ion dissociation. Formation of a negative ion double layer near a positively charged electrode would be balanced by the formation of a positive charge that is

repelled from the double layer by the field. The reverse process would occur at the negatively charged electrode, as shown in Figure 7.7.

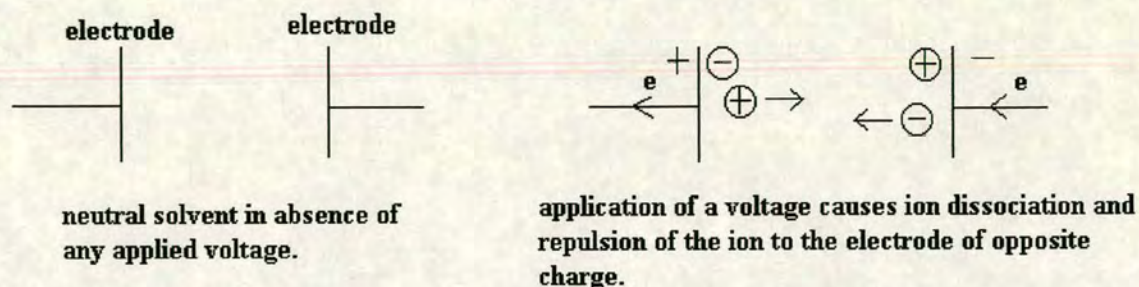


Figure 7.7. The proposed behaviour of an ionic liquid under an applied voltage.

The transmission line behaviour observed for redox active polymer modified electrodes is shown in Figure 7.8. In this system, typically the positive redox charges move along the polymer chains with negative counter-ions moving through the pores to provide electroneutrality.⁴

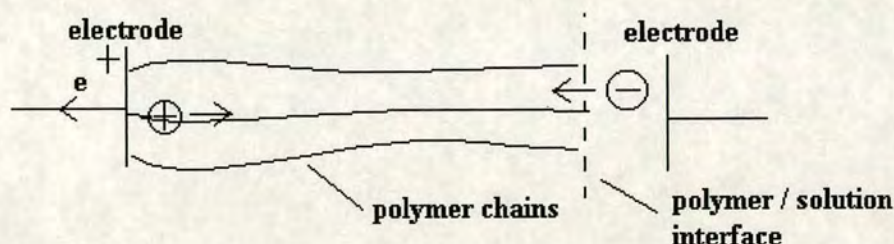


Figure 7.8. The transmission line behaviour of redox active polymer modified electrodes.

Thus, there is a redox reaction on the polymer coated electrode, with positive ions being produced at the polymer / electrode interface and the negative ions being injected at the polymer / solution interface to maintain electroneutrality. This charge injection mechanism is analogous to the processes that take place in an ionic liquid, where application of a voltage should result in the dissociation of the ion aggregates at the electrodes and the injection of one ion type from the double layer, positive ions at the anode and negative ions at the cathode. These then move through the ionic

liquid to balance charge and maintain electroneutrality. Here, a positive ion appears to be injected at one plate and a negative ion appears to be injected at the other plate, as the ions dissociate.

This mechanism differs from a conventional electrolyte solution where application of a voltage causes ions to move from the bulk solution and to align with the electrodes until the charge at the electrode is exactly balanced by the opposite charge in the diffuse double layer. There is no injection of charge from the electrode to the solution unless a redox reaction occurs. Here, no redox reaction occurs but the electronic current results in free ion formation at the electrode, which is analogous to a redox reaction. Thus, the behaviour of ionic liquids at the electrode is significantly different from the ionic aqueous solutions studied previously using AC impedance spectroscopy.

Albery *et al.*⁴ developed a transmission line for the modelling of AC impedance spectroscopy of polymer films for ions of different mobilities and this can be modified for application to ionic liquid systems.

A transmission line is generally a method of representing fundamentals of the charge movement within a system, thereby producing electronic circuit elements such as capacitors and resistors which can be related to the physical parameters of the system such as diffusion coefficients and ion concentration. When considering the response of an ionic liquid to the application of an alternating voltage the effect of ion diffusion and migration must be considered. Application of a voltage to the ionic liquid results in ion movement towards the electrode of the opposite charge but this, in turn, creates a concentration gradient within the system. This results in the diffusion of ions in the opposite direction. Thus, the driving force for the ion motion is not simply the voltage, but the voltage modified by the ion concentration. This results in the voltage in the transmission line being applied through two distributed capacitances, C_M and C_X , which correlate the effects of the concentrations of the ions

⁴ W. J. Albery and A. R. Mount, *Electroactive Polymer Electrochemistry, Part 1: Fundamentals*, Ed. by M. E. G. Lyons, Plenum Press, New York, 1994. J. Albery, C. M. Elliott and A. R. Mount, *J. Electroanal. Chem.*, 1990, **288**, 15 – 34.

M^+ and X^- at each point in the solution. This modifies the voltage, producing the driving force, which then drives the ion motion.

The Nernst-Planck equation (5) defines the flux of ions, j , within the ionic liquid and this fundamental equation allows for the effects of diffusion and migration.

$$j = D_m \left[\frac{d\bar{m}}{dz} \pm \bar{m} \left(\frac{F}{RT} \right) \left(\frac{dE}{dz} \right) \right] \quad (5)$$

D_m is the diffusion coefficient of the ion, \bar{m} is the ion concentration, E is the potential and z is the distance of ion movement. Thus, the first term on the right hand side describes the ion motion as a result of diffusion, and the second term describes ion motion (migration) as a result of the application of a voltage.

The total capacitance term that results from the first term in equation (5) can be calculated from equation (6), where A is the electrode area and L is the distance between the electrodes.

$$\frac{1}{C_\Sigma} = \left(\frac{RT}{F^2} \right) \left(\frac{1}{\bar{M}} \right) \left(\frac{1}{AL} \right) + \left(\frac{RT}{F^2} \right) \left(\frac{1}{\bar{X}} \right) \left(\frac{1}{AL} \right) = \frac{1}{C_M} + \frac{1}{C_X} \quad (5)$$

Of course, in the ionic liquid system the concentration of free cations, \bar{M} , is equal to the concentration of free anions, \bar{X} , to preserve electroneutrality. Each of these give the total *free* ion concentration, \bar{m} .

The transmission line used to represent the electrochemical behaviour of ionic liquids during AC impedance spectroscopy is shown in Figure 7.9. The transmission line contains no capacitors to take into account the double layer of ions at the electrode, as would be expected for an ionic aqueous solution (Figure 7.3), because, as explained previously, the electrons appear to be injected directly into the solution. In this way the transmission line used for the ionic liquids and the conducting polymers studied previously are very similar.

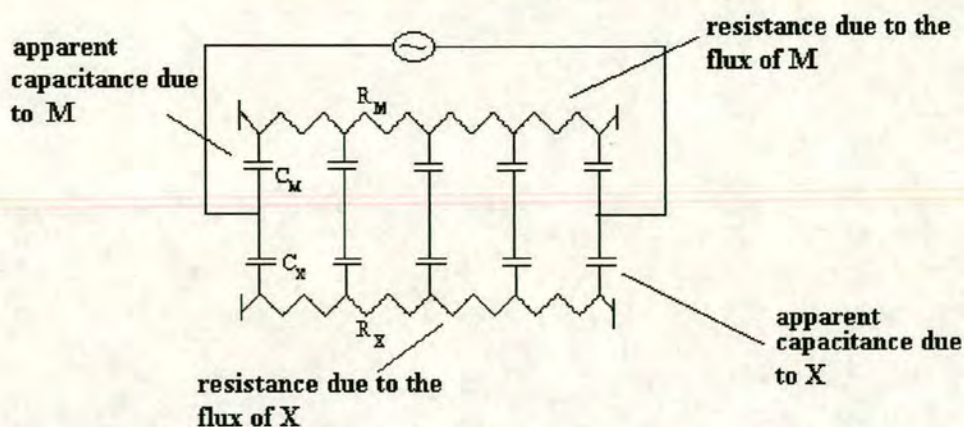


Figure 7.9. Transmission line modified to take into account the effect of diffusion and migration of the cations, M, and anions, X, and the capacitance between the two species.

The transmission line used to represent the ionic liquid can be used to explain the second unusual feature of the Nyquist plot of bmimPF_6 , which is not present in the AC impedance spectra of aqueous ionic solutions. AC impedance spectroscopy of a range of ionic liquids consistently results in plots with 45° lines at high frequency. This is known as the Warburg region, shown in Figure 7.10.

At high frequencies (at the intercept of the x-axis on the Nyquist plot) the current passes through the path of least resistance, along R_M or R_X in the transmission line, hence this portion of the plot gives information about the smallest of these resistance values. However, as the frequency is decreased and the ions are oscillating more slowly, the capacitors C_M and C_X begin to be charged, – the ions have more time to move within the system and their motion becomes increasingly coupled, with the slowest retarding the fastest, producing an increased resistance. This produces the observed 45° line. When all of the capacitors are charged the only process that is taking place is the charging and discharging of the distributed capacitance through R_M and R_X and hence, neglecting inhomogeneity effects, a vertical line is produced. This occurs at a value of $(R_M + R_X) / 3$. This can, in turn, be related to the transport number of the individual ions, and it can be shown that the high frequency intercept

$$\text{occurs at: } Z_{\text{real}} = \frac{R_M}{1 + \frac{t_-}{t_+}} = \frac{R_X}{1 + \frac{t_+}{t_-}}$$

Hence, if the transport numbers of the ions are equal, the resistance of each ion is equal, the current can pass through either R_M or R_X , and the total resistance is $R_M / 2$ or $R_X / 2$. However, if the transport numbers are different, this relationship can be used to determine the proportion of charge that passes through each resistor. This relationship is used in the mathematical modelling of the AC impedance spectroscopy of ionic liquids (section 7.2.4). Hence, analysis using this method in principle allows the parameters R_M and R_X to be determined.

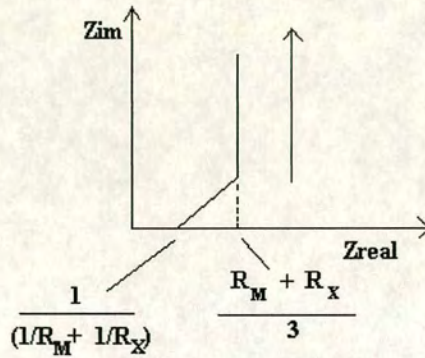


Figure 7.10. A Nyquist plot that includes a Warburg region.

7.2.4 Modelling Ionic Liquids.

To gain further information about the liquid structure of ionic liquids and their response to an alternating voltage, the behaviour of the ionic liquids was modelled using transmission line theory, fitted using SigmaPlot 3.0. If good agreement between experimental and calculated values is observed, this confirms that the transmission line used is indeed a good representation of the ionic liquid system.

The basic principle of the modelling is that the equations defining the imaginary and real impedance, (7), (8), (9) and (10) are used to calculate real and imaginary impedances from the frequency, f , of the AC perturbation. These are then compared to the experimental data.⁴

$$Z_{\text{real}} = \rho + 2\rho \left(\frac{\sinh \theta \cos \theta - \cosh \theta \sin \theta}{2\theta(\sinh^2 \theta \cos^2 \theta + \cosh^2 \theta \sin^2 \theta)} \right) + (1 - 2\theta) \left(\frac{\sinh \theta \cosh \theta - \cos \theta \sin \theta}{2\theta(\sinh^2 \theta \cos^2 \theta + \cosh^2 \theta \sin^2 \theta)} \right) \quad (7)$$

$$Z_{\text{im}} = 2\rho \left(\frac{\sinh \theta \cos \theta + \cosh \theta \sin \theta}{2\theta(\sinh^2 \theta \cos^2 \theta + \cosh^2 \theta \sin^2 \theta)} \right) - (1 - 2\theta) \left(\frac{\sinh \theta \cosh \theta + \cos \theta \sin \theta}{2\theta(\sinh^2 \theta \cos^2 \theta + \cosh^2 \theta \sin^2 \theta)} \right) \quad (8)$$

$$\rho = \frac{R_X R_M}{(R_M + R_X)^2} \quad (9)$$

$$\theta = [2\pi f C_\Sigma (R_X + R_M) / 2]^{1/2} \quad (10)$$

The modelling program then adjusts the variable parameters to provide the closest fit of calculated to experimental values. The minimum number of physical parameters are designated as variable, and then adjusted to provide the most accurate results. Initially, bmimPF₆ was modelled using two variable parameters, R and C_Σ , the total resistance and total capacitance. This model assumes that the resistances of the cation and anion, R_M and R_X , are equal and given by R and, thus, given that the ion

concentrations are equal, that the transport number of each ion is 0.5 (their diffusion coefficients are equal).

The values of capacitance and resistance for bmimPF₆ calculated using this model are shown in Table 7.1.

Temp / °C	Resistance / ohm	S.D. / ohm	Capacitance / $\times 10^{-5}$ F	S.D. / $\times 10^{-5}$ F
20	2555	18	11.58	0.39
30	1486	15	8.76	0.25
40	907	12	9.00	0.25
50	626	15	8.50	0.29

Table 7.1. Values of resistance and capacitance calculated for bmimPF₆.

Assessment of the accuracy of the fit can be made by comparison of the calculated and experimental values of real and imaginary impedance. This is often done by comparison of the experimental and calculated Nyquist plots. However, although this is good for assessing the correspondence of real and imaginary impedance data, it does not allow the variation with frequency to be assessed. This can be done by plotting the experimentally determined impedance values against those calculated by the model, as shown in Figure 7.11. The negative region of this plot shows the imaginary impedance and the positive region shows the real impedance. For all the ionic liquids modelled, good correlation between calculated and experimentally determined values of imaginary impedance were observed at all frequencies (a straight line of gradient 1 and intercept 0 is produced). The correlation was also good for the real impedance except at low frequencies. As explained previously, the lower frequency (upper) portion of the Nyquist plot would be expected to be vertical but in real systems a deviation from vertical is observed as a result of inhomogeneity of the electrode surface. There is a deviation of calculated from experimental impedance values for the real impedance because the real impedance actually increases with frequency due to inhomogeneity, which transmission line theory cannot account for.

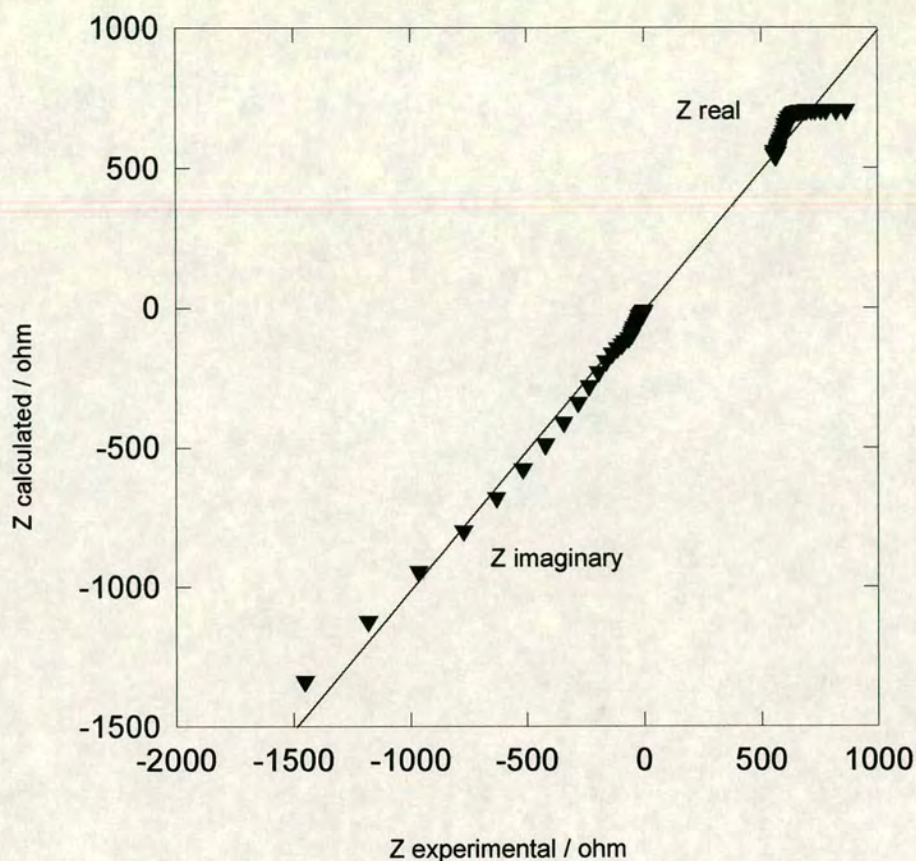


Figure 7.11. Comparison of calculated and experimental impedance values for bmimPF_6 at 30°C . Intercept = -17 ohm. Gradient = 1.007 . $r = 0.994$.

As shown in Table 7.1, mathematical modelling of bmimPF_6 allowed the total capacitance of the system, C_Σ , to be calculated. Variations in C_Σ can also be determined using the relationship between the imaginary impedance and the frequency of the applied voltage at low frequency.

The capacitance of the system given by the low frequency limit of the transmission line model and is related to the imaginary impedance of the system at low frequencies by:

$$-Z_{im} = 1 / (2\pi f C_\Sigma) \quad (11)$$

The capacitance of the ionic liquid systems can be calculated using this equation by plotting the imaginary impedance against $1/2\pi f$, which should give a straight line.

The reciprocal of the gradient of this line gives the capacitance of the system, which allows ready comparison of changes in C_{Σ} . The values of imaginary impedance measured for bmimPF₆ at a range of temperatures were plotted against $1/2\pi f$ and the results are shown in Figure 7.12.

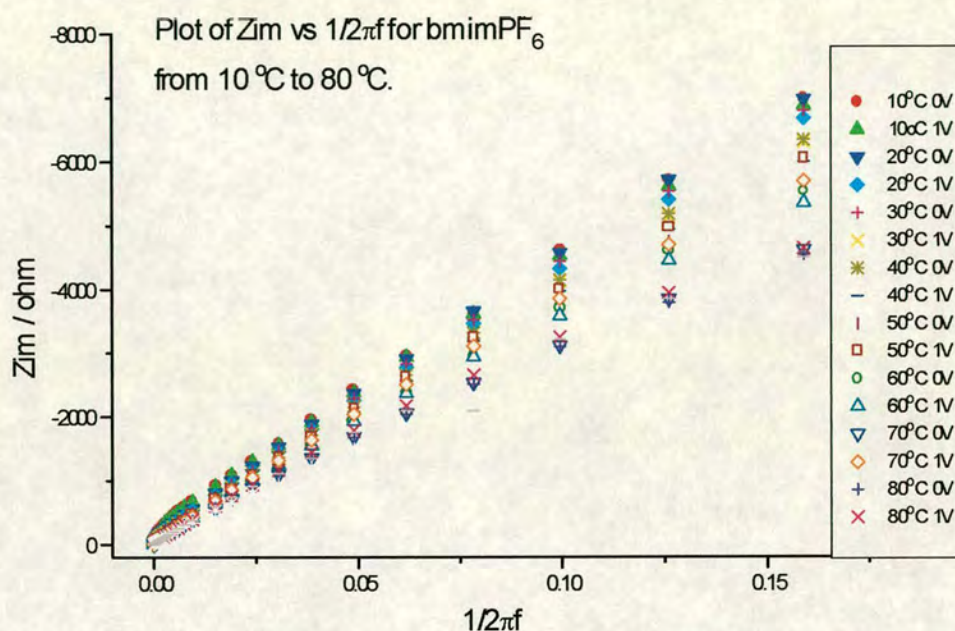


Figure 7.12. The relationship between frequency and imaginary impedance of the bmimPF₆ system.

The effect of applying a direct voltage across the bmimPF₆ systems was also studied using AC impedance spectroscopy. This was done by the application of a dc voltage of 1V across the system at the same time as the response to the small alternating voltage was monitored and the results are included in Figure 7.12.

It is clear from these results that temperature and voltage have little effect on the magnitude of the capacitance of the ionic liquid system. C_{Σ} is generally of the order of 10^{-5} to 10^{-4} F. This is comparable to the magnitude of double layer capacitances found for electrodes in aqueous and other solvent systems.⁵ This supports the theory that it is the formation of these electrode double layers that produces the free ions in

the ionic liquid, and that the ionic liquid contains relatively few free ions before a perturbation.

It must be emphasised that although calculation of the capacitance in this manner is invaluable for qualitative comparison of capacitances, determination of the capacitance through mathematical modelling of the system across all frequencies is generally considered to be more accurate as it involves fitting to all the data.

7.2.5 The Effect of Temperature on Ion Motion.

The effect of temperature on ion motion within bmimPF₆ was assessed by analysis of the change in the resistance of each ion in the transmission line with increasing temperature.

The resistance to ion motion is determined by a number of factors,⁴ such as the diffusion coefficient, D_m , and the bulk ion concentration, \bar{m} .

$$R_m = \left(\frac{RT}{F^2} \right) \left[\frac{L}{A} \right] \left(\frac{1}{D_m \bar{m}} \right) \quad (12)$$

where L/A is the cell constant, F is Faradays constant and T is the temperature of the system.

The diffusion coefficient is defined for traditional solvent systems by the Stokes Einstein equation (equation (13)), where η is the viscosity of the solvent, k is the Boltzmann constant and r is the effective radius of the ion.

$$D_m = \frac{kT}{6\pi\eta r} \quad (13)$$

The applicability of this relationship to high temperature molten salts has been studied by Bockris *et al.*⁶ Measure values of $D_m\eta / T$ were plotted against $1/r$ for a range of inorganic salts of known radii and the results were found to cluster around a

⁵ A. J. Bard and L. R. Faulkner, *Electrochemical Methods, Fundamentals and Applications*, J. Wiley & sons.

⁶ J. O'M. Bockris and A. K. N. Reddy, *Modern Electrochemistry*, Vol 1, 2nd Ed, Plenum Press.

line of gradient $k/6\pi$. This result indicates the applicability of the Stokes-Einstein equation to high temperature molten salts, but no studies have been performed to assess the applicability of this relationship to room temperature ionic liquids.

Combining equations (12) and (13) gives:

$$R_m = \frac{N_A L 6\pi \eta r}{F^2 A m} \quad (14)$$

Where N_A is Avogadro's constant. This is an important equation as it provides insight into the response of the system to a change in temperature. The temperature component of equations (12) and (13) have cancelled on combination of the two equations, indicating no direct temperature term, but there are a number of components within equation (14) that may be expected to vary with temperature. Most obviously, the viscosity of the system could reasonably be expected to change with heating and for a conventional solvent system this might be the only temperature-dependent component that need be considered. However, depending on how the ions within the ionic liquid are associated, it is possible that a change in the ionic radii or concentration with temperature could be observed. If the ions exist predominantly as individual aggregates, and these are broken up with heating, a decrease in the average ionic radii would be observed along with a concurrent increase in the ionic concentration. However, if, as proposed, the ionic liquid exists more as a "mobile lattice", with no individual ion aggregates, as has been suggested for molten salts,⁶ only the viscosity term would be expected to change with temperature.

The impedance of bmimPF_6 over a range of temperatures was measured and the results are shown in Figure 7.13.

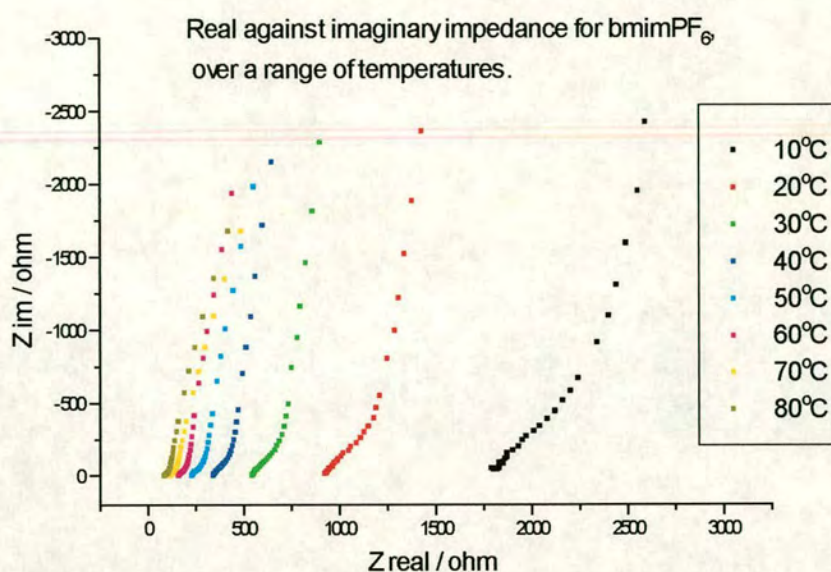


Figure 7.13. Plot of real against imaginary impedance for bmimPF_6 over a range of temperatures.

It can clearly be seen from these results and those from the mathematical modelling (Table 7.1) that the impedance of the system decreases with temperature. However, before drawing conclusions from this result it is necessary to take the effect of viscosity into consideration. To do this the viscosity of bmimPF_6 was measured over a range of temperatures. The change in viscosity with temperature was then plotted against the change in the real axis intercept, Z_{real} , with temperature and the results are shown in Figure 7.14.

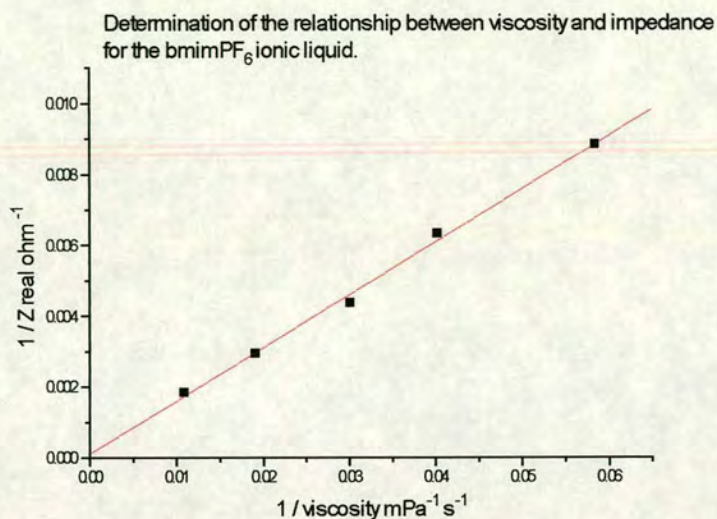


Figure 7.14. The temperature dependence of impedance and viscosity for bmimPF₆.

The linear relationship observed indicates that the decrease in impedance with temperature observed for bmimPF₆ is entirely consistent with that expected for the decreased viscosity and is not a result of a change in ionic concentration or radii.

Using the relationship given in equation (14) it is also possible to calculate the average radius of ions within the ionic liquid. Rearranging equation (14) gives:

$$r = \left(\frac{R_m F^2 \bar{m}}{N_A 6\pi\eta} \right) \left(\frac{L}{A} \right)^{-1} \quad (15)$$

where R_m is the resistance of the ion M^+ or X^- in the ionic liquid (ohm), F is Faradays constant ($C \text{ mol}^{-1}$), L/A is the cell constant, \bar{m} is the concentration of the ion (mol m^{-3}), N_A is Avogadro's constant (mol^{-1}), and η is the viscosity of the ionic liquid ($\text{Pa s} \equiv \text{N m}^{-2} \text{ s}$). This equation can be used to calculate the average radii of the ions in meters. The concentration of ions within the ionic liquid was calculated by dividing the density of the liquid by its formula weight.

A similar approach has been used by Bonhôte *et al.*⁷ and a qualitative relationship between conductivity and the other physical parameters of some ionic liquids is

reported, but no values are given. They also include a correction factor within the equation to take into account the specific interactions between the ions but again no values are given. Similarly they report the need for a factor to account for the degree of dissociation within the ionic liquid to make the Stokes-Einstein relationship more applicable. However, the work by Bockris *et al.*⁶ on high temperature molten salts seems to argue against the need for such a term.

Using equation (15) the average radius of the ions within 1-butyl-3-methylimidazolium hexafluorophosphate was calculated to be approximately 2.8×10^{-10} m. The magnitude of this value compared to that of the individual ions (the radius of a PF_6^- ion is approximately 2×10^{-10} m) supports the applicability of the Stokes-Einstein equation to ionic liquids and indicates that it is likely that the ions within the ionic liquid are not moving as aggregates but as individual ions.

The most likely outcome of these calculations is that the ionic liquid is conducting *via* the movement of ions through “holes” in the liquid. The concept of holes is a familiar one in the field of semiconductors and essentially the same principle applies here. The theory of diffusion and conduction *via* holes in a high temperature molten salt has been discussed by Bockris *et al.*⁶ and is referred to as the Swiss Cheese model.

It has been proposed that thermal motion within the ionic liquid causes ions that constitute a cluster to separate, thereby forming a hole, where the spatial arrangement of ions is such that there is a residual charge associated with it. An example is shown in Figure 7.15.

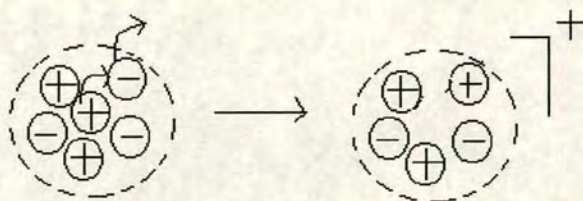


Figure 7.15. The formation of a hole within an ionic liquid.

⁷ P. Bonhôte, A. Dias, N. Papageorgiou, K. Kalyanasundaram and M. Grätzel, *Inorg. Chem.*, 1996, **35**, 1168 – 1178.

This hole formation has a thermodynamic penalty associated with it. This can be supplied from thermal energy but also a hole could be stabilised in a potential of opposite charge. Thus, when a voltage is applied across the ionic liquid, hole formation could become thermodynamically stabilised. In this case it is likely that application of a voltage across the electrodes leads to the association of a counter ion with the electrodes, leaving behind an oppositely charged hole to be ejected into solution.

C_{Σ} would then give the total concentration of positive and negative holes and the magnitude of the capacitance in these systems is of the order of a double layer, which supports the proposed mechanism of hole formation by double layer charging. Hole transport movement is effected by a neighbouring ion of opposite charge hopping into the hole. Therefore, hole transport does not require unaggregated ions hence the resistance depends on the *total* concentration of ions (equation 14).

7.2.6 The Effect of Methylation.

As outlined in Chapter 6, the effect of methylating the imidazolium ring of the ionic liquids on their melting point was significant and unexpected. Therefore, it was decided to analyse a series of mono- and dimethylated ionic liquids by AC impedance spectroscopy to further assess the effects of this change on the physical properties of these ionic liquids.

1-butyl-2,3-dimethyl imidazolium hexafluorophosphate was analysed by AC impedance spectroscopy using the same conditions as for the 1-butyl-3-methyl imidazolium hexafluorophosphate. As for bmimPF₆, the impedance was found to decrease with increasing temperature, as shown in Figure 7.16. The smaller temperature range studied is a reflection of the higher melting point of this compound compared to the monomethylated analogue.

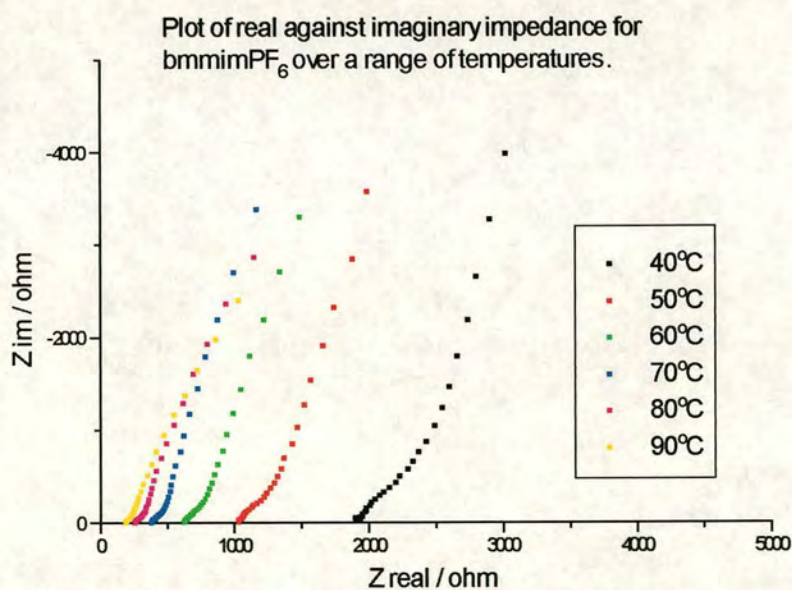


Figure 7.16. Plot of real against imaginary impedance for 1-butyl-2,3-dimethyl imidazolium hexafluorophosphate.

The change of viscosity with temperature was measured across this temperature range and the relationship between the viscosity and the resistance of the ionic liquid analysed. As for bmimPF_6 , a linear dependence was found, as shown in Figure 7.17.

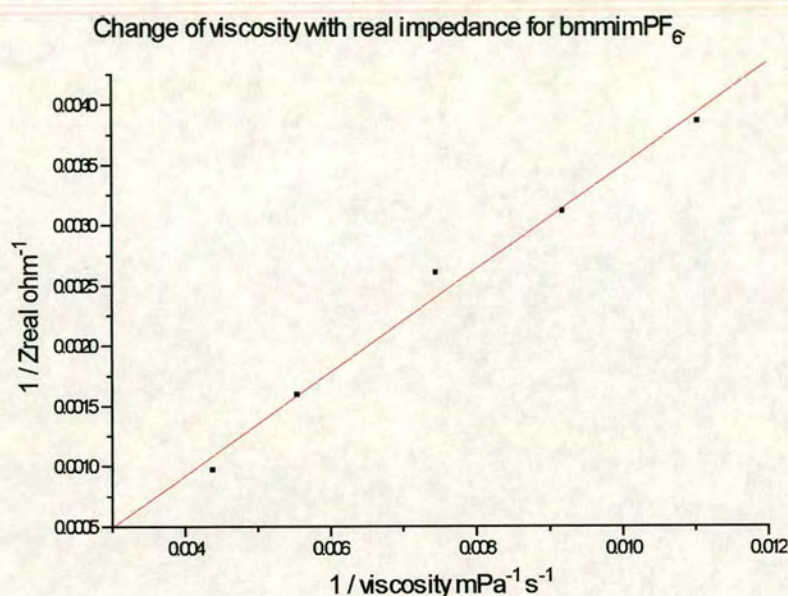


Figure 7.17. The temperature dependence of impedance and viscosity for bmmimPF_6 .

The capacitance of bmmimPF_6 was measured from these experimental results and was found to be very similar to that of bmimPF_6 . The effect of temperature on the capacitance of the bmmimPF_6 system was studied as before and again no change was observed across the temperature range studied. Similarly, little effect was observed on application of a 1V dc voltage across the system. Thus, the plot of $1/2\pi f$ against imaginary impedance gives lines of similar gradients, as shown in Figure 7.18, indicating a capacitance essentially independent of temperature and voltage. The straight line plot obtained from bmimPF_6 at 30 °C is included for comparison.

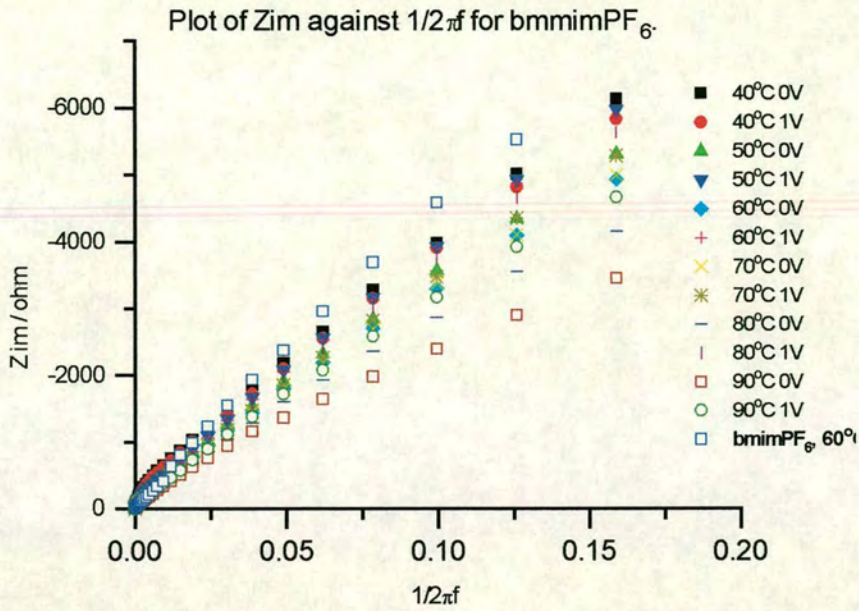


Figure 7.18. Plot of $1/2\pi f$ against imaginary impedance to determine the capacitance of the bmimPF_6 system.

Analysis of the ionic liquids by AC impedance spectroscopy was repeated for the mono and dimethylated derivatives of the tetrafluoroborate and thiocyanate ionic liquids. For all the ionic liquids studied, a linear relationship between the viscosity and impedance of the systems was observed, as shown below.

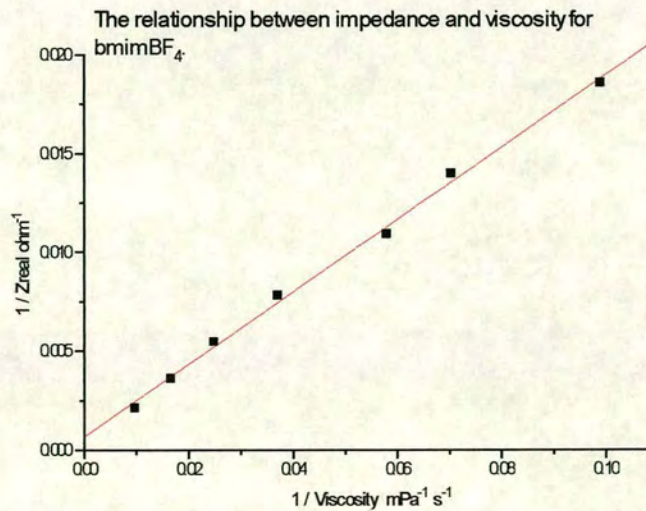


Figure 7.19. The temperature dependence of impedance and viscosity for bmimBF_4 .

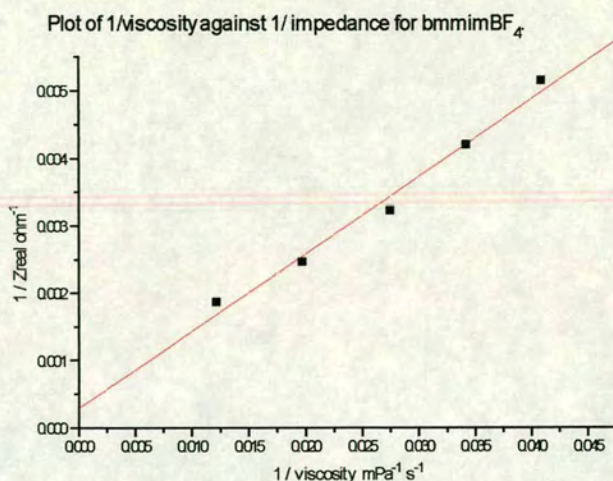


Figure 7.20. The temperature dependence of impedance and viscosity for bmimBF_4 .

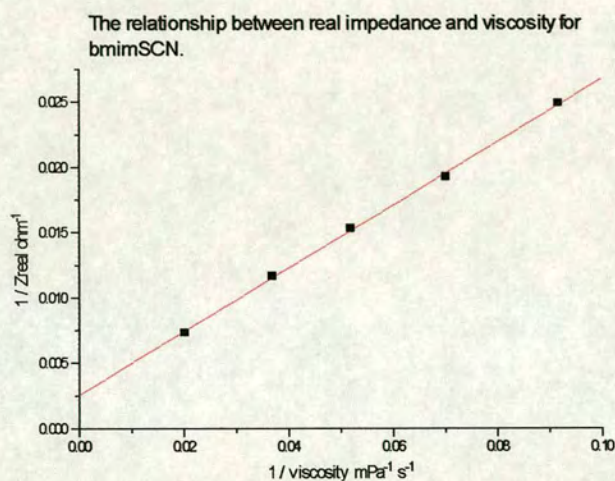


Figure 7.21. The temperature dependence of impedance and viscosity for bmimSCN .

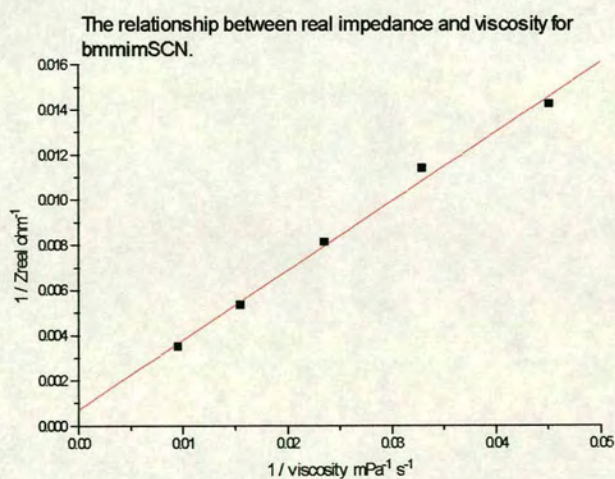


Figure 7.22. The temperature dependence of impedance and viscosity for bmmimSCN .

The capacitance values of each of these systems are of the same order of magnitude and remained constant throughout the temperature range studied and on application of a 1V voltage.

These results allow comparison of the electrochemical properties of these ionic liquids and thus the effect of changing the cation or anion on the system can be assessed. Using the viscosity and impedance data, the value of impedance for each ionic liquid at a constant value of viscosity was calculated. The impedance of each ionic liquid was calculated from the slope of the graphs, at a viscosity of 50 mPa s, and the results are given in Table 7.2.

Cation	Impedance / ohm		
	PF ₆	BF ₄	SCN
1-butyl-3-methyl imidazolium	332	268	198
1-butyl-2,3-dimethyl imidazolium	114	424	147

Table 7.2. Calculated values for the impedance of the six ionic liquids with viscosities of 50 mPa s.

The average radius of the ions within each of these ionic liquids was calculated from

equation (15) and from $Z_{\text{real}} = \frac{R_M}{1 + \frac{t_-}{t_+}} = \frac{R_X}{1 + \frac{t_+}{t_-}}$ and are given in Table 7.3.

Cation	Average Ionic Radius / x 10 ⁻¹⁰ m		
	PF ₆	BF ₄	SCN
1-butyl-3-methyl imidazolium	2.8	2.3	1.6
1-butyl-2,3-dimethyl imidazolium	1.7	2.7	1.2

Table 7.3. Average ionic radii within the mono- and di-methylated ionic liquids at 50°C.

It is evident from these results that the impedance of each of these ionic liquids (and hence their calculated average ionic radii) are very similar. This suggests that all of these ionic liquids conduct *via* hole conduction and not by the passage of large aggregates through the liquid. It is interesting to note that the plots of $1/\text{viscosity}$ against $1/Z_{\text{real}}$ for each of the ionic liquids studied have a slight positive intercept. This is postulated to be a result of the cation size getting large with increasing temperature as there is increased thermal motion acting on the alkyl chains on the imidazole ring and is consistent with the slight observed increase in the transport number of the anion with temperature.

7.2.7 The Effect of Changing the Cation.

Three ionic liquids with increasing alkyl substituent chain length, shown in Figure 7.23, were studied using AC impedance spectroscopy in an attempt to elucidate the effect of changing the chain length on the electrochemical properties of the ionic liquid.

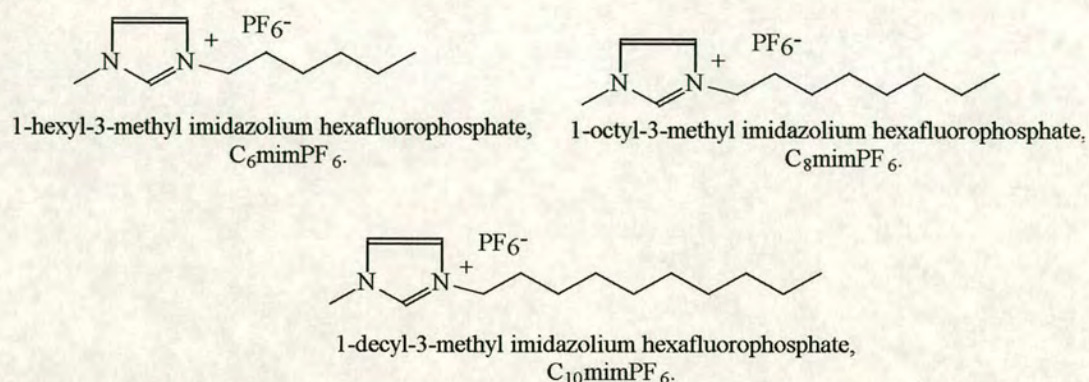


Figure 7.23. The structure and nomenclature of the three ionic liquids studied by AC impedance spectroscopy.

The Nyquist plots recorded for $C_6\text{mimPF}_6$ over a range of temperatures are shown in Figure 7.24.

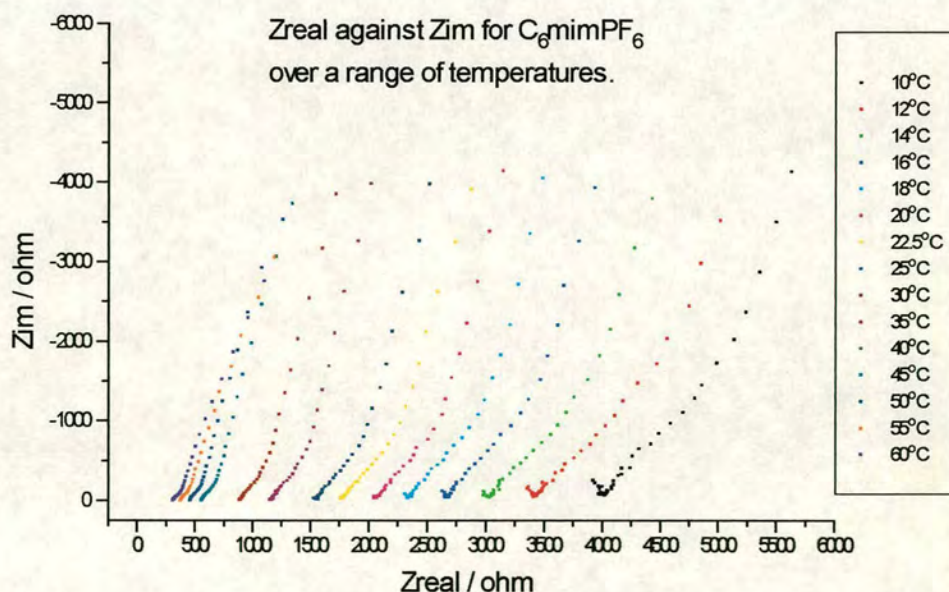


Figure 7.24. Plot of real against imaginary impedance for $C_6\text{mimPF}_6$ over a range of temperatures.

As for the butyl-substituted ionic liquids, a decrease in impedance with temperature was observed. The effect of temperature on the viscosity of this system was studied and again a linear relationship between the change in viscosity and change in impedance with temperature was observed, shown in Figure 7.25.

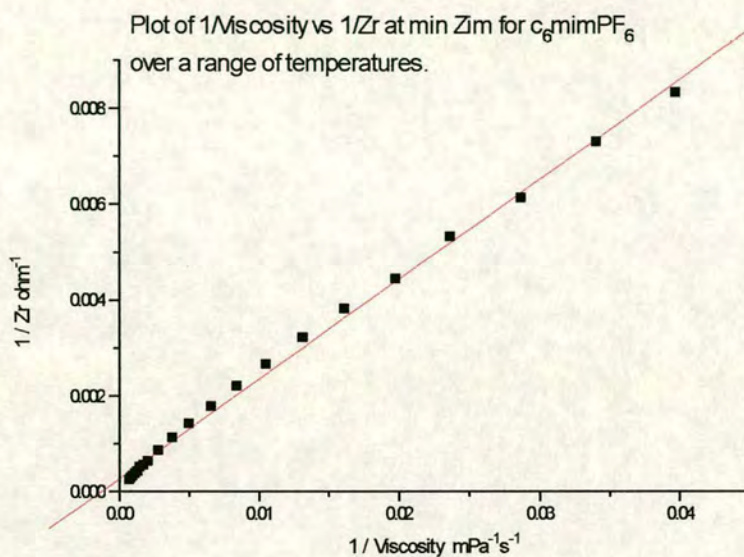


Figure 7.25. The change in viscosity and impedance with temperature for C_6mimPF_6 .

The resistance and capacitance values for C_6mimPF_6 were calculated as before using mathematical modelling. For this system three variables were used, R_M and R_X , the resistances of the individual ions, and C_Σ , the total capacitance. The largest resistance value was assigned to the resistance of the cation, R_M . The results are given in Table 7.6. An approximately constant ratio of R_M to R_X was observed throughout the temperature range studied. It was therefore possible to repeat the modelling, assuming this constant ratio, with only two variables, R_m and C_Σ , allowing greater accuracy.

Using the ratio of ionic resistances, R_M and R_X , obtained, it was possible to calculate the transport number, t , of each ion.

$$t_- = \frac{1}{1 + R_X/R_M} \quad t_+ = 1 - t_- \quad (16)$$

The transport number of the PF_6^- anion in C_6mimPF_6 was found to be approximately 0.6. It should be noted that previous modelling of the ionic liquid assumed a transport number of 0.5. However, this was found to have little effect on the resistance and capacitance values obtained.

Temp / °C	R_X / ohm	S.D. / ohm	R_M / ohm	S.D. / ohm	C_Σ / $\times 10^{-5}$ F	S.D. / $\times 10^{-5}$ F	t.	S.D.
10	5908	159	9999	345	4.21	0.12	0.63	0.06
14	4834	145	7825	290	3.59	0.11	0.62	0.06
16	3804	132	6997	267	3.61	0.11	0.65	0.06
18	3487	154	5834	271	3.29	0.01	0.63	0.06
20	3160	178	4559	272	2.79	0.07	0.59	0.06
22	2756	180	4264	274	2.91	0.08	0.61	0.06
25	2406	178	3770	266	2.87	0.08	0.61	0.06
30	1938	209	2681	277	2.70	0.07	0.72	0.07
35	1468	141	2135	198	2.69	0.08	0.69	0.10
40	1228	188	1611	234	2.50	0.09	0.57	0.11
45	945	123	1385	165	2.46	0.09	0.59	0.09
50	717	80	1296	122	2.62	0.12	0.64	0.10
55	572	67	1165	105	2.75	0.15	0.67	0.10
60	470	58	1028	92	2.71	0.17	0.69	0.10
65	406	42	788	64	3.99	0.19	0.66	0.10
70	302	32	967	66	5.69	0.38	0.76	0.11
75	234	24	1005	63	7.09	0.54	0.81	0.12
80	214	31	889	69	4.75	0.47	0.81	0.14
85	180	2	732	56	92.60	0.32	0.80	0.02
90	166	3	667	29	126.01	0.86	0.80	0.04

Table 7.4. Values of R_M , R_X and capacitance for C_6mimPF_6 .

As for the bmimPF_6 , the values of real and imaginary impedance for the C_6mimPF_6 ionic liquids were in good agreement with the experimentally determined values. A comparison of calculated and experimental results for C_6mimPF_6 at $50\text{ }^\circ\text{C}$ is shown in Figure 7.26. Again, the correlation between calculated and experimental values of imaginary impedance is excellent, but the calculated values of real impedance deviate from the measured values at low frequency, which can be attributed to the inhomogeneity of the electrode surface.

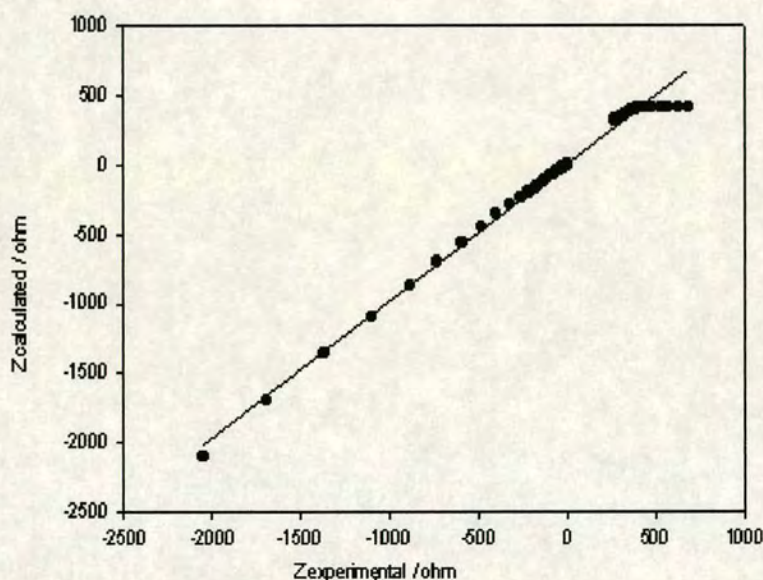


Figure 7.26. Experimental against calculated impedance for C_6mimPF_6 at $50\text{ }^\circ\text{C}$. Gradient = 0.98. Intercept = -5 ohm.

Analysis by AC impedance spectroscopy was repeated for the C_8mimPF_6 and $\text{C}_{10}\text{mimPF}_6$ ionic liquids and similar results were obtained. Again, a linear dependence of impedance on viscosity was observed, shown in Figures 7.27 and 7.28. The impedance and capacitance of these systems was found to remain constant on application of a 1V potential.

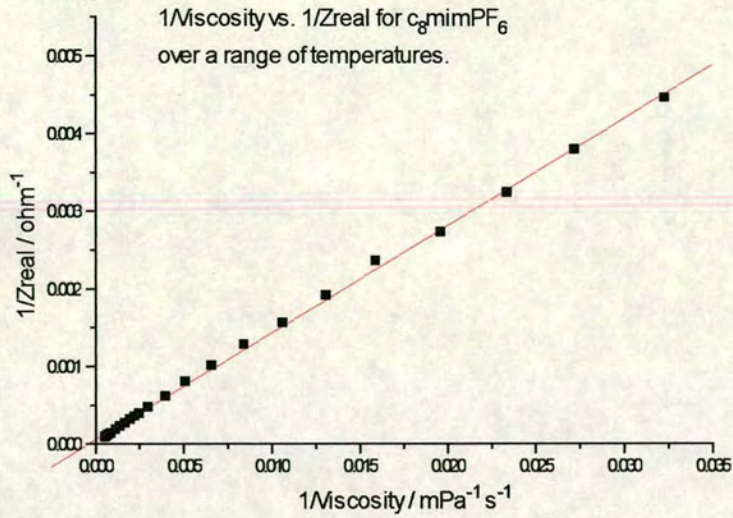


Figure 7.27. The change in viscosity and impedance with temperature for C_8mimPF_6 .

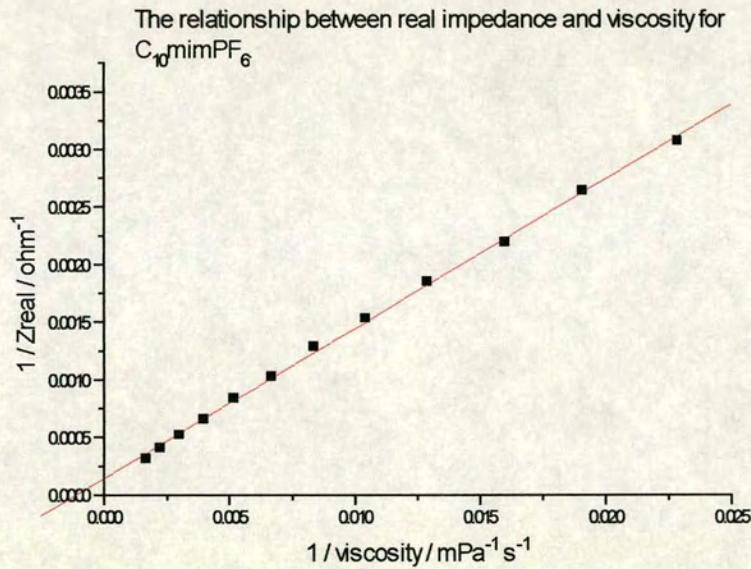


Figure 7.28. The change in viscosity and impedance with temperature for $C_{10}mimPF_6$.

As before, the resistance of each of these liquids was calculated at viscosities of 50 mPa s. The results are shown in Table 7.5.

Ionic liquid.	Impedance / ohm
C ₆ mimPF ₆	239
C ₈ mimPF ₆	361
C ₁₀ mimPF ₆	384

Table 7.5. Values of impedance for each ionic liquid at viscosities of 50 mPa s.

It can be seen from these results that as the chain length increases, the degree to which the ionic liquid impedes the passage of charge through the system also increases. This is consistent with a decrease in the mobility of the cation as a result of increased size.

The C₈mimPF₆ and C₁₀mimPF₆ ionic liquids were modelled using the same parameters as for the C₆mimPF₆ and the results are given in Table 7.6 and 7.7, respectively.

7. The Structure of Ionic Liquids in the Liquid State.

Temp / °C	R _X / ohm	S.D. / ohm	R _M / ohm	S.D. / ohm	C _Σ / x10 ⁻⁵ F	S.D. / x10 ⁻⁵ F	t-
12	15570	1676	20290	1104	4.16	0.21	0.43
16	12010	1175	15100	818	4.90	0.19	0.44
20	8453	372	11970	615	4.84	0.17	0.59
22	6564	376	11270	172	5.31	0.16	0.63
25	5532	166	9278	331	4.34	0.13	0.66
28	4524	122	8341	269	4.74	0.14	0.65
30	4138	159	6959	289	3.60	0.10	0.63
32	3620	129	6613	262	4.17	0.13	0.65
35	3011	226	5656	108	4.24	0.14	0.65
40	2619	294	3721	206	3.03	0.82	0.59
45	2050	299	2863	224	2.83	0.09	0.58
50	1584	244	2428	173	2.82	0.10	0.60
55	1355	281	1867	225	2.38	0.09	0.57
60	1190	400	1410	354	2.14	0.09	0.54
65	855	175	1422	125	2.04	0.11	0.62
70	614	113	1583	59	2.92	0.11	0.72
75	355	139	3685	5	24.79	1.47	-
80	408	148	1706	7	2.39	0.27	-
85	282	50	2748	1	44.82	1.04	-
90	226	71	3125	1	45.82	1.17	-

Table 7.6. Values of R_M, R_X and capacitance for the C₈mimPF₆ ionic liquid.

7. The Structure of Ionic Liquids in the Liquid State.

Temp / °C	R _X / ohm	S.D. / ohm	R _M / ohm	S.D. / ohm	C _Σ / x10 ⁻⁵ F	S.D. / x10 ⁻⁵ F	t	S.D.
35	4698	217	7666	377	3	0.12	0.62	0.04
40	3594	186	6355	328	2.36	0.07	0.64	0.04
45	2959	202	4735	315	2.30	0.07	0.62	0.05
50	2237	165	4118	275	2.53	0.09	0.65	0.06
55	1829	165	3171	253	2.26	0.08	0.63	0.08
60	1539	150	2520	221	2.18	0.08	0.62	0.09
65	1260	145	2017	205	2.08	0.08	0.62	0.09
70	1423	1x10 ⁶	1423	1x10 ⁶	2.04	0.16	-	-
75	869	110	1485	157	2.15	0.10	0.63	0.10
80	727	89	1295	131	2.14	0.11	0.64	0.10
85	601	75	1111	110	2.44	0.13	0.65	0.10
90	503	58	1012	90	2.72	0.15	0.67	0.10

Table 7.7. Values of R_M, R_X and capacitance for C₁₀mimPF₆. The physical parameters of the 70 °C data have excessively large S.D.s and are excluded from the transport number calculations.

The average ionic radii of the ionic liquids were calculated as before and are given in Table 7.8.

Ionic Liquid	Average Ionic Radii / x10 ⁻¹⁰ m.
C ₆ mimPF ₆	1.4
C ₈ mimPF ₆	2.0
C ₁₀ mimPF ₆	2.1

Table 7.8. The average ionic radii within the C₆, C₈ and C₁₀mimPF₆ ionic liquids at 50 °C.

As would be expected, the average ionic radii increases with chain length but the magnitude of these radii still indicate the movement of individual ions through the solution.

7.3 Analysis of Calcium Fluoride in 1-butyl-3-methyl imidazolium hexafluorophosphate.

As discussed in Chapter 4, calcium fluoride dissolved in bmimPF_6 has been successfully utilised as a medium for fluorination reactions. However, the form that the calcium fluoride takes in this ionic liquid is poorly understood. It was therefore proposed that the nature of the calcium fluoride in bmimPF_6 should be investigated. This was done using two analytical methods.

The liquid structure of calcium fluoride in bmimPF_6 was investigated using AC impedance spectroscopy. The solid structure of calcium fluoride in the dimethylated analogue, bmmimPF_6 , was analysed using x-ray powder diffraction.

The last part of this chapter compares these results and the insight into both the solid and liquid structures that was gained.

7.3.1 AC Impedance Spectroscopy.

The Nyquist plots of a 0.3 mol dm^{-3} solution of calcium fluoride in 1-butyl-3-methyl imidazolium hexafluorophosphate were recorded over a range of temperatures and compared to the neat ionic liquid. The results are shown in Figure 7.29.

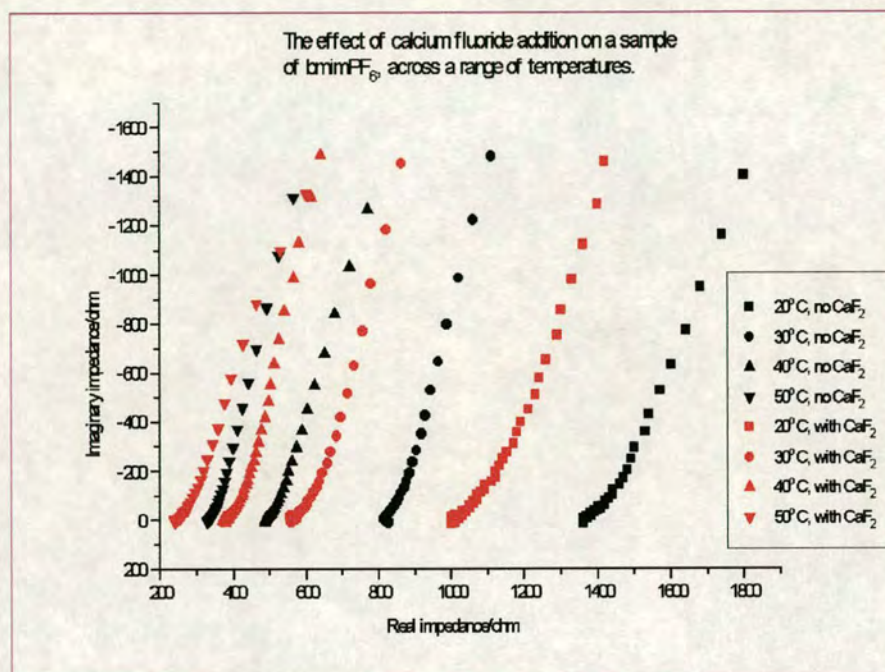


Figure 7.29. The impedance of 1-butyl-3-methyl imidazolium hexafluorophosphate with added calcium fluoride.

It can be seen from these results that addition of calcium fluoride results in a decrease in the impedance of the system.

The ratio of the resistances of the neat bmimPF_6 to that containing calcium fluoride is 1.3:1 across the temperature range studied. The ion concentration of bmimPF_6 is approximately $5 \times 10^{-3} \text{ mol cm}^{-3}$ (calculated by dividing the density by the formula weight). Thus, this resistance drop is equivalent to an increase in the bmimPF_6 ion concentration of approximately 1.5 mol cm^{-3} . However, resistance is directly proportional to ionic radius and the average ionic radius of calcium fluoride is estimated to be approximately half that of bmimPF_6 . Additionally, the calcium ion can carry twice the charge of the imidazolium cation and there are two equivalents of

fluoride ions. Allowing for these factors, the drop in impedance is consistent with the addition of a 0.3 mol cm^{-3} solution of calcium fluoride. Thus, it was concluded that all of the calcium fluoride added to the bmimPF_6 had dissociated and dispersed within the ionic liquid, thereby contributing to the drop in resistance, and was not merely incorporated as undissociated aggregates.

The bmimPF_6 system containing calcium fluoride was modelled using the same parameters as for the bmimPF_6 system. This system is more complex than that of the neat bmimPF_6 as it contains four different ions of different sizes and proportions so for modelling purposes the transport number was again fixed at 0.5 and only one value of resistance was calculated, shown in Table 7.9.

Temp / °C	Resistance / ohm	S.D. / ohm	Capacitance / $\times 10^{-5} \text{ F}$	S.D. / $\times 10^{-5} \text{ F}$
20	1910	11	9.84	0.21
30	1058	13	7.88	0.19
40	702	12	6.76	0.15
50	501	14	7.04	0.20

Table 7.9. Values of resistance and capacitance calculated for 0.3 mol dm^{-3} solution of CaF_2 in bmimPF_6 .

The similar values of the capacitance of this system that were observed experimentally over the temperature range studied again suggests double layer hole formation.

As previously, good correlation between the calculated and experimental impedance values were obtained, as shown in Figure 7.30, with the exception of the low frequency deviation in real impedance observed previously and attributed to inhomogeneity.

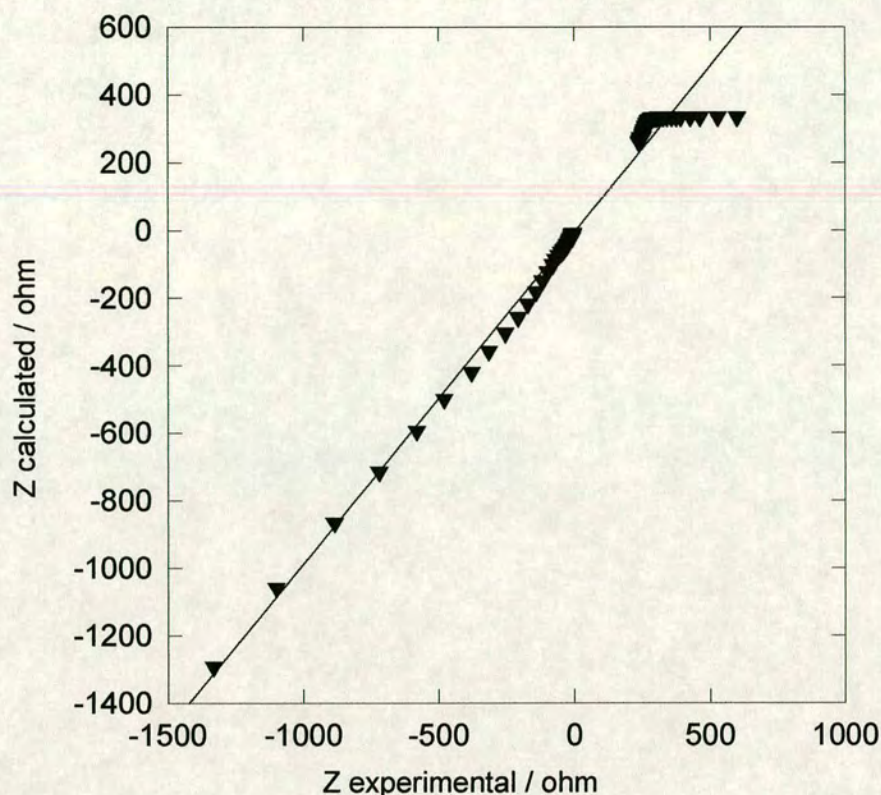


Figure 7.30. Correlation between calculated and experimental impedance for CaF_2 in bmimPF_6 . Gradient = 0.98, Intercept = -6 ohm.

The structure of calcium fluoride in a number of ionic liquids has also been studied by Extended X-ray Absorption Fine Structure (EXAFS) using the Synchrotron Radiation source at the Daresbury Laboratory. The studies were performed looking at the calcium ion and the results of these investigations are being analysed. It is hoped that these will give more information about the environment surrounding the calcium ion.

7.3.2 Powder Diffraction.

Following the successful analysis of the liquid structure of calcium fluoride in 1-butyl-3-methyl imidazolium hexafluorophosphate by AC impedance spectroscopy it was proposed that study of the mixture by x-ray powder diffraction could provide further insight into the nature of calcium fluoride within the ionic liquid. The methylated ionic liquid 1-butyl-2,3-dimethyl imidazolium hexafluorophosphate, bmmimPF₆, is ideal for this analysis as it is a solid at room temperature and thus allows for analysis by x-ray powder diffraction.

A 0.5 mol dm⁻³ solution of calcium fluoride in 1-butyl-2,3-dimethyl imidazolium hexafluorophosphate was prepared and filtered to remove any undissolved calcium fluoride. The solution was then allowed to solidify and ground up for analysis. The powder diffraction spectrum obtained for this mixture is shown in Figure 7.31, and compared to that of the neat bmmimPF₆. The powder diffraction pattern of neat calcium fluoride was collected under the same conditions and is shown in Figure 7.32.

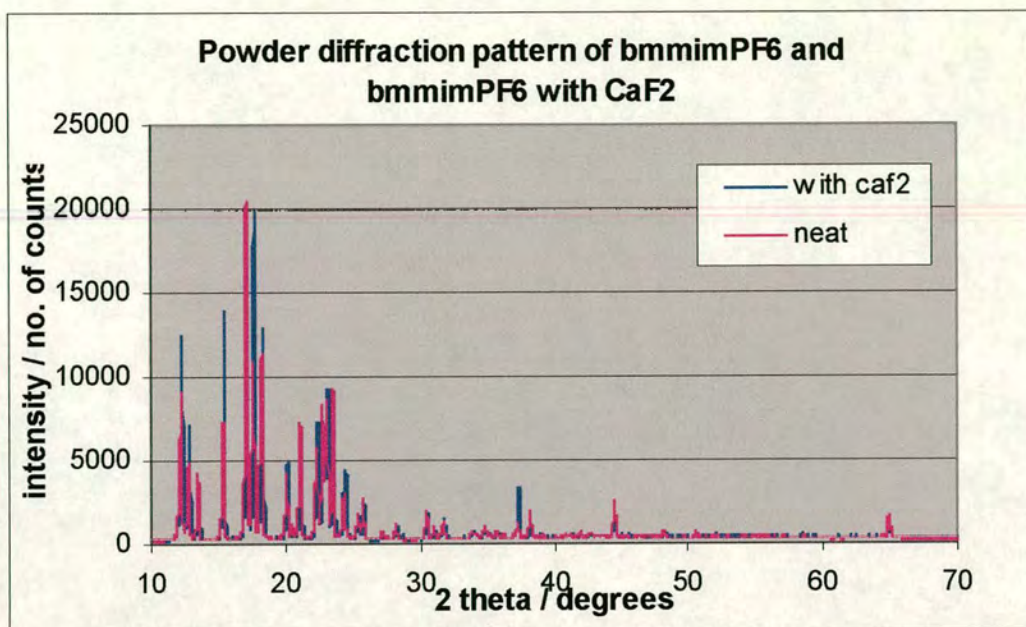


Figure 7.31. The powder diffraction pattern of bmmimPF_6 and bmmimPF_6 with calcium fluoride. All spectra were recorded using Cu radiation.

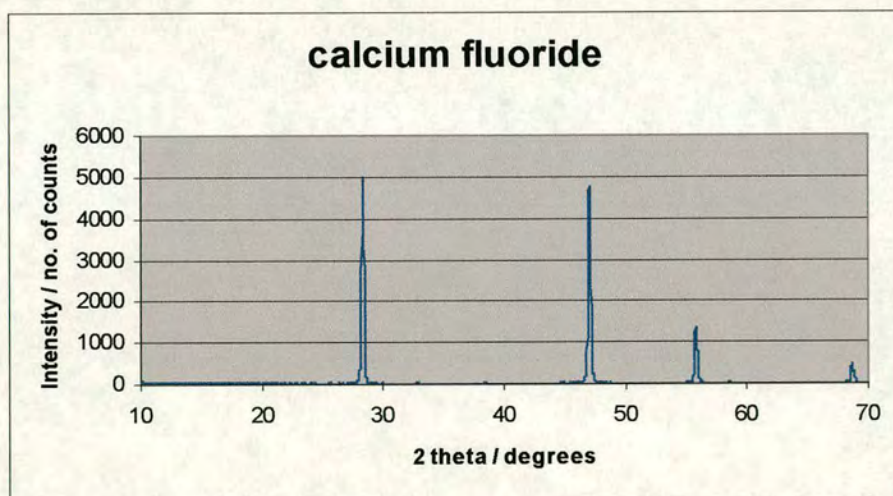


Figure 7.32. The powder diffraction pattern of calcium fluoride.

It is clear from comparison of these two spectra that there is no free polycrystalline calcium fluoride present in the mixture of bmmimPF_6 and CaF_2 .

One possible explanation for this is that the calcium fluoride is present within the sample in a non-crystalline form, or as nano-crystallites. However, powder diffraction spectra of small crystallites normally exhibit significant broadening of the background spectrum and this is not observed.

It can also be seen from Figure 7.31 that addition of calcium fluoride appears to result in a shift in the peaks within the powder diffraction spectrum. This can be seen in more detail in Figure 7.33, where the spectrum of the samples between 10° and 25° is shown.

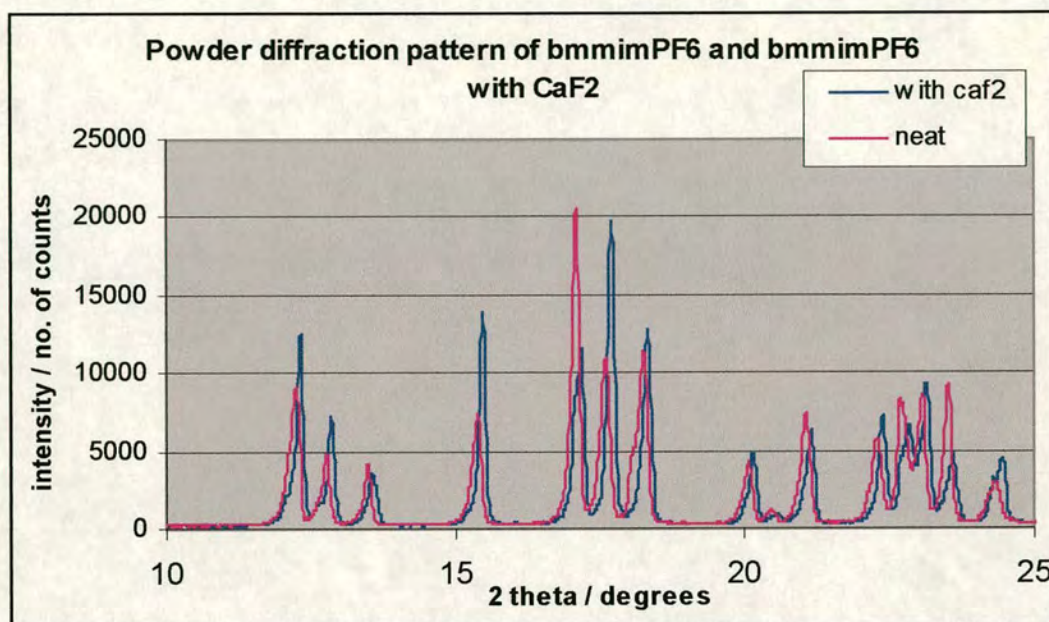


Figure 7.33. The enlarged powder diffraction pattern of bmmimPF₆ and bmmimPF₆ with calcium fluoride.

This result suggests a change in the size of the unit cell of the bmmimPF₆ on addition of calcium fluoride.

To eliminate the possibility that this peak shift was solely a result of poor calibration of the apparatus, the spectra were re-recorded using silicon as an internal reference. A small quantity of silicon was ground into each sample and the spectra recorded as before. The powder diffraction patterns obtained are shown in Figure 7.34. For clarity the part of the samples between 10° and 30° is shown in Figure 7.35.

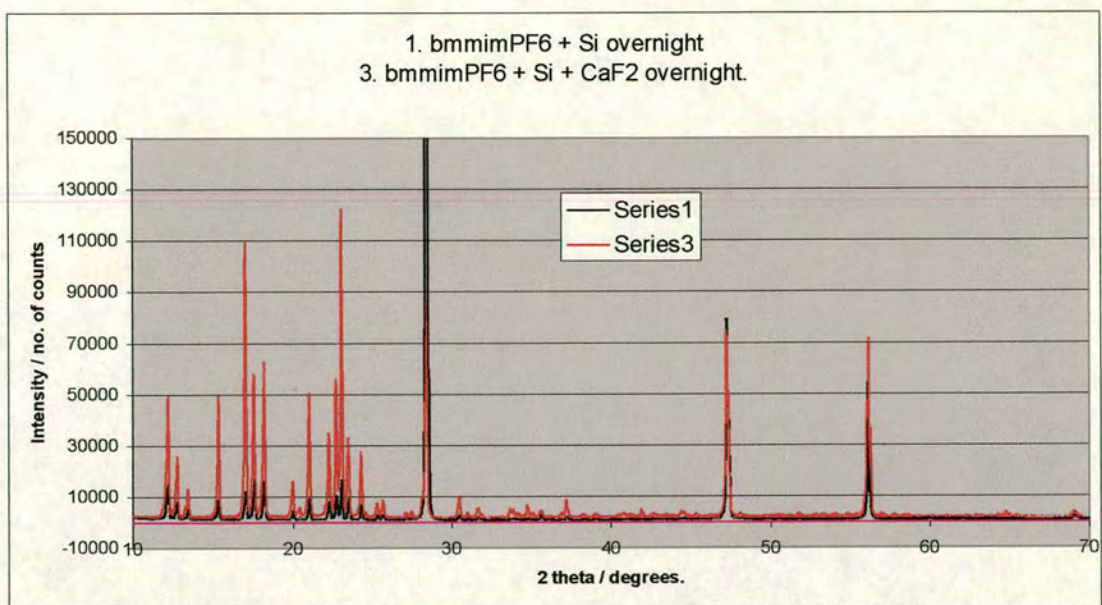


Figure 7.34. Powder diffraction patterns of bmmimPF₆ and bmmimPF₆ with calcium fluoride, with silicon as an internal reference.

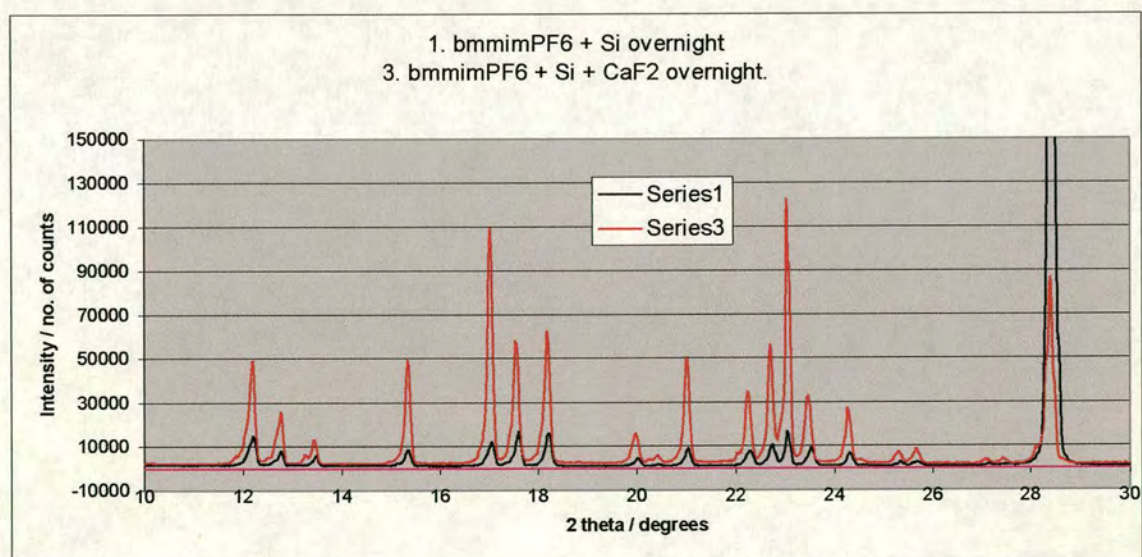


Figure 7.35. Enlarged x-ray powder diffraction pattern of bmmimPF₆ and bmmimPF₆ with calcium fluoride and silicon. The silicon peak at 28° clearly occurs at the same scattering angle for both samples.

As observed previously, there is a shift in peak position on addition of calcium fluoride to the bmmimPF₆. However, the peaks attributable to the silicon, at 28°, 48°

and 57° , lie at the same value of scattering angle for both samples. This confirms the calibration of the instrument is correct and that the apparent change in cell size is a real effect. Addition of the calcium fluoride results in a shift in the peak position to lower scattering angle, consistent with an *increase* in cell size.

This observation suggests that the calcium fluoride has been incorporated into the ionic liquid as dissociated ions and is not merely present in undissociated aggregates. This is consistent with the conclusions reached by analysis of the liquid structure of CaF_2 in bmimPF_6 by AC impedance spectroscopy.

7.4 Conclusions.

AC impedance has been used for the first time to study room temperature ionic liquids. These systems were found to behave in a significantly different way to more conventional ionic aqueous solutions.

In the absence of an electric field, ionic liquids appear to exist as a neutral sea of ions, like a “mobile lattice”. Application of an alternating voltage results in the dissociation of the neutral ionic liquid at the electrode, the formation of a double layer and the ejection of the counterion from the double layer. The ionic liquid appears to then conduct *via* a hole transport mechanism. Thus, there are a small number of free ions and hole transport uses all of the ions, both free and aggregated.

This ion dissociation mechanism is analogous to the charge injection mechanism that takes place during the AC impedance spectroscopy of redox active polymers, which has been studied in some detail, and thus similar transmission lines can be used to represent both systems. The response of a number of ionic liquids to an alternating voltage was successfully modelled and values for the resistance of the individual ions and the total capacitance of each system were obtained. Good correlation between the calculated and experimental results was obtained, indicating that the ionic liquids are well represented by the transmission line used.

AC impedance spectroscopy was used to study mono and dimethylated butyl-substituted ionic liquids, and ionic liquids with increasing size of cation substituent, and very similar results were obtained for each. The average ionic radii of each ionic liquid was calculated to lie between 1.5 and 3 Å and correlated well with the calculated average sizes of the individual ions. This result also indicates that conductance occurs within these systems *via* movement of individual ions and not by the movement of large ion aggregates.

The impedance of the ionic liquids was found to decrease with temperature in direct relation to the resultant decrease in the viscosity of the system. This result, and the observation of a constant capacitance, C_{Σ} , with temperature, also suggests that the presence of large individual aggregates within the ionic liquid is unlikely, and that a neutral sea of ions is a more accurate qualitative description.

The transport number of the negative ion within a range of ionic liquids was calculated to be approximately 0.6. However, this value appears to increase slightly at high temperatures. It is proposed that this is a result of the ions effectively changing shape as the thermal energy of the system increases and they have more energy to rotate. The ionic liquids are modelled by treating the ions as spheres. The validity of this assumption, and the change in the overall shape of the ions as the thermal energy increases, has not been assessed. This is suggested as an interesting area for future work.

The effect of addition of calcium fluoride to the bmimPF₆ ionic liquid was studied. Results were consistent with complete dissociation and dispersion of the salt within the ionic liquid. The successful use of this medium for fluorination reactions further supports the presence of free dissociated fluoride ions within the ionic liquid.

Likewise, x-ray powder diffraction analysis of calcium fluoride in bmmimPF₆ indicated the incorporation of the calcium fluoride into the ionic liquid as dissociated ions and not as isolated clusters.

8 The Structure of Ionic Liquids in the Solid State.

8.1 Introduction.

The precise nature and extent of the interactions between the cation and anion of substituted imidazolium ionic liquids has been debated for a number of years, but information on these interactions has been hindered by a lack of high quality crystal structures. The liquid structures of some of these species have been studied and the presence of hydrogen bonds between the anion and the hydrogen at the 2-position of the cation alluded to from NMR and IR evidence. However, the extent of this hydrogen bonding was unknown and the nature of any interactions between the anion and the other ring hydrogens, H4 and H5, has not been explicitly discussed. X-ray crystallography is an important tool in the elucidation of the solid state structures of imidazolium-based ionic liquids and this structural information is important in the drive to understand the relationship between the structure and the physical properties of these room temperature ionic liquids.

As outlined in Chapter 6, there are still many unanswered questions regarding the relationship between the structure and the physical properties of imidazolium-based ionic liquids. The effect of changes to the cation, particularly with regard to the effect of methylation of the imidazolium ring on melting point, is largely unexplored. Similarly, the significant effect of changing anion, such as the dramatic difference in the hydrophobicity between the hexafluorophosphate and tetrafluoroborate salts, also raises a number of questions. The lack of crystal structures for any of these butyl-

substituted species was identified as a significant hindrance to enhancing the understanding of the structure-property relationships of these species.

Five crystal structures of butyl-substituted imidazolium ionic liquids have been collected and the structural differences between these structures have been analysed in an attempt to enhance our understanding of the differences between these species.

This section describes the investigations into the relationship between structure and physical properties that have been performed on 1-butyl-3-methyl imidazolium ionic liquids by analysis by x-ray crystallography.

In the light of these results, the crystal structures of related ionic liquids that have been published in the literature have been examined in detail, with specific attention being paid to interactions between cations and anions.

8.2 The Effect of Changing the Cation.

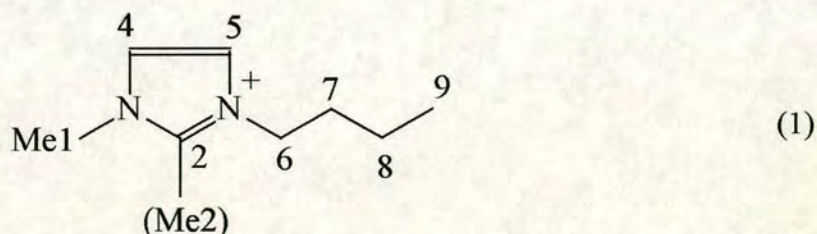
As described in Chapter 5, it has been observed that methylation at the 2-position of the imidazolium ring resulted in an unexpected increase in the melting point of the imidazolium ionic liquid. This is contrary to what would be predicted based on the extent of hydrogen bonding within these compounds - this would be expected to decrease on methylation owing to the removal of the acidic proton in the 2-position. It was proposed that comparison of the crystal structures of mono and di-methylated structures could help explain this phenomenon. For the purpose of this investigation, only close-contact distances between atoms that lie within the sum of their van der Waals radii are reported. This cut-off distance was chosen to allow consistent comparison of the hydrogen bonding within each of the crystal structures.

8.2.1 1-butyl-3-methyl imidazolium chloride.

1-butyl-3-methyl imidazolium chloride is an extremely important ionic liquid as it is used as the precursor to the much-used tetrafluoroborate and hexafluorophosphate ionic liquids. Despite this, few structural studies have been performed on this species and the results of many of these investigations have been inconclusive, particularly with regard to the extent of hydrogen bonding within these species (see Chapter 3).

The crystal structures of the imidazolium ionic liquids were obtained by allowing the materials to solidify slowly on the inner walls of a Schlenk tube or on a microscope slide under nitrogen. The solids formed as a crystalline mass, from which a suitable single crystal can be cut. When dealing with the chloride species, care must be taken to cut and load the crystals under nitrogen as these compounds are extremely hygroscopic and exposure to air results in the absorption of water and the materials become liquids.

Detailed crystallographic data are collected in the Appendix. The numbering scheme used for all of the crystal structures detailed is shown in (1).



Five imidazolium cations surround each chloride within the bmimCl structure, as shown in Figure 8.1. The close contacts between the anion and cation within the crystal structure of 1-butyl-3-methyl imidazolium chloride are given in Table 8.1.

Bond	Distance / Å
Cl – H2	2.47
Cl – H6	2.78
Cl – H6	2.88
Cl – Me	2.91
Cl – Me	2.91

Table 8.1. Close contacts within the crystal structure of bmimCl.

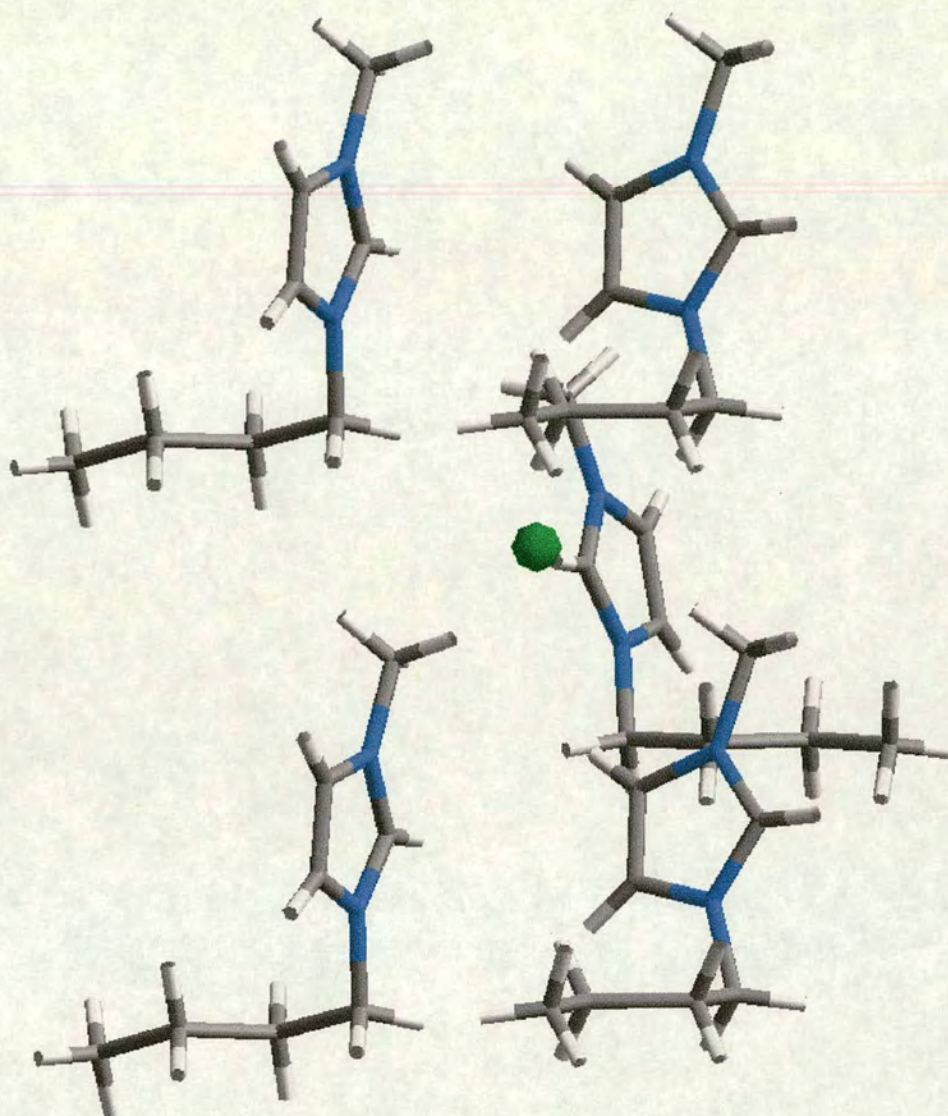


Figure 8.1. Part of the crystal structure of 1-butyl-3-methyl imidazolium chloride showing the environment around a chloride ion.

As expected, the shortest hydrogen bond is between the chloride and H2, but the structure is in no way dominated by this interaction. On the contrary, four of the close contacts are to other hydrogens on the substituted imidazolium. This surprising result suggests that the importance of this Cl – H2 hydrogen bond may have been overestimated.

8.2.2 1-butyl-2,3-dimethyl imidazolium chloride.

The effect of methylation in the 2-position was studied by analysis of the crystal structure of 1-butyl-2,3-dimethyl imidazolium chloride, shown in Figure 8.2.

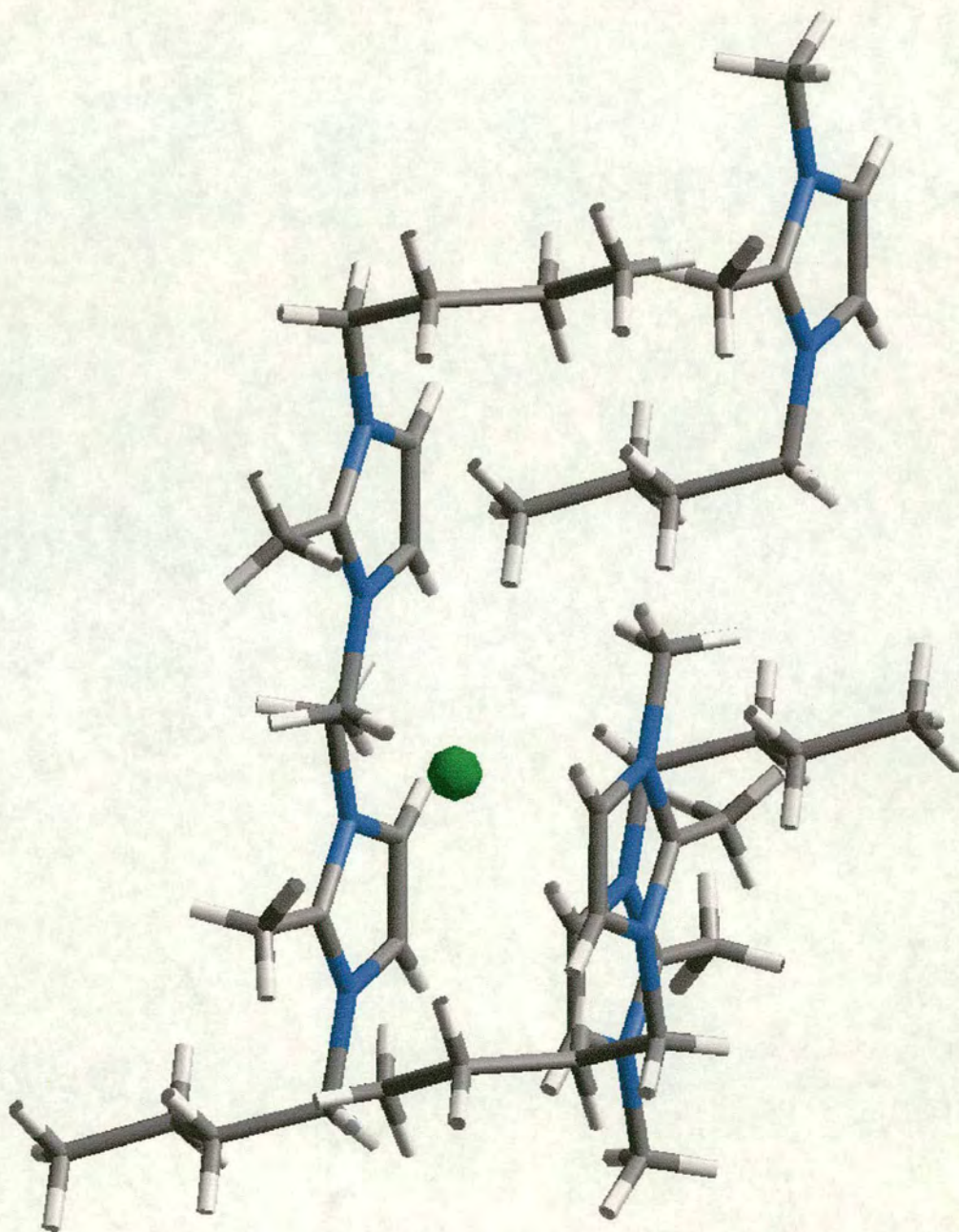


Figure 8.2. Molecular structure of 1-butyl-2,3-dimethyl imidazolium chloride, bmmimCl.

As for the mono-methylated species, the dimethylated structure crystallises with five imidazolium rings around each chloride ion. However, the number of hydrogen bonds that the chloride anion now forms has increased from five to seven, as detailed in Table 8.2.

Bond	Distance / Å
Cl – H5	2.59
Cl – H4	2.67
Cl to H on Me1	2.75
Cl to H on Me2	2.78
Cl to H on Me1	2.85
Cl to H on Me2	2.88
Cl to H9	2.90

Table 8.2. Close contacts within the crystal structure of 1-butyl-2,3-dimethyl imidazolium chloride.

Thus, although the strongest of the hydrogen bonds has been removed upon methylation, the importance of the other hydrogen bonds remains and the number of these bonds is actually increased. This provides a convincing explanation for the increase in melting point that occurs on methylation of the imidazolium ring.

The effect of methylation on the internal geometry of the cation was analysed by comparison of the bond lengths and angles of each species. It was concluded that this substitution has no significant effect on the internal geometry of the cation, within the limits of the resolution of these structures.

8.3 The Effect of Changing the Anion.

The crystal structures of bmimCl and bmmimCl allowed the effect of changes to the cation on structure to be assessed. It was therefore proposed that a similar analysis of the crystal structures of ionic liquids with different anions should be performed with a view to investigation of the effect of anion on structure. The studies were performed using two different cations.

The crystal structure of 1-butyl-3-methyl imidazolium bromide allows comparison of the chloride and bromide species and thus assessment of the effect of different halides.

The crystal structures of 1-butyl-2,3-dimethyl imidazolium hexafluorophosphate and tetrafluoroborate allows the effect of changes to the anion within the dimethylated ionic liquids to be assessed. Analysis of the tetrafluoroborate and hexafluorophosphate derivatives is of particular interest as it is these anions that are most commonly used, and no crystal structure of a tetrafluoroborate-based ionic liquid has been published.

Elucidation of the crystal structure of 1-butyl-2-phenyl-3-methyl imidazolium hexafluorophosphate enables comparison of the effect of addition of a methyl and a phenyl group to the cation to be assessed.

8.3.1 1-butyl-3-methyl imidazolium bromide.

The crystal structure of bmimBr is similar to that of bmimCl in that it displays relatively few close contacts between the anion and cation. The structure is shown in Figure 8.3 and the close contacts are listed in Table 8.3.

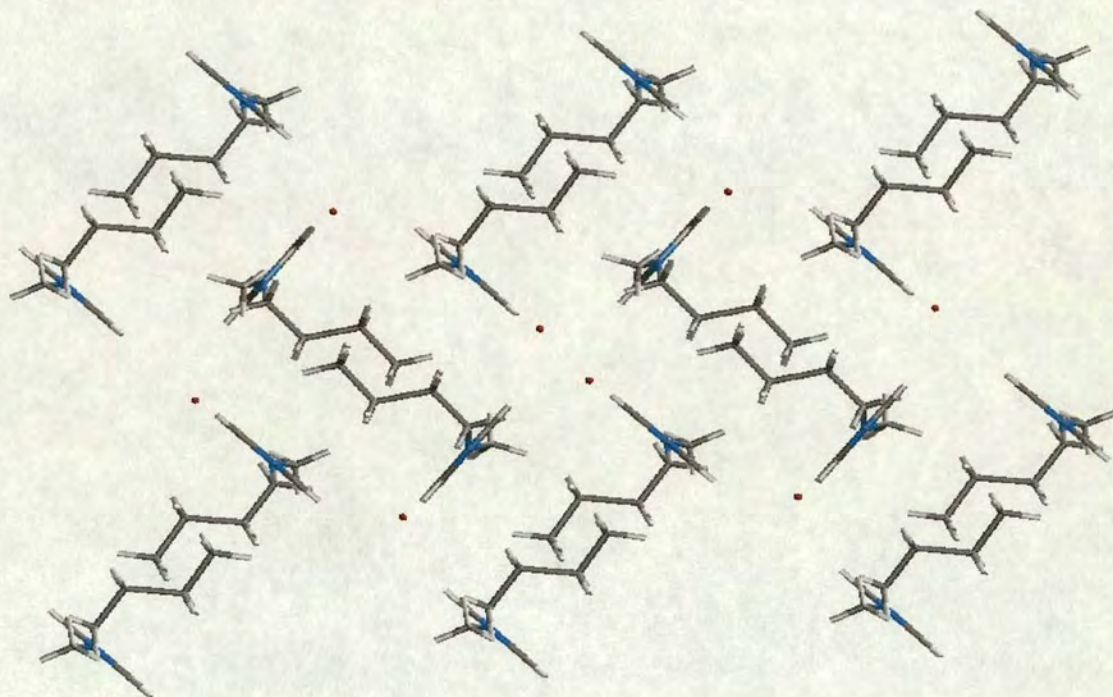


Figure 8.3. The crystal structure of bmimBr.

Close contact	Distance / Å
Br – H2	2.63
Br – H on Me	2.81
Br – H6	2.81
Br – H6	2.90

Table 8.3. Close contacts within the bmimBr crystal structure.

It can be seen from Figure 8.3 that the imidazolium rings within the bmimBr crystal structure lie in a series of interlocking chains, unlike those in the chloride analogue that shows no stacking. BmimBr also differs from bmimCl in that it exhibits disorder within the crystal structure. However, like the chloride derivative, it can be seen that

there are relatively few close contacts between the anion and cation. As expected, the shortest of these involves the acidic H2, but close contacts to other hydrogens on the cation also play a significant role. Thus, in this compound, as for bmimCl, the importance of the role of the H2 in hydrogen bonding appears to have been overemphasised.

8.3.2 1-butyl-2,3-dimethyl imidazolium hexafluorophosphate.

The crystal structure of bmmimPF₆ is shown in Figure 8.4 and the closest contacts involving the PF₆ groups are given in Table 8.4.

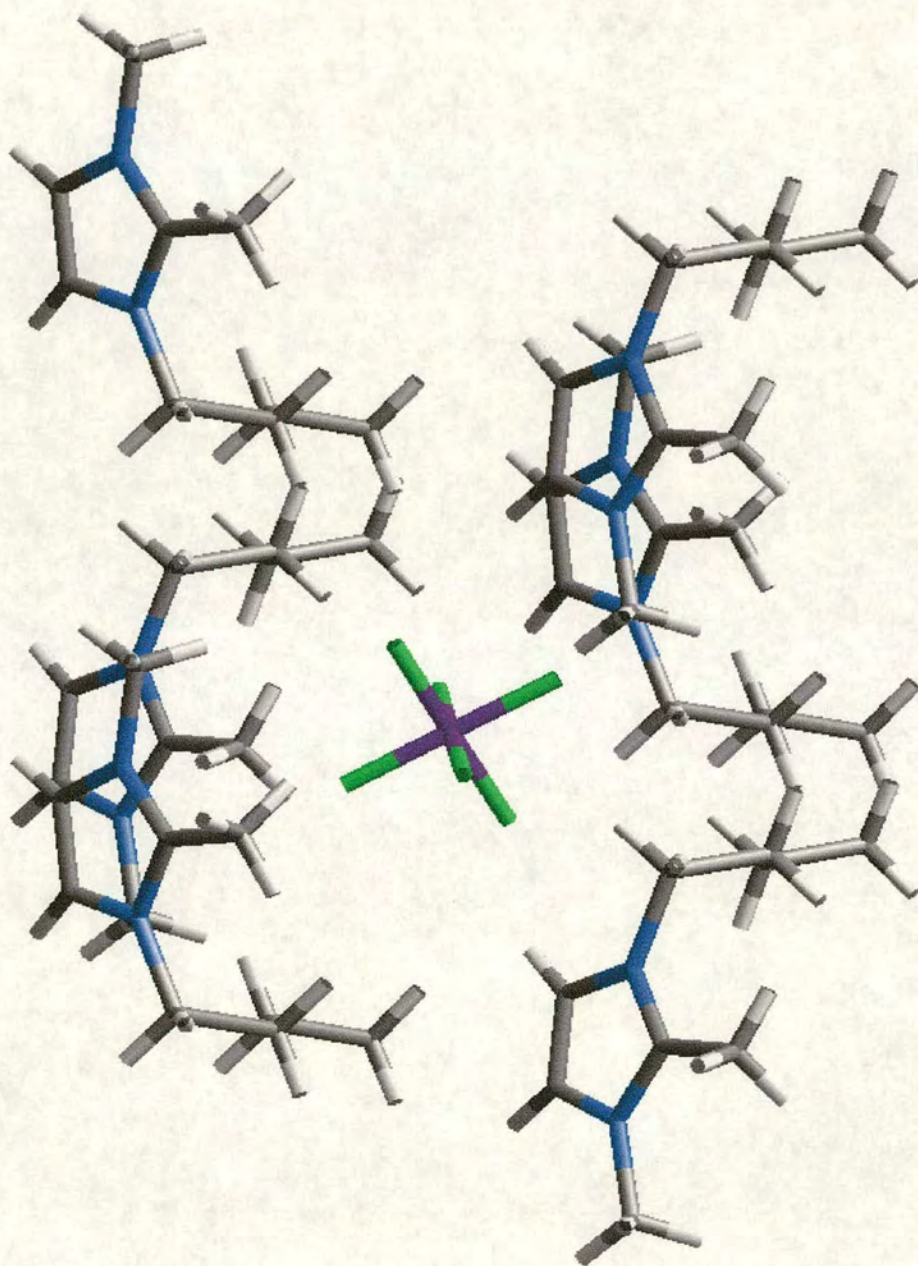


Figure 8.4. Part of the crystal structure of 1-butyl-2,3-dimethyl imidazolium hexafluorophosphate showing the environment around the PF₆⁻ anion.

Close contact	Distance / Å
F – H4	2.46
F – H6	2.49
F – H7	2.57
F – H on Me1	2.57
F – H on Me2	2.59
F – H5	2.60
F – H on Me2	2.60
F – H6	2.61
F – H4	2.62
F – H on Me1	2.64
F – H5	2.66

Table 8.4. Close contacts within the crystal structure of 1-butyl-2,3-dimethyl imidazolium hexafluorophosphate.

Six imidazolium rings surround each PF_6 anion giving a total of eleven hydrogen bonds between the ions, again emphasising the significant extent of hydrogen bonding that exists within these structures.

It is interesting to note that there is no published crystal structure of 1-butyl-3-methyl imidazolium hexafluorophosphate. This is no doubt a result of the fact that bmimPF_6 forms a glass rather than a polycrystalline solid at low temperatures. The formation of a glass indicates that there is short-range order but no long-range order in the solid. It is possible that for the bmimPF_6 the dominant interaction between the PF_6 group and H2 is also present in the liquid phase, and that on cooling this interaction remains dominant and “locks” the orientation of the cations and anions in such a way that the regular packing arrangement required for a polycrystalline solid cannot be achieved. For the bmmimPF_6 , the structure is not dominated by any one particular interaction and so on cooling, the cations and anions are able to orientate themselves in such a way to give a structure with long range order.

8.3.2.1 1-butyl-2,3-dimethyl imidazolium tetrafluoroborate.

One of the effects of changing the anion from PF_6 to BF_4 that is immediately obvious is an increase in the degree of disorder. Within the crystal structure of bmmimBF_4 , shown in Figures 8.5 and 8.6, the BF_4 anion exists in two different environments and one of these is disordered.

Only four imidazole rings surround the fully ordered BF_4 , but there remains six hydrogen-bonding contacts associated with this ion, as detailed in Table 8.5.

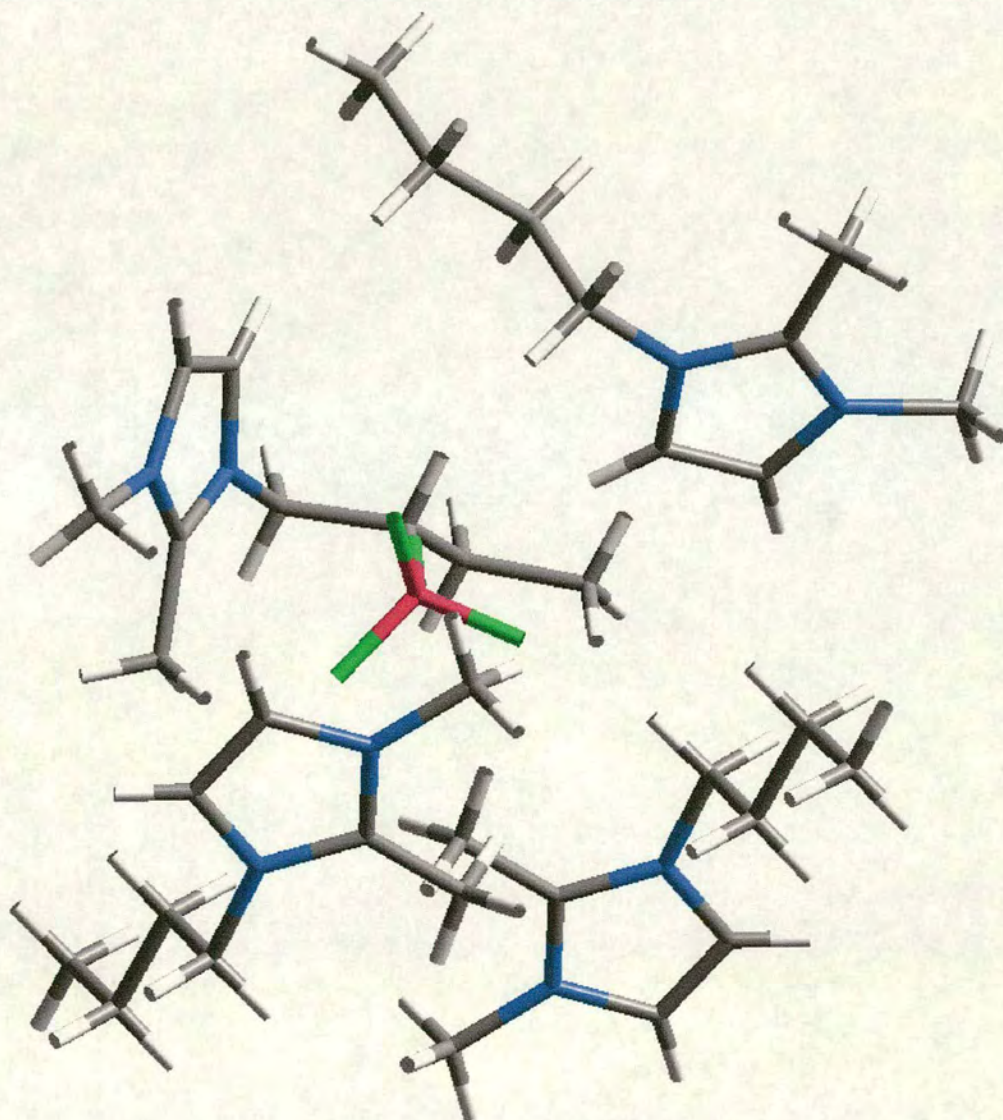
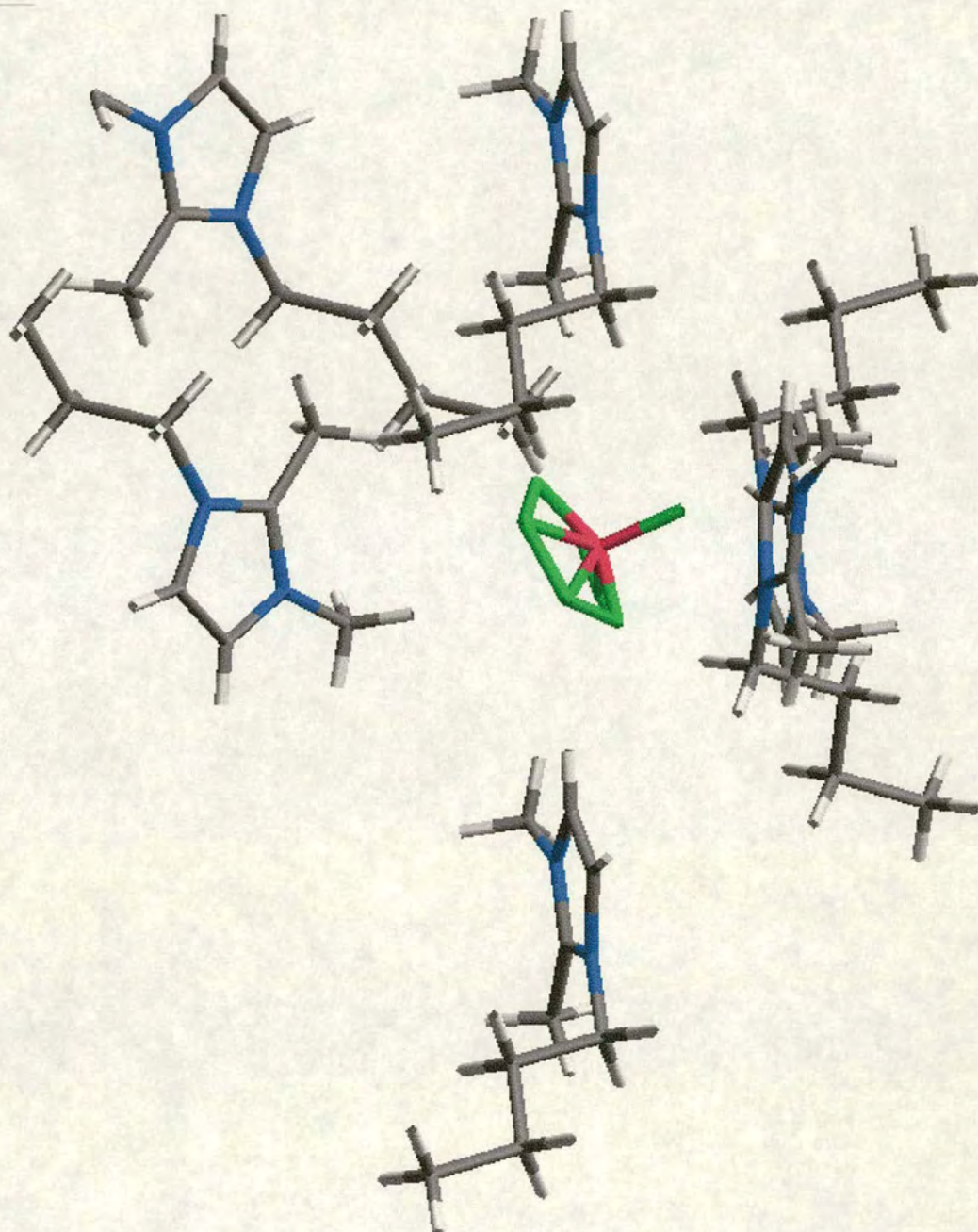


Figure 8.5. The environment of the fully ordered BF_4 anion in bmmimBF_4 .

Bond	Distance / Å
F – H4	2.33
F – H5	2.44
F – H on Me2	2.46
F – H on Me1	2.48
F – H on Me2	2.54
F – H on Me2	2.57

Table 8.5. Hydrogen bond distances to the ordered BF_4 anion.Figure 8.6. The environment of the disordered BF_4 ion in bmmimBF_4 .

Five imidazole rings surround each disordered BF_4 ion. 85% of the occupancy of this structure has 7 inter-ionic hydrogen bonds and 15% has 6 inter-ionic hydrogen bonds. The lengths of these interactions are given in Tables 8.6 and 8.7.

Bond	Distance / Å
B – H5	2.27
B – H on Me2	2.28
B – H on Me2	2.34
B – H6	2.56
B – H6	2.56
B – H on Me1	2.62

Table 8.6. Hydrogen bond distances for the 85% occupied BF_4 anion within the bmmim BF_4 crystal structure.

Bond	Distance / Å
B – H4	2.27
B – H5	2.27
B – H8	2.43
B – H on Me1	2.48
B – H on Me2	2.52
B – H9	2.59
B – H6	2.62

Table 8.7. Hydrogen bond distances for the 15% occupied BF_4 anion within the bmmim BF_4 crystal structure.

The effect of changing the anion on the internal geometry of the cation was assessed experimentally by analysis of these crystal structures and again no change was observed.

The densities of the crystals of each species are given in Table 8.8 and show a significant change with anion.

Ionic liquid.	Density / Mg m^{-3}
BmmimCl	1.210
Bmmim BF_4	1.298
Bmmim PF_6	1.521

Table 8.8. Densities of bmmimCl, bmmim BF_4 and bmmim PF_6 as determined from the crystal structures.

This trend reflects the increasing mass of the anion in each of these structures. Hence, the effect of replacing the strongly co-ordinating chloride ion with the less co-ordinating BF_4 or PF_6 anions, which might be expected to result in a decrease in interionic interactions and a resultant drop in density, is overshadowed by the effect of the significantly increased mass. However, it is probably this decrease in co-ordinating ability that is responsible for the significant decrease in the melting points of the BF_4 and PF_6 species compared to the chloride analogue (see section 6.2).

8.4 The Effect of Substitution of a Phenyl Group.

The effect of substitution of a methyl group to the cation of imidazolium ionic liquids has been assessed by comparison of the crystal structures of mono- and dimethylated species. Comparison of this with the effect of the addition of a phenyl group to the imidazolium ring is also possible by comparison of the crystal structures of 1-butyl-2,3-dimethyl imidazolium hexafluorophosphate and 1-butyl-2-phenyl-3-methyl imidazolium hexafluorophosphate. The crystal structure of 1-butyl-2-phenyl-3-methyl imidazolium hexafluorophosphate is shown in Figure 8.7.

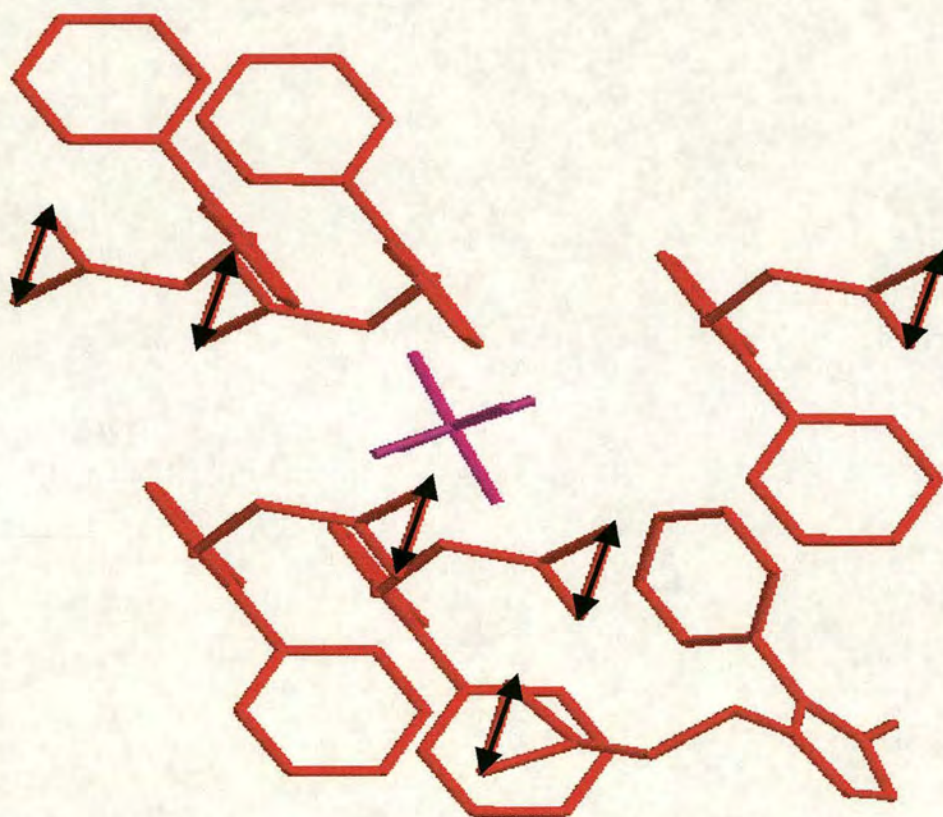


Figure 8.7. The crystal structure of 1-butyl-2-phenyl-3-methyl imidazolium hexafluorophosphate. Black arrows indicate disorder between two positions.

The extent of hydrogen bonding within this ionic liquid was analysed by studying the number of interactions between the cation and anion and these are given in Table 8.9.

Close contact.	Distance / Å
F – H6	2.39
F – H7	2.42
F – H on Ph	2.47
F – H7	2.57
F – H on Me	2.60
F – H on Ph	2.62
F – H4	2.63

Table 8.9. Close contacts within the crystal structure of 1-butyl-2-phenyl-3-methyl imidazolium hexafluorophosphate.

The most striking difference between this crystal structure and that of 1-butyl-2,3-dimethyl imidazolium hexafluorophosphate is that in this species there is disorder at the tip of the butyl group.

The arrows in Figure 8.7 have been added to indicate the location of this disorder and to show that the carbon at the tip of the butyl group essentially exists in two different positions within the crystal structure with 50 % occupancy.

This crystal structure was collected at 220 K, and so it was decided to investigate the effect of temperature on this disorder by collection of another data set at 293 K. Although an increase in temperature would be expected to result in a slight increase in the vibrational amplitudes of all atoms in the crystal, the crystal structure at 293 K shows that there is a marked increase in the degree of disorder of the butyl group such that it is now the two end carbon atoms of the butyl chain that are disordered. The two crystal structures are superimposed for comparison in Figure 8.8. The structure recorded at room temperature is shown in yellow.

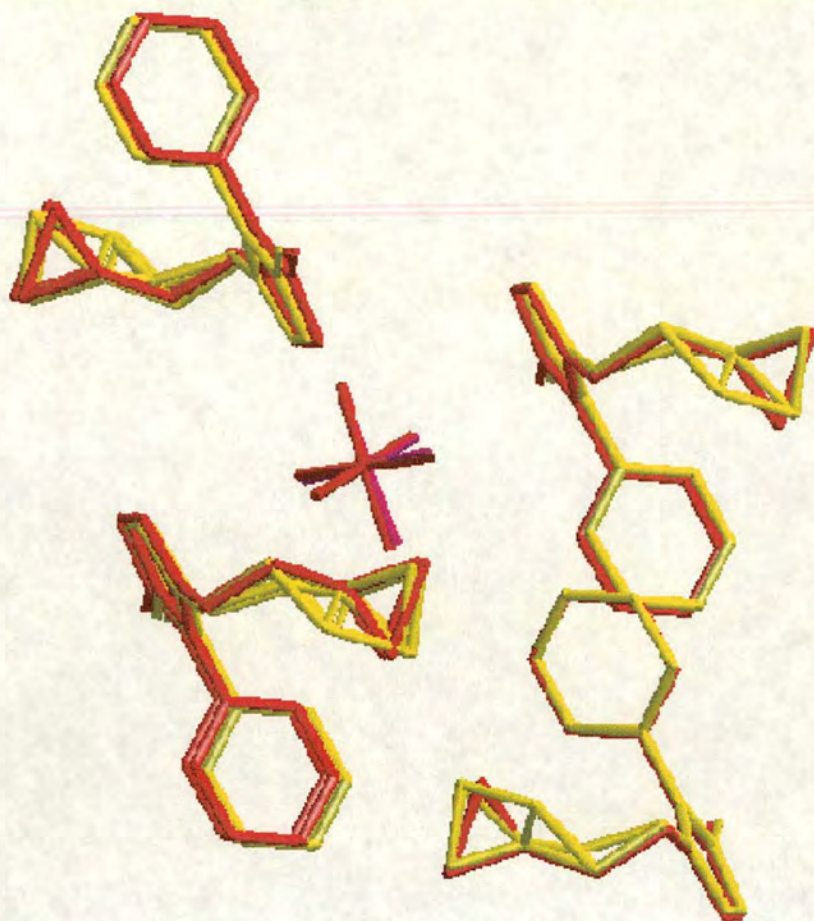


Figure 8.8. The crystal structures of 1-butyl-2-phenyl-3-methyl imidazolium hexafluorophosphate at 220 K and 293 K.

It is interesting to note that this disorder of the butyl group is not observed in any of the crystal structures of the mono- or di-methylated imidazolium ionic liquids.

It is proposed that this is because the dominant interactions (other than the electrostatic interaction between cations and anions) within this structure are those between the phenyl rings. It is the optimisation of these interactions that dictates the orientation of the cations within the solid, with the directional interactions between the cation and the anion being of secondary importance. There is only one close contact between the PF_6 and the backbone of the imidazolium ring in this structure compared to four in the dimethylated species. It is proposed that there are fewer interactions to the butyl group in this structure and thus it is less restricted in its movement and disorder is observed. The internal geometry of the cation is unaffected by changing the nature of the 2-substituent.

8.5 Structural Trends within Published Ionic Liquid Crystal Structures.

Following the successful elucidation of the solid state structure of a range of butyl-substituted imidazolium ionic liquids, the published crystal structures of similar imidazolium-based ionic liquids were re-assessed to determine whether similar structural trends were apparent. Using the Cambridge Structural Database it is possible to analyse published crystal structures to gain additional structural information that is not included in the original literature. For each of the structures studied, the environment surrounding an individual anion was investigated and the number of close contacts determined. Thus, in a similar manner to that described previously, analysis of the extent of hydrogen bonding within each ionic liquid was possible and the effect of structural changes could be assessed.

To date, only two crystal structures of butyl-substituted imidazolium ionic liquids have been published, presumably due to their relatively low melting point and the general difficulty of growing crystals of these compounds. However, the crystal structures of the ethyl-substituted imidazolium ionic liquids have been investigated in more detail and a comparison of some of these crystal structures gives some insight into the nature of imidazolium ionic liquids in the solid form.

The first crystal structure of an imidazolium-based ionic liquid was published in 1986 by Abdul-Sada *et al.* and described the structure of the ethyl-substituted species, emimI.¹ They reported the existence of hydrogen bonding within the structure, the first hard evidence of such bonding, but only with reference to the interaction of the iodide with the methyl and H2 hydrogen atoms. No indication of any hydrogen bonding to the other ring hydrogens was reported.

In 1995 Elaiwi *et al.* published the structure of the analogous emimBr as well as emimI and emimAlBr₄ thereby enabling some assessment of the effect of changing the anion on the crystal structure.² The internal dimensions of the imidazolium ring

¹ A. Abdul-Sada, A M. Greenway, P. B. Hitchcock, T. J. Mohammed, K. R. Seddon and J. A. Zora, *J. Chem. Soc., Chem. Commun.*, 1986, 1753 – 1754.

² A. Elaiwi, P. B. Hitchcock, K. R. Seddon, N. Srinivasan, Y. Tan, T. Welton and J. A. Zora, *J. Chem. Soc., Dalton Trans.*, 1995, 3467 – 3471.

are largely unaffected by the change in anion and the crystals of the iodide and bromide species are isomorphous. However, unlike Abdul-Sada, Elaiwi reports the presence of hydrogen bonding between the anion and all three of the ring hydrogens within each species, although those to H4 and H5 are longer than those to H2.

The crystal structure of emimCl, published by Dymeck *et al.*³ is anomalous in that it shows four unique imidazolium cations and four unique chlorides in each unit cell. The crystal structure as a whole is considerably more complicated than those of the bromide and iodide analogues, which contain only one crystallographically distinct cation and anion. They report that hydrogen bonding is evident between the chloride anions and H2, H4 and H5 on the imidazolium rings, but each of the four distinct chlorides display different numbers and combinations of hydrogen bonds. However, as for the bromide and iodide species, the hydrogen bonding between the anion and the cation is significant and not restricted to the interactions between the anion and the H2 proton of the cation, as was previously supposed.

The data for this crystal structure are poor (R factor > 10 %) and disorder is observed at both the carbons of the ethyl chain - probably exacerbated by collection of the data at room temperature - so comparison of this species with the iodide and bromide species is not easy. Additionally, the crystal structure data published in the Cambridge Structural Database does not include hydrogen placement. Assessment of the hydrogen bonding within this structure would entail placing the hydrogens using the Cambridge Structural Database and is invalidated by the large degree of uncertainty involved owing to the poor quality of the data. However, another member of the research group at Edinburgh has collected the crystal structure of emimCl so this is used to compare the structures of the three species.⁴ This structure is similar to that published, in that it contains four inequivalent imidazolium cations in each cell, two of which are disordered. The distance of the closest contacts between the anions and the hydrogens of the imidazole rings for each species are shown in Table 8.10. It is clear from these results that an increase in the anion size

³ C. J. Dymeck, JR, D. A. Grossie, A. V. Fratini and W. W. Adams, *J. Molecular Structure*, 1989, **213**, 25 – 34.

⁴ D. Sanders. University of Edinburgh, 2001.

results in a corresponding increase in the length of the closest contacts between the anion and cation.

Close contact	Distance / Å		
	EmimCl X = Cl	EmimBr X = Br	EmimI X = I
X – H2	2.45	2.78	2.93
X – H4	2.74	2.89	3.13
X – H5	2.63	2.97	3.17

Table 8.10. Comparison of the C – X close contacts within emimX ionic liquids. X = anion.

The crystal structure of emimNO₂ and emimNO₃ have been published and show significant hydrogen bonding, this time to the oxygen atoms of the anion and most significantly to H2. The change in anion from nitrite to nitrate results in a change from a hexagonal packing arrangement of cations to a vertical stacking arrangement, similar to that observed in the emimCl species. The emimI and emimBr also exhibit stacking of the imidazolium ring. In contrast, the crystal structure of emimPF₆ exhibits no such stacking.⁵ The existence of significant hydrogen bonding between the cation and anion is, however, still evident in the emimPF₆ species and it is again interesting to note that while the interactions to the H2 ring hydrogen are the strongest of the interactions they are by no means exclusive. The close contacts within this structure were determined using the data published in the Cambridge Structural Database and are given in Table 8.11.

⁵ J. Fuller, R. T. Carlin, H. C. DeLong and D. Haworth, *J. Chem. Soc., Chem. Commun.*, 1994, 299 – 300.

Close contact	Distance / Å
F – H2	2.56
F – H2	2.68
F – H2	2.70
F – H5	2.69
F – H5	2.65
F – H6	2.64

Table 8.11. Close contacts less than 2.70Å within the emimPF₆ crystal structure.

Hence, further examination of the published crystal structures shows that, as for the butyl-substituted species, while the hydrogen bonding between the anion and the H2 is indeed important, those to the other ring hydrogens are also significant.

In an attempt to assess the significance of the hydrogen bonding to the H4 and H5 ring protons, Abdul-Sada *et al.* synthesised a number of emim compounds with methyl substituents at the 2-position.⁶ However, this investigation was performed prior to the publication of the emimCl crystal structure and was initiated predominantly as an attempt to predict the nature of the emimCl crystal structure. Hence, no comparison of the mono and di-methylated chloride species is made, either crystallographically or in terms of any changes in the physical properties of the species observed upon methylation. Again, this can be done by further analysis of the published data. The crystal structure of 1-ethyl-2,3-dimethyl imidazolium chloride displays six close contacts between the anion and cation, as shown in Table 8.12.

⁶ A. K. Abdul-Sada, S. Al-Juaid, A. M. Greenway and P. B. Hitchcock, *Struct. Chem.*, 1990, **1**, 391 – 394.

Close contact	Distance / Å
Cl – H4	2.54
Cl – H on Me2	2.59
Cl – H6	2.69
Cl – H on Me1	2.81
Cl – H on Me1	2.81
Cl – H6	2.86

Table 8.12. Close contacts within 1-ethyl-2,3-dimethyl imidazolium chloride.

The importance of hydrogen bonding to the H4 and H5 position can also be assessed using a different approach, by analysis of the crystal structure of the tetra-methylated species 1,3,4,5-tetramethyl imidazolium chloride.⁷ Analysis of this crystal structure data elucidates the effect of removing all the ring hydrogens other than the most acidic. Surprisingly, the result is not an increase in the amount of hydrogen bonding to the H2 proton. On the contrary, each chloride shows only one interaction with hydrogen at this position - the rest of the hydrogen bonds within this structure are present between the chloride and the hydrogens on the methyl groups. A list of the seven close contacts to each chloride is given in Table 8.13.

Close contact	Distance / Å
Cl – H2	2.42
Cl – H on Me1	2.67
Cl – H on Me1	2.74
Cl – H on Me1	2.75
Cl – H on Me1	2.84
Cl – H on Me4	2.85

Table 8.13. Close contacts within the crystal structure of 1,3,4,5-tetramethyl imidazolium chloride. Me1 refers to methyl group adjacent to 2-position, Me4 refers to the methyl on backbone of imidazolium ring. Me1 ≡ Me3 and Me4 ≡ Me5 as structure is symmetrically substituted.

⁷ N. Kuhn, J. Fahl, R. Fawzi, C. Maichle-Möbmer and M. Steinmann, *Z. Naturforschung, Teil B*, 1998, **53**, 720 – 726.

The two crystal structures of butyl-substituted imidazolium ionic liquids that have been published confirm the involvement of all the ring hydrogens in hydrogen bonding. Dullius *et al.* report the crystal structure of bis(1-*n*-butyl-3-methyl imidazolium) tetrachloropalladate, (bmim)₂PdCl₄ which is reported as a catalyst precursor and not as an ionic liquid.⁸ The crystal structure shows that the PdCl₄²⁻ anion is only hydrogen bonded to three imidazolium groups – these are bonds to the acidic H2, bonds to the tip of the butyl group, and bonds to H5 on the imidazolium ring, as detailed in Table 8.14. Again it is interesting to note that, as observed for the other butyl-substituted species, hydrogen bonding between the anion and cation is not restricted to the H2 of the imidazolium ring.

Close contact	Distance / Å
Cl – H9	2.69
Cl – H5	2.72
Cl – H2	2.89
Cl – H2	2.90

Table 8.14. Close contacts within the crystal structure of [bmim]₂[PdCl₄]. Each close contact is observed twice for each anion. The numbering scheme used has been changed for consistency with that used in the rest of this investigation.

The crystal structure of 1-butyl-3-methylimidazolium tetraphenylborate, bmimBPh₄, was published in 2000.⁹ Unsurprisingly, the hydrogen bonding observed between the cation and anion in this crystal structure is dominated by the interactions of the imidazole and phenyl groups. These groups probably help initiate crystallisation - indeed the melting point of this species is much higher at 134 °C - and as such probably result in a significantly different crystal structure than those expected for the BF₄ and PF₆ species. One of the phenyl groups is aligned such that all of the hydrogen atoms lie within the sum of their van der Waals radii of the H2 of the imidazolium ring allowing six different hydrogen bonds, detailed in Table 8.15.

⁸ J. E. L. Dullius, P. A. Z. Suarez, S. Einloft, R. F. de Souza and J. Dupont, *Organometallics*, 1998, 17, 815 – 819.

There are also five additional hydrogen bonds between the anion, which has close contacts to three imidazolium rings and the cation.

Close contact	Distance / Å
Hydrogens on phenyl – H1	2.67, 2.68, 2.69, 2.75, 2.77, 2.81.
Ph – H7	2.73
Ph – H5	2.76
Ph – H5	2.76
Ph – H4	2.79
Ph – H5	2.79
Ph – H on Me	2.82

Table 8.15. Close contact within the crystal structure of bmimBPh₄. Numbering scheme has been altered for consistency with that used previously.

⁹ J. Dupont, P. A. Z. Suarez, R. F. de Souza, R. A. Burrow and J. Kintzinger, *Chem. Eur. J.*, 2000, **6**, 13, 2377 – 2381.

8.6 Conclusions.

The crystal structures of 1-butyl-3-methyl imidazolium chloride and 1-butyl-2,3-dimethyl imidazolium chloride have allowed the effect of methylation of the imidazolium ring at the 2-position to be assessed. It was predicted that methylation at this position would reduce the extent of hydrogen bonding within the species by removal of the acidic H2. By contrast, this substitution resulted in an unexpected increase in the melting points of the ionic liquids. It can be seen by analysis of the crystal structures of these species that methylation actually resulted in an increase in the hydrogen bonding within these systems. The loss of the shortest contact between the anion and the H2 is more than compensated for by an increase in the number of close contacts between the anion and the other hydrogens on the cation. Thus, a melting point increase is observed.

The effect of changing the anion on the crystal structures of imidazolium ionic liquids was also assessed through analysis of the crystal structures of 1-butyl-2,3-dimethyl imidazolium hexafluorophosphate and tetrafluoroborate. These species also exhibit significant hydrogen bonding between the cation and anion, thereby explaining their high melting points. Anion disorder is observed in the 1-butyl-2,3-dimethyl imidazolium tetrafluoroborate species and cation disorder is observed within the crystal structure of 1-butyl-2-phenyl-3-methyl imidazolium hexafluorophosphate.

Analysis of the crystal structures of other imidazolium-based ionic liquids that have been published confirms the observation that, while the hydrogen bonding to the H2 is important, it is by no means exclusive and its importance has previously been overemphasised.

Appendix.

1 X-ray Crystallography.

A1. 1-butyl-3-methyl imidazolium chloride.

Empirical formula	$C_8 H_{15} Cl N_2$ $[N_2C_3H_3(Me)C_4H_9]^+Cl^-$
Formula weight	174.67
Wavelength	0.71073 Å
Temperature	150(2) K
Crystal System	Orthorhombic
Space group	Pna2(1)
Unit cell dimensions	a = 10.0494(14) Å α = 90 deg. b = 11.3375(16) Å β = 90 deg. c = 8.2866(11) Å γ = 90 deg.
Volume	944.1(2) Å ³
Number of reflections for cell	2388 (2.5 < theta < 26.5 deg.)
Z	4
Density (calculated)	1.229 Mg/m ³
Absorption coefficient	0.347 mm ⁻¹
F(000)	376
Crystal description	Colourless rod
Crystal size	0.28 x 0.07 x 0.06 mm
Theta range for data collection	2.71 to 26.39 deg
Index ranges	-12 ≤ h ≤ 7, -14 ≤ k ≤ 14, -10 ≤ l ≤ 10
Reflections collected	5090
Independent reflections	1848 [R(int) = 0.0305]
Scan type	phi and omega scans
Absorption correction	Sadabs (Tmin= 0.821, Tmax=0.928)

Solution	direct (SHELXS-97 (Sheldrick, 1990))
Refinement type	Full-matrix least-squares on F^2
Program used for refinement	SHELXL-97
Hydrogen atom placement	geometric
Hydrogen atom treatment	riding
Data / restraints/ parameters	1848/1/102
Goodness-of-fit on F^2	1.090
Conventional R [$F > 4\sigma(F)$]	R1 = 0.0429 [1710 data]
Weighted R (F^2 and all data)	wR2 = 0.0886
Absolute structure parameter	0.11(10)
Extinction coefficient	0
Final maximum delta/sigma	0.000
Weighting scheme	calc $w=1/[\sigma^2(F_o^2)+(0.0334P)^2+0.4474P]$ where $P=(F_o^2+2F_c^2)/3$
Largest diff. Peak and hole	0.211 and -0.239 e. \AA^{-3}

Table A1. Crystal data, solution and refinement for 1-butyl-3-methyl imidazolium chloride.

Bond	Length / \AA
N(1)-C(2)	1.324(4)
N(1)-C(5)	1.374(4)
N(1)-C(6)	1.483(4)
C(2)-N(3)	1.328(5)
N(3)-C(4)	1.379(4)
N(3)-C(10)	1.461(4)
C(4)-C(5)	1.343(3)
C(6)-C(7)	1.509(4)
C(7)-C(8)	1.515(4)
C(8)-C(9)	1.512(4)

Table A2. Bond lengths for 1-butyl-3-methyl imidazolium chloride.

Bond	Angle / $^\circ$
C(9)-C(8)-C(7)	112.5(2)
C(2)-N(1)-C(5)	109.3(3)
C(2)-N(1)-C(6)	124.9(2)
C(5)-N(1)-C(6)	125.8(3)
N(1)-C(2)-N(3)	108.19(19)
C(2)-N(3)-C(4)	108.5(3)
C(2)-N(3)-C(10)	124.7(2)
C(4)-N(3)-C(10)	126.8(3)
C(5)-C(4)-N(3)	107.3(3)
C(4)-C(5)-N(1)	106.7(3)
N(1)-C(6)-C(7)	110.7(2)
C(6)-C(7)-C(8)	114.3(2)

Table A3. Bond angles for 1-butyl-3-methyl imidazolium chloride.

A2. 1-butyl-3-methyl imidazolium bromide.

Empirical formula	$C_8 H_{15} Br N_2$ $[N_2C_3H_3(Me)Bu]^+ Br^-$
Formula weight	219.13
Wavelength	0.71073 Å
Temperature	150(2) K
Crystal System	Orthorhombic
Space group	Pnma
Unit cell dimensions	a = 10.033(3) Å α = 90 deg. b = 8.424(2) Å β = 90 deg. c = 11.816(3) Å γ = 90 deg.
Volume	998.7(5) Å ³
Number of reflections for cell	2493 (2.5 < theta < 26.5 deg.)
Z	4
Density (calculated)	1.457 Mg/m ³
Absorption coefficient	4.062 mm ⁻¹
F(000)	448
Crystal description	Colourless block
Crystal size	1.5 x 0.66 x 0.63 mm
Theta range for data collection	2.66 to 26.48 deg
Index ranges	-12 ≤ h ≤ 12, -9 ≤ k ≤ 10, -10 ≤ l ≤ 14
Reflections collected	4852
Independent reflections	1077 [R(int) = 0.0883]
Scan type	phi and omega scans
Absorption correction	Sadabs (Tmin= 0.316, Tmax=1.000)
Solution	Patterson (SHELXS-97 (Sheldrick, 1990))
Refinement type	Full-matrix least-squares on F ²
Program used for refinement	SHELXL-97
Hydrogen atom placement	geometric
Hydrogen atom treatment	riding

Data / restraints/ parameters	1077/0/77
Goodness-of-fit on F^2	1.139
Conventional R [$F > 4\sigma(F)$]	R1 = 0.0745 [866 data]
Weighted R (F^2 and all data)	wR2 = 0.2018
Extinction coefficient	0.009(5)
Final maximum delta/sigma	0.000
Weighting scheme	calc $w=1/[\sigma^2(F_o^2)+(0.0997P)^2+7.6606P]$ where $P=(F_o^2+2F_c^2)/3$
Largest diff. Peak and hole	1.891 and -1.378 e.Å ⁻³

Table A3. Crystal data, solution and refinement for 1-butyl-3-methyl imidazolium bromide.

Bond	Length / Å
N(1)-C(2)	1.304(9)
N(1)-C(5)	1.393(10)
N(1)-C(10)	1.45(2)
N(1)-C(6)	1.560(19)
C(2)-N(1)#1	1.304(9)
C(5)-C(5)#1	1.303(17)
C(6)-C(7)	1.50(3)
C(7)-C(8)	1.50(2)
C(8)-C(9)	1.52(2)

Table A4. Bond lengths for 1-butyl-3-methyl imidazolium bromide.

Bond	Angle / °
C(2)-N(1)-C(5)	107.7(7)
C(2)-N(1)-C(10)	125.6(11)
C(5)-N(1)-C(10)	124.2(11)
C(2)-N(1)-C(6)	122.6(10)
C(5)-N(1)-C(6)	126.6(10)
C(10)-N(1)-C(6)	30.1(9)
N(1)-C(2)-N(1)#1	109.9(10)
C(5)#1-C(5)-N(1)	107.4(5)
C(7)-C(6)-N(1)	117.1(14)
C(6)-C(7)-C(8)	114.1(14)
C(7)-C(8)-C(9)	112.3(15)

Table A5. Bond angles for 1-butyl-3-methyl imidazolium bromide.

A3. 1-butyl-2,3-dimethyl imidazolium chloride.

Empirical formula	$C_9 H_{17} Cl N_2$ $C_3H_2N_2(Me)_2(nBu)$
Formula weight	188.70
Wavelength	0.71073 Å
Temperature	150(2) K
Crystal System	Monoclinic
Space group	P2(1)/n
Unit cell dimensions	a = 8.3045(6) Å α = 90 deg. b = 11.6621(9) Å β = 90.7400(10) deg. c = 10.6994(8) Å γ = 90 deg.
Volume	1036.13(13) Å ³
Number of reflections for cell	4420 (2.5 < theta < 53 deg.)
Z	4
Density (calculated)	1.210 Mg/m ³
Absorption coefficient	0.321 mm ⁻¹
F(000)	408
Crystal description	Colourless block
Crystal size	0.38 x 0.24 x 0.17 mm
Theta range for data collection	2.58 to 26.41 deg.
Index ranges	-10 ≤ h ≤ 10, -8 ≤ k ≤ 14, -13 ≤ l ≤ 11
Reflections collected	5607
Independent reflections	2123 [R(int) = 0.0184]
Scan type	phi and omega scans
Absorption correction	Sadabs (Tmin= 0.629, Tmax=0.928)
Solution	Patterson (SHELXS-97 (Sheldrick, 1990))
Refinement type	Full-matrix least-squares on F ²
Program used for refinement	SHELXL-97
Hydrogen atom placement	difmap
Hydrogen atom treatment	refined freely

Data / restraints/ parameters	2123/0/177
Goodness-of-fit on F^2	0.941
Conventional R [$F > 4\sigma(F)$]	R1 = 0.0293 [1766 data]
Weighted R (F^2 and all data)	wR2 = 0.0766
Extinction coefficient	0
Final maximum delta/sigma	0.001
Weighting scheme	calc $w=1/[\sigma^2(F_o^2)+(0.0503P)^2+0.0000P]$ where $P=(F_o^2+2F_c^2)/3$
Largest diff. Peak and hole	0.227 and -0.338 e.Å ⁻³

Table A6. Crystal data, solution and refinement for 1-butyl-2,3-dimethyl imidazolium chloride.

Bond	Length / Å
N(1)-C(2)	1.3355(16)
N(1)-C(5)	1.3808(16)
N(1)-C(6)	1.4727(16)
C(2)-N(3)	1.3340(15)
C(2)-C(11)	1.4744(18)
N(3)-C(4)	1.3807(16)
N(3)-C(10)	1.4654(16)
C(4)-C(5)	1.3402(18)
C(6)-C(7)	1.5151(18)
C(7)-C(8)	1.5155(18)
C(8)-C(9)	1.5107(19)

Table A7. Bond lengths for 1-butyl-2,3-methyl imidazolium chloride.

Bond	Angle / °
C(9)-C(8)-C(7)	111.99(12)
C(2)-N(1)-C(5)	109.03(10)
C(2)-N(1)-C(6)	125.61(12)
C(5)-N(1)-C(6)	125.35(11)
N(1)-C(2)-N(3)	107.53(11)
C(2)-N(3)-C(4)	109.19(10)
C(2)-N(3)-C(10)	125.02(11)
C(4)-N(3)-C(10)	125.79(11)
C(5)-C(4)-N(3)	107.03(11)
C(4)-C(5)-N(1)	107.21(11)
N(1)-C(6)-C(7)	112.13(10)
C(6)-C(7)-C(8)	113.63(12)

Table A8. Bond angles for 1-butyl-2,3-dimethyl imidazolium chloride.

A4. 1-butyl-2,3-dimethyl imidazolium tetrafluoroborate.

Empirical formula	$C_9 H_{17} B F_4 N_2$ $C_3N_2H_2 (Me)_2 {}^nBu \cdot BF_4$
Formula weight	240.06
Wavelength	1.54178 Å
Temperature	150(2) K
Crystal System	Monoclinic
Space group	P2(1)/c
Unit cell dimensions	a = 13.033(7) Å α = 90 deg. b = 11.261(6) Å β = 93.44(6) deg. c = 16.770(13) Å γ = 90 deg.
Volume	2457(3) Å ³
Number of reflections for cell	49 (15 < theta < 22 deg.)
Z	8
Density (calculated)	1.298 Mg/m ³
Absorption coefficient	1.042 mm ⁻¹
F(000)	1008
Crystal description	Colourless plate
Crystal size	0.31 x 0.21 x 0.06 mm
Theta range for data collection	3.40 to 69.66 deg.
Index ranges	-15<=h<=15, 0<=k<=13, -18<=l<=20
Reflections collected	4496
Independent reflections	4496 [R(int) = 0.0000]
Scan type	Omega-2theta
Solution	direct (sir92)
Refinement type	Full-matrix least-squares on F ²
Program used for refinement	SHELXL-97
Hydrogen atom placement	geometric
Hydrogen atom treatment	riding
Data / restraints/ parameters	4496/0/309
Goodness-of-fit on F ²	0.971

Conventional R [$F > 4\sigma(F)$]	R1 = 0.0848 [1888 data]
Weighted R (F^2 and all data)	R1 = 0.0848 [1888 data]
Extinction coefficient	0.0005(2)
Final maximum delta/sigma	0.000
Weighting scheme	calc $w=1/[\sigma^2(Fo^2)+(0.0931P)^2+0.0000P]$ where $P=(Fo^2+2Fc^2)/3$
Largest diff. Peak and hole	0.324 and -0.250 e. \AA^{-3}

Table A9. Crystal data, solution and refinement for bmmimBF₄.

Bond	Length / \AA
B(1A)- F(3A)	1.375(7)
B(1A)- F(1A)	1.377(7)
B(1A)- F(2A)	1.377(7)
B(1A)- F(4A)	1.385(7)
B(1B)- F(1B')	1.18(2)
B(1B)- F(3B')	1.31(4)
B(1B)- F(1B)	1.336(8)
B(1B)- F(4B)	1.352(7)
B(1B)- F(2B)	1.366(9)
B(1B)- F(2B')	1.38(3)
B(1B)- F(3B)	1.385(9)
N(1A)- C(2A)	1.341(6)
N(1A)- C(5A)	1.390(7)
N(1A)- C(6A)	1.479(6)
C(2A)- N(3A)	1.336(6)
C(2A)- C(21A)	1.474(7)
N(3A)- C(4A)	1.374(6)
N(3A)- C(10A)	1.460(6)
C(4A)- C(5A)	1.344(7)
C(6A)- C(7A)	1.508(8)
C(7A)- C(8A)	1.524(7)
C(8A)- C(9A)	1.511(8)
N(1B)- C(2B)	1.344(6)
N(1B)- C(5B)	1.380(7)
N(1B)- C(6B)	1.466(7)
C(2B)- N(3B)	1.331(7)
C(2B)- C(21B)	1.485(7)
N(3B)- C(4B)	1.378(7)
N(3B)- C(10B)	1.469(7)
C(4B)- C(5B)	1.330(8)
C(6B)- C(7B)	1.521(7)
C(7B)- C(8B)	1.515(7)
C(8B)- C(9B)	1.522(8)

Table A 10. Bond lengths for 1-butyl-2,3-dimethyl imidazolium tetrafluoroborate.

Bond	Angle / °		
F(3A)-B(1A)-F(1A)	109.9(5)	C(2A)-N(1A)-C(6A)	127.2(5)
F(3A)-B(1A)-F(2A)	109.6(5)	C(5A)-N(1A)-C(6A)	123.6(4)
F(1A)-B(1A)-F(2A)	109.4(5)	N(3A)-C(2A)-N(1A)	107.4(5)
F(3A)-B(1A)-F(4A)	108.8(5)	N(3A)-C(2A)-C(21A)	126.3(5)
F(1A)-B(1A)-F(4A)	109.9(5)	N(1A)-C(2A)-C(21A)	126.3(5)
F(2A)-B(1A)-F(4A)	109.2(5)	C(2A)-N(3A)-C(4A)	109.3(4)
F(1B')-B(1B)-F(3B')	112(2)	C(2A)-N(3A)-C(10A)	125.9(4)
F(1B')-B(1B)-F(1B)	150.8(14)	C(4A)-N(3A)-C(10A)	124.8(5)
F(3B')-B(1B)-F(1B)	66.9(18)	C(5A)-C(4A)-N(3A)	107.7(5)
F(1B')-B(1B)-F(4B)	100.5(14)	C(4A)-C(5A)-N(1A)	106.5(5)
F(3B')-B(1B)-F(4B)	108.5(17)	N(1A)-C(6A)-C(7A)	111.5(4)
F(1B)-B(1B)-F(4B)	107.5(6)	C(6A)-C(7A)-C(8A)	112.0(5)
F(1B')-B(1B)-F(2B)	64.9(14)	C(9A)-C(8A)-C(7A)	112.6(5)
F(3B')-B(1B)-F(2B)	47.2(17)	C(2B)-N(1B)-C(5B)	108.3(5)
F(1B)-B(1B)-F(2B)	109.5(7)	C(2B)-N(1B)-C(6B)	126.3(5)
F(4B)-B(1B)-F(2B)	113.7(6)	C(5B)-N(1B)-C(6B)	125.1(5)
F(1B')-B(1B)-F(2B')	110(2)	N(3B)-C(2B)-N(1B)	107.2(5)
F(3B')-B(1B)-F(2B')	110(2)	N(3B)-C(2B)-C(21B)	125.9(5)
F(1B)-B(1B)-F(2B')	49.3(14)	N(1B)-C(2B)-C(21B)	126.9(5)
F(4B)-B(1B)-F(2B')	115.5(13)	C(2B)-N(3B)-C(4B)	109.8(5)
F(2B)-B(1B)-F(2B')	130.5(13)	C(2B)-N(3B)-C(10B)	125.8(5)
F(1B')-B(1B)-F(3B)	53.5(14)	C(4B)-N(3B)-C(10B)	124.4(5)
F(3B')-B(1B)-F(3B)	139.3(17)	C(5B)-C(4B)-N(3B)	106.6(5)
F(1B)-B(1B)-F(3B)	106.9(6)	N(1B)-C(6B)-C(7B)	111.6(4)
F(4B)-B(1B)-F(3B)	111.4(6)	C(4B)-C(5B)-N(1B)	108.2(5)
F(2B)-B(1B)-F(3B)	107.6(7)	C(8B)-C(7B)-C(6B)	112.8(5)
F(2B')-B(1B)-F(3B)	58.4(15)	C(7B)-C(8B)-C(9B)	111.9(5)
C(2A)-N(1A)-C(5A)	109.0(4)		

Table A11. Bond angles for 1-butyl-2,3-dimethyl imidazolium tetrafluoroborate.

A5. 1-butyl-2,3-dimethyl imidazolium hexafluorophosphate.

Empirical formula	$C_9 H_{17} F_6 N_2 P$ $C_3 N_2 H_2 (Me)_2 {}^n Bu . PF_6$
Formula weight	298.22
Wavelength	0.71073 Å
Temperature	150(2) K
Crystal System	Monoclinic
Space group	Cc
Unit cell dimensions	a = 15.381(6) Å α = 90 deg. b = 8.603(3) Å β = 122.353(4) deg. c = 11.652(5) Å γ = 90 deg.
Volume	1302.5(9) Å ³
Number of reflections for cell	1827 (2.5 < theta < 26 deg.)
Z	4
Density (calculated)	1.521 Mg/m ³
Absorption coefficient	0.268 mm ⁻¹
F(000)	616
Crystal description	Colourless plate
Crystal size	0.54 x 0.36 x 0.07 mm
Theta range for data collection	2.84 to 26.39 deg.
Index ranges	-13 ≤ h ≤ 19, -10 ≤ k ≤ 10, -14 ≤ l ≤ 13
Reflections collected	3491
Independent reflections	1976 [R(int) = 0.0220]
Scan type	phi and omega scans
Solution	direct (SHELXS-97 (Sheldrick, 1990))
Refinement type	Full-matrix least-squares on F ²
Program used for refinement	SHELXL-97
Hydrogen atom placement	geometric
Hydrogen atom treatment	riding and rotating
Data / restraints/ parameters	1976/2/166
Goodness-of-fit on F ²	1.053

Conventional R [$F > 4\sigma(F)$]	R1 = 0.0366 [1773 data]
Weighted R (F^2 and all data)	wR2 = 0.0961
Extinction coefficient	0
Final maximum delta/sigma	0.000
Weighting scheme	calc $w = 1/[\sigma^2(F_o^2) + (0.0623P)^2 + 0.0000P]$ where $P = (F_o^2 + 2F_c^2)/3$
Largest diff. Peak and hole	0.305 and -0.211 e.Å ⁻³

Table A12. Crystal data for 1-butyl-2,3-dimethyl imidazolium hexafluorophosphate.

Bond	Length / Å
P(1)-F(4)	1.5702(19)
P(1)-F(1)	1.590(2)
P(1)-F(6)	1.5926(19)
P(1)-F(3)	1.595(2)
P(1)-F(5)	1.595(2)
P(1)-F(2)	1.606(2)
N(1)-C(2)	1.332(4)
N(1)-C(5)	1.379(3)
N(1)-C(6)	1.477(3)
C(2)-N(3)	1.324(4)
C(2)-C(11)	1.481(4)
N(3)-C(4)	1.385(3)
N(3)-C(10)	1.465(3)
C(4)-C(5)	1.328(4)
C(6)-C(7)	1.517(4)
C(7)-C(8)	1.512(4)
C(8)-C(9)	1.515(5)

Table A13. Bond lengths for 1-butyl-2,3-dimethyl imidazolium hexafluorophosphate.

Bond	Angle / °
F(4)-P(1)-F(1)	91.61(13)
F(4)-P(1)-F(6)	178.93(13)
F(1)-P(1)-F(6)	88.48(13)
F(4)-P(1)-F(3)	91.07(11)
F(1)-P(1)-F(3)	90.14(12)
F(6)-P(1)-F(3)	90.00(11)
F(4)-P(1)-F(5)	90.42(13)
F(1)-P(1)-F(5)	177.77(14)
F(6)-P(1)-F(5)	89.48(13)
F(3)-P(1)-F(5)	90.76(12)
F(4)-P(1)-F(2)	89.37(12)
F(1)-P(1)-F(2)	89.78(11)
F(6)-P(1)-F(2)	89.56(11)
F(3)-P(1)-F(2)	179.55(11)
F(5)-P(1)-F(2)	89.31(11)
C(9)-C(8)-C(7)	113.0(3)
C(2)-N(1)-C(5)	108.9(2)
C(2)-N(1)-C(6)	126.3(2)
C(5)-N(1)-C(6)	124.7(2)
N(1)-C(2)-N(3)	107.7(2)
C(2)-N(3)-C(4)	109.0(2)
C(2)-N(3)-C(10)	126.1(2)
C(4)-N(3)-C(10)	124.8(2)
C(5)-C(4)-N(3)	107.0(2)
C(4)-C(5)-N(1)	107.4(2)
N(1)-C(6)-C(7)	111.2(2)
C(6)-C(7)-C(8)	114.3(2)
N(3)-C(2)-C(11)	125.6(3)
N(1)-C(2)-C(11)	126.6(3)

Table A14. Bond angles for 1-butyl-2,3-dimethyl imidazolium hexafluorophosphate.

A6. 1-butyl-2-phenyl-3-methyl imidazolium hexafluorophosphate.

Empirical formula	C ₁₄ H ₁₉ F ₆ N ₂ P C ₁₄ H ₁₉ N ₂ ⁺ .PF ₆ ⁻
Formula weight	360.28
Wavelength	0.71073 Å
Temperature	150(2) K
Crystal System	Monoclinic
Space group	C2/c
Unit cell dimensions	a = 15.843(2) Å α = 90 deg. b = 8.6700(13) Å β = 95.302(3) deg. c = 24.895(4) Å γ = 90 deg.
Volume	3405.0(9) Å ³
Number of reflections for cell	4129 (4 < theta < 58 deg.)
Z	8
Density (calculated)	1.406 Mg/m ³
Absorption coefficient	0.219 mm ⁻¹
F(000)	1488
Crystal description	colourless block
Crystal size	0.50 x 0.40 x 0.14 mm
Theta range for data collection	1.64 to 22.49 deg.
Index ranges	-16 ≤ h ≤ 16, -9 ≤ k ≤ 9, -26 ≤ l ≤ 13
Reflections collected	6754
Independent reflections	2230 [R(int) = 0.0622]
Scan type	Phi and Omega Scans
Solution	direct (SHELXS-97 (Sheldrick, 1990))
Refinement type	Full-matrix least-squares on F ²
Program used for refinement	SHELXL-97
Hydrogen atom placement	geometric
Hydrogen atom treatment	Mixed
Data / restraints/ parameters	2230/91/236
Goodness-of-fit on F ²	1.046

Conventional R [$F > 4\sigma(F)$]	R1 = 0.0978 [1400 data]
Weighted R (F^2 and all data)	wR2 = 0.3031
Extinction coefficient	0.0036(11)
Final maximum delta/sigma	0.007
Weighting scheme	calc $w = 1/[\sigma^2(F_o^2) + (0.2000P)^2 + 0.0000P]$ where $P = (F_o^2 + 2F_c^2)/3$
Largest diff. Peak and hole	0.636 and -0.366 e.Å ⁻³

Table A15. Crystal data, solution and refinement for 1-butyl-2,3-dimethyl imidazolium hexafluorophosphate.

Bond	Length / Å		
P(1)-F(4)	1.528(5)	C(6)-C(7)	1.493(7)
P(1)-F(1)	1.547(5)	C(6)-C(7')	1.495(10)
P(1)-F(6)	1.504(5)	C(7)-C(8)	1.474(8)
P(1)-F(3)	1.525(5)	C(7')-C(8')	1.496(8)
P(1)-F(5)	1.471(5)	C(8)-C(9)	1.473(9)
P(1)-F(2)	1.520(5)	C(8')-C(9')	1.481(8)
N(1)-C(2)	1.325(6)	C(2)-C(21)	1.450(7)
N(1)-C(5)	1.354(6)	C(21)-C(22)	1.375(8)
N(1)-C(6)	1.455(7)	C(21)-C(26)	1.389(8)
C(2)-N(3)	1.338(6)	C(22)-C(23)	1.376(9)
N(3)-C(4)	1.351(6)	C(23)-C(24)	1.339(10)
N(3)-C(10)	1.462(7)	C(24)-C(25)	1.348(9)
C(4)-C(5)	1.299(8)	C(25)-C(26)	1.367(8)

Table A16. Bond lengths for 1-butyl-2,3-dimethyl imidazolium hexafluorophosphate.

Bond	Angle / °		
C(2)-N(1)-C(5)	109.1(5)	C(25)-C(26)-C(21)	118.7(6)
C(2)-N(1)-C(6)	126.0(5)	C(2)-N(3)-C(4)	109.4(5)
C(5)-N(1)-C(6)	125.0(5)	C(2)-N(3)-C(10)	125.6(5)
N(1)-C(6)-C(7)	115.5(7)	C(4)-N(3)-C(10)	124.9(5)
N(1)-C(6)-C(7')	105.6(13)	C(5)-C(4)-N(3)	107.3(5)
C(7)-C(6)-C(7')	24.3(13)	C(4)-C(5)-N(1)	108.3(5)
C(8)-C(7)-C(6)	109.4(9)	F(5)-P(1)-F(6)	176.8(5)
C(9)-C(8)-C(7)	116.0(11)	F(5)-P(1)-F(2)	92.5(4)
C(6)-C(7')-C(8')	111(2)	F(6)-P(1)-F(2)	89.2(4)
C(9')-C(8')-C(7')	105.9(15)	F(5)-P(1)-F(3)	88.2(4)
N(1)-C(2)-N(3)	106.0(5)	F(6)-P(1)-F(3)	90.1(4)
N(1)-C(2)-C(21)	127.5(5)	F(2)-P(1)-F(3)	179.1(4)
N(3)-C(2)-C(21)	126.6(5)	F(5)-P(1)-F(4)	91.5(4)
C(22)-C(21)-C(26)	119.5(6)	F(6)-P(1)-F(4)	91.1(4)
C(22)-C(21)-C(2)	120.7(5)	F(2)-P(1)-F(4)	93.1(4)
C(26)-C(21)-C(2)	119.7(5)	F(3)-P(1)-F(4)	86.4(4)
C(21)-C(22)-C(23)	119.3(7)	F(5)-P(1)-F(1)	89.4(4)
C(24)-C(23)-C(22)	120.9(7)	F(6)-P(1)-F(1)	88.1(4)
C(23)-C(24)-C(25)	120.1(7)	F(2)-P(1)-F(1)	85.1(4)
C(24)-C(25)-C(26)	121.4(7)	F(3)-P(1)-F(1)	95.4(4)
		F(4)-P(1)-F(1)	178.0(4)

Table A17. Bond angles for 1-butyl-2,3-dimethyl imidazolium hexafluorophosphate.

2. Conferences and Lecture Courses Attended.

Date	Conference / course.
16 th February 1999	Inorganic Synthesis, The University of Edinburgh.
20-22 nd April 1999	The University of Edinburgh Inorganic Section Meeting, Firlush Field Centre.
2 nd July 1999	Butler Electrochemistry Meeting, University of St. Andrews.
24 – 26 th August 1999	The University of Edinburgh Physical Section Meeting, Firlush Field Centre.
20-21 st September 1999	University of Scotland Inorganic Club, Heriot-Watt University.
17 – 20 th April 2000	RSC Annual Conference, UMIST, Manchester.
26 – 28 th April 2000	The University of Edinburgh Inorganic Section Meeting, Firlush Field Centre.
15 – 20 th June 2000	EPSRC-funded research Councils' Graduate School, The University of Stirling.
9 – 14 th July 2000	34 th International Conference on Coordination Chemistry, The University of Edinburgh.
22 – 24 th August 2000	The University of Edinburgh Physical Section Meeting, Firlush Field Centre.
13 – 14 th September 2000	University of Scotland Inorganic Club, University of Strathclyde, Glasgow.
1 – 5 th April 2001	The American Chemical Society Conference, San Diego, California.
25 – 27 th April 2001	The University of Edinburgh Inorganic Section Meeting, Firlush Field Centre.
17 – 18 th May 2001	Avecia Conference, Grasmere, Lake District.
12 th June 2001	Exotic Instruments in Chemistry, The University of Edinburgh.

Additionally, I attended the nearly all of the inorganic and material section meetings.